Star Formation

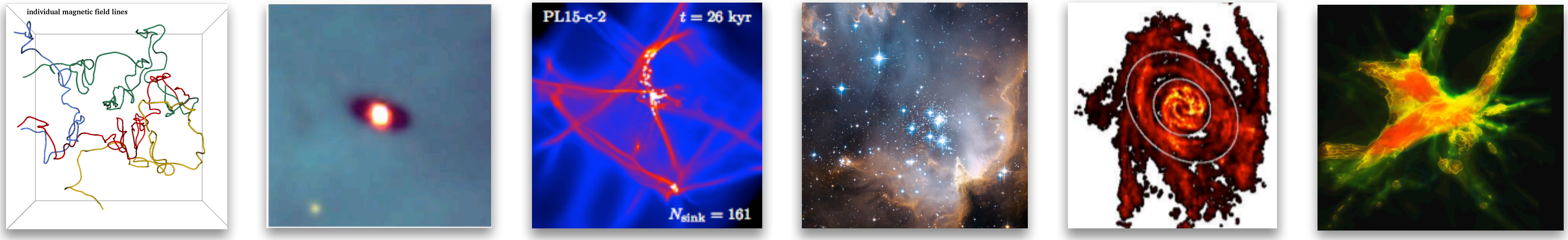

Ralf Klessen

Universität Heidelberg, Zentrum für Astronomie
Institut für Theoretische Astrophysik

thanks to ...

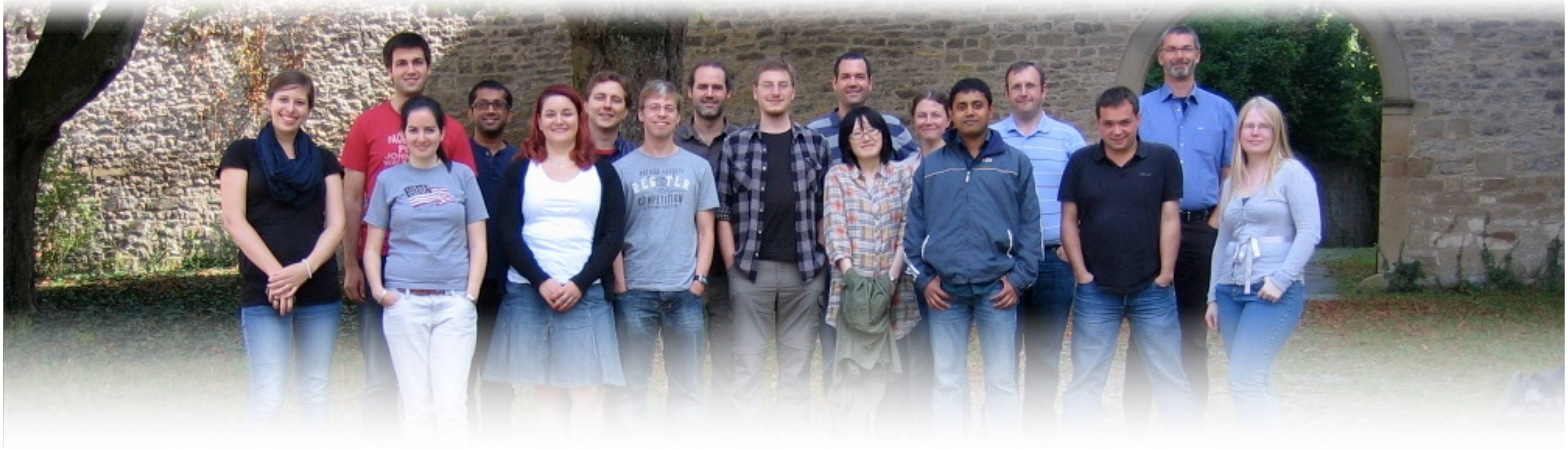

... people in the group in Heidelberg:

Christian Baczynski, Erik Bertram, Frank Bigiel, Rachel Chicharro, Roxana Chira, Paul Clark, Gustavo Dopcke, Jayanta Dutta, Volker Gaibler, Simon Glover, Lukas Konstandin, Faviola Molina, Mei Sasaki, Jennifer Schober, Rahul Shetty, Rowan Smith, László Szűcs, Svitlana Zhukovska

... former group members:

Robi Banerjee, Ingo Berentzen, Christoph Federrath, Philipp Girichidis, Thomas Greif, Milica Micic, Thomas Peters, Dominik Schleicher, Stefan Schmeja, Sharanya Sur

... many collaborators abroad!

Deutsche
Forschungsgemeinschaft
DFG

BADEN-
WÜRTTEMBERG
STIFTUNG
Wir stiften Zukunft

HGSFP

IMPRS

Disclaimer

- I try to cover the field as broadly as possible, however, there will clearly be a bias towards my personal interests and many examples will be from my own work.

Schedule

- Formation of molecular clouds
- Origin and statistical characteristics of ISM turbulence and introduction to star (cluster) formation
- Stellar initial mass function

Literature

- Books
  - Stahler, S., & Palla, F., 2004, "The Formation of Stars" (Weinheim: Wiley-VCH)
  - Osterbrock, D., & Farland, G., 2006, "Astrophysics of Gaseous Nebulae & Active Galactic Nuclei, 2nd ed. (Sausalito: Univ. Science Books)
  - Bodenheimer, P. 2012, "Principles of Star Formation" (Springer Verlag)
  - Draine, B. 2011, "Physics of the Interstellar and Intergalactic Medium" (Princeton Series in Astrophysics)

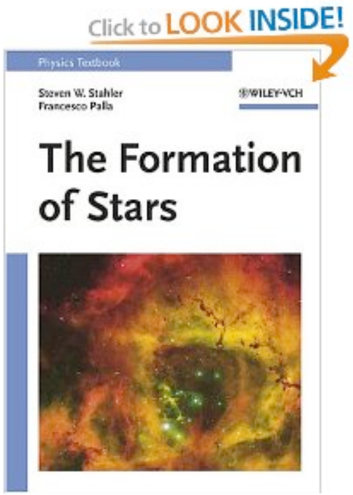
Click to LOOK INSIDE!

Physics Textbook

Steven W. Stahler
Francesco Palla

WILEY-VCH

The Formation of Stars

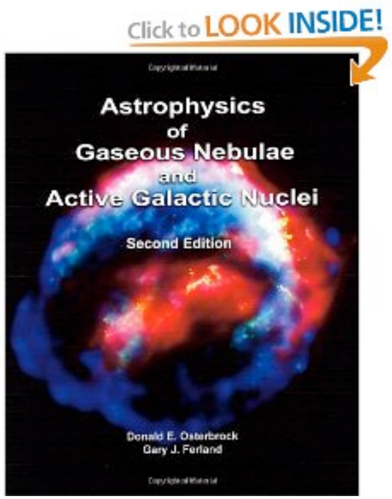
Click to LOOK INSIDE!

Astrophysics
of
Gaseous Nebulae
and
Active Galactic Nuclei

Second Edition

Donald E. Osterbrock
Gary J. Ferland

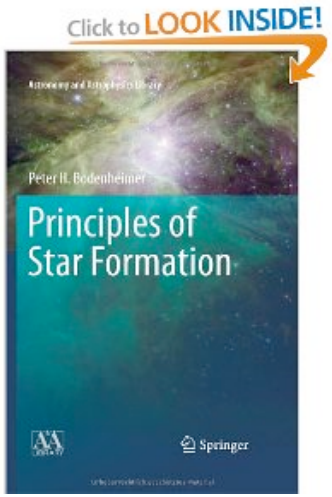
Click to LOOK INSIDE!

Peter H. Bodenheimer

Principles of
Star Formation

Springer

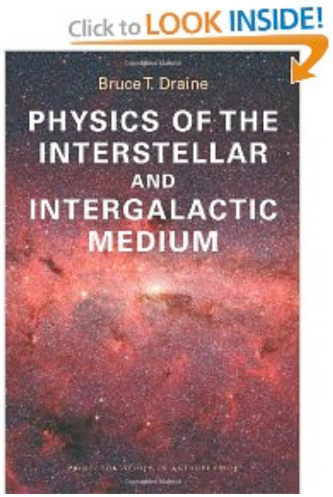
Click to LOOK INSIDE!

Bruce T. Draine

PHYSICS OF THE
INTERSTELLAR
AND
INTERGALACTIC
MEDIUM

- Books
  - Stahler, S., & Palla, F., 2004, "The Formation of Stars" (Weinheim: Wiley-VCH)
  - Osterbrock, D., & Farland, G., 2006, "Astrophysics of Gaseous Nebulae & Active Galactic Nuclei, 2nd ed. (Sausalito: Univ. Science Books)
  - Bodenheimer, P. 2012, "Principles of Star Formation" (Springer Verlag)
  - Draine, B. 2011, "Physics of the Interstellar and Intergalactic Medium" (Princeton Series in Astrophysics)

Literature

- Review Articles
  - Mac Low, M.-M., Klessen, R.S., 2004, "The control of star formation by supersonic turbulence", Rev. Mod. Phys., 76, 125 - 194
  - Zinnecker, H., Yorke, McKee, C.F., Ostriker, E.C., 2008, "Toward Understanding Massive Star Formation", ARA&A, 45, 481 - 563
  - McKee, C.F., Ostriker, E.C., 2008, "Theory of Star Formation", ARA&A, 45, 565 - 687
  - Bromm, V., Larson, R.B., 2004, "The first stars", ARA&A, 42, 79 - 118

inventory of Galactic disc component

- **stellar disc**
  - thin disc (80% of mass): stars of all ages 0-12Gyr
  - thick disc (5% of mass): older stars with lower metallicity
- **interstellar medium (ISM)**
  - gas (15% of mass): hot, warm, and cool component (atomic and molecular)
  - dust (<1% of gas mass): well mixed with the cool gas
  - cosmic rays: relativistic particles
  - magnetic fields: frozen to the gas (field lines are co-moving with the gas); energy density comparable to the kinetic energy of gas

Interstellar Matter: ISM

Abundances, scaled to 1.000.000 H atoms

element		atomic number	abundance
hydrogen	H	1	1.000.000
deuterium	$_1H^2$	1	16
helium	He	2	68.000
carbon	C	6	420
nitrogen	N	7	90
oxygen	O	8	700
neon	Ne	10	100
sodium	Na	11	2
magnesium	Mg	12	40
aluminium	Al	13	3
silicium	Si	14	38
sulfur	S	16	20
calcium	Ca	20	2
iron	Fe	26	34
nickel	Ni	28	2

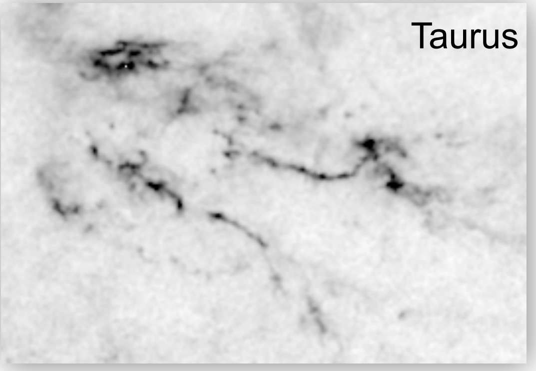

hydrogen is by far the most abundant element (more than 90% in number).

Phases of the ISM

Because hydrogen is the dominating element, the classification scheme is based on its chemical state:

ionized atomic hydrogeN	*HII* (H^+)
neutraler atomic hydrogen	*HI* (H)
molecular hydrogen	H_2

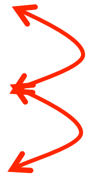

ionization

dissociation

different regions consist of almost 100% of the appropriate phase, the transition regions between HII, H and H_2 are very thin.

star formation always takes place in dense and cold molecular clouds.

Phases of the ISM

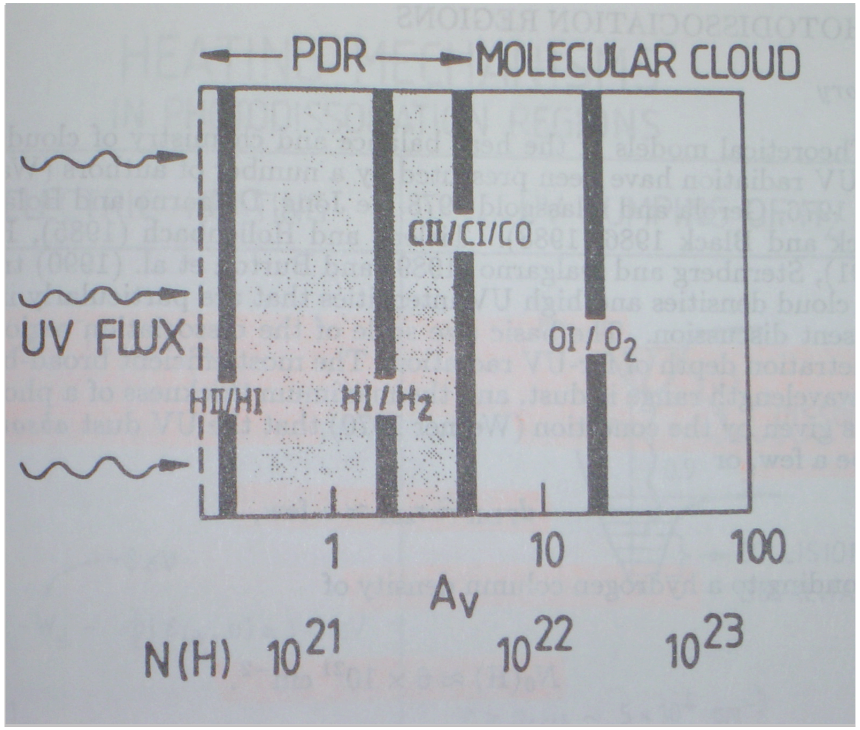

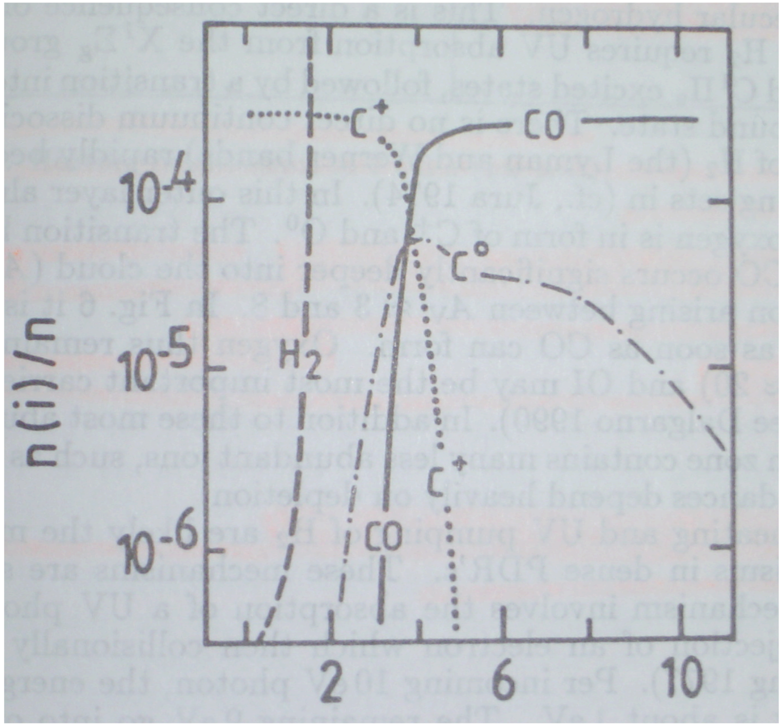

A_V

HII ⟷ **HI** ⟷ **H_2** ⟶

density / column density increases ⟶

A_V denotes the extinction, the attenuation of radiation due to absorption (mostly on dust grains)

Life-cycle of ISM

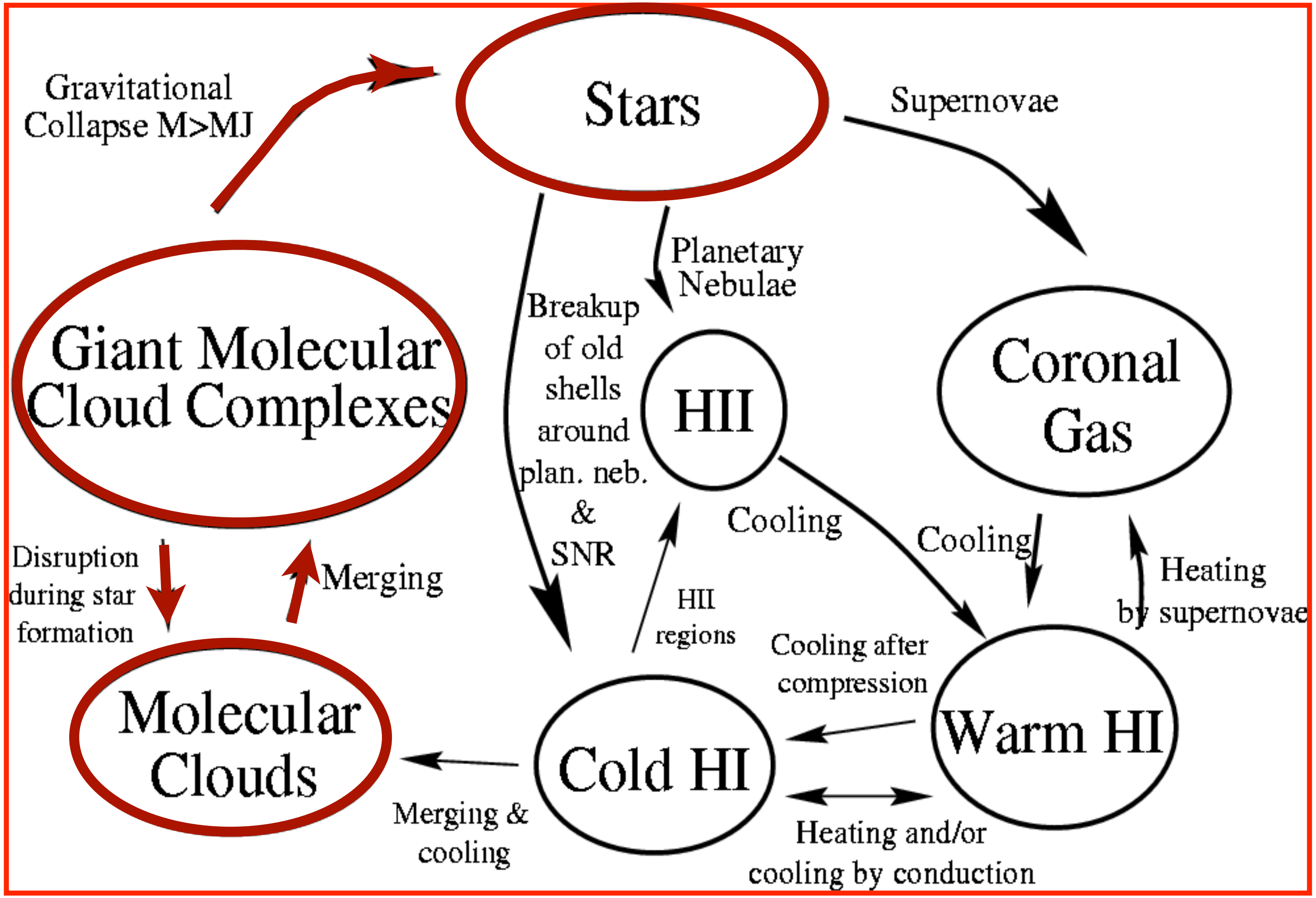

Data from Thomas Dame, CfA Harvard

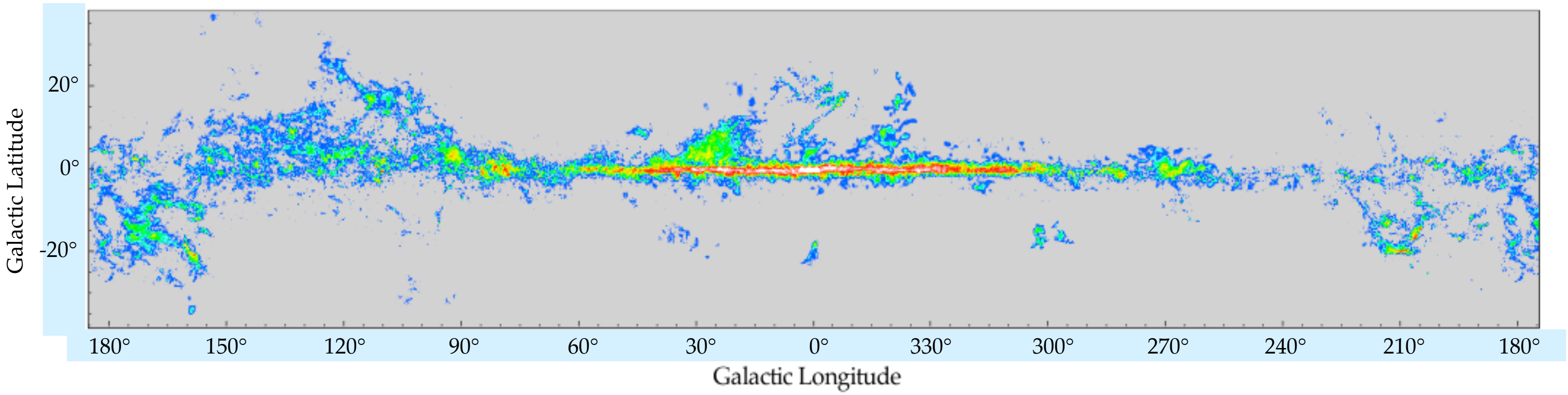

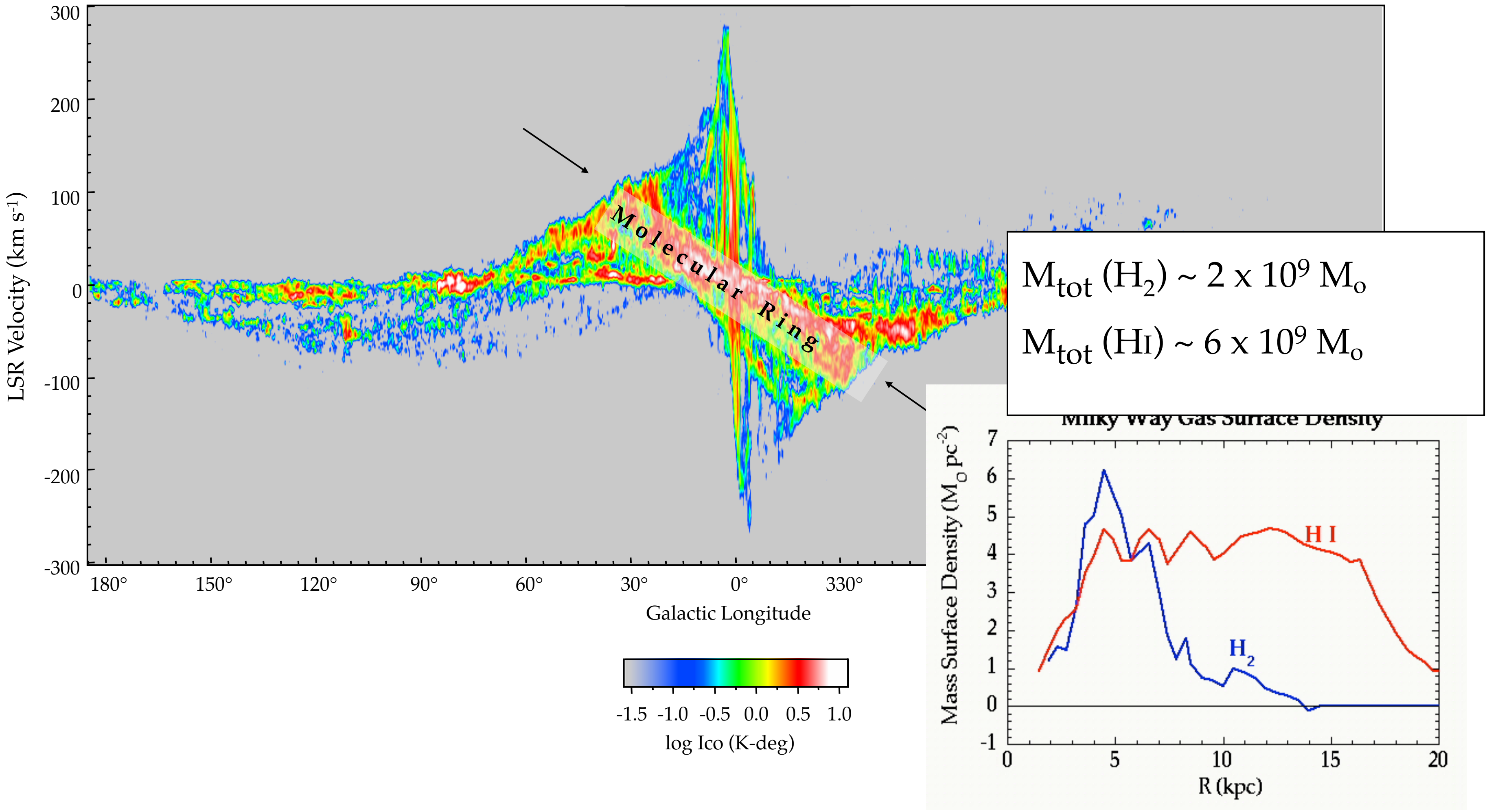

M_{tot} (H_2) ~ 2 x 10^9 M_o

M_{tot} (HI) ~ 6 x 10^9 M_o

Predicted $N(H_2)$ (“IRAS - H I”)

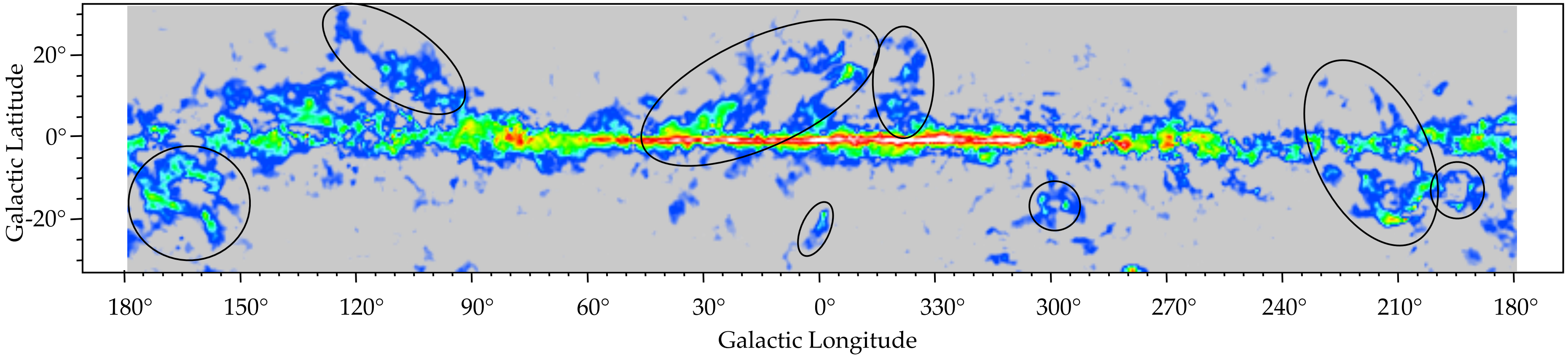

Observed Velocity-Integrated CO

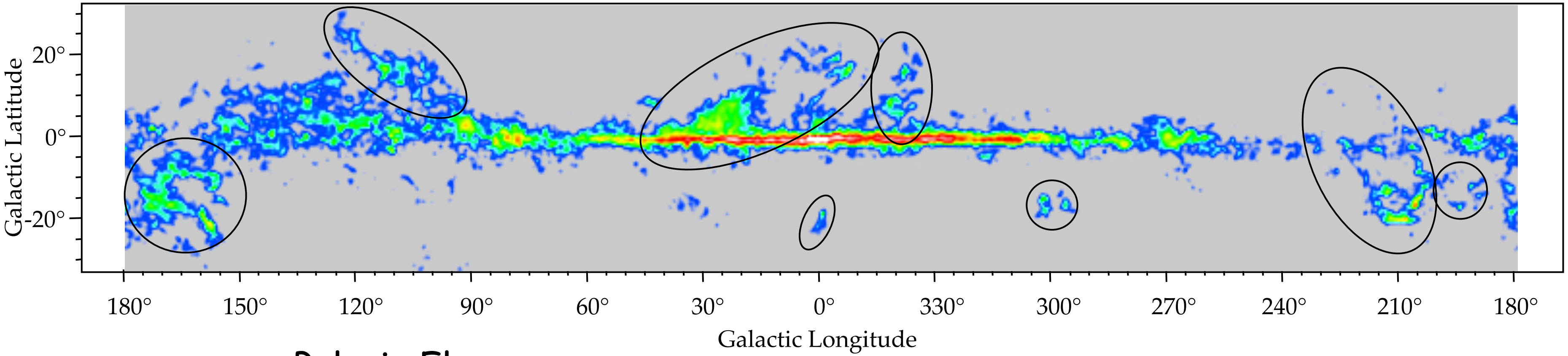

Polaris Flare
Cepheus

Ophiuchus | Lupus

Orion

Taurus

λ-Ori

RCrA

Chamaeleon

ata from Thomas Dame, CfA Harvard

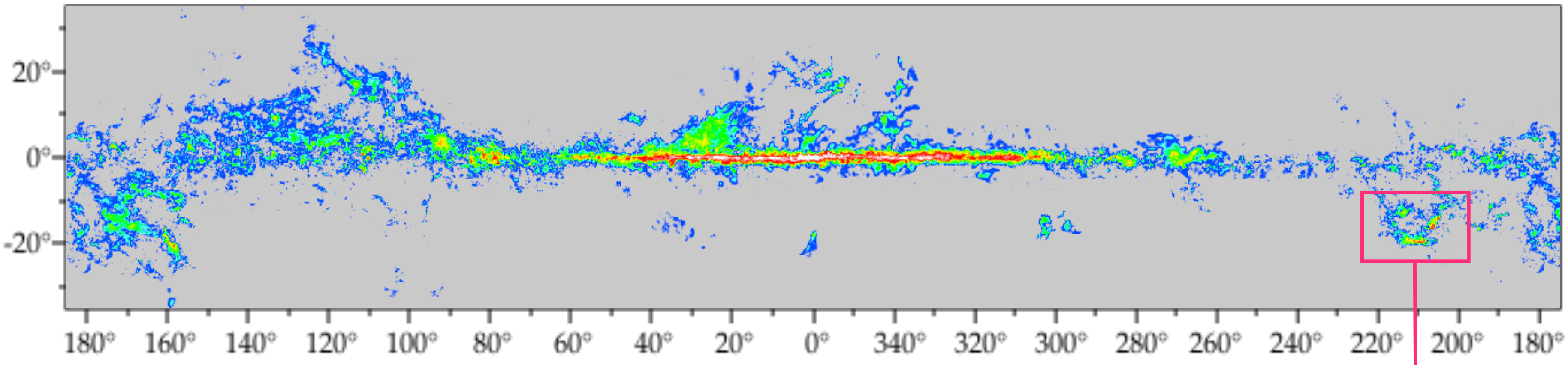

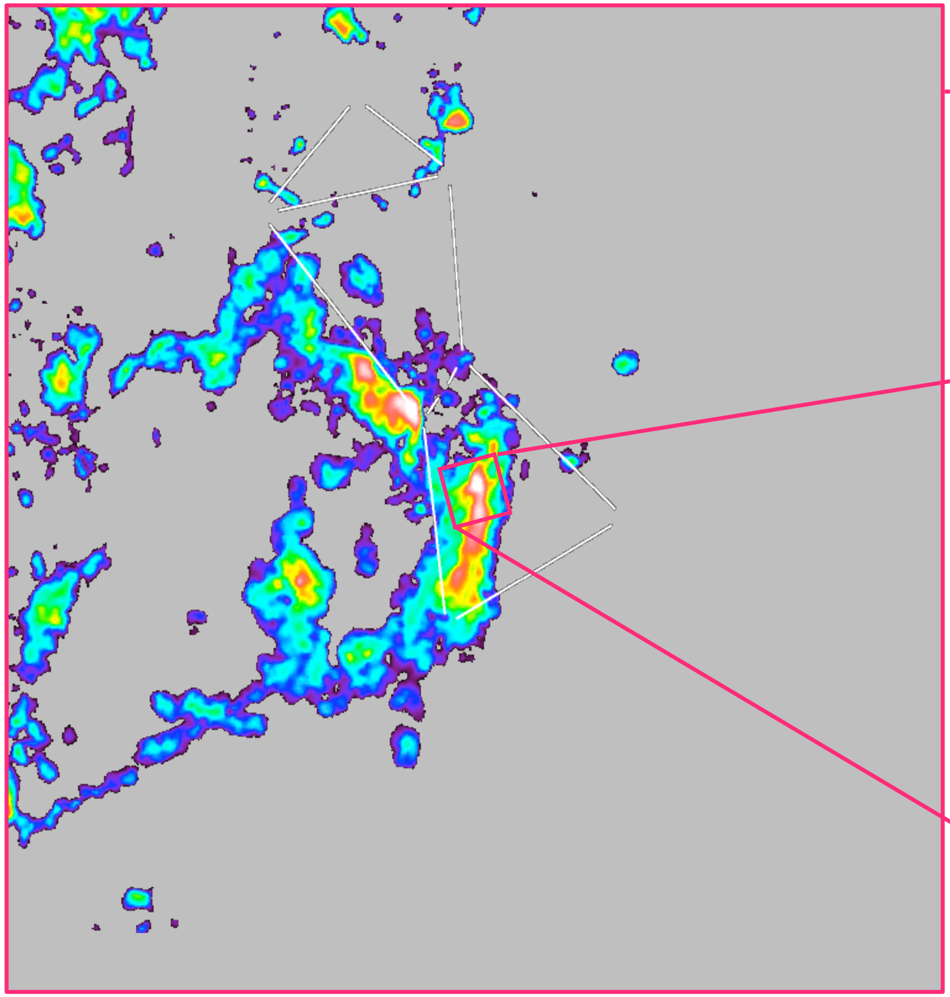

data from T. Dame (CfA Harvard)

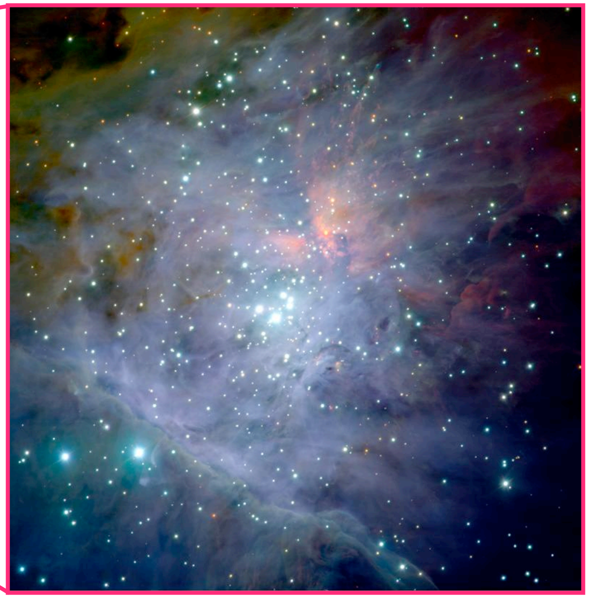

Orion Nebula Cluster (ESO, VLT, M. McCaughrean)

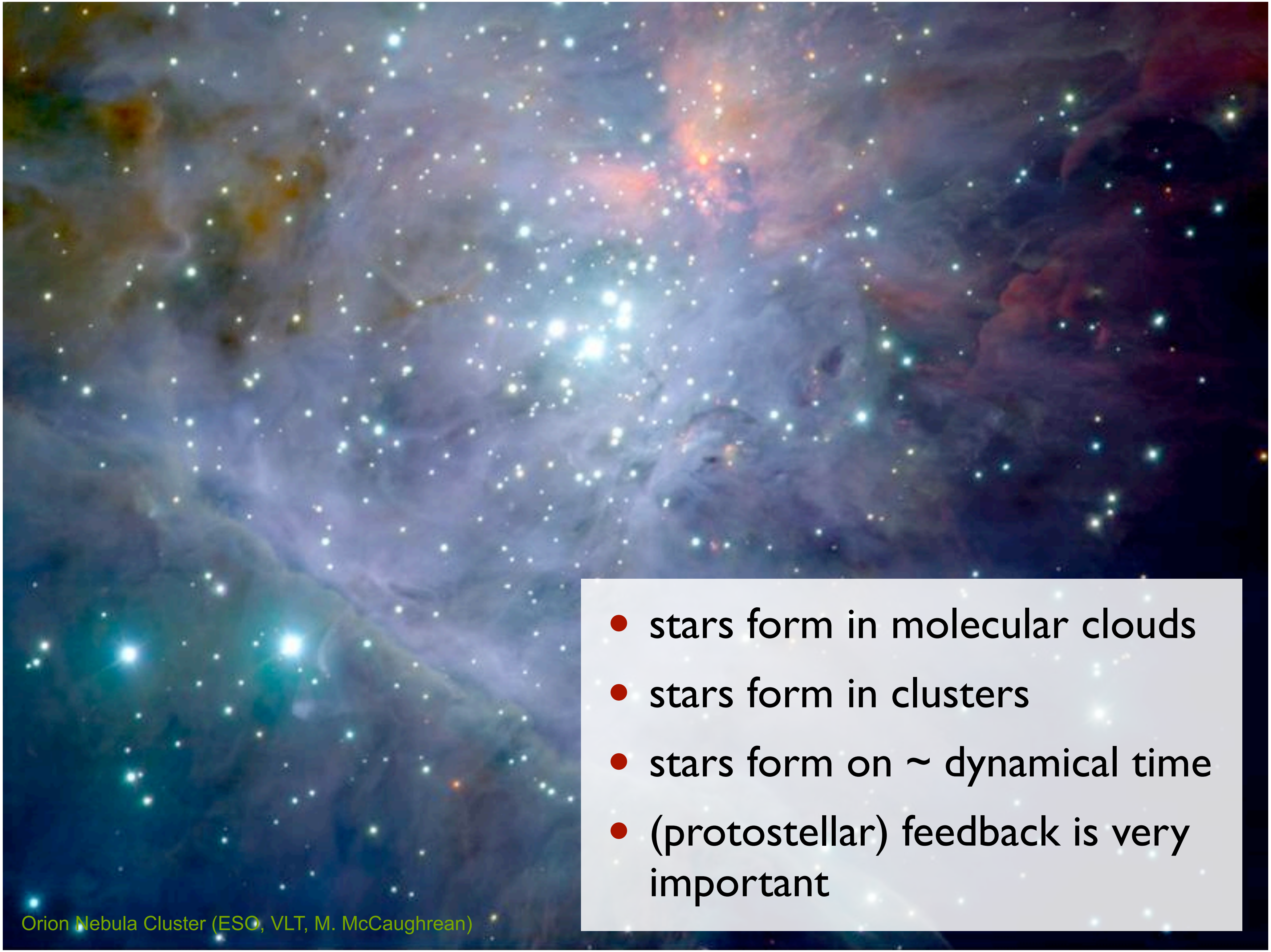

Orion Nebula Cluster (ESO, VLT, M. McCaughrean)

- stars form in molecular clouds
- stars form in clusters
- stars form on ~ dynamical time
- (protostellar) feedback is very important

- strong feedback: UV radiation from Θ1C Orionis affects star formation on all cluster scales

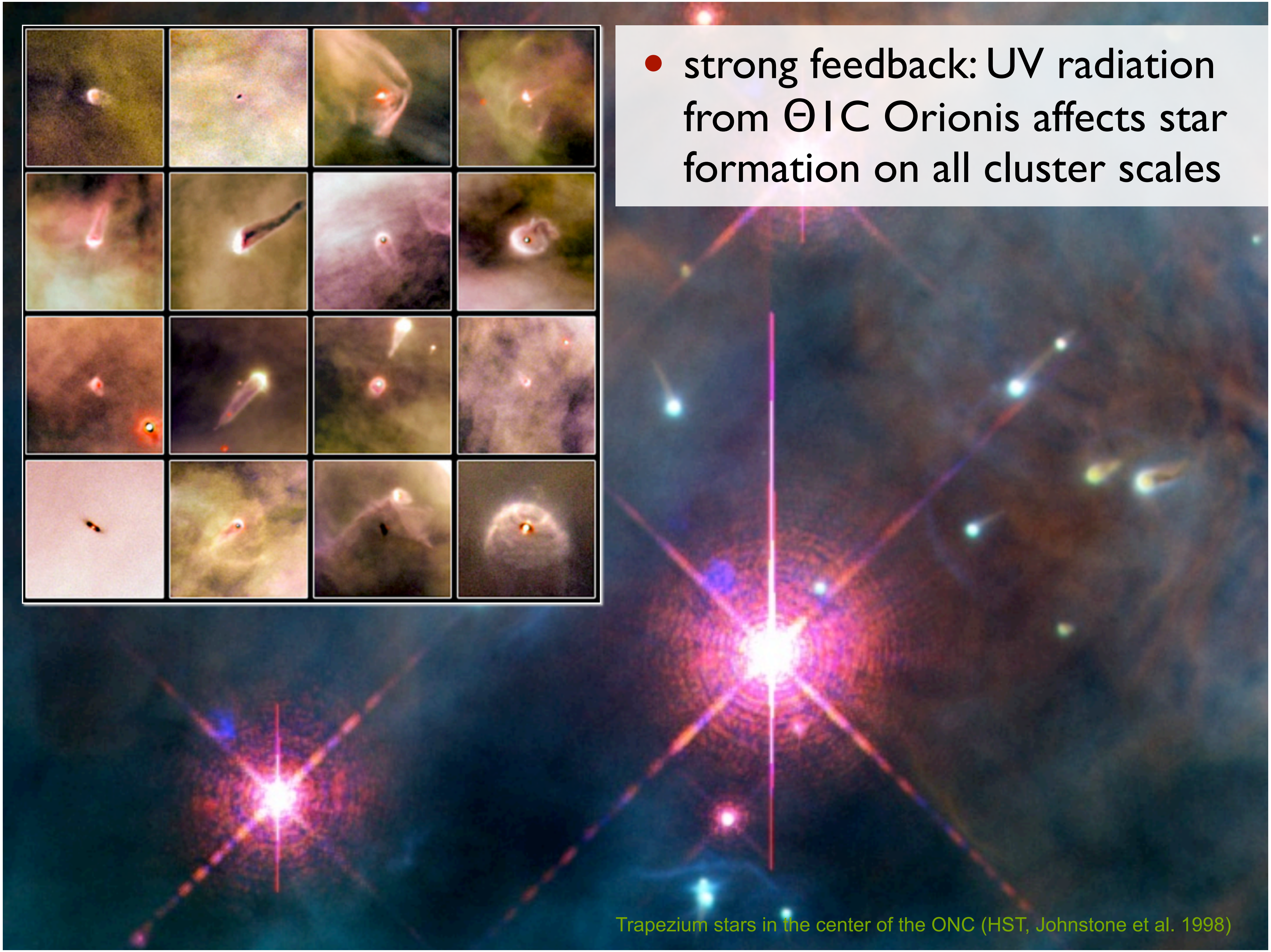

Trapezium stars in the center of the ONC (HST, Johnstone et al. 1998)

eventually, clusters like the ONC (1 Myr) will evolve into clusters like the Pleiades (100 Myr)

Pleiades (DSS, Palomar Observatory Sky Survey)

nearby molecular clouds

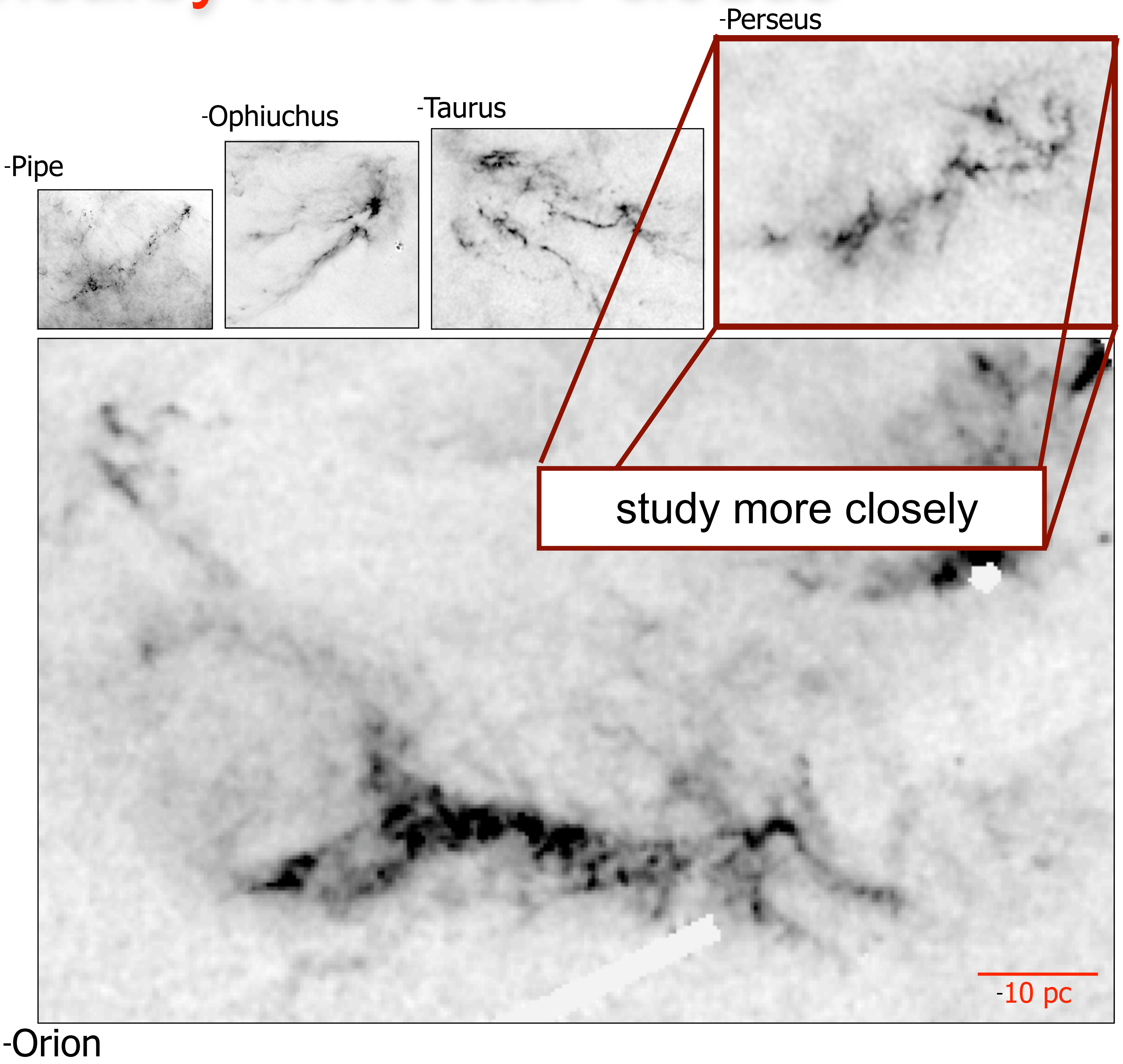

study more closely

scales to same scale

(from A. Goodman)

what drives ISM turbulence?

- seems to be driven on large scales, little difference between star-forming and non-SF clouds
  ---> rules out internal sources
- proposals in the literature
  - supernovae
  - expanding HII regions / stellar winds / outflows
  - spiral density waves
  - magneto-rotational instability
  - more recent idea: accretion onto disk

what drives ISM turbulence?

some energetic arguments...

energy decay by turbulent dissipation:

$$\dot{e} \simeq -(1/2)\rho v_{\rm rms}^3 / L_{\rm d}$$

$$= -(3 \times 10^{-27}\ {\rm erg\,cm^{-3}\,s^{-1}}) \left(\frac{n}{1\ {\rm cm^{-3}}} \right)$$

$$\times \left(\frac{v_{\rm rms}}{10\ {\rm km\,s^{-1}}} \right)^3 \left(\frac{L_{\rm d}}{100\ {\rm pc}} \right)^{-1},$$

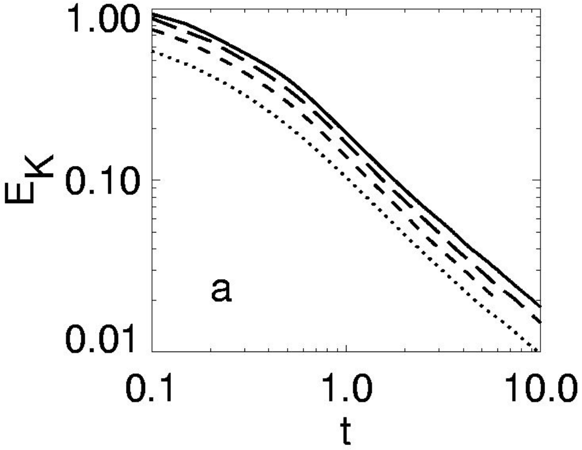

(Mac Low et al. 1999)

decay timescale:

$$\tau_{\rm d} = e/\dot{e} \simeq L_{\rm d}/v_{\rm rms}$$

$$= (9.8\ {\rm Myr}) \left(\frac{L_{\rm d}}{100\ {\rm pc}} \right) \left(\frac{v_{\rm rms}}{10\ {\rm km\,s^{-1}}} \right)^{-1},$$

(from Mac Low & Klessen, 2004)

what drives ISM turbulence?

magneto-rotational instability:

$$\dot{e} = (3 \times 10^{-29}\ \mathrm{erg\,cm^{-3}\,s^{-1}}) \left(\frac{B}{3\,\mu\mathrm{G}}\right)^2 \left(\frac{\Omega}{(220\ \mathrm{Myr})^{-1}}\right).$$

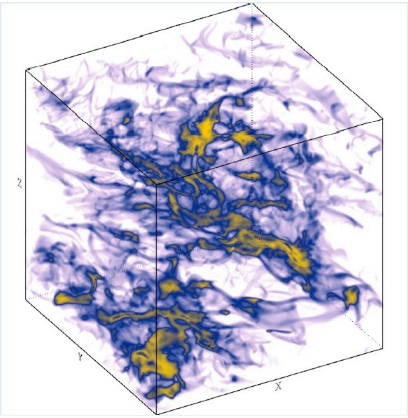

(from Piotek & Ostriker 2005)

gravitational instability (spiral waves)

$$\begin{aligned}\dot{e} &\simeq G(\Sigma_g/H)^2 \lambda^2 \Omega \\ &\simeq (4 \times 10^{-29}\ \mathrm{erg\,cm^{-3}\,s^{-1}}) \\ &\quad \times \left(\frac{\Sigma_g}{10 M_\odot\ \mathrm{pc}^{-2}}\right)^2 \left(\frac{H}{100\ \mathrm{pc}}\right)^{-2} \\ &\quad \times \left(\frac{\lambda}{100\ \mathrm{pc}}\right)^2 \left(\frac{\Omega}{(220\ \mathrm{Myr})^{-1}}\right),\end{aligned}$$

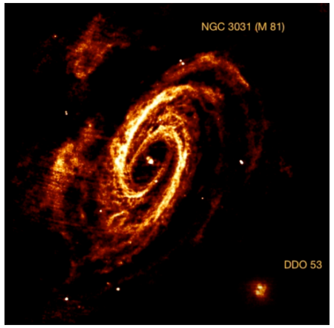

(from Walter et al. 2008)

(from Mac Low & Klessen, 2004)

what drives ISM turbulence?

protostellar outflows

$$\dot{e} = \frac{1}{2} f_{\rm w} \eta_{\rm w} \frac{\dot{\Sigma}_*}{H} v_{\rm w}^2$$

$$\simeq (2\times10^{\boxed{-28}}\ \text{erg cm}^{-3}\ \text{s}^{-1}) \left(\frac{H}{200\ \text{pc}}\right)^{-1} \left(\frac{f_{\rm w}}{0.4}\right)$$

$$\times \left(\frac{v_{\rm w}}{200\ \text{km s}^{-1}}\right) \left(\frac{v_{\rm rms}}{10\ \text{km s}^{-1}}\right)$$

$$\times \left(\frac{\dot{\Sigma}_*}{4.5\times10^{-9} M_\odot\ \text{pc}^{-2}\ \text{yr}^{-1}}\right),$$

(Li & Nakamura 2006, Wang et al. 2010 vs.
Banerjee et al. 2008)

expanding HII regions

$$\dot{e} = \frac{\langle \delta p \rangle \mathcal{N}(>1) v_i}{V t_i}$$

$$= (3\times10^{\boxed{-30}}\ \text{erg s} \qquad ^{-3})$$

$$\times \left(\frac{N_{\rm H}}{1.5\times10^{22}\ \text{cm}^{-2}}\right)^{-3/14} \left(\frac{M_{cl}}{10^6 M_\odot}\right)^{1/14}$$

$$\times \left(\frac{\langle M_* \rangle}{440 M_\odot}\right) \left(\frac{\mathcal{N}(>1)}{650}\right) \left(\frac{v_i}{10\ \text{km s}^{-1}}\right)$$

$$\times \left(\frac{H_c}{100\ \text{pc}}\right)^{-1} \left(\frac{R_{sf}}{15\ \text{kpc}}\right)^{-2} \left(\frac{t_i}{18.5\ \text{Myr}}\right)^{-1}$$

(note: different numbers by Matzner 2002)

(from Mac Low & Klessen, 2004)

what drives ISM turbulence?

supernovae

$$\dot{e} = \frac{\sigma_{SN}\eta_{SN}E_{SN}}{\pi R_{sf}^2 H_c}$$

$$= (3\times 10^{\enclose{circle}{-26}}\ \mathrm{erg\ s^{-1}\ cm^{-3}})\left(\frac{\eta_{SN}}{0.1}\right)\left(\frac{\sigma_{SN}}{1\ \ \mathrm{SNu}}\right)$$

$$\times\left(\frac{H_c}{100\ \ \mathrm{pc}}\right)^{-1}\left(\frac{R_{sf}}{15\ \ \mathrm{kpc}}\right)^{-2}\left(\frac{E_{SN}}{10^{51}\ \ \mathrm{erg}}\right).$$

in star-forming parts of the disk, clearly SN provide enough energy to compensate for the decay of ISM turbulence.

BUT: what is outside the disk?

(from Mac Low & Klessen, 2004)

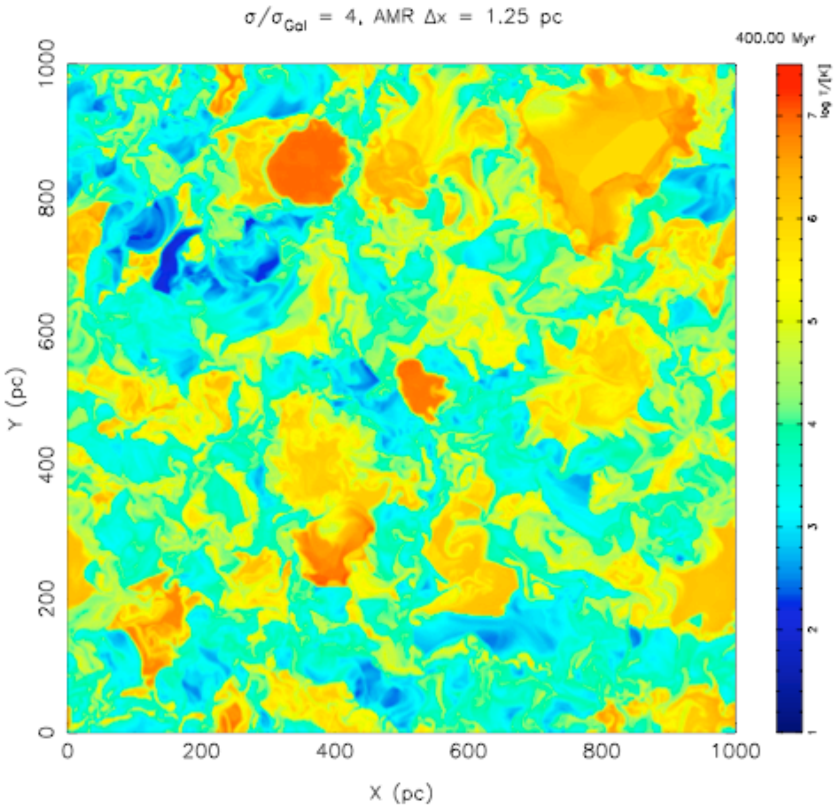

(distribution of temperature in SN driven disk turbulence, by de Avillez & Breitschwerdt 2004)

accretion driven turbulence

- yet another thought:
  - astrophysical objects *form* by *accretion* of ambient material
  - the *kinetic energy* associated with this process is a key agent *driving internal turbulence*.
  - this works on *ALL* scales:
    - galaxies
    - molecular clouds
    - protostellar accretion disks

Klessen & Hennebelle (2010, A&A)

concept

- turbulence decays on a crossing time

$$\tau_\mathrm{d} \approx \frac{L_\mathrm{d}}{\sigma}$$

- energy decay rate

$$\dot{E}_\mathrm{decay} \approx \frac{E}{\tau_\mathrm{d}} = -\frac{1}{2}\frac{M\sigma^3}{L_\mathrm{d}}$$

- kinetic energy of infalling material

$$\dot{E}_\mathrm{in} = \frac{1}{2}\dot{M}_\mathrm{in}v_\mathrm{in}^2$$

- can both values match, modulo some efficiency?

$$\epsilon = \left|\frac{\dot{E}_\mathrm{decay}}{\dot{E}_\mathrm{in}}\right|$$

(Field et al.. 2008, MNRAS, 385, 181, Mac Low & Klessen 2004, RMP, 76, 125)

some estimates from convergent flow studies

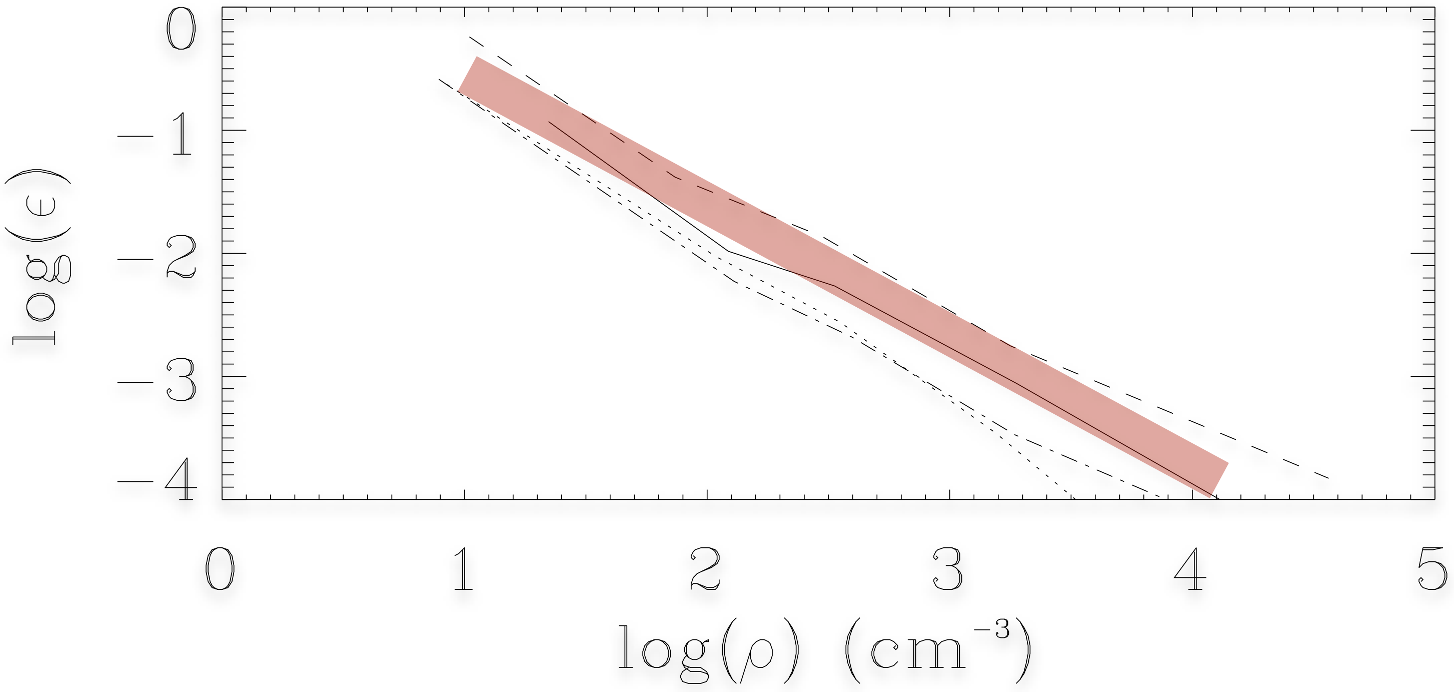

Klessen & Hennebelle (2010)

application to galaxies

- underlying assumption
  - galaxy is in steady state
    ---> accretion rate equals star formation rate
  - what is the required efficiency for the method to work?
- study Milky Way and 11 THINGS
  - excellent observational data in HI:
    velocity dispersion, column density, rotation curve

11 THINGS galaxies

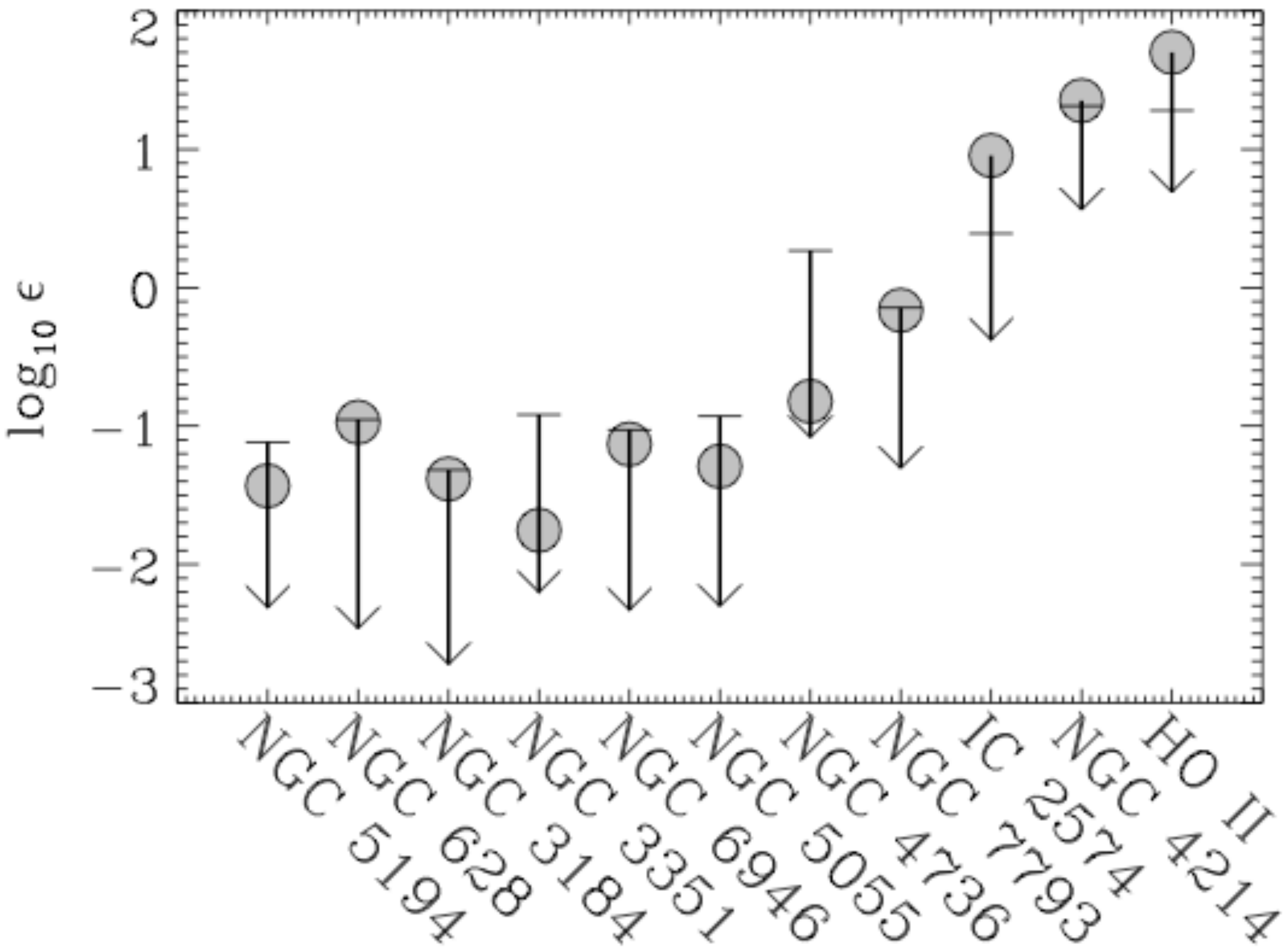

some further thoughts

- method works for Milky Way type galaxies:
  - required efficiencies are ~1% only!
- relevant for outer disks (extended HI disks)
  - there are not other sources of turbulence (certainly not stellar sources, maybe MRI)
- works well for molecular clouds
  - example clouds in the LMC (Fukui et al.)
- potentially interesting for TTS
  - model reproduces dM/dt - M relation (e.g Natta et al. 2006, Muzerolle et al. 2005, Muhanty et al. 2005, Calvet et al. 2004, etc.)

molecular cloud formation

molecular cloud formation

- star formation on galactic scales
  → requires understanding of
  formation of molecular clouds
- questions
  - *where* and *when* do molecular clouds form?
  - *what* are their properties?
  - *how* do stars form in their interior?
  - global correlations? → *Schmidt law*

molecular cloud formation

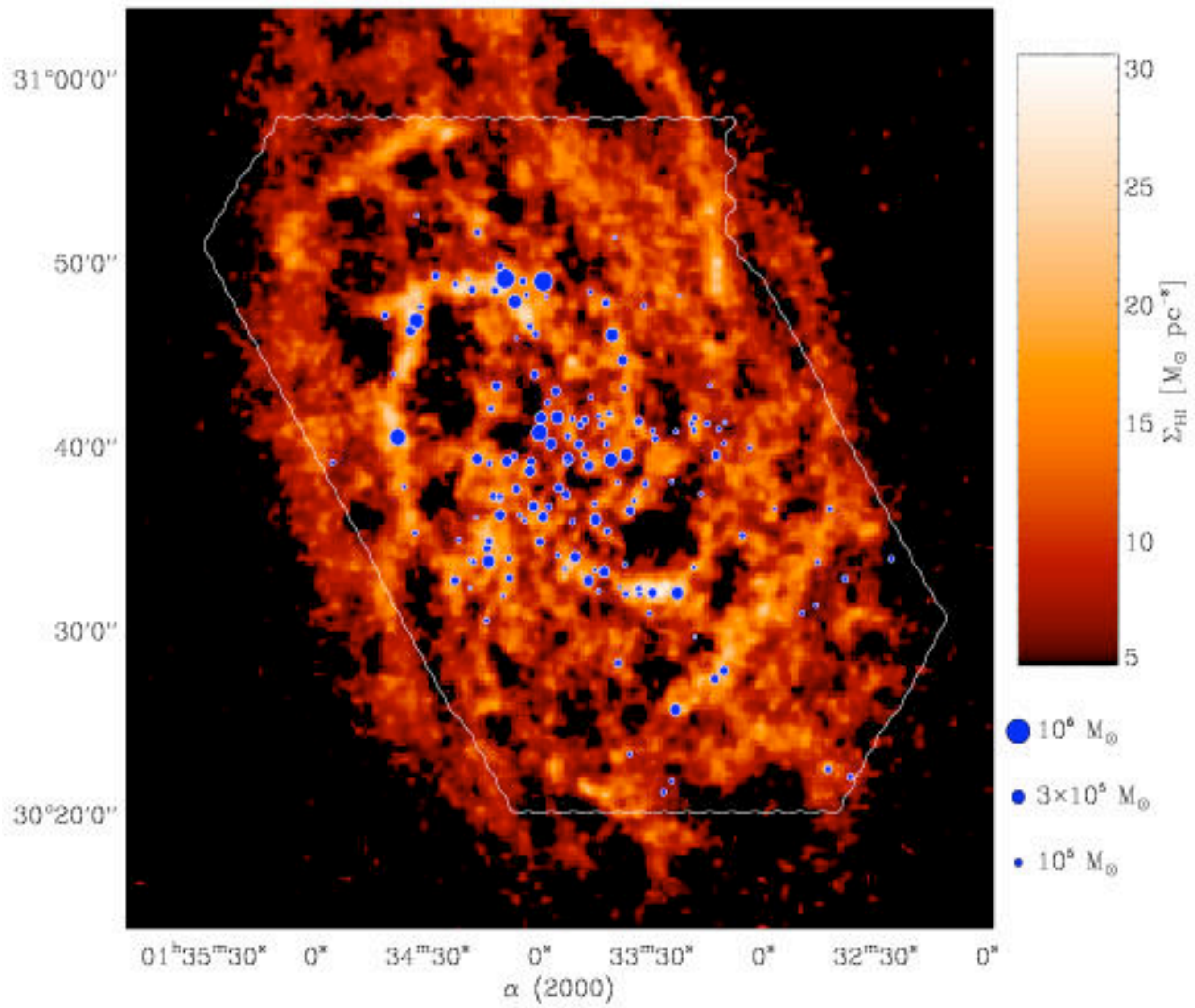

Thesis:

Molecular clouds form at *stagnation points* of large-scale convergent flows, mostly triggered by global (or external) perturbations.

(Deul & van der Hulst 1987, Blitz et al. 2004)

correlation with large-scale perturbations

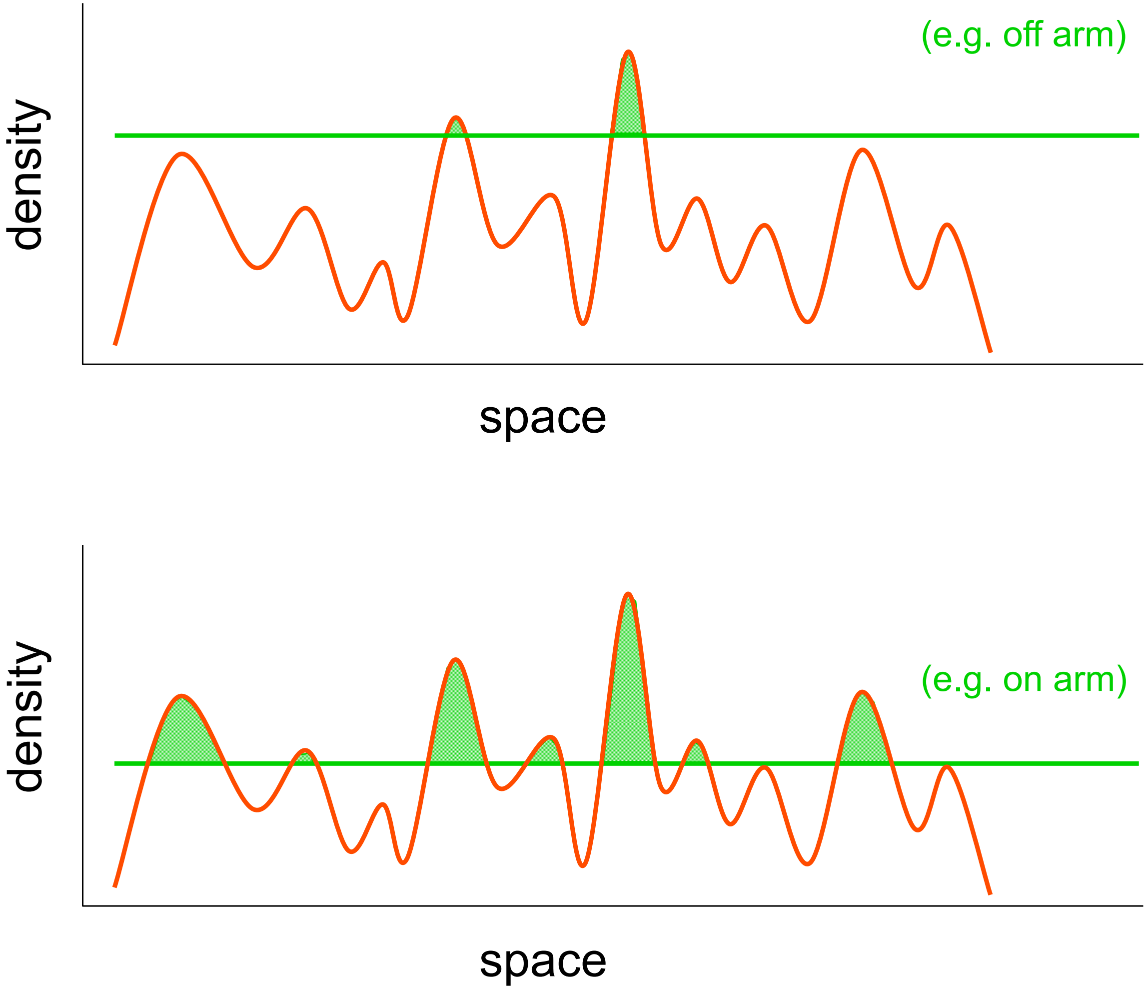

density/temperature fluctuations in warm atomar ISM are caused by *thermal/ gravitational instability* and/ or *supersonic turbulence*

some fluctuations are *dense* enough to *form H_2* within "*reasonable time*"

→ *molecular cloud*

external perturbuations (i.e. potential changes) *increase* likelihood

star formation on *global* scales

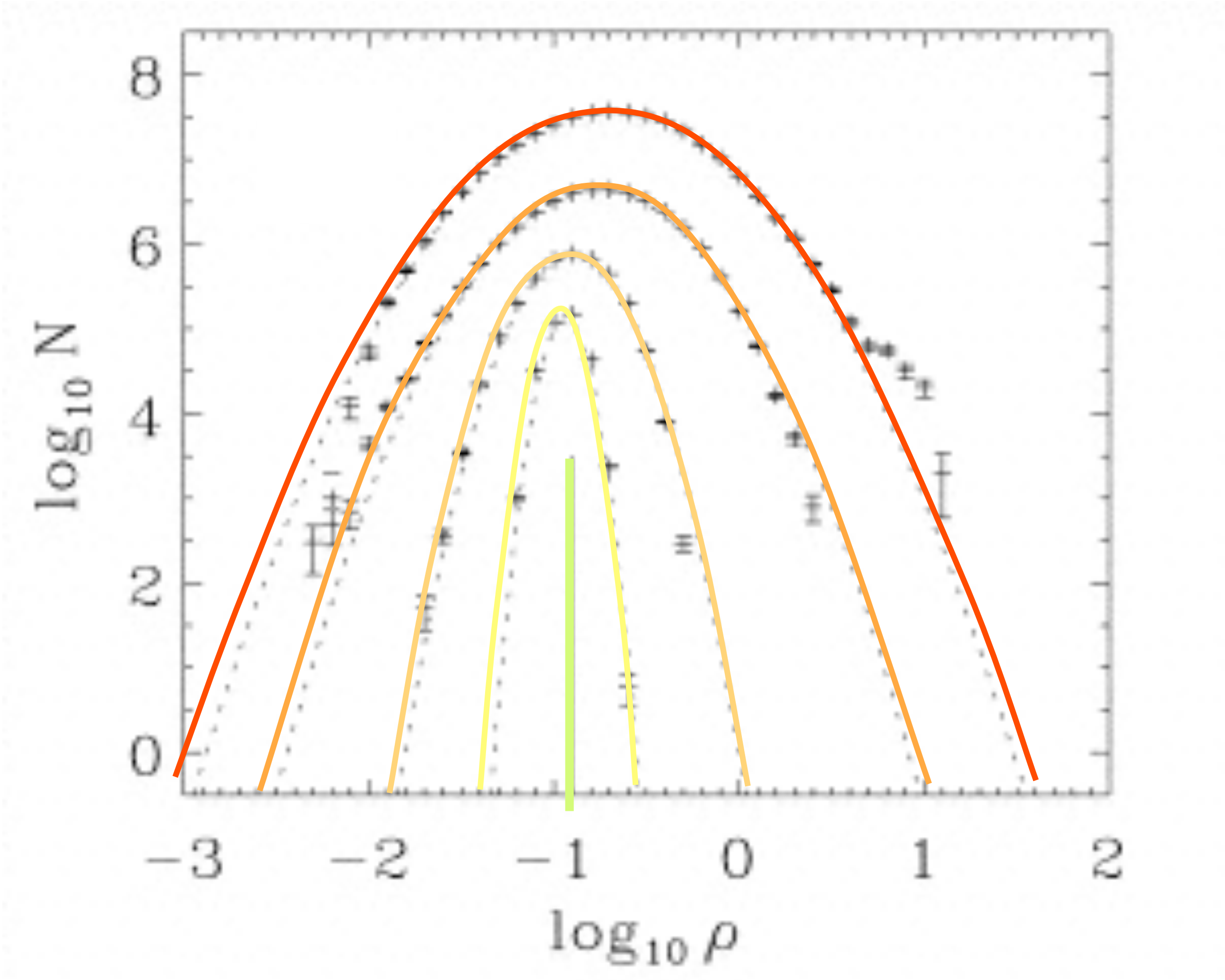

probability distribution function of the density *(ρ-pdf)*

varying rms Mach numbers:

M1 > M2 > M3 > M4 > 0

mass weighted ρ-pdf, each shifted by ΔlogN=1

(from Klessen, 2001; also Gazol et al. 2005, Krumholz & McKee 2005, Glover & Mac Low 2007ab)

star formation on *global* scales

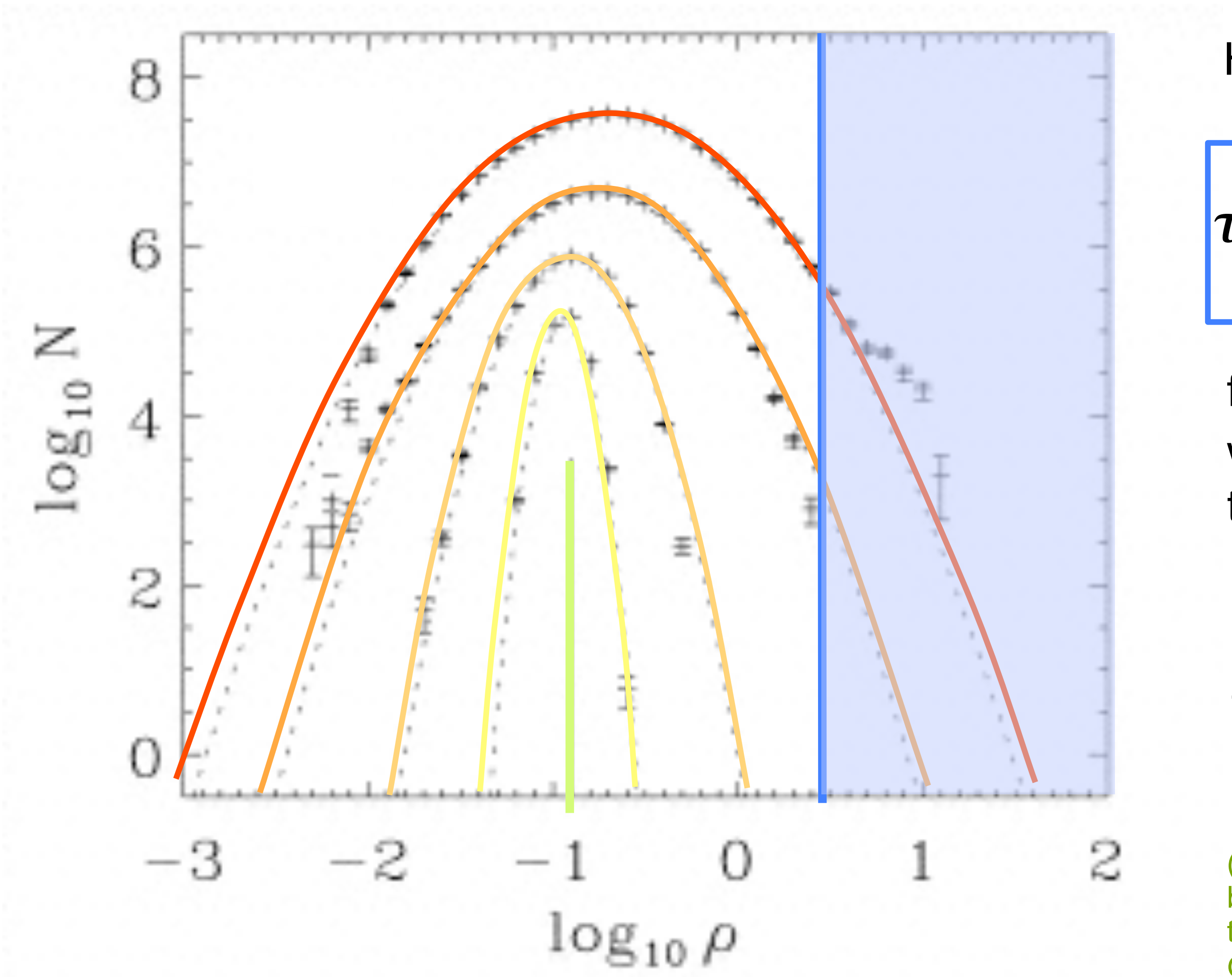

mass weighted ρ-pdf, each shifted by ΔlogN=1

(rate from Hollenback, Werner, & Salpeter 1971)

H_2 formation rate:

$$\boxed{\tau_{H_2} \approx \frac{1.5\,\mathrm{Gyr}}{n_H / 1\mathrm{cm}^{-3}}}$$

for $n_H \geq 100$ cm^{-3}, H_2 forms within 10 Myr, this is about the lifetime of typical MC's.

in turbulent gas, the H_2 fraction can become very high on short timescale

(for models with coupling between cloud dynamics and time-dependent chemistry, see Glover & Mac Low 2007a,b)

star formation on *global* scales

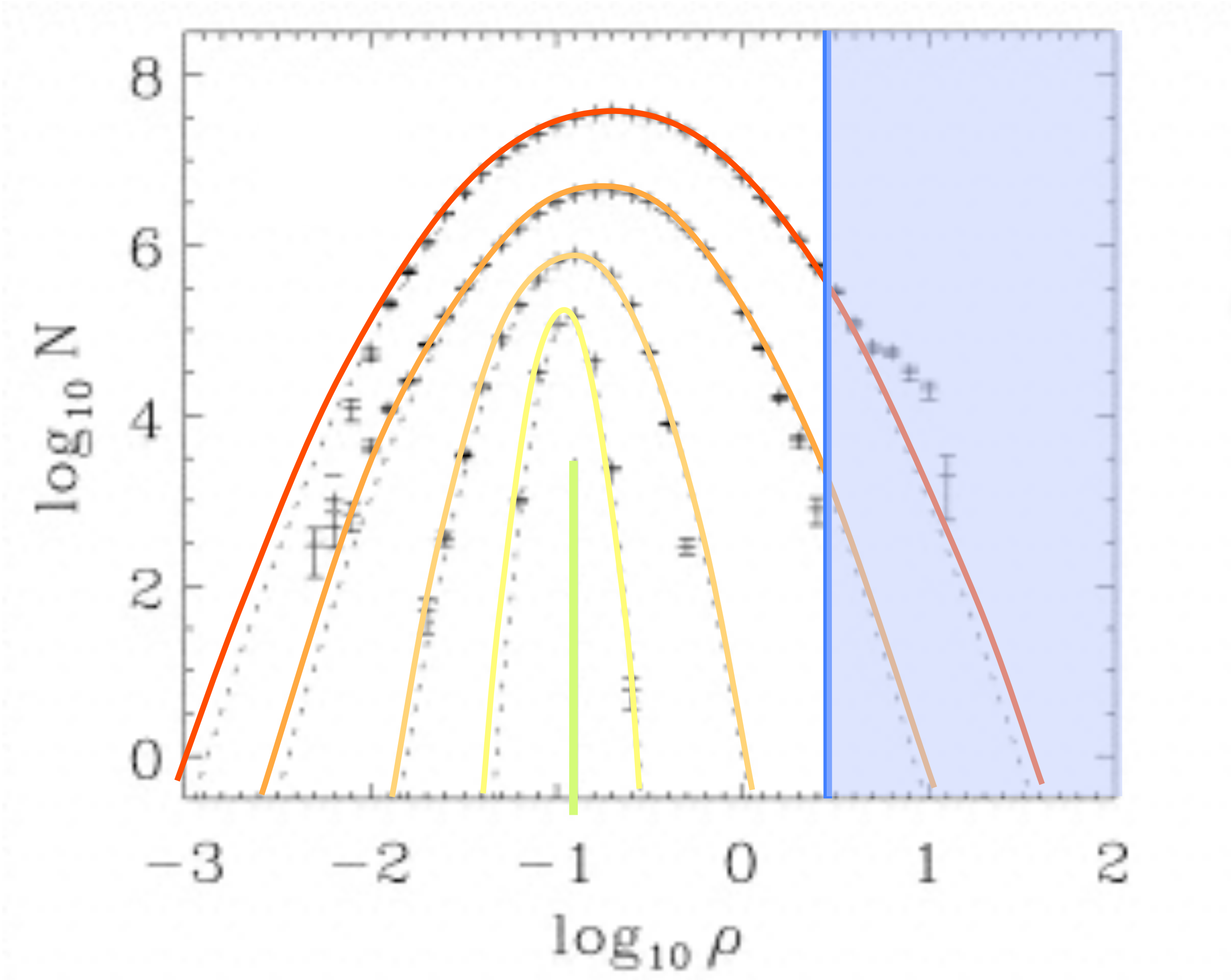

mass weighted ρ-pdf, each shifted by ΔlogN=1

(rate from Hollenback, Werner, & Salpeter 1971)

BUT: *it doesn't work*
(at least not so easy):

Chemistry has a memory effect!

H2 forms more quickly in high-density regions as it gets destroyed in low-density parts.

(for models with coupling between cloud dynamics and time-dependent chemistry, see Glover & Mac Low 2007a,b)

SFR estimates from the PDF

log density PDF:

$$p_s(s) = \frac{1}{\sqrt{2\pi\sigma_s^2}} \exp\left(-\frac{(s-s_0)^2}{2\sigma_s^2}\right)$$

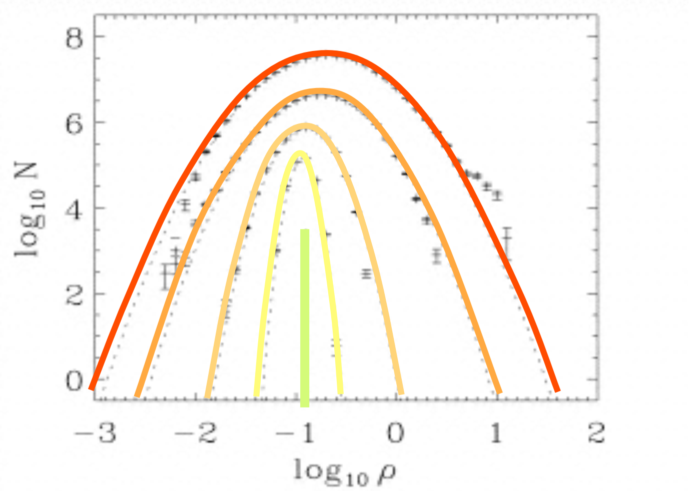

$$s \equiv \ln\left(\rho/\rho_0\right) .$$

log density, normalized to the mean

relation between mean density and turbulent Mach number M and magnetic field strength β:

$$s_0 = -\frac{1}{2}\sigma_s^2$$

$$\sigma_s^2 = \ln\left(1 + b^2\mathcal{M}^2 \frac{\beta}{\beta+1}\right)$$

$$\sigma_s^2 = \ln\left(1 + b^2\mathcal{M}^2 \frac{2\mathcal{M}_\mathrm{A}^2}{\mathcal{M}^2 + 2\mathcal{M}_\mathrm{A}^2}\right)$$

e.g. Padoan & Nordlund 2002, Krumholz & McKee 2005, Hennebelle & Chabrier 2009, Federrath & Klessen 2012, Molina et al. 2012

SFR estimates from the PDF

star formation rate (Msun/yr) in terms of the SF efficiency per free-fall time $\mathrm{SFR}_{\mathrm{ff}}$

$$\mathrm{SFR} \equiv \frac{M_{\mathrm{c}}}{t_{\mathrm{ff}}(\rho_0)}\,\mathrm{SFR}_{\mathrm{ff}}\,.$$

$$\mathrm{SFR}_{\mathrm{ff}} = \frac{\epsilon}{\phi_t}\int_{s_{\mathrm{crit}}}^{\infty}\frac{t_{\mathrm{ff}}(\rho_0)}{t_{\mathrm{ff}}(\rho)}\,\frac{\rho}{\rho_0}\,p(s)\,\mathrm{d}s\,.$$

SF efficiency per free-fall time

$$t_{\mathrm{ff}}(\rho) \equiv \left(\frac{3\pi}{32G\rho}\right)^{1/2}$$

free-fall time

e.g. Padoan & Nordlund 2002, Krumholz & McKee 2005, Hennebelle & Chabrier 2009, Federrath & Klessen 2012

SFR estimates from the PDF

comparison and extension of existing models

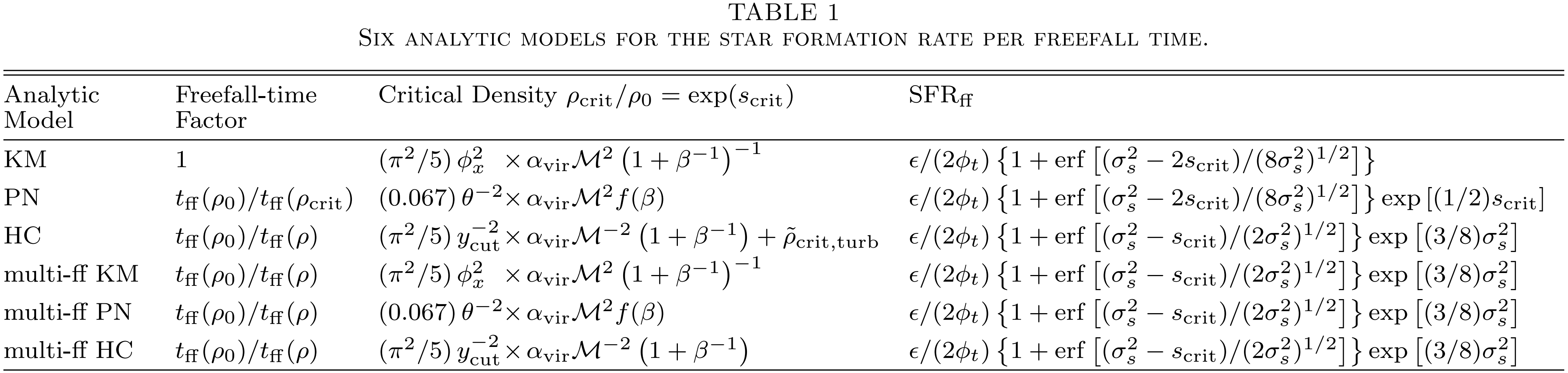

TABLE 1
SIX ANALYTIC MODELS FOR THE STAR FORMATION RATE PER FREEFALL TIME.

Analytic Model	Freefall-time Factor	Critical Density $\rho_{\rm crit}/\rho_0 = \exp(s_{\rm crit})$	$\mathrm{SFR}_{\rm ff}$
KM	1	$(\pi^2/5)\,\phi_x^2 \times \alpha_{\rm vir}\mathcal{M}^2\left(1+\beta^{-1}\right)^{-1}$	$\epsilon/(2\phi_t)\,\left\{1+\mathrm{erf}\left[(\sigma_s^2-2s_{\rm crit})/(8\sigma_s^2)^{1/2}\right]\right\}$
PN	$t_{\rm ff}(\rho_0)/t_{\rm ff}(\rho_{\rm crit})$	$(0.067)\,\theta^{-2}\times\alpha_{\rm vir}\mathcal{M}^2 f(\beta)$	$\epsilon/(2\phi_t)\,\left\{1+\mathrm{erf}\left[(\sigma_s^2-2s_{\rm crit})/(8\sigma_s^2)^{1/2}\right]\right\}\exp\left[(1/2)s_{\rm crit}\right]$
HC	$t_{\rm ff}(\rho_0)/t_{\rm ff}(\rho)$	$(\pi^2/5)\,y_{\rm cut}^{-2}\times\alpha_{\rm vir}\mathcal{M}^{-2}\left(1+\beta^{-1}\right)+\tilde{\rho}_{\rm crit,turb}$	$\epsilon/(2\phi_t)\,\left\{1+\mathrm{erf}\left[(\sigma_s^2-s_{\rm crit})/(2\sigma_s^2)^{1/2}\right]\right\}\exp\left[(3/8)\sigma_s^2\right]$
multi-ff KM	$t_{\rm ff}(\rho_0)/t_{\rm ff}(\rho)$	$(\pi^2/5)\,\phi_x^2 \times \alpha_{\rm vir}\mathcal{M}^2\left(1+\beta^{-1}\right)^{-1}$	$\epsilon/(2\phi_t)\,\left\{1+\mathrm{erf}\left[(\sigma_s^2-s_{\rm crit})/(2\sigma_s^2)^{1/2}\right]\right\}\exp\left[(3/8)\sigma_s^2\right]$
multi-ff PN	$t_{\rm ff}(\rho_0)/t_{\rm ff}(\rho)$	$(0.067)\,\theta^{-2}\times\alpha_{\rm vir}\mathcal{M}^2 f(\beta)$	$\epsilon/(2\phi_t)\,\left\{1+\mathrm{erf}\left[(\sigma_s^2-s_{\rm crit})/(2\sigma_s^2)^{1/2}\right]\right\}\exp\left[(3/8)\sigma_s^2\right]$
multi-ff HC	$t_{\rm ff}(\rho_0)/t_{\rm ff}(\rho)$	$(\pi^2/5)\,y_{\rm cut}^{-2}\times\alpha_{\rm vir}\mathcal{M}^{-2}\left(1+\beta^{-1}\right)$	$\epsilon/(2\phi_t)\,\left\{1+\mathrm{erf}\left[(\sigma_s^2-s_{\rm crit})/(2\sigma_s^2)^{1/2}\right]\right\}\exp\left[(3/8)\sigma_s^2\right]$

Federrath & Klessen 2012

SFR estimates from the PDF

comparison between analytic models and numerical simulations

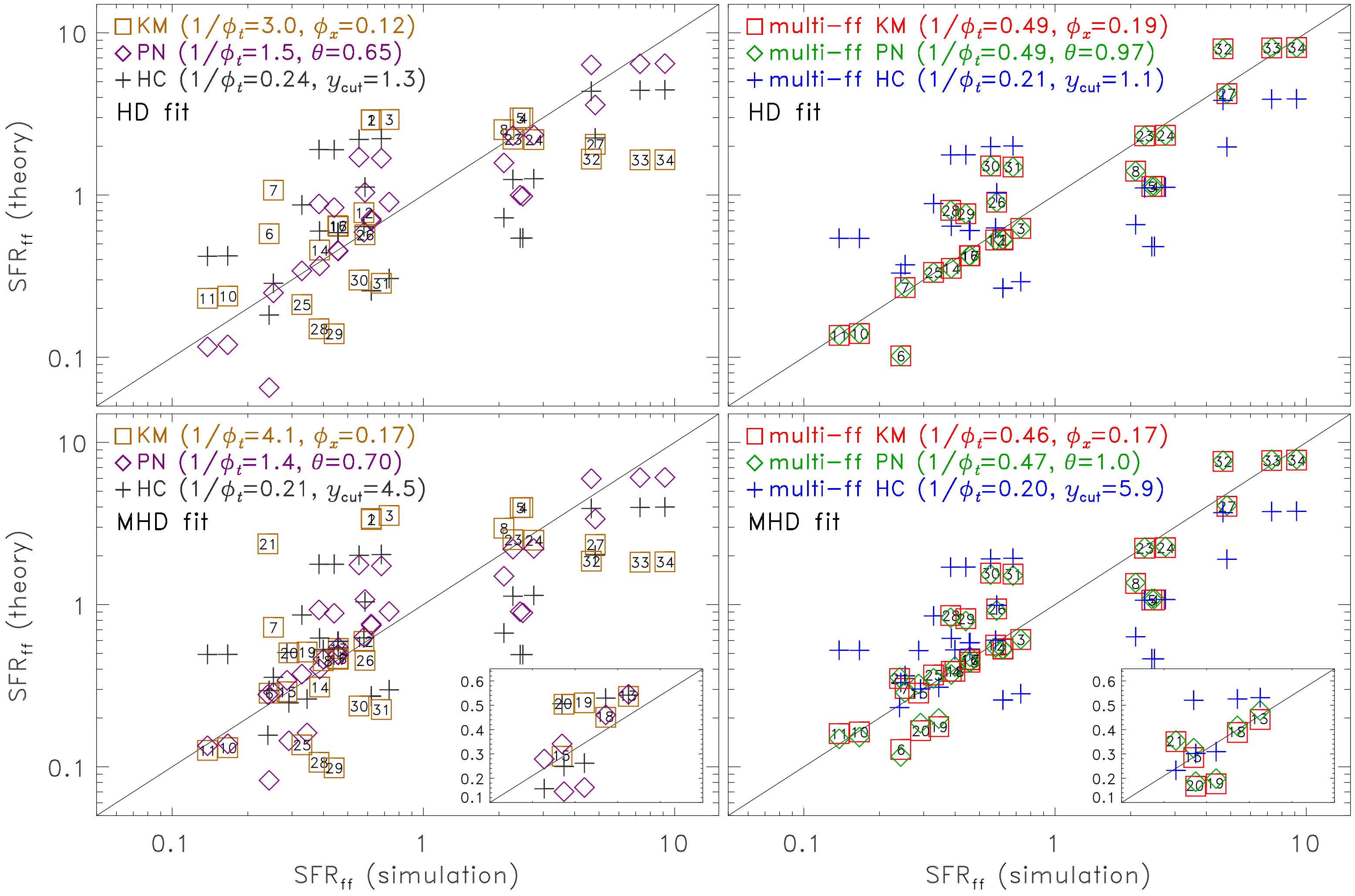

Federrath & Klessen 2012

SFR estimates from the PDF

comparison between numerical simulations and observations

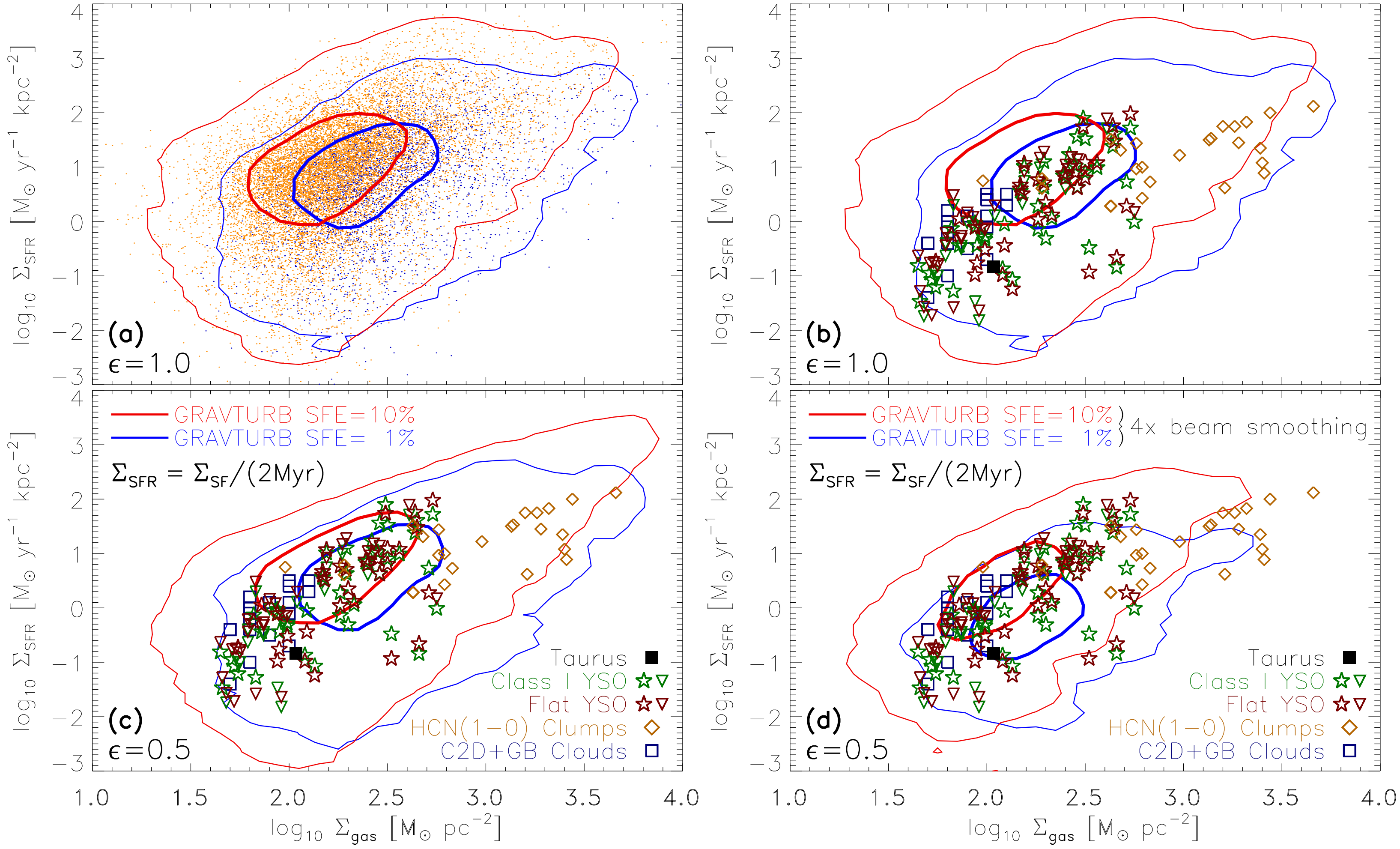

Federrath & Klessen 2012

modeling galactic SF

SPH calculations of self-gravitating disks of stars and (isothermal) gas in dark-matter potential, sink particles measure local collapse --> star formation

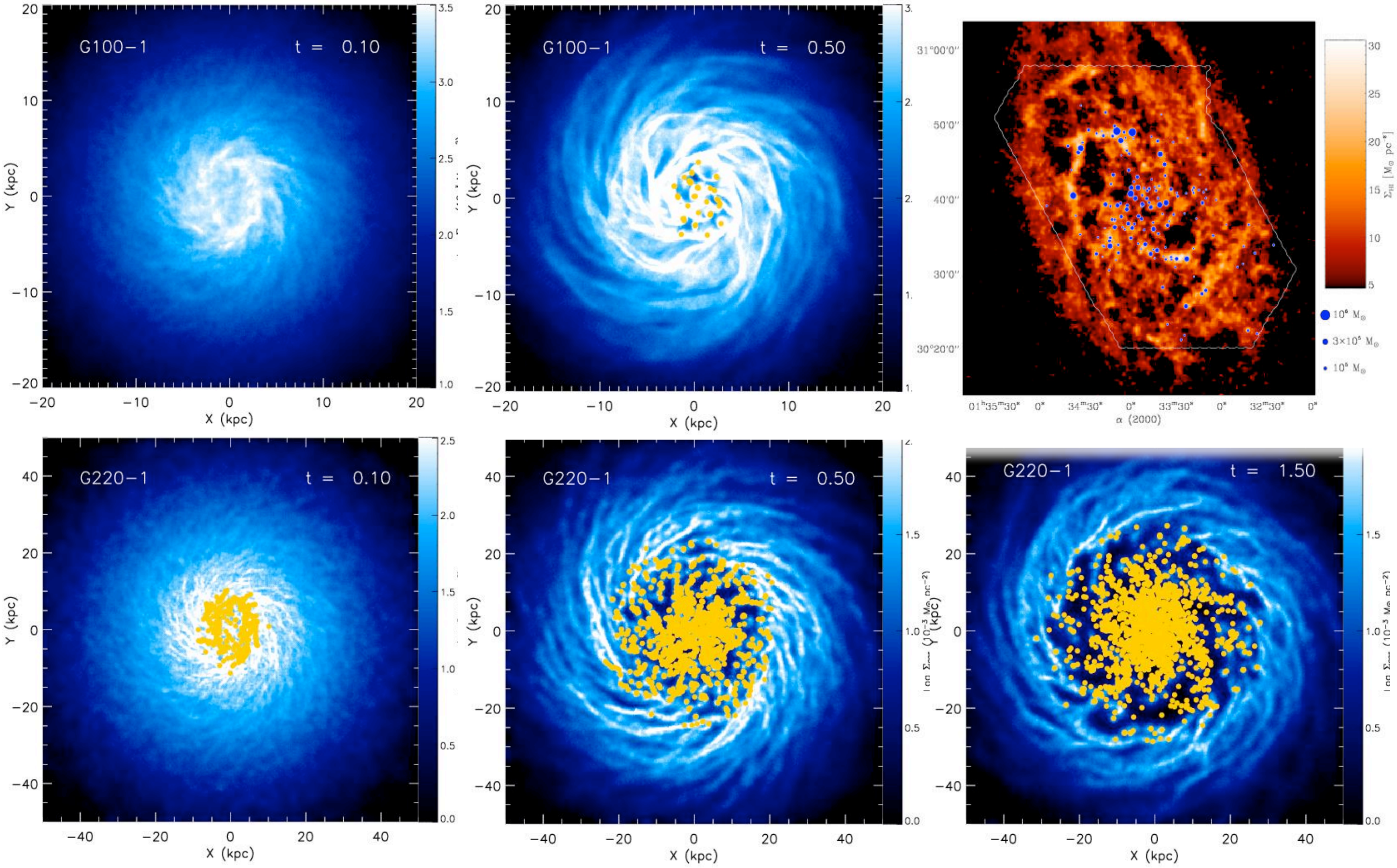

(Li, Mac Low, & Klessen, 2005, ApJ, 620,L19 - L22)

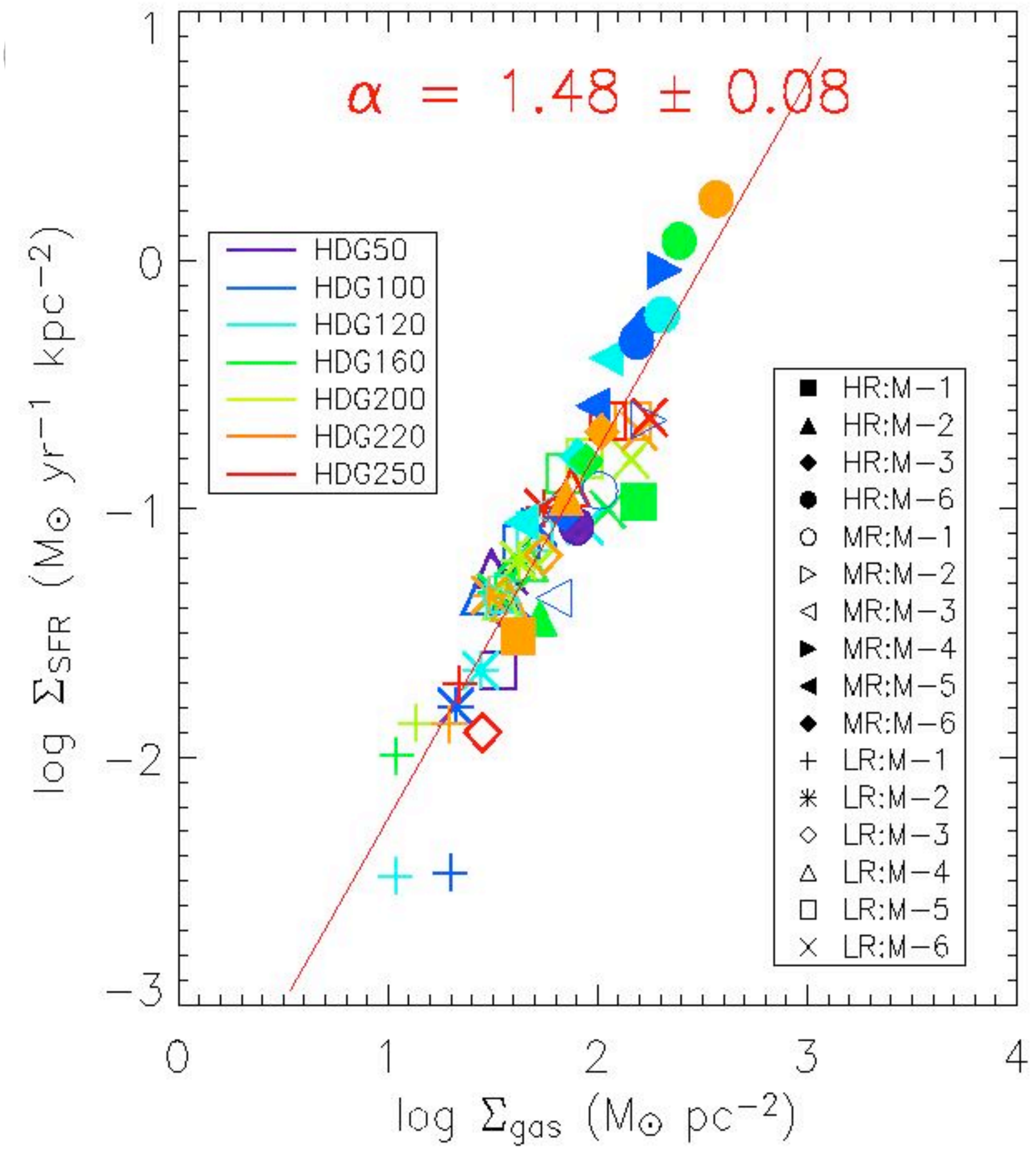

(Li, Mac Low, & Klessen, 2005, ApJ, 620, L19 - L22)

We find correlation between *star formation rate* and *gas surface density:*

$$\boxed{\Sigma_{SFR} \propto \Sigma_{gas}^{1.5}}$$

global Schmidt law

observed Schmidt law

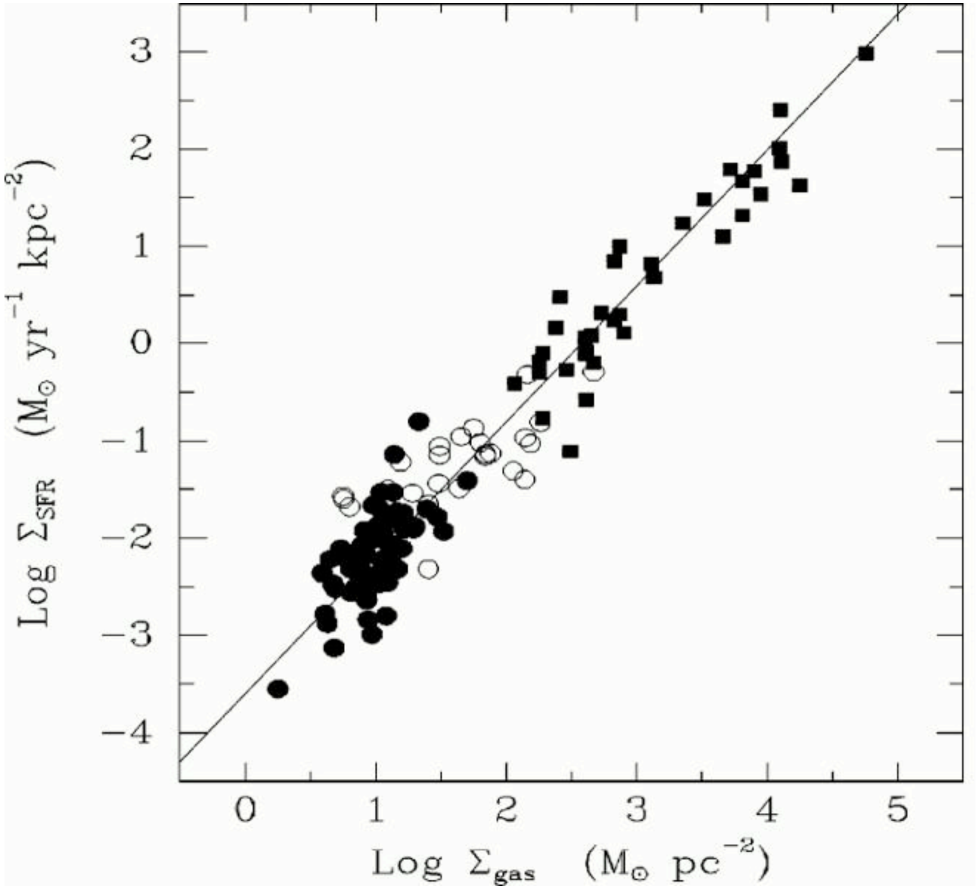

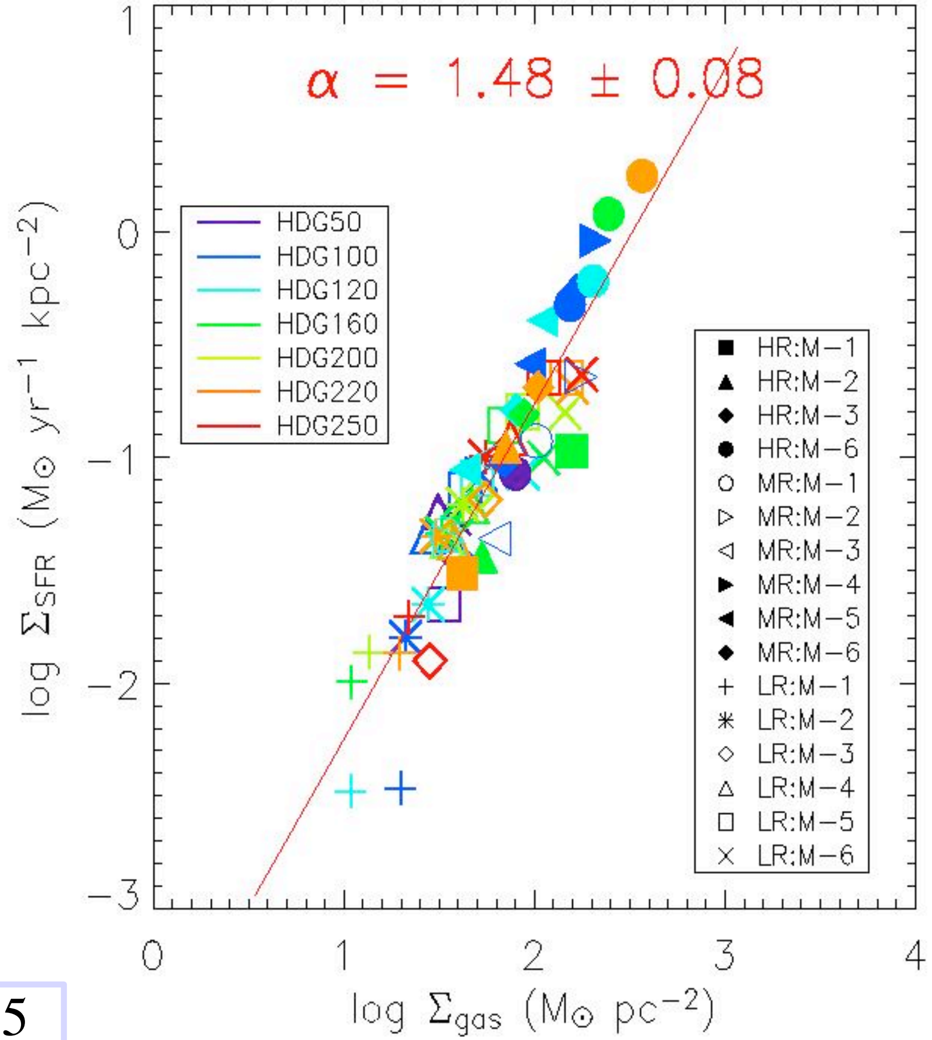

in both cases:

$$\boxed{\Sigma_{\mathrm{SFR}} \propto \Sigma_{\mathrm{gas}}^{1.5}}$$

(from Kennicutt 1998)

molecular cloud formation

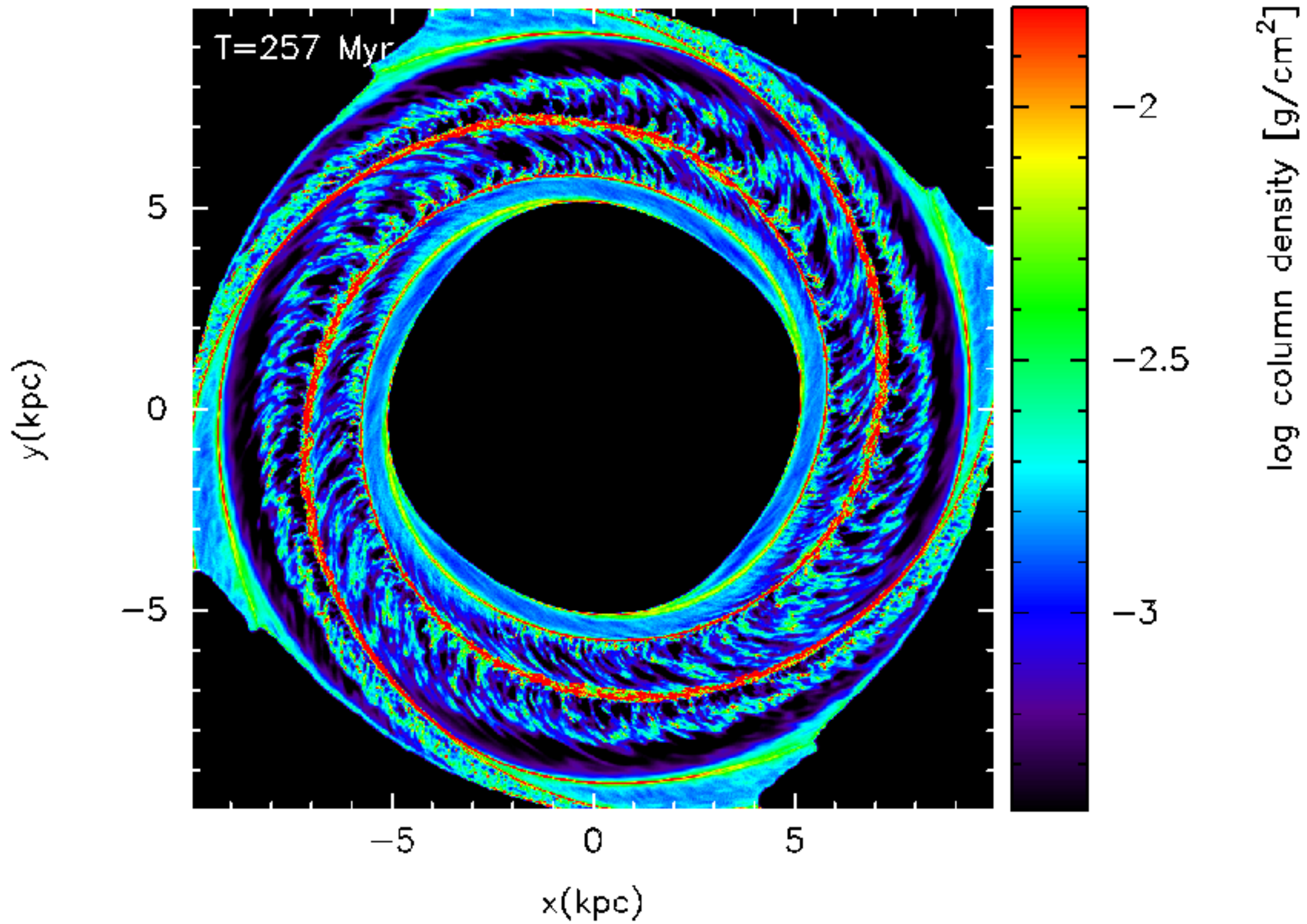

(from Dobbs et al. 2008)

molecular cloud formation

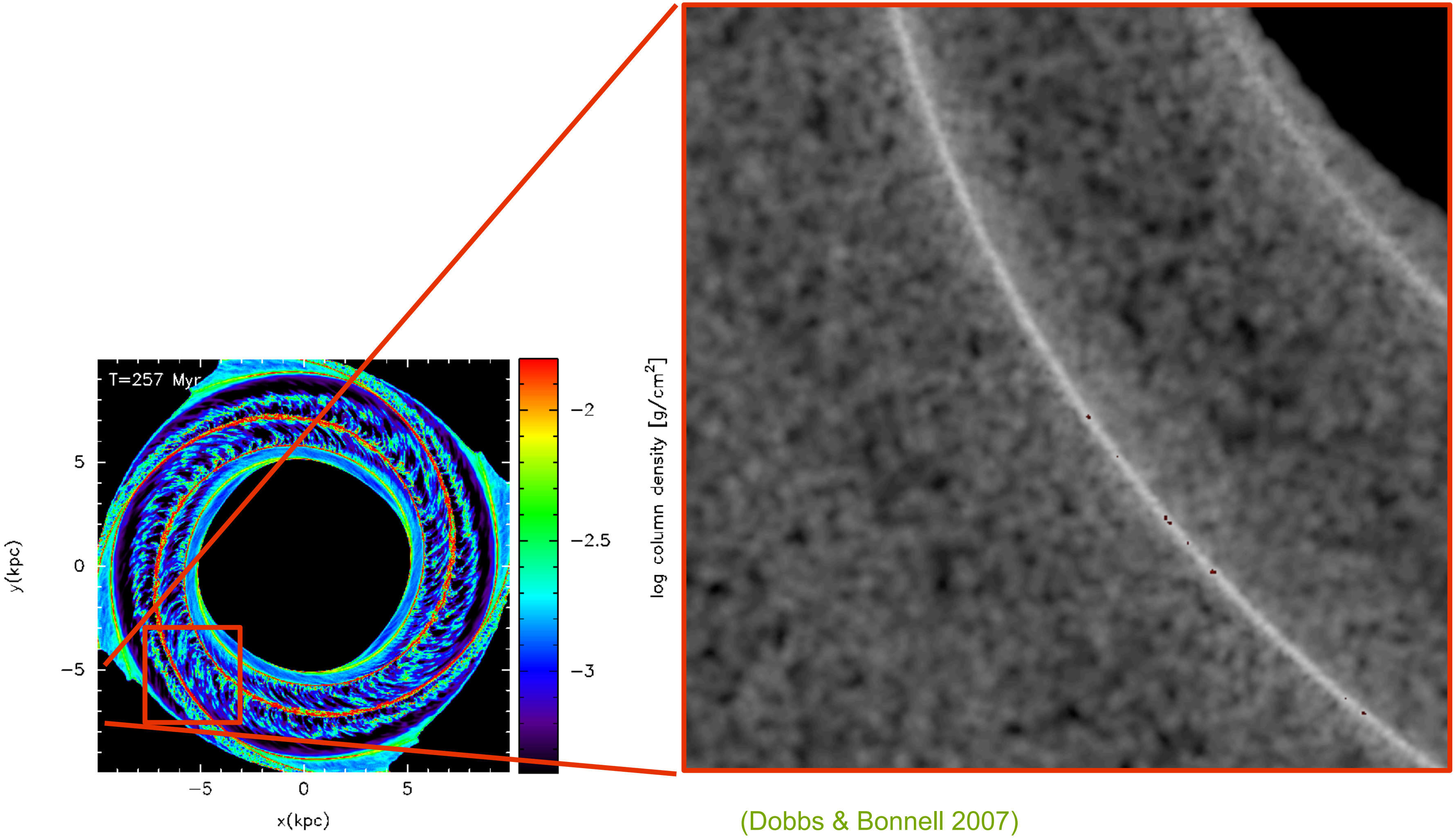

(Dobbs & Bonnell 2007)

molecular cloud formation

molecular gas fraction as function of time

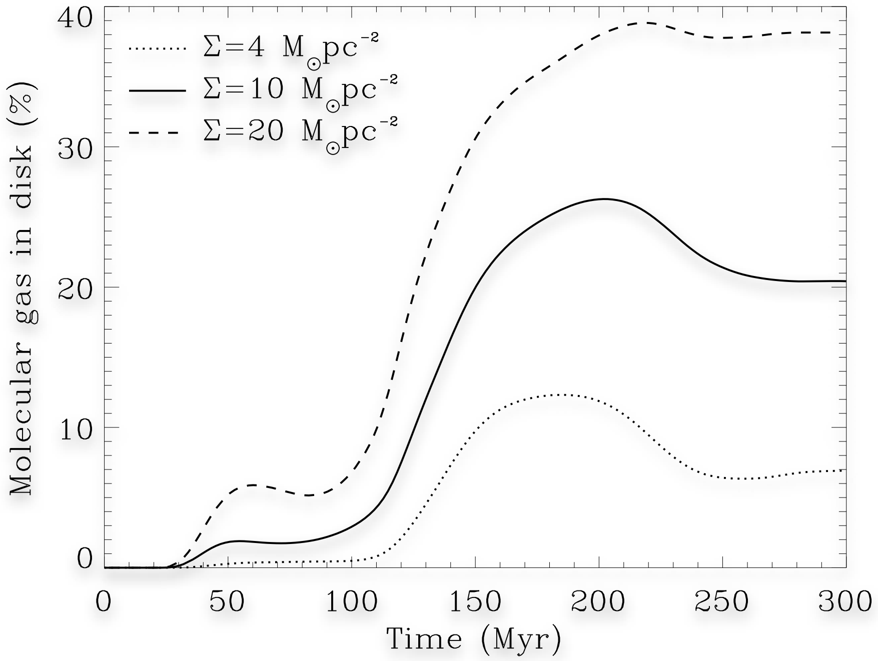

molecular gas fraction as function of density

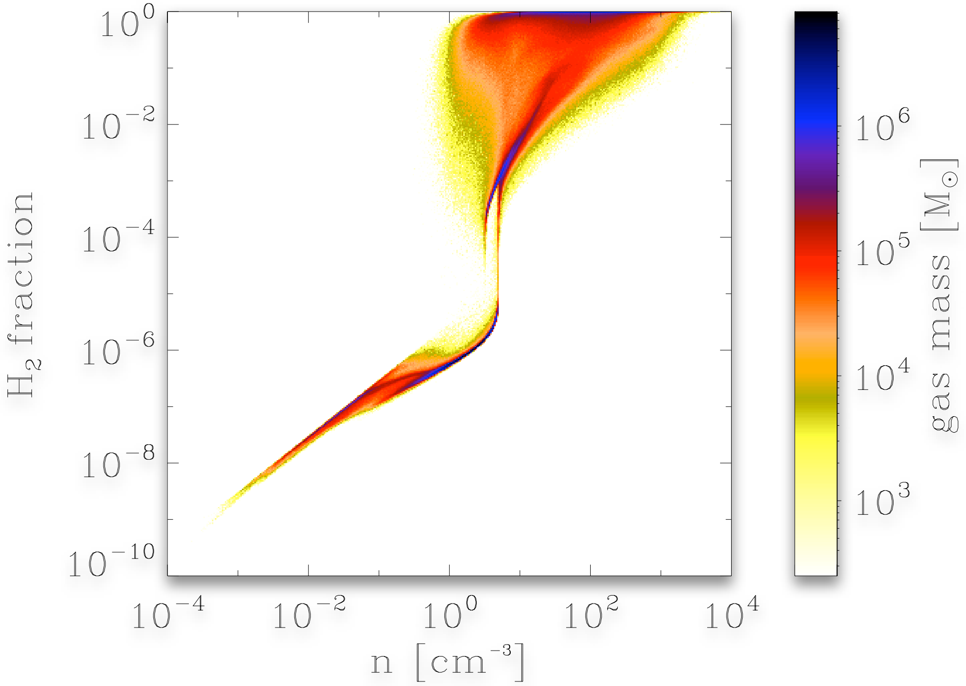

(Dobbs et al. 2008)

molecular cloud formation

molecular gas fraction of fluid
element as function of time

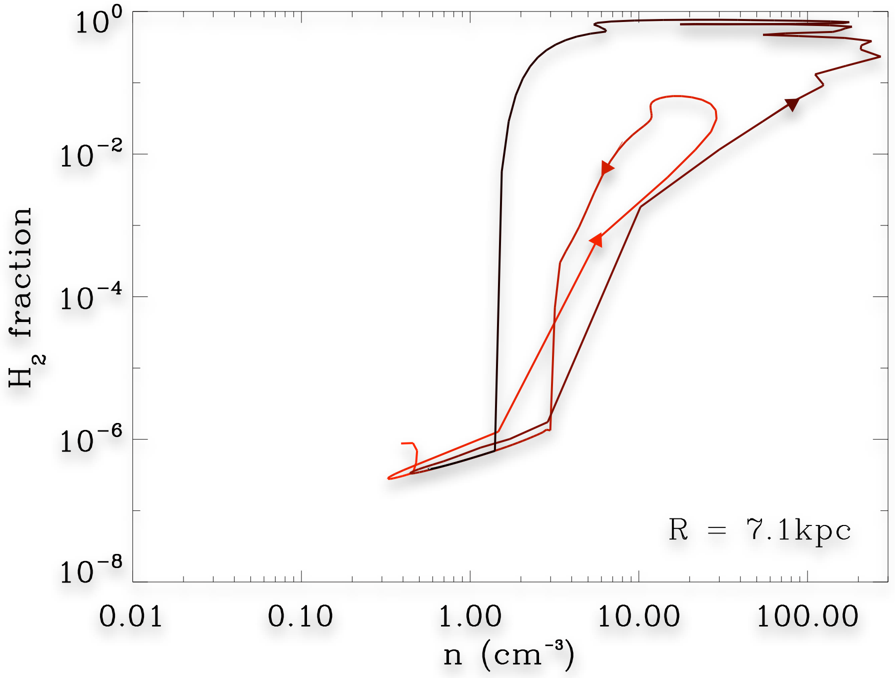

molecular gas fraction as function of density

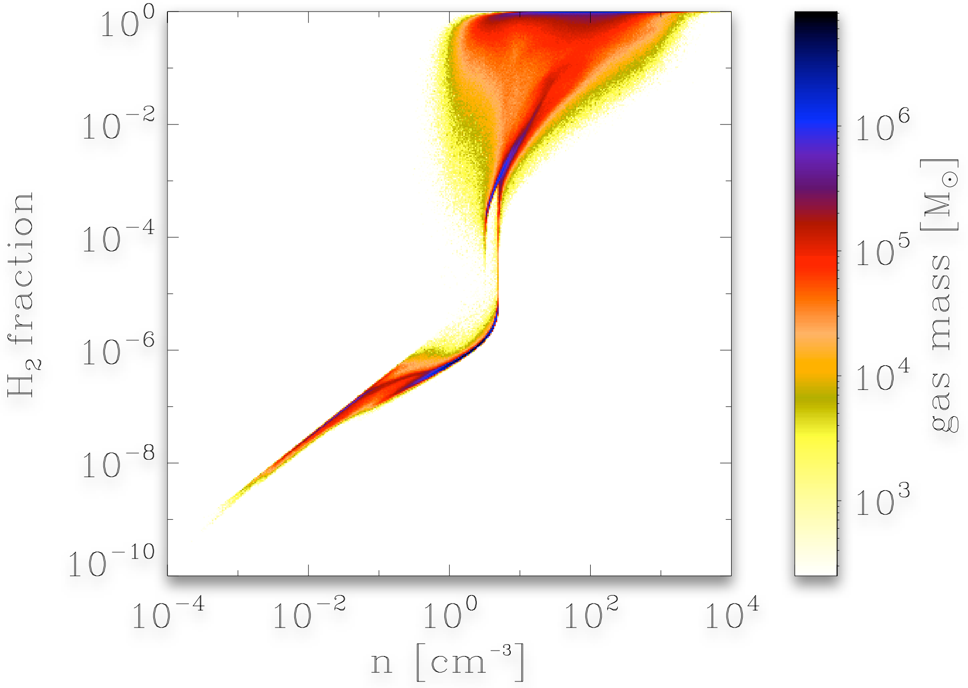

(Dobbs et al. 2008)

modeling chemistry

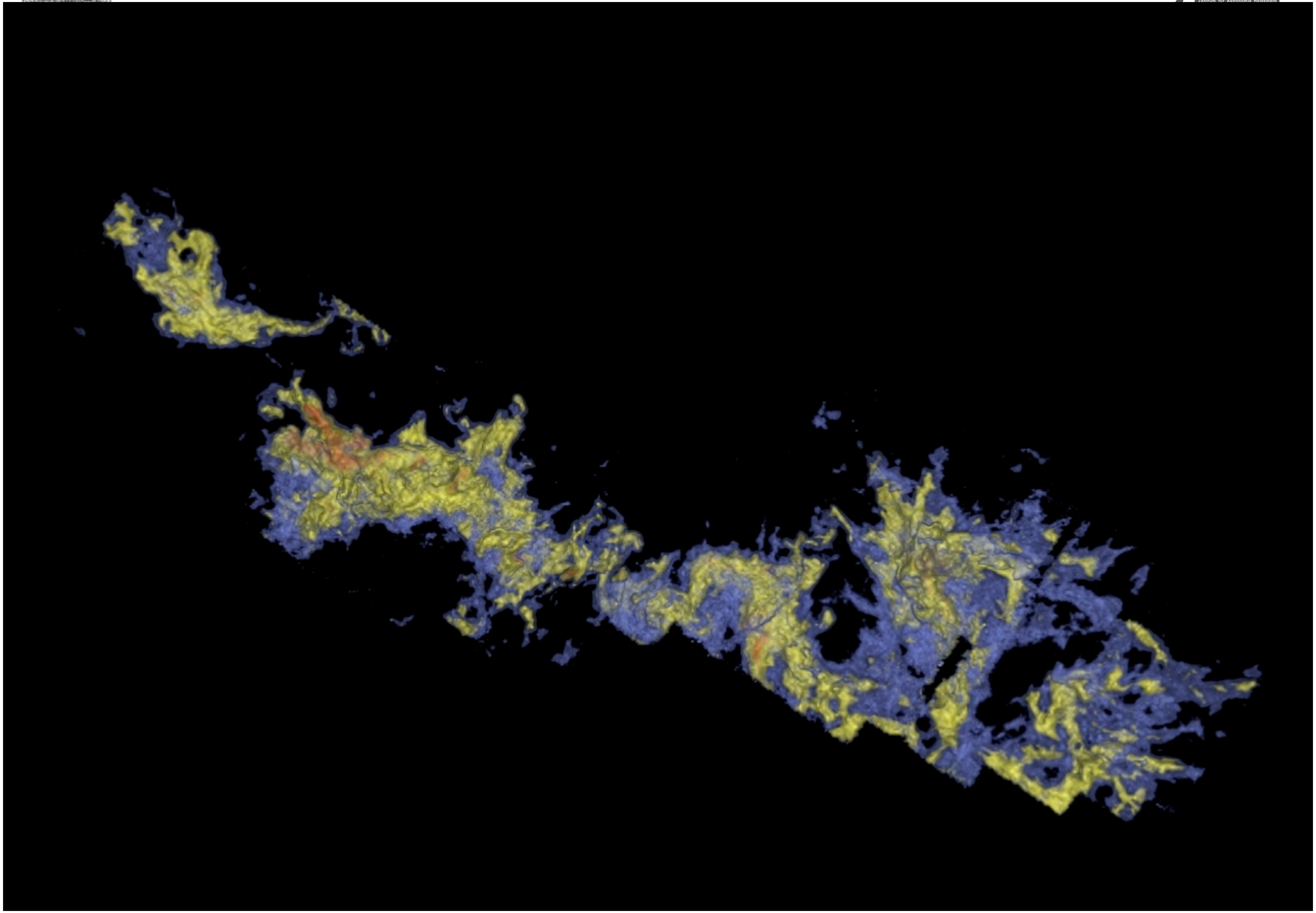

image from Alyssa Goodman: COMPLETE survey

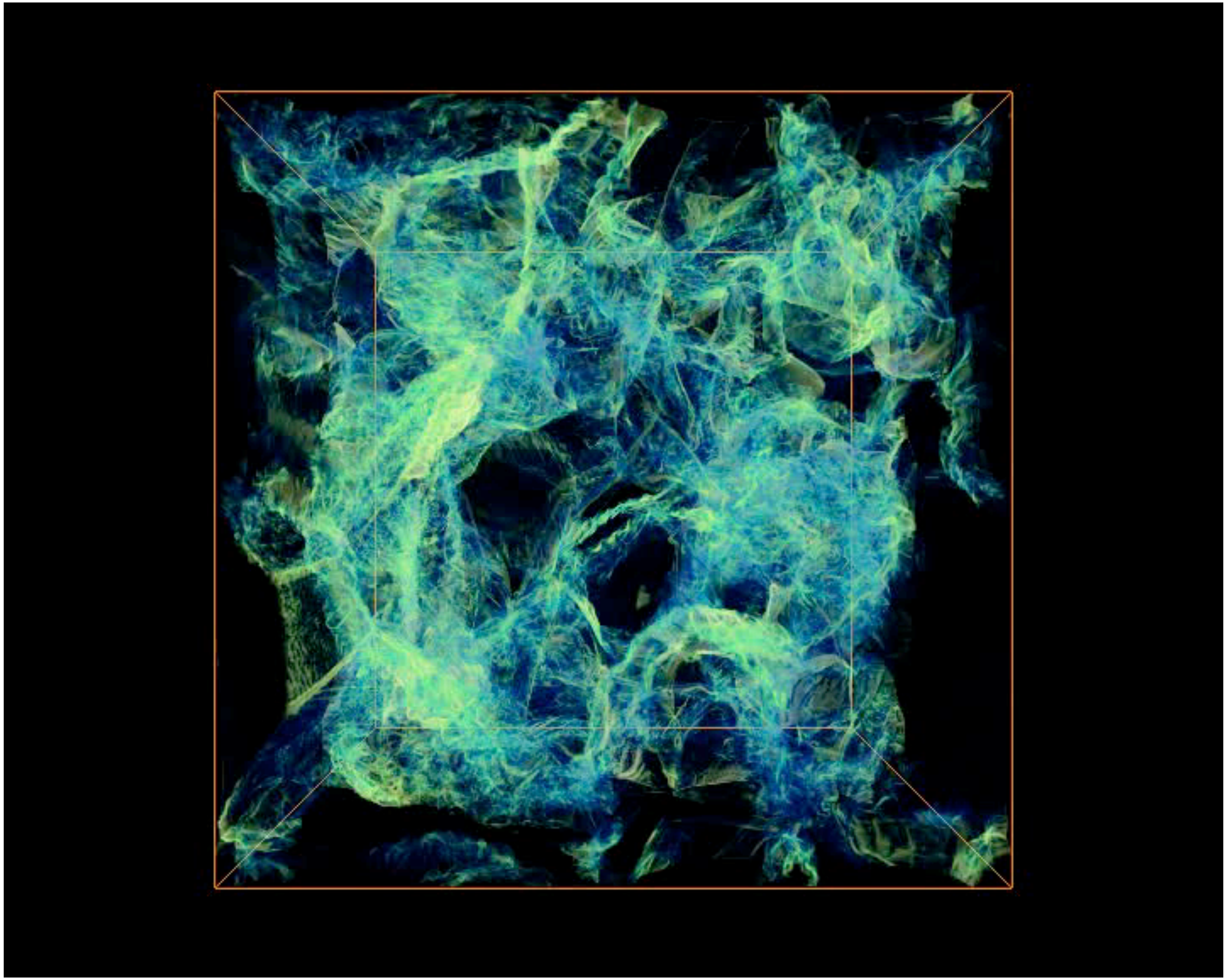

(movie from Christoph Federrath)

experimental set-up

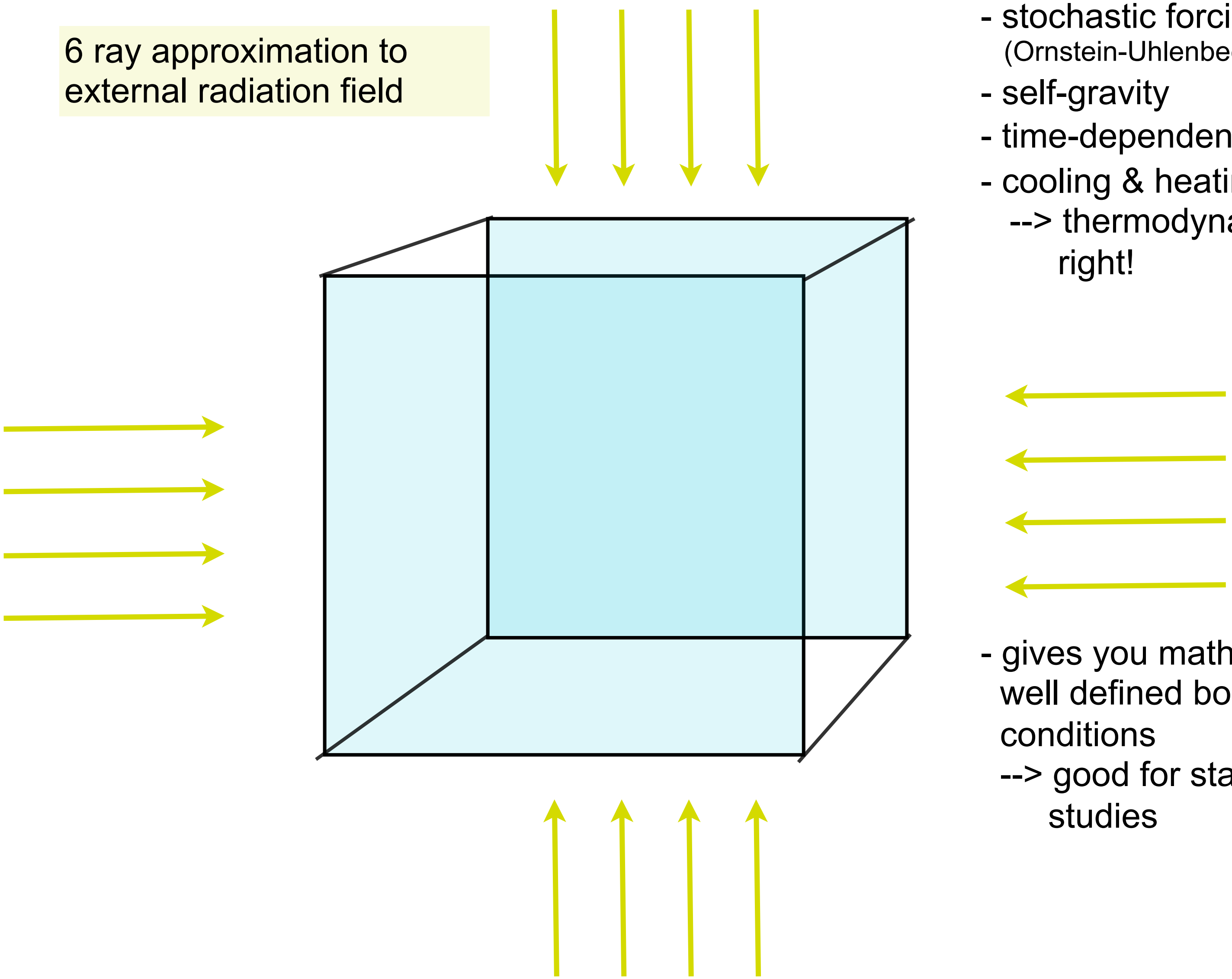

6 ray approximation to
external radiation field

- AMR MHD (B = 2 muG)
- stochastic forcing
  (Ornstein-Uhlenbeck)
- self-gravity
- time-dependent chemistry
- cooling & heating processes
  --> thermodynamics done
  right!

- gives you mathematically
  well defined boundary
  conditions
  --> good for statistical
  studies

chemical model 0

- 32 chemical species
  - 17 in instantaneous equilibrium:

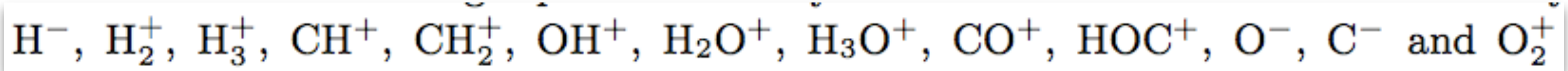

H^-, H_2^+, H_3^+, CH^+, CH_2^+, OH^+, H_2O^+, H_3O^+, CO^+, HOC^+, O^-, C^- and O_2^+

  - 19 full non-equilibrium evolution

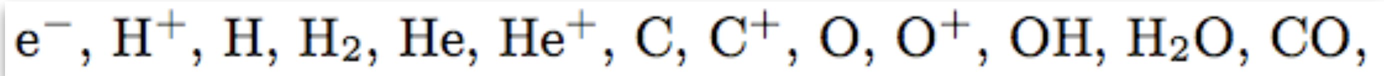

e^-, H^+, H, H_2, He, He^+, C, C^+, O, O^+, OH, H_2O, CO,

C_2, O_2, HCO^+, CH, CH_2 and CH_3^+

- 218 reactions
- various heating and cooling processes

(Glover, Federrath, Mac Low, Klessen, 2010, MNRS, 404, 2)

chemical model 1

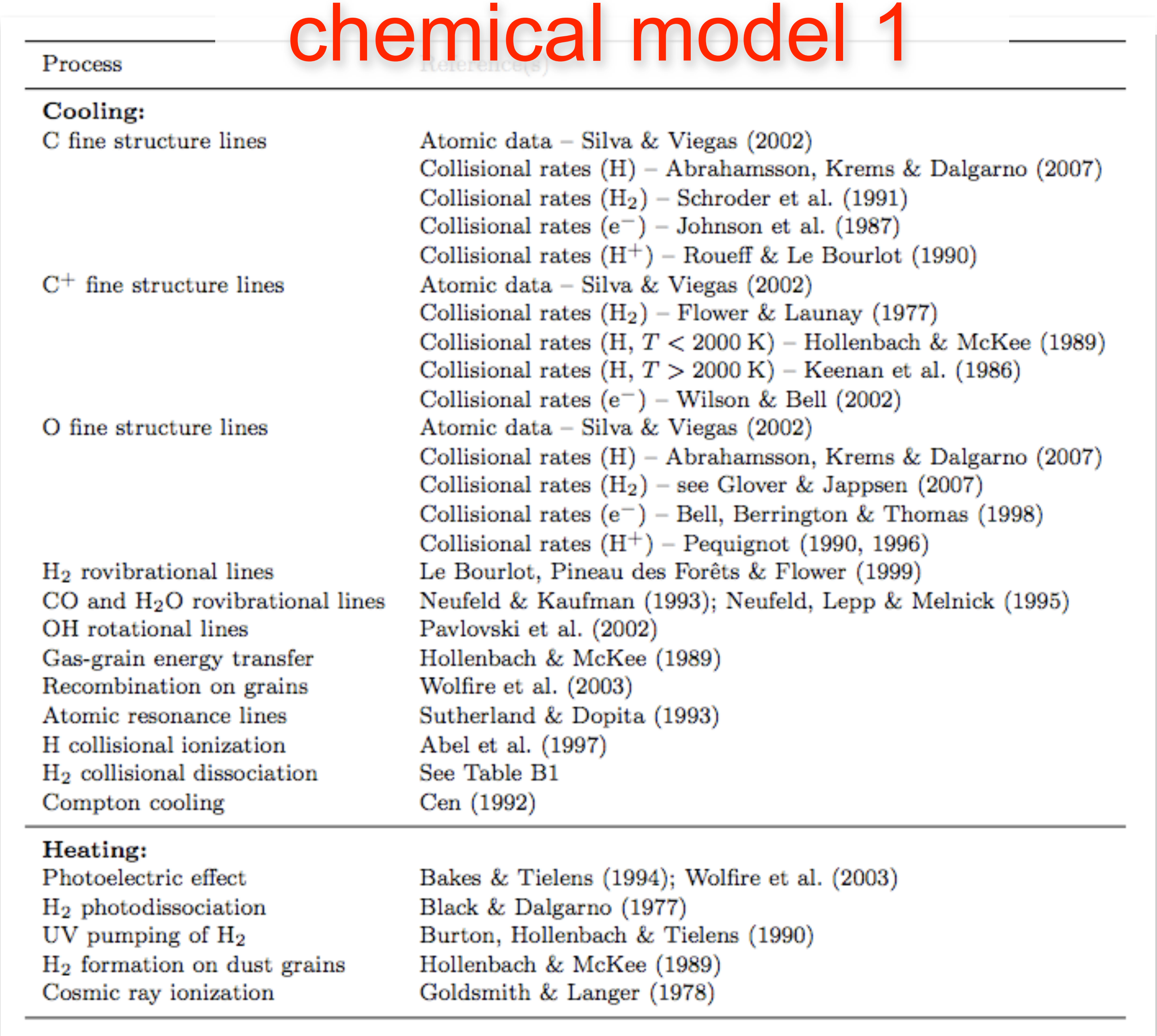

Process	Reference(s)
Cooling:	
C fine structure lines	Atomic data – Silva & Viegas (2002)
	Collisional rates (H) – Abrahamsson, Krems & Dalgarno (2007)
	Collisional rates (H_2) – Schroder et al. (1991)
	Collisional rates (e^-) – Johnson et al. (1987)
	Collisional rates (H^+) – Roueff & Le Bourlot (1990)
C^+ fine structure lines	Atomic data – Silva & Viegas (2002)
	Collisional rates (H_2) – Flower & Launay (1977)
	Collisional rates (H, $T < 2000$ K) – Hollenbach & McKee (1989)
	Collisional rates (H, $T > 2000$ K) – Keenan et al. (1986)
	Collisional rates (e^-) – Wilson & Bell (2002)
O fine structure lines	Atomic data – Silva & Viegas (2002)
	Collisional rates (H) – Abrahamsson, Krems & Dalgarno (2007)
	Collisional rates (H_2) – see Glover & Jappsen (2007)
	Collisional rates (e^-) – Bell, Berrington & Thomas (1998)
	Collisional rates (H^+) – Pequignot (1990, 1996)
H_2 rovibrational lines	Le Bourlot, Pineau des Forêts & Flower (1999)
CO and H_2O rovibrational lines	Neufeld & Kaufman (1993); Neufeld, Lepp & Melnick (1995)
OH rotational lines	Pavlovski et al. (2002)
Gas-grain energy transfer	Hollenbach & McKee (1989)
Recombination on grains	Wolfire et al. (2003)
Atomic resonance lines	Sutherland & Dopita (1993)
H collisional ionization	Abel et al. (1997)
H_2 collisional dissociation	See Table B1
Compton cooling	Cen (1992)
Heating:	
Photoelectric effect	Bakes & Tielens (1994); Wolfire et al. (2003)
H_2 photodissociation	Black & Dalgarno (1977)
UV pumping of H_2	Burton, Hollenbach & Tielens (1990)
H_2 formation on dust grains	Hollenbach & McKee (1989)
Cosmic ray ionization	Goldsmith & Langer (1978)

(Glover, Federrath, Mac Low, Klessen, 2010, MNRS, 404, 2)

chemical model 2

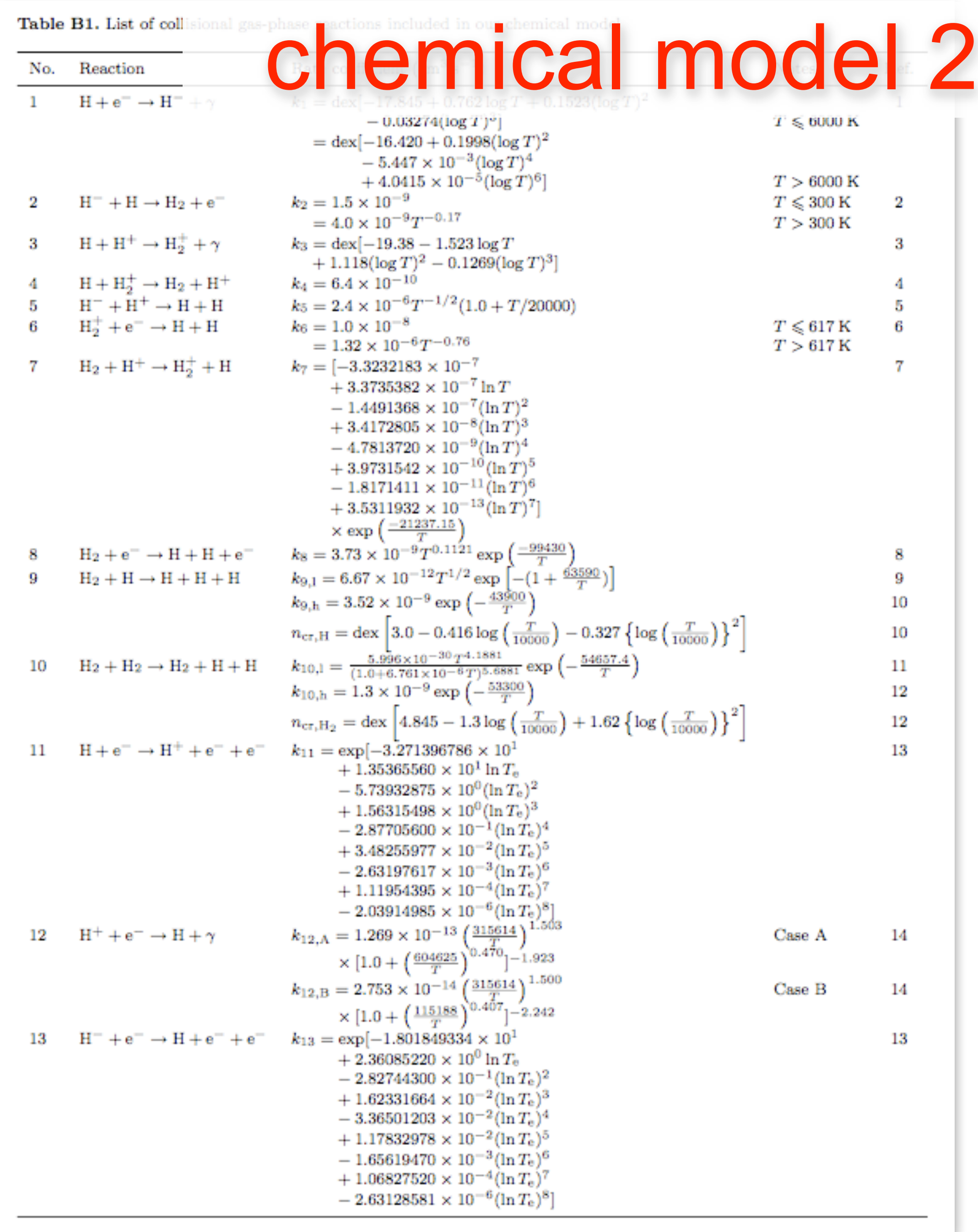

Table B1. List of collisional gas-phase reactions included in our chemical model

No.	Reaction	Rate coefficient (cm^3 s^{-1})	Notes	Ref.
1	$H + e^- \rightarrow H^- + \gamma$	$k_1 = \mathrm{dex}[-17.845 + 0.762 \log T + 0.1523 (\log T)^2 - 0.03274 (\log T)^3]$	$T \leqslant 6000$ K	1
		$= \mathrm{dex}[-16.420 + 0.1998 (\log T)^2 - 5.447 \times 10^{-3} (\log T)^4 + 4.0415 \times 10^{-5} (\log T)^6]$	$T > 6000$ K	
2	$H^- + H \rightarrow H_2 + e^-$	$k_2 = 1.5 \times 10^{-9}$	$T \leqslant 300$ K	2
		$= 4.0 \times 10^{-9} T^{-0.17}$	$T > 300$ K	
3	$H + H^+ \rightarrow H_2^+ + \gamma$	$k_3 = \mathrm{dex}[-19.38 - 1.523 \log T + 1.118 (\log T)^2 - 0.1269 (\log T)^3]$		3
4	$H + H_2^+ \rightarrow H_2 + H^+$	$k_4 = 6.4 \times 10^{-10}$		4
5	$H^- + H^+ \rightarrow H + H$	$k_5 = 2.4 \times 10^{-6} T^{-1/2} (1.0 + T/20000)$		5
6	$H_2^+ + e^- \rightarrow H + H$	$k_6 = 1.0 \times 10^{-8}$	$T \leqslant 617$ K	6
		$= 1.32 \times 10^{-6} T^{-0.76}$	$T > 617$ K	
7	$H_2 + H^+ \rightarrow H_2^+ + H$	$k_7 = [-3.3232183 \times 10^{-7} + 3.3735382 \times 10^{-7} \ln T - 1.4491368 \times 10^{-7} (\ln T)^2 + 3.4172805 \times 10^{-8} (\ln T)^3 - 4.7813720 \times 10^{-9} (\ln T)^4 + 3.9731542 \times 10^{-10} (\ln T)^5 - 1.8171411 \times 10^{-11} (\ln T)^6 + 3.5311932 \times 10^{-13} (\ln T)^7] \times \exp\left(\frac{-21237.15}{T}\right)$		7
8	$H_2 + e^- \rightarrow H + H + e^-$	$k_8 = 3.73 \times 10^{-9} T^{0.1121} \exp\left(\frac{-99430}{T}\right)$		8
9	$H_2 + H \rightarrow H + H + H$	$k_{9,l} = 6.67 \times 10^{-12} T^{1/2} \exp\left[-(1 + \frac{63590}{T})\right]$		9
		$k_{9,h} = 3.52 \times 10^{-9} \exp\left(-\frac{43900}{T}\right)$		10
		$n_{cr,H} = \mathrm{dex}\left[3.0 - 0.416 \log\left(\frac{T}{10000}\right) - 0.327 \left\{\log\left(\frac{T}{10000}\right)\right\}^2\right]$		10
10	$H_2 + H_2 \rightarrow H_2 + H + H$	$k_{10,l} = \frac{5.996 \times 10^{-30} T^{4.1881}}{(1.0 + 6.761 \times 10^{-6} T)^{5.6881}} \exp\left(-\frac{54657.4}{T}\right)$		11
		$k_{10,h} = 1.3 \times 10^{-9} \exp\left(-\frac{53300}{T}\right)$		12
		$n_{cr,H_2} = \mathrm{dex}\left[4.845 - 1.3 \log\left(\frac{T}{10000}\right) + 1.62 \left\{\log\left(\frac{T}{10000}\right)\right\}^2\right]$		12
11	$H + e^- \rightarrow H^+ + e^- + e^-$	$k_{11} = \exp[-3.271396786 \times 10^1 + 1.35365560 \times 10^1 \ln T_e - 5.73932875 \times 10^0 (\ln T_e)^2 + 1.56315498 \times 10^0 (\ln T_e)^3 - 2.87705600 \times 10^{-1} (\ln T_e)^4 + 3.48255977 \times 10^{-2} (\ln T_e)^5 - 2.63197617 \times 10^{-3} (\ln T_e)^6 + 1.11954395 \times 10^{-4} (\ln T_e)^7 - 2.03914985 \times 10^{-6} (\ln T_e)^8]$		13
12	$H^+ + e^- \rightarrow H + \gamma$	$k_{12,A} = 1.269 \times 10^{-13} \left(\frac{315614}{T}\right)^{1.503} \times \left[1.0 + \left(\frac{604625}{T}\right)^{0.470}\right]^{-1.923}$	Case A	14
		$k_{12,B} = 2.753 \times 10^{-14} \left(\frac{315614}{T}\right)^{1.500} \times \left[1.0 + \left(\frac{115188}{T}\right)^{0.407}\right]^{-2.242}$	Case B	14
13	$H^- + e^- \rightarrow H + e^- + e^-$	$k_{13} = \exp[-1.801849334 \times 10^1 + 2.36085220 \times 10^0 \ln T_e - 2.82744300 \times 10^{-1} (\ln T_e)^2 + 1.62331664 \times 10^{-2} (\ln T_e)^3 - 3.36501203 \times 10^{-2} (\ln T_e)^4 + 1.17832978 \times 10^{-2} (\ln T_e)^5 - 1.65619470 \times 10^{-3} (\ln T_e)^6 + 1.06827520 \times 10^{-4} (\ln T_e)^7 - 2.63128581 \times 10^{-6} (\ln T_e)^8]$		13

(Glover, Federrath, Mac Low, Klessen, 2010, MNRS, 404, 2)

chemical model 2

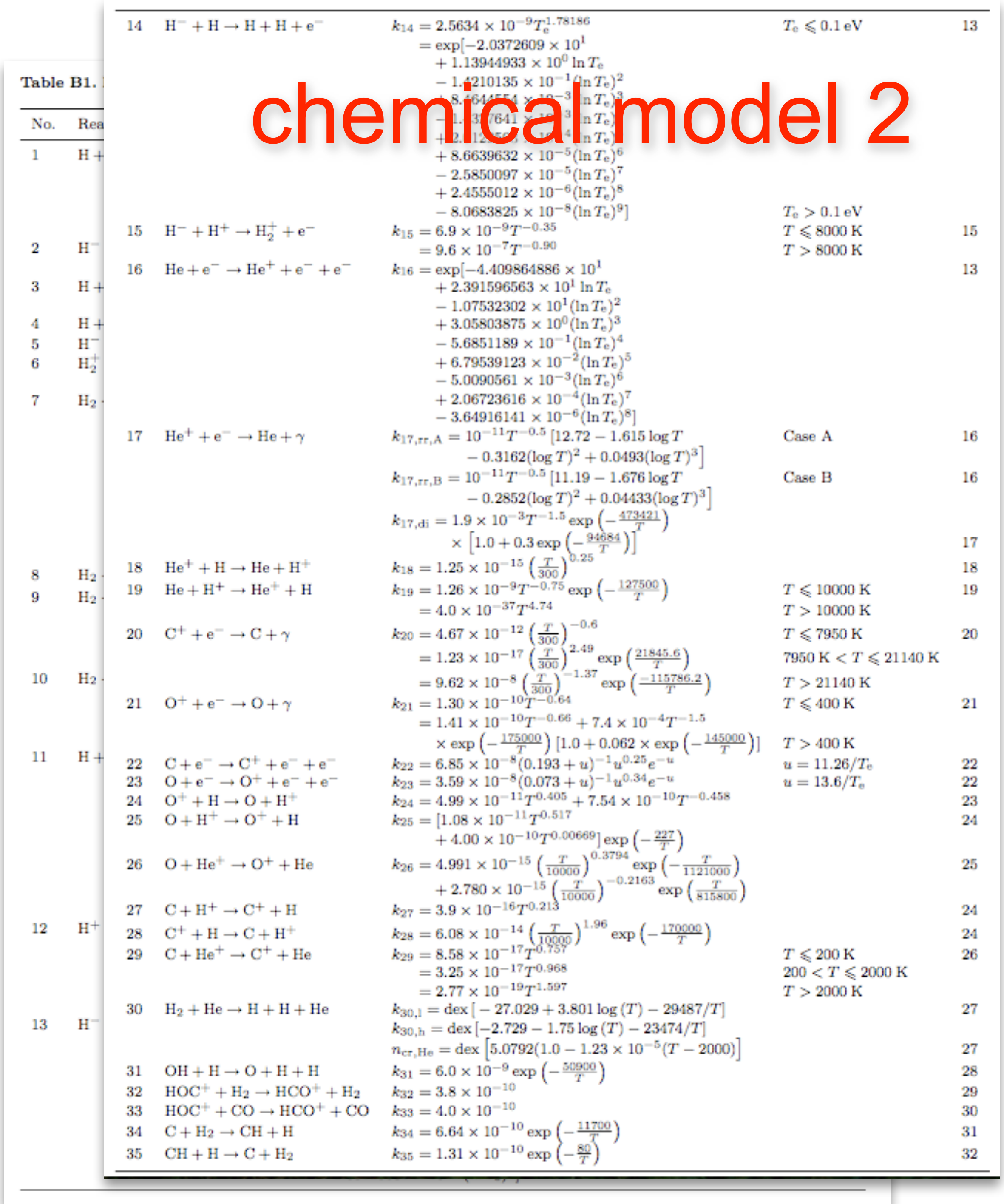

Table B1.

No.	Rea
1	H +
2	H^-
3	H +
4	H +
5	H^-
6	H_2^+
7	H_2
8	H_2
9	H_2
10	H_2
11	H +
12	H^+
13	H^-

14	$H^- + H \rightarrow H + H + e^-$	$k_{14} = 2.5634 \times 10^{-9} T_e^{1.78186}$	$T_e \leqslant 0.1$ eV	13
		$= \exp[-2.0372609 \times 10^{1}$ $+ 1.13944933 \times 10^{0} \ln T_e$ $- 1.4210135 \times 10^{-1} (\ln T_e)^2$ $+ 8.4644554 \times 10^{-3} (\ln T_e)^3$ $- 1.4327641 \times 10^{-3} (\ln T_e)^4$ $+ 2.0122503 \times 10^{-4} (\ln T_e)^5$ $+ 8.6639632 \times 10^{-5} (\ln T_e)^6$ $- 2.5850097 \times 10^{-5} (\ln T_e)^7$ $+ 2.4555012 \times 10^{-6} (\ln T_e)^8$ $- 8.0683825 \times 10^{-8} (\ln T_e)^9]$	$T_e > 0.1$ eV	
15	$H^- + H^+ \rightarrow H_2^+ + e^-$	$k_{15} = 6.9 \times 10^{-9} T^{-0.35}$	$T \leqslant 8000$ K	15
		$= 9.6 \times 10^{-7} T^{-0.90}$	$T > 8000$ K	
16	$He + e^- \rightarrow He^+ + e^- + e^-$	$k_{16} = \exp[-4.409864886 \times 10^{1}$ $+ 2.391596563 \times 10^{1} \ln T_e$ $- 1.07532302 \times 10^{1} (\ln T_e)^2$ $+ 3.05803875 \times 10^{0} (\ln T_e)^3$ $- 5.6851189 \times 10^{-1} (\ln T_e)^4$ $+ 6.79539123 \times 10^{-2} (\ln T_e)^5$ $- 5.0090561 \times 10^{-3} (\ln T_e)^6$ $+ 2.06723616 \times 10^{-4} (\ln T_e)^7$ $- 3.64916141 \times 10^{-6} (\ln T_e)^8]$		13
17	$He^+ + e^- \rightarrow He + \gamma$	$k_{17,\mathrm{rr,A}} = 10^{-11} T^{-0.5} [12.72 - 1.615 \log T$ $- 0.3162 (\log T)^2 + 0.0493 (\log T)^3]$	Case A	16
		$k_{17,\mathrm{rr,B}} = 10^{-11} T^{-0.5} [11.19 - 1.676 \log T$ $- 0.2852 (\log T)^2 + 0.04433 (\log T)^3]$	Case B	16
		$k_{17,\mathrm{di}} = 1.9 \times 10^{-3} T^{-1.5} \exp\left(-\frac{473421}{T}\right)$ $\times \left[1.0 + 0.3 \exp\left(-\frac{94684}{T}\right)\right]$		17
18	$He^+ + H \rightarrow He + H^+$	$k_{18} = 1.25 \times 10^{-15} \left(\frac{T}{300}\right)^{0.25}$		18
19	$He + H^+ \rightarrow He^+ + H$	$k_{19} = 1.26 \times 10^{-9} T^{-0.75} \exp\left(-\frac{127500}{T}\right)$	$T \leqslant 10000$ K	19
		$= 4.0 \times 10^{-37} T^{4.74}$	$T > 10000$ K	
20	$C^+ + e^- \rightarrow C + \gamma$	$k_{20} = 4.67 \times 10^{-12} \left(\frac{T}{300}\right)^{-0.6}$	$T \leqslant 7950$ K	20
		$= 1.23 \times 10^{-17} \left(\frac{T}{300}\right)^{2.49} \exp\left(\frac{21845.6}{T}\right)$	$7950 \mathrm{~K} < T \leqslant 21140$ K	
		$= 9.62 \times 10^{-8} \left(\frac{T}{300}\right)^{-1.37} \exp\left(\frac{-115786.2}{T}\right)$	$T > 21140$ K	
21	$O^+ + e^- \rightarrow O + \gamma$	$k_{21} = 1.30 \times 10^{-10} T^{-0.64}$	$T \leqslant 400$ K	21
		$= 1.41 \times 10^{-10} T^{-0.66} + 7.4 \times 10^{-4} T^{-1.5}$ $\times \exp\left(-\frac{175000}{T}\right) [1.0 + 0.062 \times \exp\left(-\frac{145000}{T}\right)]$	$T > 400$ K	
22	$C + e^- \rightarrow C^+ + e^- + e^-$	$k_{22} = 6.85 \times 10^{-8} (0.193 + u)^{-1} u^{0.25} e^{-u}$	$u = 11.26/T_e$	22
23	$O + e^- \rightarrow O^+ + e^- + e^-$	$k_{23} = 3.59 \times 10^{-8} (0.073 + u)^{-1} u^{0.34} e^{-u}$	$u = 13.6/T_e$	22
24	$O^+ + H \rightarrow O + H^+$	$k_{24} = 4.99 \times 10^{-11} T^{0.405} + 7.54 \times 10^{-10} T^{-0.458}$		23
25	$O + H^+ \rightarrow O^+ + H$	$k_{25} = [1.08 \times 10^{-11} T^{0.517}$ $+ 4.00 \times 10^{-10} T^{0.00669}] \exp\left(-\frac{227}{T}\right)$		24
26	$O + He^+ \rightarrow O^+ + He$	$k_{26} = 4.991 \times 10^{-15} \left(\frac{T}{10000}\right)^{0.3794} \exp\left(-\frac{T}{1121000}\right)$ $+ 2.780 \times 10^{-15} \left(\frac{T}{10000}\right)^{-0.2163} \exp\left(\frac{T}{815800}\right)$		25
27	$C + H^+ \rightarrow C^+ + H$	$k_{27} = 3.9 \times 10^{-16} T^{0.213}$		24
28	$C^+ + H \rightarrow C + H^+$	$k_{28} = 6.08 \times 10^{-14} \left(\frac{T}{10000}\right)^{1.96} \exp\left(-\frac{170000}{T}\right)$		24
29	$C + He^+ \rightarrow C^+ + He$	$k_{29} = 8.58 \times 10^{-17} T^{0.757}$	$T \leqslant 200$ K	26
		$= 3.25 \times 10^{-17} T^{0.968}$	$200 < T \leqslant 2000$ K	
		$= 2.77 \times 10^{-19} T^{1.597}$	$T > 2000$ K	
30	$H_2 + He \rightarrow H + H + He$	$k_{30,\mathrm{l}} = \mathrm{dex}[-27.029 + 3.801 \log(T) - 29487/T]$ $k_{30,\mathrm{h}} = \mathrm{dex}[-2.729 - 1.75 \log(T) - 23474/T]$		27
		$n_{\mathrm{cr,He}} = \mathrm{dex}\left[5.0792(1.0 - 1.23 \times 10^{-5}(T - 2000)\right]$		27
31	$OH + H \rightarrow O + H + H$	$k_{31} = 6.0 \times 10^{-9} \exp\left(-\frac{50900}{T}\right)$		28
32	$HOC^+ + H_2 \rightarrow HCO^+ + H_2$	$k_{32} = 3.8 \times 10^{-10}$		29
33	$HOC^+ + CO \rightarrow HCO^+ + CO$	$k_{33} = 4.0 \times 10^{-10}$		30
34	$C + H_2 \rightarrow CH + H$	$k_{34} = 6.64 \times 10^{-10} \exp\left(-\frac{11700}{T}\right)$		31
35	$CH + H \rightarrow C + H_2$	$k_{35} = 1.31 \times 10^{-10} \exp\left(-\frac{80}{T}\right)$		32

(Glover, Federrath, Mac Low, Klessen, 2010, MNRS, 404, 2)

chemical model 2

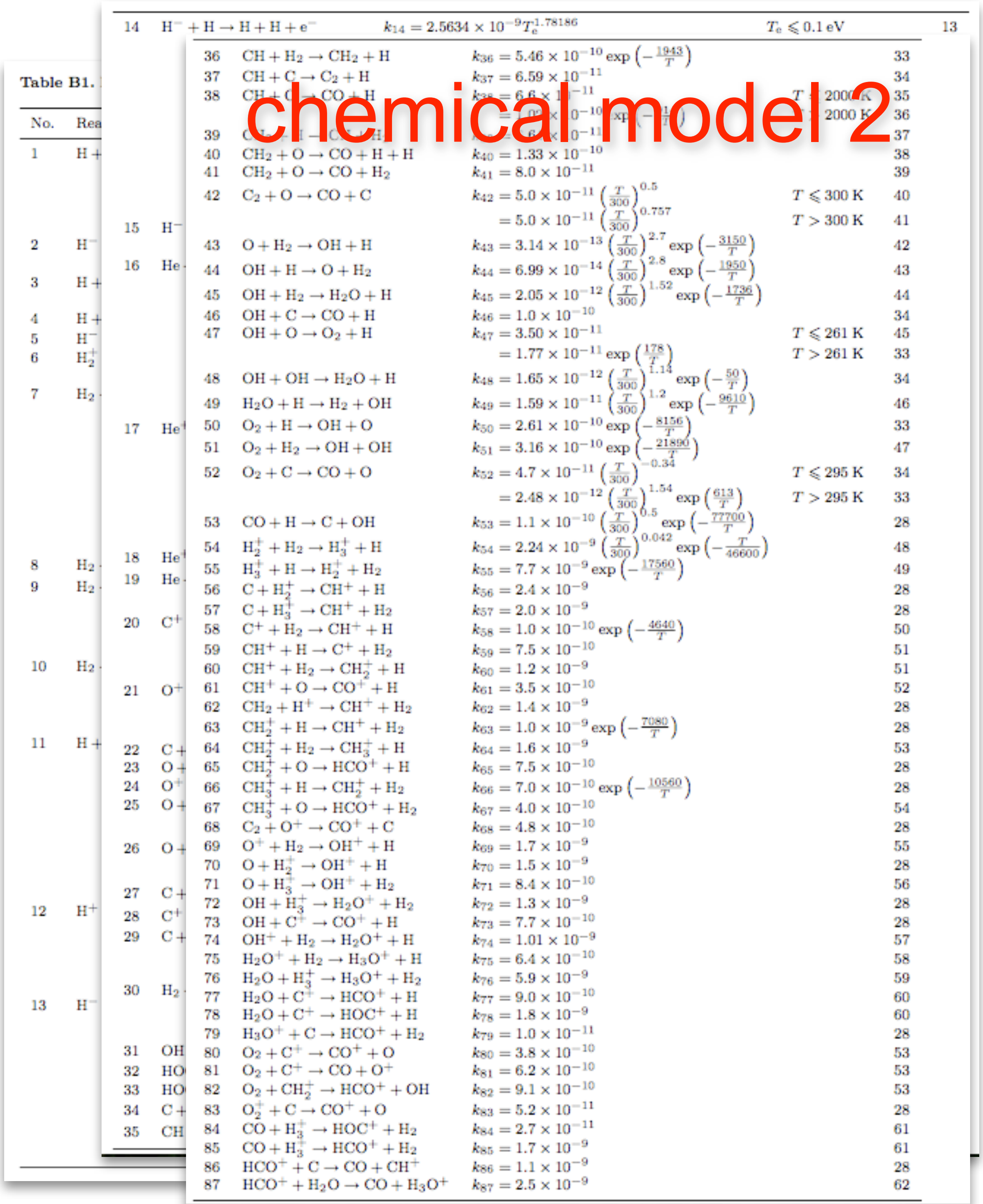

Table B1.

No. Rea

1 H +

2 H^-

3 H +

4 H +

5 H^-

6 H_2^+

7 H_2

8 H_2

9 H_2

10 H_2

11 H +

12 H^+

13 H^-

14 $H^- + H \rightarrow H + H + e^-$ $k_{14} = 2.5634 \times 10^{-9} T_e^{1.78186}$ $T_e \leqslant 0.1$ eV 13

15 H^-

16 He

17 He^+

18 He^+

19 He

20 C^+

21 O^+

22 C +

23 O +

24 O^+

25 O +

26 O +

27 C +

28 C^+

29 C +

30 H_2

31 OH

32 HO

33 HO

34 C +

35 CH

36	$CH + H_2 \rightarrow CH_2 + H$	$k_{36} = 5.46 \times 10^{-10} \exp\left(-\frac{1943}{T}\right)$		33
37	$CH + C \rightarrow C_2 + H$	$k_{37} = 6.59 \times 10^{-11}$		34
38	$CH +$ [illegible] $\rightarrow CO + H$	$k_{38} = 6.6 \times 10^{-11}$	T [illegible] 2000 K	35
		$= 1.02 \times 10^{-10} \exp\left(-\frac{[illegible]}{T}\right)$	T [illegible] 2000 K	36
39	[illegible]	[illegible]		37
40	$CH_2 + O \rightarrow CO + H + H$	$k_{40} = 1.33 \times 10^{-10}$		38
41	$CH_2 + O \rightarrow CO + H_2$	$k_{41} = 8.0 \times 10^{-11}$		39
42	$C_2 + O \rightarrow CO + C$	$k_{42} = 5.0 \times 10^{-11} \left(\frac{T}{300}\right)^{0.5}$	$T \leqslant 300$ K	40
		$= 5.0 \times 10^{-11} \left(\frac{T}{300}\right)^{0.757}$	$T > 300$ K	41
43	$O + H_2 \rightarrow OH + H$	$k_{43} = 3.14 \times 10^{-13} \left(\frac{T}{300}\right)^{2.7} \exp\left(-\frac{3150}{T}\right)$		42
44	$OH + H \rightarrow O + H_2$	$k_{44} = 6.99 \times 10^{-14} \left(\frac{T}{300}\right)^{2.8} \exp\left(-\frac{1950}{T}\right)$		43
45	$OH + H_2 \rightarrow H_2O + H$	$k_{45} = 2.05 \times 10^{-12} \left(\frac{T}{300}\right)^{1.52} \exp\left(-\frac{1736}{T}\right)$		44
46	$OH + C \rightarrow CO + H$	$k_{46} = 1.0 \times 10^{-10}$		34
47	$OH + O \rightarrow O_2 + H$	$k_{47} = 3.50 \times 10^{-11}$	$T \leqslant 261$ K	45
		$= 1.77 \times 10^{-11} \exp\left(\frac{178}{T}\right)$	$T > 261$ K	33
48	$OH + OH \rightarrow H_2O + H$	$k_{48} = 1.65 \times 10^{-12} \left(\frac{T}{300}\right)^{1.14} \exp\left(-\frac{50}{T}\right)$		34
49	$H_2O + H \rightarrow H_2 + OH$	$k_{49} = 1.59 \times 10^{-11} \left(\frac{T}{300}\right)^{1.2} \exp\left(-\frac{9610}{T}\right)$		46
50	$O_2 + H \rightarrow OH + O$	$k_{50} = 2.61 \times 10^{-10} \exp\left(-\frac{8156}{T}\right)$		33
51	$O_2 + H_2 \rightarrow OH + OH$	$k_{51} = 3.16 \times 10^{-10} \exp\left(-\frac{21890}{T}\right)$		47
52	$O_2 + C \rightarrow CO + O$	$k_{52} = 4.7 \times 10^{-11} \left(\frac{T}{300}\right)^{-0.34}$	$T \leqslant 295$ K	34
		$= 2.48 \times 10^{-12} \left(\frac{T}{300}\right)^{1.54} \exp\left(\frac{613}{T}\right)$	$T > 295$ K	33
53	$CO + H \rightarrow C + OH$	$k_{53} = 1.1 \times 10^{-10} \left(\frac{T}{300}\right)^{0.5} \exp\left(-\frac{77700}{T}\right)$		28
54	$H_2^+ + H_2 \rightarrow H_3^+ + H$	$k_{54} = 2.24 \times 10^{-9} \left(\frac{T}{300}\right)^{0.042} \exp\left(-\frac{T}{46600}\right)$		48
55	$H_3^+ + H \rightarrow H_2^+ + H_2$	$k_{55} = 7.7 \times 10^{-9} \exp\left(-\frac{17560}{T}\right)$		49
56	$C + H_2^+ \rightarrow CH^+ + H$	$k_{56} = 2.4 \times 10^{-9}$		28
57	$C + H_3^+ \rightarrow CH^+ + H_2$	$k_{57} = 2.0 \times 10^{-9}$		28
58	$C^+ + H_2 \rightarrow CH^+ + H$	$k_{58} = 1.0 \times 10^{-10} \exp\left(-\frac{4640}{T}\right)$		50
59	$CH^+ + H \rightarrow C^+ + H_2$	$k_{59} = 7.5 \times 10^{-10}$		51
60	$CH^+ + H_2 \rightarrow CH_2^+ + H$	$k_{60} = 1.2 \times 10^{-9}$		51
61	$CH^+ + O \rightarrow CO^+ + H$	$k_{61} = 3.5 \times 10^{-10}$		52
62	$CH_2 + H^+ \rightarrow CH^+ + H_2$	$k_{62} = 1.4 \times 10^{-9}$		28
63	$CH_2^+ + H \rightarrow CH^+ + H_2$	$k_{63} = 1.0 \times 10^{-9} \exp\left(-\frac{7080}{T}\right)$		28
64	$CH_2^+ + H_2 \rightarrow CH_3^+ + H$	$k_{64} = 1.6 \times 10^{-9}$		53
65	$CH_2^+ + O \rightarrow HCO^+ + H$	$k_{65} = 7.5 \times 10^{-10}$		28
66	$CH_3^+ + H \rightarrow CH_2^+ + H_2$	$k_{66} = 7.0 \times 10^{-10} \exp\left(-\frac{10560}{T}\right)$		28
67	$CH_3^+ + O \rightarrow HCO^+ + H_2$	$k_{67} = 4.0 \times 10^{-10}$		54
68	$C_2 + O^+ \rightarrow CO^+ + C$	$k_{68} = 4.8 \times 10^{-10}$		28
69	$O^+ + H_2 \rightarrow OH^+ + H$	$k_{69} = 1.7 \times 10^{-9}$		55
70	$O + H_2^+ \rightarrow OH^+ + H$	$k_{70} = 1.5 \times 10^{-9}$		28
71	$O + H_3^+ \rightarrow OH^+ + H_2$	$k_{71} = 8.4 \times 10^{-10}$		56
72	$OH + H_3^+ \rightarrow H_2O^+ + H_2$	$k_{72} = 1.3 \times 10^{-9}$		28
73	$OH + C^+ \rightarrow CO^+ + H$	$k_{73} = 7.7 \times 10^{-10}$		28
74	$OH^+ + H_2 \rightarrow H_2O^+ + H$	$k_{74} = 1.01 \times 10^{-9}$		57
75	$H_2O^+ + H_2 \rightarrow H_3O^+ + H$	$k_{75} = 6.4 \times 10^{-10}$		58
76	$H_2O + H_3^+ \rightarrow H_3O^+ + H_2$	$k_{76} = 5.9 \times 10^{-9}$		59
77	$H_2O + C^+ \rightarrow HCO^+ + H$	$k_{77} = 9.0 \times 10^{-10}$		60
78	$H_2O + C^+ \rightarrow HOC^+ + H$	$k_{78} = 1.8 \times 10^{-9}$		60
79	$H_3O^+ + C \rightarrow HCO^+ + H_2$	$k_{79} = 1.0 \times 10^{-11}$		28
80	$O_2 + C^+ \rightarrow CO^+ + O$	$k_{80} = 3.8 \times 10^{-10}$		53
81	$O_2 + C^+ \rightarrow CO + O^+$	$k_{81} = 6.2 \times 10^{-10}$		53
82	$O_2 + CH_2^+ \rightarrow HCO^+ + OH$	$k_{82} = 9.1 \times 10^{-10}$		53
83	$O_2^+ + C \rightarrow CO^+ + O$	$k_{83} = 5.2 \times 10^{-11}$		28
84	$CO + H_3^+ \rightarrow HOC^+ + H_2$	$k_{84} = 2.7 \times 10^{-11}$		61
85	$CO + H_3^+ \rightarrow HCO^+ + H_2$	$k_{85} = 1.7 \times 10^{-9}$		61
86	$HCO^+ + C \rightarrow CO + CH^+$	$k_{86} = 1.1 \times 10^{-9}$		28
87	$HCO^+ + H_2O \rightarrow CO + H_3O^+$	$k_{87} = 2.5 \times 10^{-9}$		62

(Glover, Federrath, Mac Low, Klessen, 2010, MNRS, 404, 2)

chemical model 2

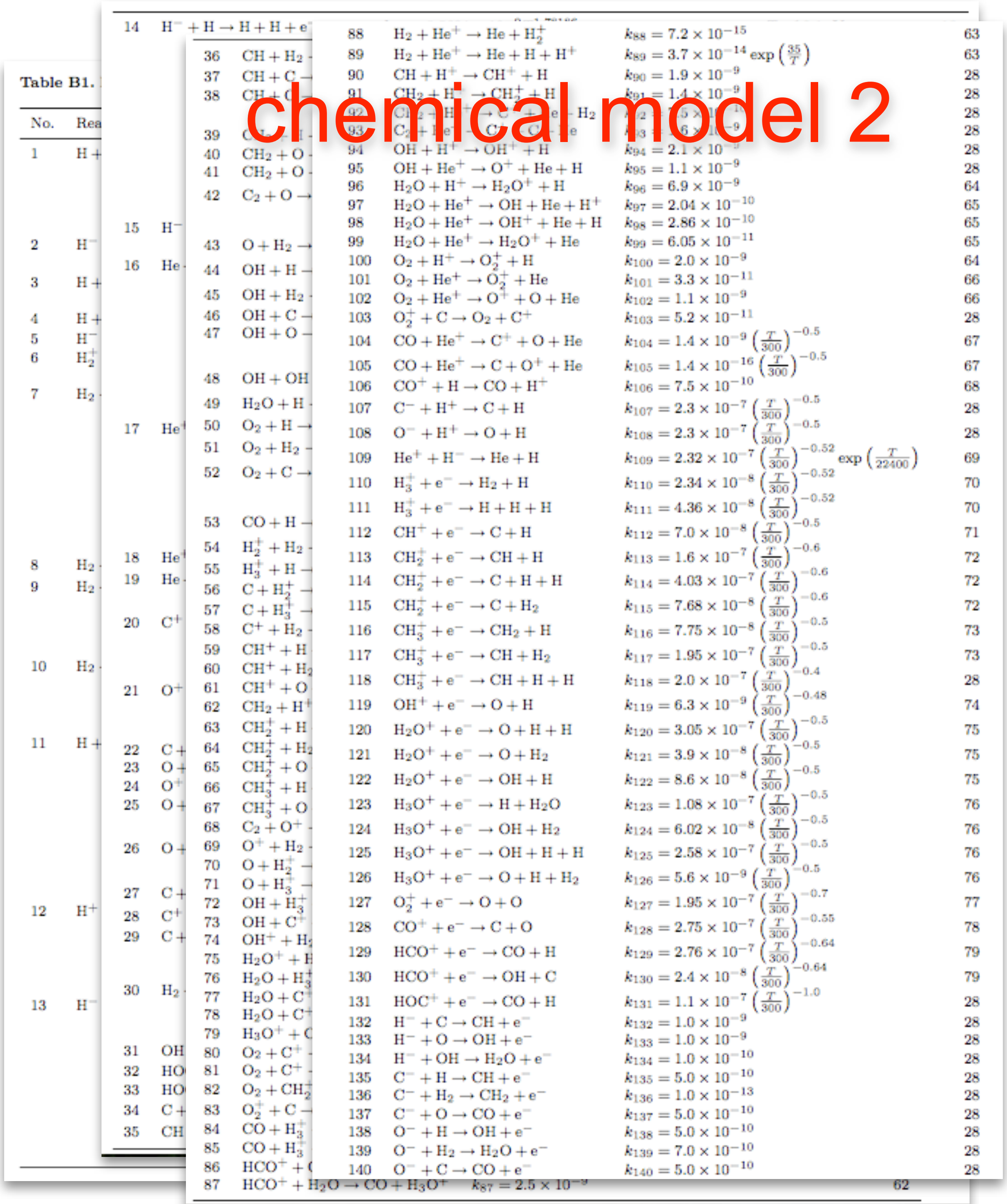

88	$H_2 + He^+ \rightarrow He + H_2^+$	$k_{88} = 7.2 \times 10^{-15}$	63
89	$H_2 + He^+ \rightarrow He + H + H^+$	$k_{89} = 3.7 \times 10^{-14} \exp\left(\frac{35}{T}\right)$	63
90	$CH + H^+ \rightarrow CH^+ + H$	$k_{90} = 1.9 \times 10^{-9}$	28
91	$CH_2 + H^+ \rightarrow CH_2^+ + H$	$k_{91} = 1.4 \times 10^{-9}$	28
92	$CH_2 + He^+ \rightarrow C^+ + He + H_2$	$k_{92} = 7.5 \times 10^{-10}$	28
93	$C_2 + He^+ \rightarrow C^+ + C + He$	$k_{93} = 1.6 \times 10^{-9}$	28
94	$OH + H^+ \rightarrow OH^+ + H$	$k_{94} = 2.1 \times 10^{-9}$	28
95	$OH + He^+ \rightarrow O^+ + He + H$	$k_{95} = 1.1 \times 10^{-9}$	28
96	$H_2O + H^+ \rightarrow H_2O^+ + H$	$k_{96} = 6.9 \times 10^{-9}$	64
97	$H_2O + He^+ \rightarrow OH + He + H^+$	$k_{97} = 2.04 \times 10^{-10}$	65
98	$H_2O + He^+ \rightarrow OH^+ + He + H$	$k_{98} = 2.86 \times 10^{-10}$	65
99	$H_2O + He^+ \rightarrow H_2O^+ + He$	$k_{99} = 6.05 \times 10^{-11}$	65
100	$O_2 + H^+ \rightarrow O_2^+ + H$	$k_{100} = 2.0 \times 10^{-9}$	64
101	$O_2 + He^+ \rightarrow O_2^+ + He$	$k_{101} = 3.3 \times 10^{-11}$	66
102	$O_2 + He^+ \rightarrow O^+ + O + He$	$k_{102} = 1.1 \times 10^{-9}$	66
103	$O_2^+ + C \rightarrow O_2 + C^+$	$k_{103} = 5.2 \times 10^{-11}$	28
104	$CO + He^+ \rightarrow C^+ + O + He$	$k_{104} = 1.4 \times 10^{-9} \left(\frac{T}{300}\right)^{-0.5}$	67
105	$CO + He^+ \rightarrow C + O^+ + He$	$k_{105} = 1.4 \times 10^{-16} \left(\frac{T}{300}\right)^{-0.5}$	67
106	$CO^+ + H \rightarrow CO + H^+$	$k_{106} = 7.5 \times 10^{-10}$	68
107	$C^- + H^+ \rightarrow C + H$	$k_{107} = 2.3 \times 10^{-7} \left(\frac{T}{300}\right)^{-0.5}$	28
108	$O^- + H^+ \rightarrow O + H$	$k_{108} = 2.3 \times 10^{-7} \left(\frac{T}{300}\right)^{-0.5}$	28
109	$He^+ + H^- \rightarrow He + H$	$k_{109} = 2.32 \times 10^{-7} \left(\frac{T}{300}\right)^{-0.52} \exp\left(\frac{T}{22400}\right)$	69
110	$H_3^+ + e^- \rightarrow H_2 + H$	$k_{110} = 2.34 \times 10^{-8} \left(\frac{T}{300}\right)^{-0.52}$	70
111	$H_3^+ + e^- \rightarrow H + H + H$	$k_{111} = 4.36 \times 10^{-8} \left(\frac{T}{300}\right)^{-0.52}$	70
112	$CH^+ + e^- \rightarrow C + H$	$k_{112} = 7.0 \times 10^{-8} \left(\frac{T}{300}\right)^{-0.5}$	71
113	$CH_2^+ + e^- \rightarrow CH + H$	$k_{113} = 1.6 \times 10^{-7} \left(\frac{T}{300}\right)^{-0.6}$	72
114	$CH_2^+ + e^- \rightarrow C + H + H$	$k_{114} = 4.03 \times 10^{-7} \left(\frac{T}{300}\right)^{-0.6}$	72
115	$CH_2^+ + e^- \rightarrow C + H_2$	$k_{115} = 7.68 \times 10^{-8} \left(\frac{T}{300}\right)^{-0.6}$	72
116	$CH_3^+ + e^- \rightarrow CH_2 + H$	$k_{116} = 7.75 \times 10^{-8} \left(\frac{T}{300}\right)^{-0.5}$	73
117	$CH_3^+ + e^- \rightarrow CH + H_2$	$k_{117} = 1.95 \times 10^{-7} \left(\frac{T}{300}\right)^{-0.5}$	73
118	$CH_3^+ + e^- \rightarrow CH + H + H$	$k_{118} = 2.0 \times 10^{-7} \left(\frac{T}{300}\right)^{-0.4}$	28
119	$OH^+ + e^- \rightarrow O + H$	$k_{119} = 6.3 \times 10^{-9} \left(\frac{T}{300}\right)^{-0.48}$	74
120	$H_2O^+ + e^- \rightarrow O + H + H$	$k_{120} = 3.05 \times 10^{-7} \left(\frac{T}{300}\right)^{-0.5}$	75
121	$H_2O^+ + e^- \rightarrow O + H_2$	$k_{121} = 3.9 \times 10^{-8} \left(\frac{T}{300}\right)^{-0.5}$	75
122	$H_2O^+ + e^- \rightarrow OH + H$	$k_{122} = 8.6 \times 10^{-8} \left(\frac{T}{300}\right)^{-0.5}$	75
123	$H_3O^+ + e^- \rightarrow H + H_2O$	$k_{123} = 1.08 \times 10^{-7} \left(\frac{T}{300}\right)^{-0.5}$	76
124	$H_3O^+ + e^- \rightarrow OH + H_2$	$k_{124} = 6.02 \times 10^{-8} \left(\frac{T}{300}\right)^{-0.5}$	76
125	$H_3O^+ + e^- \rightarrow OH + H + H$	$k_{125} = 2.58 \times 10^{-7} \left(\frac{T}{300}\right)^{-0.5}$	76
126	$H_3O^+ + e^- \rightarrow O + H + H_2$	$k_{126} = 5.6 \times 10^{-9} \left(\frac{T}{300}\right)^{-0.5}$	76
127	$O_2^+ + e^- \rightarrow O + O$	$k_{127} = 1.95 \times 10^{-7} \left(\frac{T}{300}\right)^{-0.7}$	77
128	$CO^+ + e^- \rightarrow C + O$	$k_{128} = 2.75 \times 10^{-7} \left(\frac{T}{300}\right)^{-0.55}$	78
129	$HCO^+ + e^- \rightarrow CO + H$	$k_{129} = 2.76 \times 10^{-7} \left(\frac{T}{300}\right)^{-0.64}$	79
130	$HCO^+ + e^- \rightarrow OH + C$	$k_{130} = 2.4 \times 10^{-8} \left(\frac{T}{300}\right)^{-0.64}$	79
131	$HOC^+ + e^- \rightarrow CO + H$	$k_{131} = 1.1 \times 10^{-7} \left(\frac{T}{300}\right)^{-1.0}$	28
132	$H^- + C \rightarrow CH + e^-$	$k_{132} = 1.0 \times 10^{-9}$	28
133	$H^- + O \rightarrow OH + e^-$	$k_{133} = 1.0 \times 10^{-9}$	28
134	$H^- + OH \rightarrow H_2O + e^-$	$k_{134} = 1.0 \times 10^{-10}$	28
135	$C^- + H \rightarrow CH + e^-$	$k_{135} = 5.0 \times 10^{-10}$	28
136	$C^- + H_2 \rightarrow CH_2 + e^-$	$k_{136} = 1.0 \times 10^{-13}$	28
137	$C^- + O \rightarrow CO + e^-$	$k_{137} = 5.0 \times 10^{-10}$	28
138	$O^- + H \rightarrow OH + e^-$	$k_{138} = 5.0 \times 10^{-10}$	28
139	$O^- + H_2 \rightarrow H_2O + e^-$	$k_{139} = 7.0 \times 10^{-10}$	28
140	$O^- + C \rightarrow CO + e^-$	$k_{140} = 5.0 \times 10^{-10}$	28

87 $HCO^+ + H_2O \rightarrow CO + H_3O^+$ $k_{87} = 2.5 \times 10^{-9}$ 62

(Glover, Federrath, Mac Low, Klessen, 2010, MNRS, 404, 2)

chemical model 2

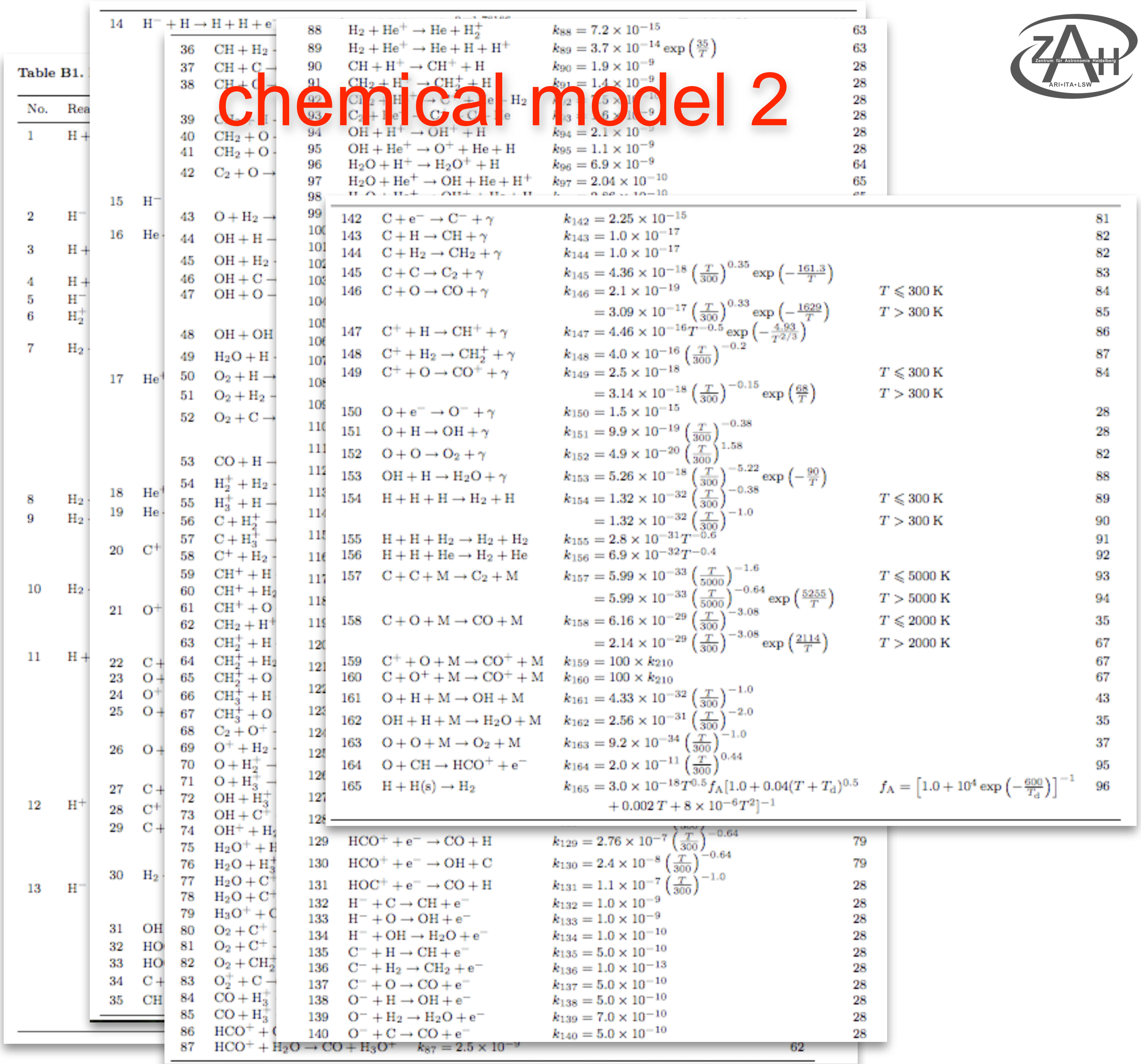

Table B1.

88	$H_2 + He^+ \rightarrow He + H_2^+$	$k_{88} = 7.2 \times 10^{-15}$	63
89	$H_2 + He^+ \rightarrow He + H + H^+$	$k_{89} = 3.7 \times 10^{-14} \exp\left(\frac{35}{T}\right)$	63
90	$CH + H^+ \rightarrow CH^+ + H$	$k_{90} = 1.9 \times 10^{-9}$	28
91	$CH_2 + H^+ \rightarrow CH_2^+ + H$	$k_{91} = 1.4 \times 10^{-9}$	28
92	$CH_2 + He^+ \rightarrow C^+ + He + H_2$	$k_{92} = 7.5 \times 10^{-10}$	28
93	$C_2 + He^+ \rightarrow C^+ + C + He$	$k_{93} = 1.6 \times 10^{-9}$	28
94	$OH + H^+ \rightarrow OH^+ + H$	$k_{94} = 2.1 \times 10^{-9}$	28
95	$OH + He^+ \rightarrow O^+ + He + H$	$k_{95} = 1.1 \times 10^{-9}$	28
96	$H_2O + H^+ \rightarrow H_2O^+ + H$	$k_{96} = 6.9 \times 10^{-9}$	64
97	$H_2O + He^+ \rightarrow OH + He + H^+$	$k_{97} = 2.04 \times 10^{-10}$	65
129	$HCO^+ + e^- \rightarrow CO + H$	$k_{129} = 2.76 \times 10^{-7} \left(\frac{T}{300}\right)^{-0.64}$	79
130	$HCO^+ + e^- \rightarrow OH + C$	$k_{130} = 2.4 \times 10^{-8} \left(\frac{T}{300}\right)^{-0.64}$	79
131	$HOC^+ + e^- \rightarrow CO + H$	$k_{131} = 1.1 \times 10^{-7} \left(\frac{T}{300}\right)^{-1.0}$	28
132	$H^- + C \rightarrow CH + e^-$	$k_{132} = 1.0 \times 10^{-9}$	28
133	$H^- + O \rightarrow OH + e^-$	$k_{133} = 1.0 \times 10^{-9}$	28
134	$H^- + OH \rightarrow H_2O + e^-$	$k_{134} = 1.0 \times 10^{-10}$	28
135	$C^- + H \rightarrow CH + e^-$	$k_{135} = 5.0 \times 10^{-10}$	28
136	$C^- + H_2 \rightarrow CH_2 + e^-$	$k_{136} = 1.0 \times 10^{-13}$	28
137	$C^- + O \rightarrow CO + e^-$	$k_{137} = 5.0 \times 10^{-10}$	28
138	$O^- + H \rightarrow OH + e^-$	$k_{138} = 5.0 \times 10^{-10}$	28
139	$O^- + H_2 \rightarrow H_2O + e^-$	$k_{139} = 7.0 \times 10^{-10}$	28
140	$O^- + C \rightarrow CO + e^-$	$k_{140} = 5.0 \times 10^{-10}$	28

142	$C + e^- \rightarrow C^- + \gamma$	$k_{142} = 2.25 \times 10^{-15}$		81
143	$C + H \rightarrow CH + \gamma$	$k_{143} = 1.0 \times 10^{-17}$		82
144	$C + H_2 \rightarrow CH_2 + \gamma$	$k_{144} = 1.0 \times 10^{-17}$		82
145	$C + C \rightarrow C_2 + \gamma$	$k_{145} = 4.36 \times 10^{-18} \left(\frac{T}{300}\right)^{0.35} \exp\left(-\frac{161.3}{T}\right)$		83
146	$C + O \rightarrow CO + \gamma$	$k_{146} = 2.1 \times 10^{-19}$	$T \leqslant 300$ K	84
		$= 3.09 \times 10^{-17} \left(\frac{T}{300}\right)^{0.33} \exp\left(-\frac{1629}{T}\right)$	$T > 300$ K	85
147	$C^+ + H \rightarrow CH^+ + \gamma$	$k_{147} = 4.46 \times 10^{-16} T^{-0.5} \exp\left(-\frac{4.93}{T^{2/3}}\right)$		86
148	$C^+ + H_2 \rightarrow CH_2^+ + \gamma$	$k_{148} = 4.0 \times 10^{-16} \left(\frac{T}{300}\right)^{-0.2}$		87
149	$C^+ + O \rightarrow CO^+ + \gamma$	$k_{149} = 2.5 \times 10^{-18}$	$T \leqslant 300$ K	84
		$= 3.14 \times 10^{-18} \left(\frac{T}{300}\right)^{-0.15} \exp\left(\frac{68}{T}\right)$	$T > 300$ K	
150	$O + e^- \rightarrow O^- + \gamma$	$k_{150} = 1.5 \times 10^{-15}$		28
151	$O + H \rightarrow OH + \gamma$	$k_{151} = 9.9 \times 10^{-19} \left(\frac{T}{300}\right)^{-0.38}$		28
152	$O + O \rightarrow O_2 + \gamma$	$k_{152} = 4.9 \times 10^{-20} \left(\frac{T}{300}\right)^{1.58}$		82
153	$OH + H \rightarrow H_2O + \gamma$	$k_{153} = 5.26 \times 10^{-18} \left(\frac{T}{300}\right)^{-5.22} \exp\left(-\frac{90}{T}\right)$		88
154	$H + H + H \rightarrow H_2 + H$	$k_{154} = 1.32 \times 10^{-32} \left(\frac{T}{300}\right)^{-0.38}$	$T \leqslant 300$ K	89
		$= 1.32 \times 10^{-32} \left(\frac{T}{300}\right)^{-1.0}$	$T > 300$ K	90
155	$H + H + H_2 \rightarrow H_2 + H_2$	$k_{155} = 2.8 \times 10^{-31} T^{-0.6}$		91
156	$H + H + He \rightarrow H_2 + He$	$k_{156} = 6.9 \times 10^{-32} T^{-0.4}$		92
157	$C + C + M \rightarrow C_2 + M$	$k_{157} = 5.99 \times 10^{-33} \left(\frac{T}{5000}\right)^{-1.6}$	$T \leqslant 5000$ K	93
		$= 5.99 \times 10^{-33} \left(\frac{T}{5000}\right)^{-0.64} \exp\left(\frac{5255}{T}\right)$	$T > 5000$ K	94
158	$C + O + M \rightarrow CO + M$	$k_{158} = 6.16 \times 10^{-29} \left(\frac{T}{300}\right)^{-3.08}$	$T \leqslant 2000$ K	35
		$= 2.14 \times 10^{-29} \left(\frac{T}{300}\right)^{-3.08} \exp\left(\frac{2114}{T}\right)$	$T > 2000$ K	67
159	$C^+ + O + M \rightarrow CO^+ + M$	$k_{159} = 100 \times k_{210}$		67
160	$C + O^+ + M \rightarrow CO^+ + M$	$k_{160} = 100 \times k_{210}$		67
161	$O + H + M \rightarrow OH + M$	$k_{161} = 4.33 \times 10^{-32} \left(\frac{T}{300}\right)^{-1.0}$		43
162	$OH + H + M \rightarrow H_2O + M$	$k_{162} = 2.56 \times 10^{-31} \left(\frac{T}{300}\right)^{-2.0}$		35
163	$O + O + M \rightarrow O_2 + M$	$k_{163} = 9.2 \times 10^{-34} \left(\frac{T}{300}\right)^{-1.0}$		37
164	$O + CH \rightarrow HCO^+ + e^-$	$k_{164} = 2.0 \times 10^{-11} \left(\frac{T}{300}\right)^{0.44}$		95
165	$H + H(s) \rightarrow H_2$	$k_{165} = 3.0 \times 10^{-18} T^{0.5} f_A [1.0 + 0.04(T + T_d)^{0.5}$ $+ 0.002\,T + 8 \times 10^{-6} T^2]^{-1}$	$f_A = \left[1.0 + 10^4 \exp\left(-\frac{600}{T_d}\right)\right]^{-1}$	96

(Glover, Federrath, Mac Low, Klessen, 2010, MNRAS, 404, 2)

chemical model 2

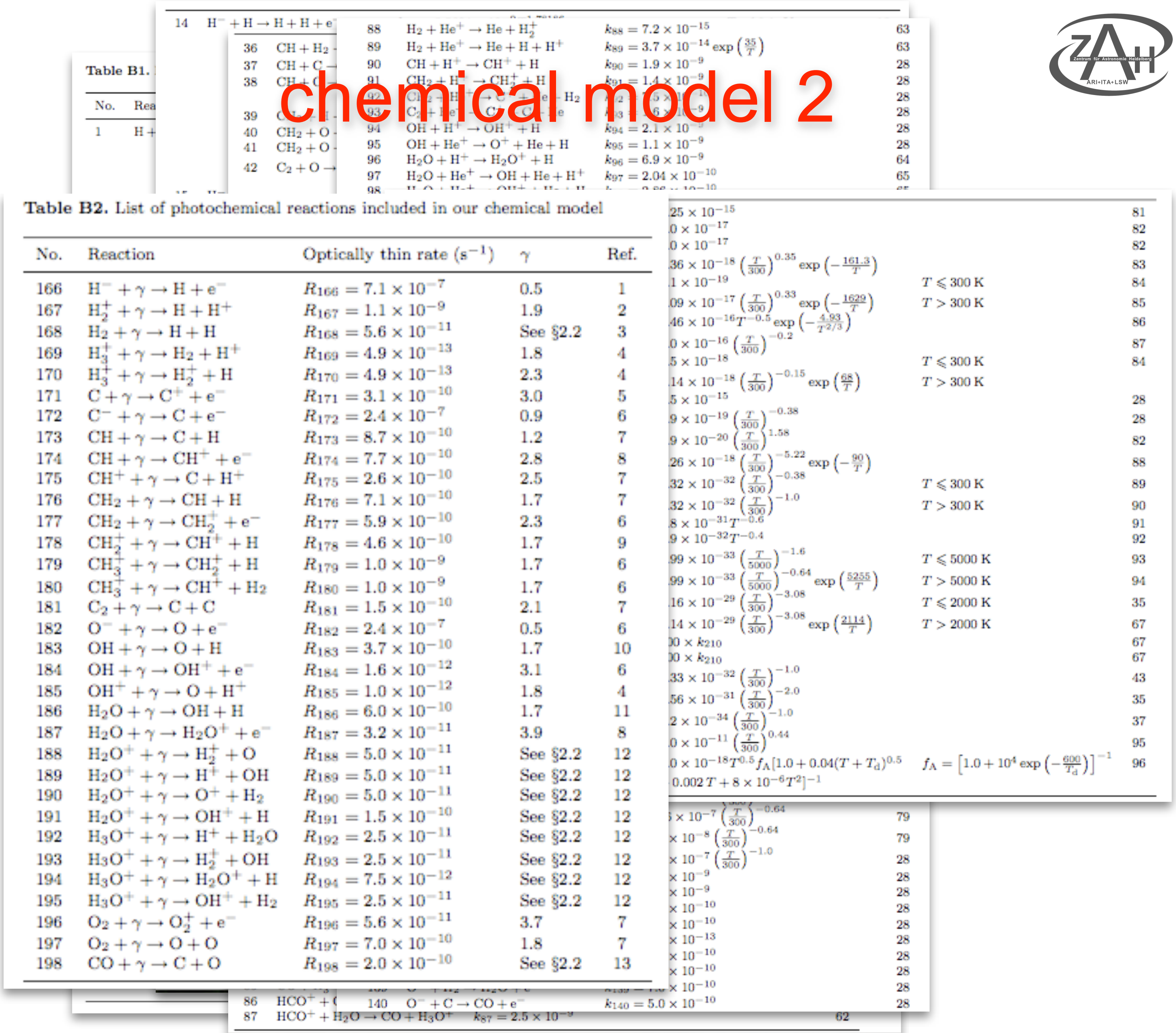

88	$H_2 + He^+ \rightarrow He + H_2^+$	$k_{88} = 7.2 \times 10^{-15}$	63
89	$H_2 + He^+ \rightarrow He + H + H^+$	$k_{89} = 3.7 \times 10^{-14} \exp\left(\frac{35}{T}\right)$	63
90	$CH + H^+ \rightarrow CH^+ + H$	$k_{90} = 1.9 \times 10^{-9}$	28
91	$CH_2 + H^+ \rightarrow CH_2^+ + H$	$k_{91} = 1.4 \times 10^{-9}$	28
92	$CH_2 + He^+ \rightarrow C^+ + He + H_2$	$k_{92} = 7.5 \times 10^{-10}$	28
93	$C_2 + He^+ \rightarrow C^+ + C + He$	$k_{93} = 1.6 \times 10^{-9}$	28
94	$OH + H^+ \rightarrow OH^+ + H$	$k_{94} = 2.1 \times 10^{-9}$	28
95	$OH + He^+ \rightarrow O^+ + He + H$	$k_{95} = 1.1 \times 10^{-9}$	28
96	$H_2O + H^+ \rightarrow H_2O^+ + H$	$k_{96} = 6.9 \times 10^{-9}$	64
97	$H_2O + He^+ \rightarrow OH + He + H^+$	$k_{97} = 2.04 \times 10^{-10}$	65

Table B2. List of photochemical reactions included in our chemical model

No.	Reaction	Optically thin rate (s^{-1})	γ	Ref.
166	$H^- + \gamma \rightarrow H + e^-$	$R_{166} = 7.1 \times 10^{-7}$	0.5	1
167	$H_2^+ + \gamma \rightarrow H + H^+$	$R_{167} = 1.1 \times 10^{-9}$	1.9	2
168	$H_2 + \gamma \rightarrow H + H$	$R_{168} = 5.6 \times 10^{-11}$	See §2.2	3
169	$H_3^+ + \gamma \rightarrow H_2 + H^+$	$R_{169} = 4.9 \times 10^{-13}$	1.8	4
170	$H_3^+ + \gamma \rightarrow H_2^+ + H$	$R_{170} = 4.9 \times 10^{-13}$	2.3	4
171	$C + \gamma \rightarrow C^+ + e^-$	$R_{171} = 3.1 \times 10^{-10}$	3.0	5
172	$C^- + \gamma \rightarrow C + e^-$	$R_{172} = 2.4 \times 10^{-7}$	0.9	6
173	$CH + \gamma \rightarrow C + H$	$R_{173} = 8.7 \times 10^{-10}$	1.2	7
174	$CH + \gamma \rightarrow CH^+ + e^-$	$R_{174} = 7.7 \times 10^{-10}$	2.8	8
175	$CH^+ + \gamma \rightarrow C + H^+$	$R_{175} = 2.6 \times 10^{-10}$	2.5	7
176	$CH_2 + \gamma \rightarrow CH + H$	$R_{176} = 7.1 \times 10^{-10}$	1.7	7
177	$CH_2 + \gamma \rightarrow CH_2^+ + e^-$	$R_{177} = 5.9 \times 10^{-10}$	2.3	6
178	$CH_2^+ + \gamma \rightarrow CH^+ + H$	$R_{178} = 4.6 \times 10^{-10}$	1.7	9
179	$CH_3^+ + \gamma \rightarrow CH_2^+ + H$	$R_{179} = 1.0 \times 10^{-9}$	1.7	6
180	$CH_3^+ + \gamma \rightarrow CH^+ + H_2$	$R_{180} = 1.0 \times 10^{-9}$	1.7	6
181	$C_2 + \gamma \rightarrow C + C$	$R_{181} = 1.5 \times 10^{-10}$	2.1	7
182	$O^- + \gamma \rightarrow O + e^-$	$R_{182} = 2.4 \times 10^{-7}$	0.5	6
183	$OH + \gamma \rightarrow O + H$	$R_{183} = 3.7 \times 10^{-10}$	1.7	10
184	$OH + \gamma \rightarrow OH^+ + e^-$	$R_{184} = 1.6 \times 10^{-12}$	3.1	6
185	$OH^+ + \gamma \rightarrow O + H^+$	$R_{185} = 1.0 \times 10^{-12}$	1.8	4
186	$H_2O + \gamma \rightarrow OH + H$	$R_{186} = 6.0 \times 10^{-10}$	1.7	11
187	$H_2O + \gamma \rightarrow H_2O^+ + e^-$	$R_{187} = 3.2 \times 10^{-11}$	3.9	8
188	$H_2O^+ + \gamma \rightarrow H_2^+ + O$	$R_{188} = 5.0 \times 10^{-11}$	See §2.2	12
189	$H_2O^+ + \gamma \rightarrow H^+ + OH$	$R_{189} = 5.0 \times 10^{-11}$	See §2.2	12
190	$H_2O^+ + \gamma \rightarrow O^+ + H_2$	$R_{190} = 5.0 \times 10^{-11}$	See §2.2	12
191	$H_2O^+ + \gamma \rightarrow OH^+ + H$	$R_{191} = 1.5 \times 10^{-10}$	See §2.2	12
192	$H_3O^+ + \gamma \rightarrow H^+ + H_2O$	$R_{192} = 2.5 \times 10^{-11}$	See §2.2	12
193	$H_3O^+ + \gamma \rightarrow H_2^+ + OH$	$R_{193} = 2.5 \times 10^{-11}$	See §2.2	12
194	$H_3O^+ + \gamma \rightarrow H_2O^+ + H$	$R_{194} = 7.5 \times 10^{-12}$	See §2.2	12
195	$H_3O^+ + \gamma \rightarrow OH^+ + H_2$	$R_{195} = 2.5 \times 10^{-11}$	See §2.2	12
196	$O_2 + \gamma \rightarrow O_2^+ + e^-$	$R_{196} = 5.6 \times 10^{-11}$	3.7	7
197	$O_2 + \gamma \rightarrow O + O$	$R_{197} = 7.0 \times 10^{-10}$	1.8	7
198	$CO + \gamma \rightarrow C + O$	$R_{198} = 2.0 \times 10^{-10}$	See §2.2	13

25×10^{-15}		81
0×10^{-17}		82
0×10^{-17}		82
$36 \times 10^{-18} \left(\frac{T}{300}\right)^{0.35} \exp\left(-\frac{161.3}{T}\right)$		83
1×10^{-19}	$T \leqslant 300$ K	84
$09 \times 10^{-17} \left(\frac{T}{300}\right)^{0.33} \exp\left(-\frac{1629}{T}\right)$	$T > 300$ K	85
$46 \times 10^{-16} T^{-0.5} \exp\left(-\frac{4.93}{T^{2/3}}\right)$		86
$0 \times 10^{-16} \left(\frac{T}{300}\right)^{-0.2}$		87
5×10^{-18}	$T \leqslant 300$ K	84
$14 \times 10^{-18} \left(\frac{T}{300}\right)^{-0.15} \exp\left(\frac{68}{T}\right)$	$T > 300$ K	
5×10^{-15}		28
$9 \times 10^{-19} \left(\frac{T}{300}\right)^{-0.38}$		28
$9 \times 10^{-20} \left(\frac{T}{300}\right)^{1.58}$		82
$26 \times 10^{-18} \left(\frac{T}{300}\right)^{-5.22} \exp\left(-\frac{90}{T}\right)$		88
$32 \times 10^{-32} \left(\frac{T}{300}\right)^{-0.38}$	$T \leqslant 300$ K	89
$32 \times 10^{-32} \left(\frac{T}{300}\right)^{-1.0}$	$T > 300$ K	90
$8 \times 10^{-31} T^{-0.6}$		91
$9 \times 10^{-32} T^{-0.4}$		92
$99 \times 10^{-33} \left(\frac{T}{5000}\right)^{-1.6}$	$T \leqslant 5000$ K	93
$99 \times 10^{-33} \left(\frac{T}{5000}\right)^{-0.64} \exp\left(\frac{5255}{T}\right)$	$T > 5000$ K	94
$16 \times 10^{-29} \left(\frac{T}{300}\right)^{-3.08}$	$T \leqslant 2000$ K	35
$14 \times 10^{-29} \left(\frac{T}{300}\right)^{-3.08} \exp\left(\frac{2114}{T}\right)$	$T > 2000$ K	67
$00 \times k_{210}$		67
$00 \times k_{210}$		67
$33 \times 10^{-32} \left(\frac{T}{300}\right)^{-1.0}$		43
$56 \times 10^{-31} \left(\frac{T}{300}\right)^{-2.0}$		35
$2 \times 10^{-34} \left(\frac{T}{300}\right)^{-1.0}$		37
$0 \times 10^{-11} \left(\frac{T}{300}\right)^{0.44}$		95
$0 \times 10^{-18} T^{0.5} f_A [1.0 + 0.04(T + T_d)^{0.5}$ $0.002\, T + 8 \times 10^{-6} T^2]^{-1}$	$f_A = \left[1.0 + 10^4 \exp\left(-\frac{600}{T_d}\right)\right]^{-1}$	96

(Glover, Federrath, Mac Low, Klessen, 2010, MNRAS, 404, 2)

chemical model 2

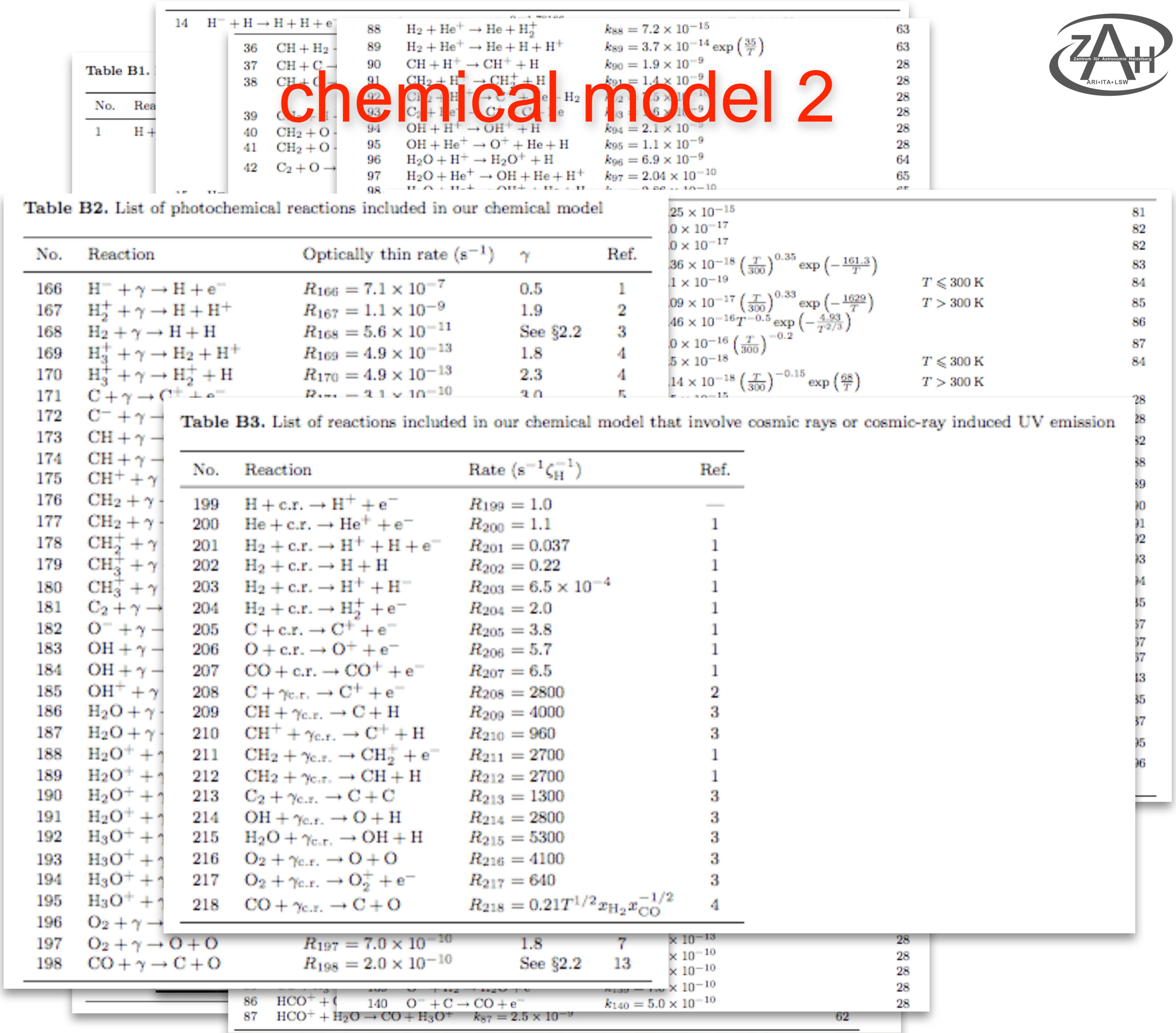

14	$H^- + H \rightarrow H + H + e^-$		
36	$CH + H_2$		
37	$CH + C$		
38	$CH + C$		
39			
40	$CH_2 + O$		
41	$CH_2 + O$		
42	$C_2 + O \rightarrow$		
88	$H_2 + He^+ \rightarrow He + H_2^+$	$k_{88} = 7.2 \times 10^{-15}$	63
89	$H_2 + He^+ \rightarrow He + H + H^+$	$k_{89} = 3.7 \times 10^{-14} \exp\left(\frac{35}{T}\right)$	63
90	$CH + H^+ \rightarrow CH^+ + H$	$k_{90} = 1.9 \times 10^{-9}$	28
91	$CH_2 + H^+ \rightarrow CH_2^+ + H$	$k_{91} = 1.4 \times 10^{-9}$	28
92	[illegible]	[illegible]	28
93	[illegible]	[illegible]	28
94	$OH + H^+ \rightarrow OH^+ + H$	$k_{94} = 2.1 \times 10^{-9}$	28
95	$OH + He^+ \rightarrow O^+ + He + H$	$k_{95} = 1.1 \times 10^{-9}$	28
96	$H_2O + H^+ \rightarrow H_2O^+ + H$	$k_{96} = 6.9 \times 10^{-9}$	64
97	$H_2O + He^+ \rightarrow OH + He + H^+$	$k_{97} = 2.04 \times 10^{-10}$	65

25×10^{-15}		81
0×10^{-17}		82
0×10^{-17}		82
$36 \times 10^{-18} \left(\frac{T}{300}\right)^{0.35} \exp\left(-\frac{161.3}{T}\right)$		83
1×10^{-19}	$T \leqslant 300$ K	84
$09 \times 10^{-17} \left(\frac{T}{300}\right)^{0.33} \exp\left(-\frac{1629}{T}\right)$	$T > 300$ K	85
$46 \times 10^{-16} T^{-0.5} \exp\left(-\frac{4.93}{T^{2/3}}\right)$		86
$0 \times 10^{-16} \left(\frac{T}{300}\right)^{-0.2}$		87
5×10^{-18}	$T \leqslant 300$ K	84
$14 \times 10^{-18} \left(\frac{T}{300}\right)^{-0.15} \exp\left(\frac{68}{T}\right)$	$T > 300$ K	

Table B2. List of photochemical reactions included in our chemical model

No.	Reaction	Optically thin rate (s^{-1})	γ	Ref.
166	$H^- + \gamma \rightarrow H + e^-$	$R_{166} = 7.1 \times 10^{-7}$	0.5	1
167	$H_2^+ + \gamma \rightarrow H + H^+$	$R_{167} = 1.1 \times 10^{-9}$	1.9	2
168	$H_2 + \gamma \rightarrow H + H$	$R_{168} = 5.6 \times 10^{-11}$	See §2.2	3
169	$H_3^+ + \gamma \rightarrow H_2 + H^+$	$R_{169} = 4.9 \times 10^{-13}$	1.8	4
170	$H_3^+ + \gamma \rightarrow H_2^+ + H$	$R_{170} = 4.9 \times 10^{-13}$	2.3	4
171	$C + \gamma \rightarrow C^+ + e^-$	$R_{171} = 3.1 \times 10^{-10}$	3.0	5
172	$C^- + \gamma \rightarrow$			
173	$CH + \gamma \rightarrow$			
174	$CH + \gamma \rightarrow$			
175	$CH^+ + \gamma$			
176	$CH_2 + \gamma$			
177	$CH_2 + \gamma$			
178	$CH_2^+ + \gamma$			
179	$CH_3^+ + \gamma$			
180	$CH_3^+ + \gamma$			
181	$C_2 + \gamma \rightarrow$			
182	$O^- + \gamma \rightarrow$			
183	$OH + \gamma \rightarrow$			
184	$OH + \gamma \rightarrow$			
185	$OH^+ + \gamma$			
186	$H_2O + \gamma$			
187	$H_2O + \gamma$			
188	$H_2O^+ + \gamma$			
189	$H_2O^+ + \gamma$			
190	$H_2O^+ + \gamma$			
191	$H_2O^+ + \gamma$			
192	$H_3O^+ + \gamma$			
193	$H_3O^+ + \gamma$			
194	$H_3O^+ + \gamma$			
195	$H_3O^+ + \gamma$			
196	$O_2 + \gamma \rightarrow$			
197	$O_2 + \gamma \rightarrow O + O$	$R_{197} = 7.0 \times 10^{-10}$	1.8	7
198	$CO + \gamma \rightarrow C + O$	$R_{198} = 2.0 \times 10^{-10}$	See §2.2	13

Table B3. List of reactions included in our chemical model that involve cosmic rays or cosmic-ray induced UV emission

No.	Reaction	Rate ($s^{-1} \zeta_H^{-1}$)	Ref.
199	$H + c.r. \rightarrow H^+ + e^-$	$R_{199} = 1.0$	—
200	$He + c.r. \rightarrow He^+ + e^-$	$R_{200} = 1.1$	1
201	$H_2 + c.r. \rightarrow H^+ + H + e^-$	$R_{201} = 0.037$	1
202	$H_2 + c.r. \rightarrow H + H$	$R_{202} = 0.22$	1
203	$H_2 + c.r. \rightarrow H^+ + H^-$	$R_{203} = 6.5 \times 10^{-4}$	1
204	$H_2 + c.r. \rightarrow H_2^+ + e^-$	$R_{204} = 2.0$	1
205	$C + c.r. \rightarrow C^+ + e^-$	$R_{205} = 3.8$	1
206	$O + c.r. \rightarrow O^+ + e^-$	$R_{206} = 5.7$	1
207	$CO + c.r. \rightarrow CO^+ + e^-$	$R_{207} = 6.5$	1
208	$C + \gamma_{c.r.} \rightarrow C^+ + e^-$	$R_{208} = 2800$	2
209	$CH + \gamma_{c.r.} \rightarrow C + H$	$R_{209} = 4000$	3
210	$CH^+ + \gamma_{c.r.} \rightarrow C^+ + H$	$R_{210} = 960$	3
211	$CH_2 + \gamma_{c.r.} \rightarrow CH_2^+ + e^-$	$R_{211} = 2700$	1
212	$CH_2 + \gamma_{c.r.} \rightarrow CH + H$	$R_{212} = 2700$	1
213	$C_2 + \gamma_{c.r.} \rightarrow C + C$	$R_{213} = 1300$	3
214	$OH + \gamma_{c.r.} \rightarrow O + H$	$R_{214} = 2800$	3
215	$H_2O + \gamma_{c.r.} \rightarrow OH + H$	$R_{215} = 5300$	3
216	$O_2 + \gamma_{c.r.} \rightarrow O + O$	$R_{216} = 4100$	3
217	$O_2 + \gamma_{c.r.} \rightarrow O_2^+ + e^-$	$R_{217} = 640$	3
218	$CO + \gamma_{c.r.} \rightarrow C + O$	$R_{218} = 0.21 T^{1/2} x_{H_2} x_{CO}^{-1/2}$	4

86	$HCO^+ + C$		
87	$HCO^+ + H_2O \rightarrow CO + H_3O^+$	$k_{87} = 2.5 \times 10^{-9}$	62
140	$O^- + C \rightarrow CO + e^-$	$k_{140} = 5.0 \times 10^{-10}$	28

(Glover, Federrath, Mac Low, Klessen, 2010, MNRS, 404, 2)

HI to H2 conversion rate

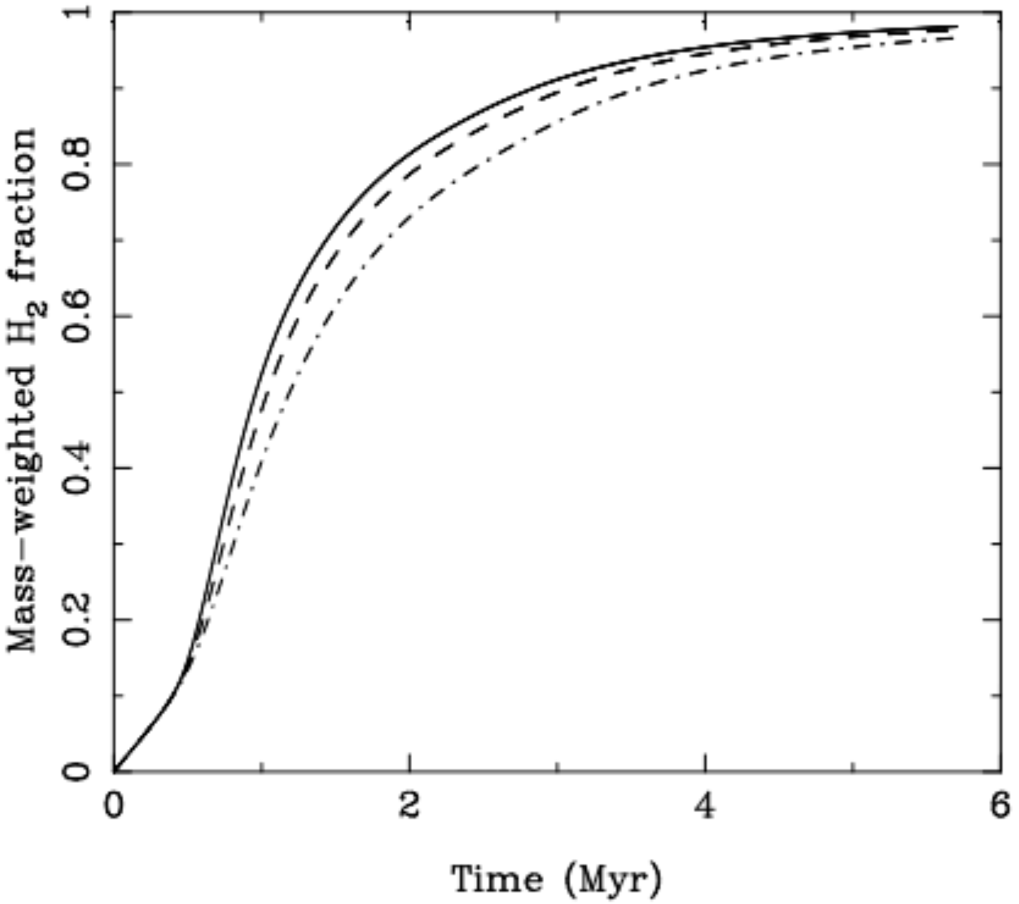

Figure 4. Time evolution of the mass-weighted H_2 abundance in simulations R1, R2 and R3, which have numerical resolutions of 64^3 zones (dot-dashed), 128^3 zones (dashed) and 256^3 zones (solid), respectively.

(Glover, Federrath, Mac Low, Klessen, 2010)

HI to H2 conversion rate

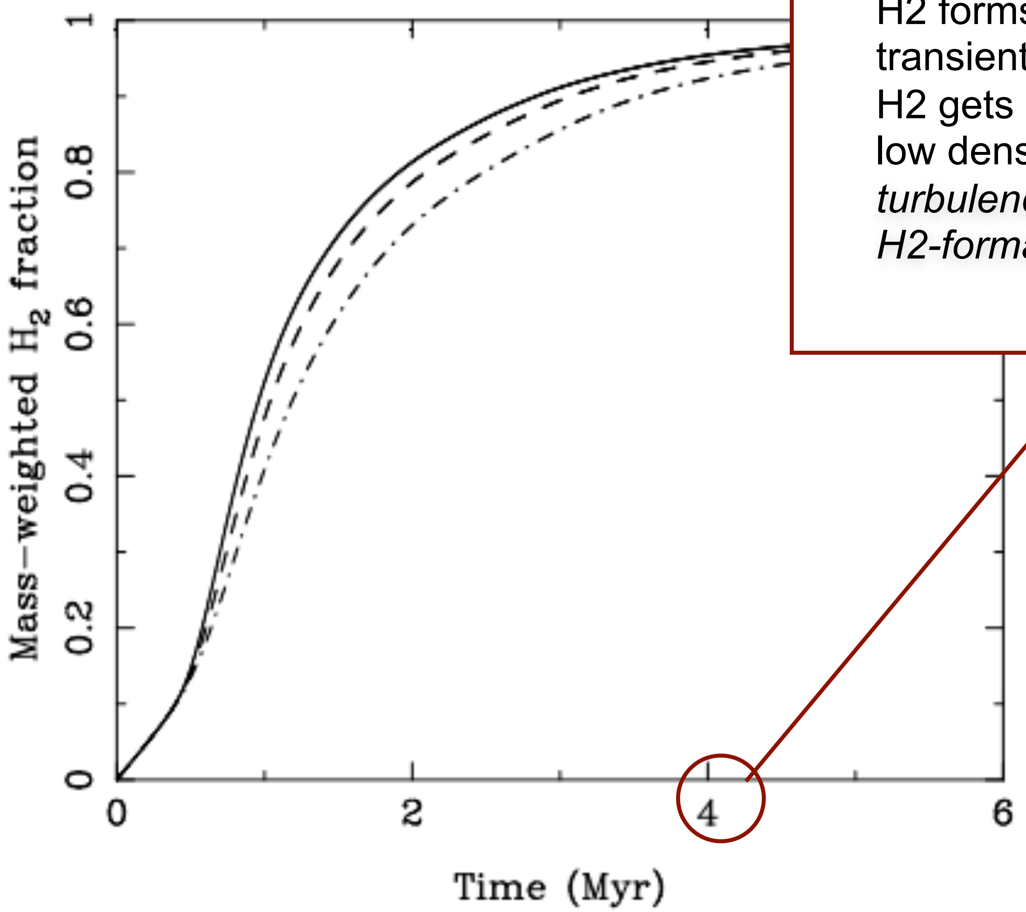

H2 forms rapidly in shocks / transient density fluctuations / H2 gets destroyed slowly in low density regions / *result: turbulence greatly enhances H2-formation rate*

Figure 4. Time evolution of the mass-weighted H_2 abundance in simulations R1, R2 and R3, which have numerical resolutions of 64^3 zones (dot-dashed), 128^3 zones (dashed) and 256^3 zones (solid), respectively.

(Glover, Federrath, Mac Low, Klessen, 2010)

HI to H2 conversion rate

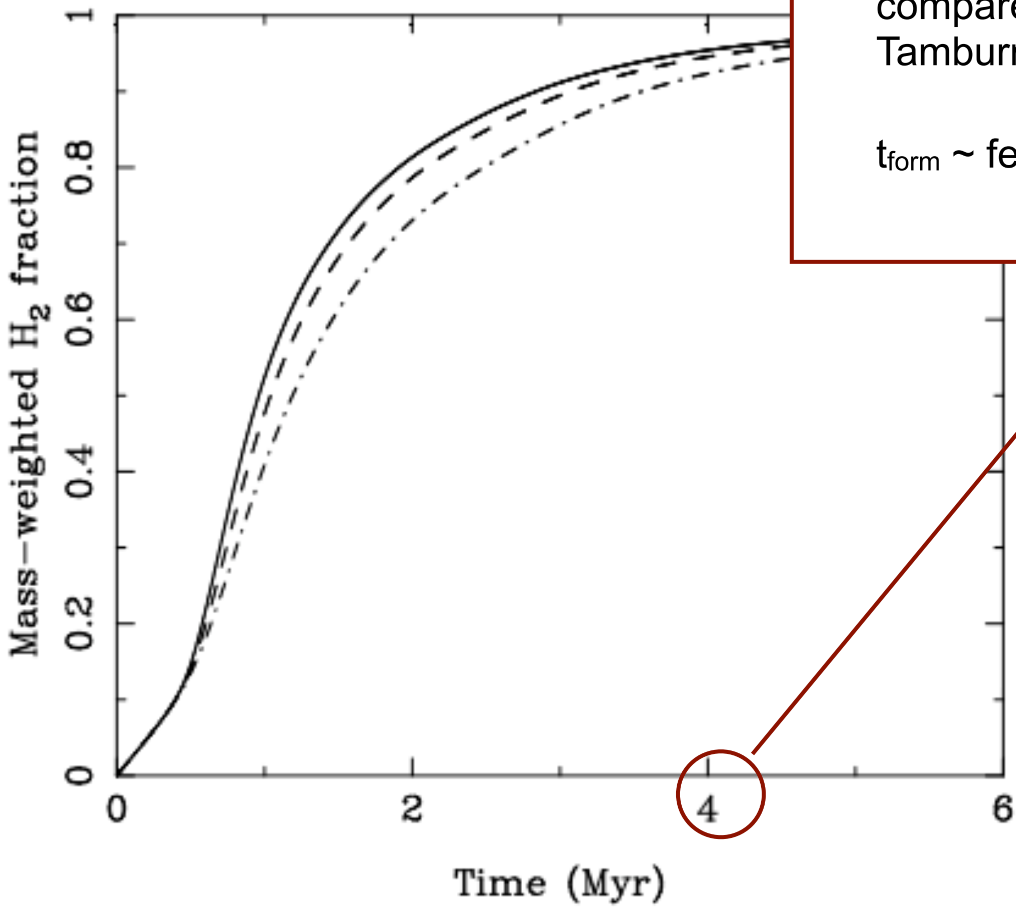

compare to data from
Tamburro et al. (2008) study:

t_{form} ~ few x 10^6 years

Figure 4. Time evolution of the mass-weighted H_2 abundance in simulations R1, R2 and R3, which have numerical resolutions of 64^3 zones (dot-dashed), 128^3 zones (dashed) and 256^3 zones (solid), respectively.

(Glover, Federrath, Mac Low, Klessen, 2010)

CO, C^+ formation rates

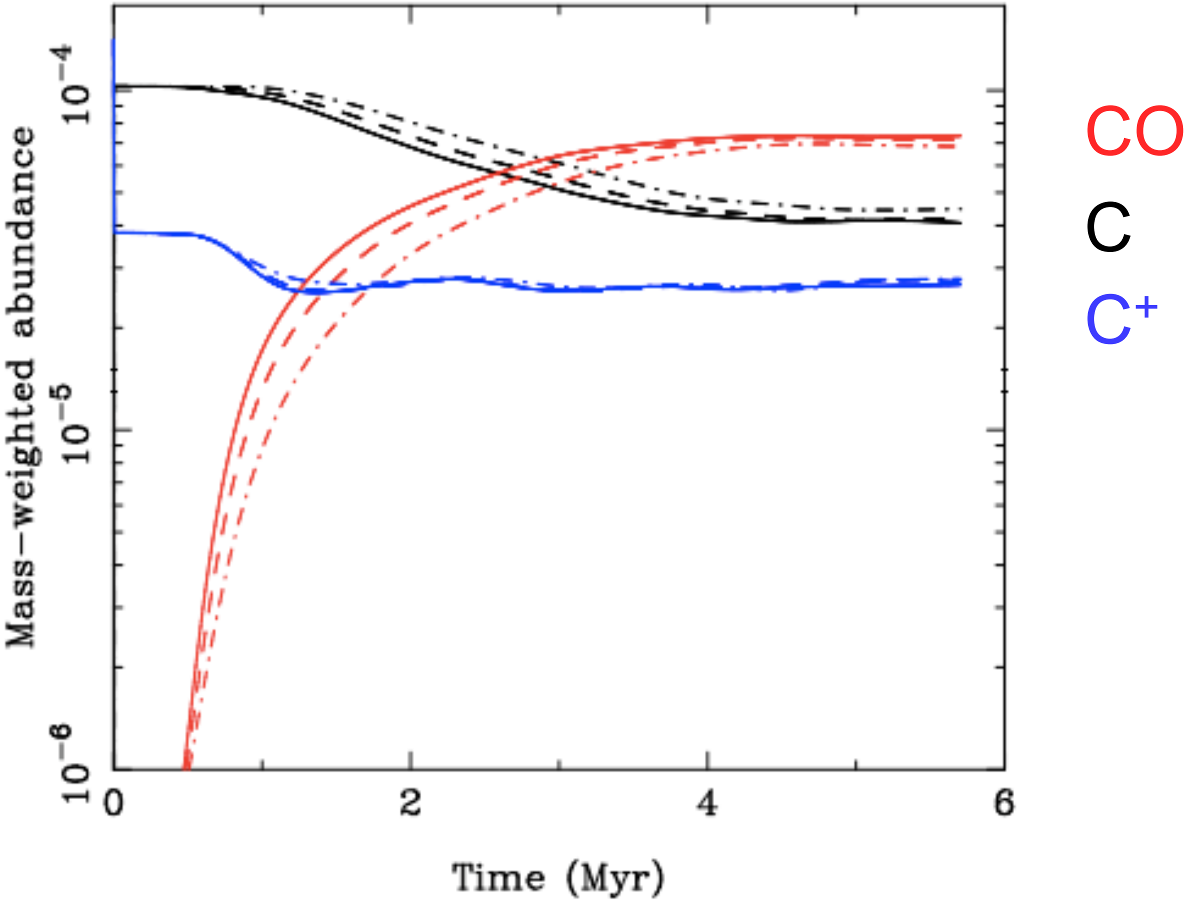

Figure 5. Time evolution of the mass-weighted abundances of atomic carbon (black lines), CO (red lines), and C^+ (blue lines) in simulations with numerical resolutions of 64^3 zones (dot-dashed), 128^3 zones (dashed) and 256^3 zones (solid).

(Glover, Federrath, Mac Low, Klessen, 2010)

effects of chemistry 1

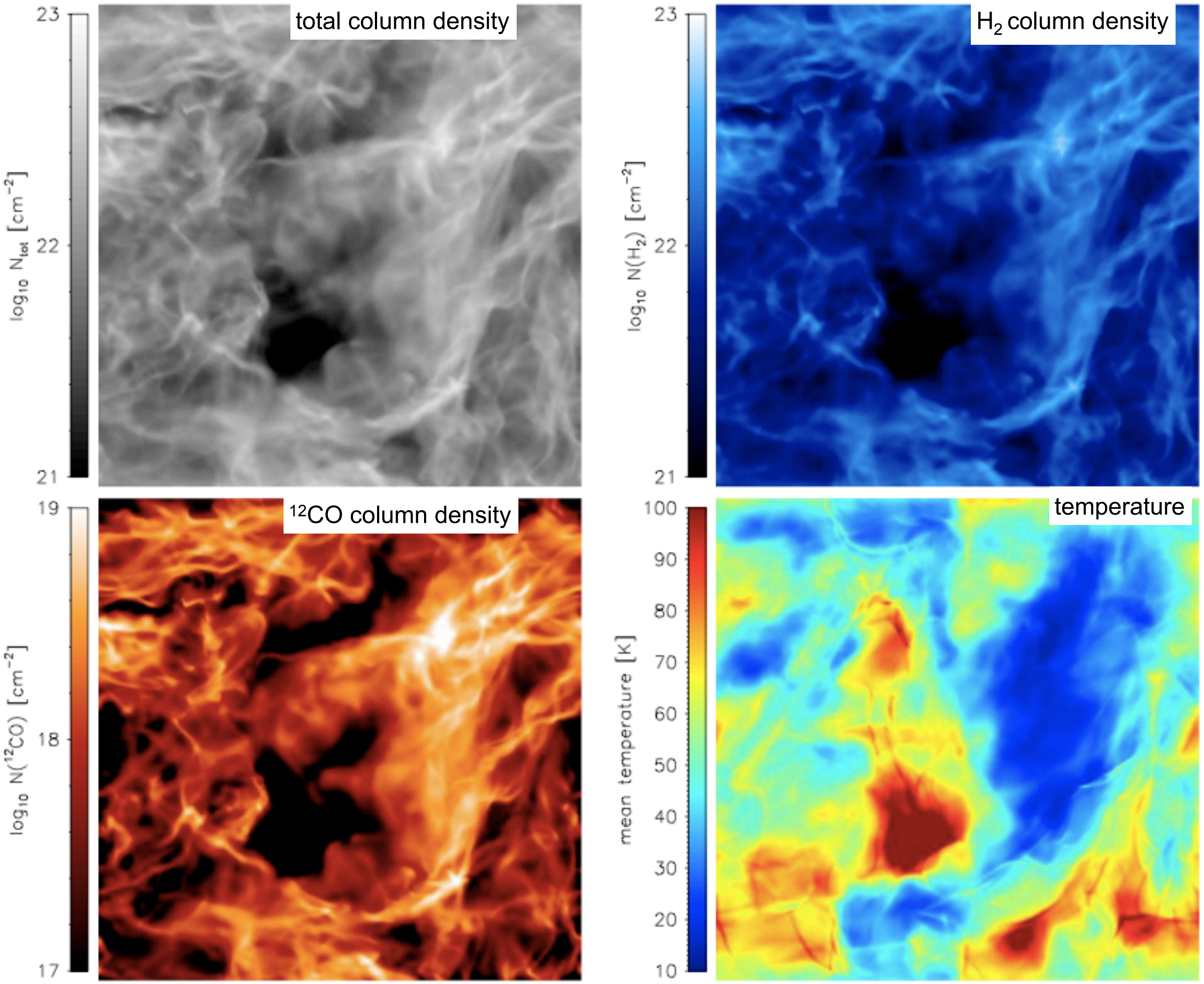

(Glover, Federrath, Mac Low, Klessen, 2010)

effects of chemistry 2

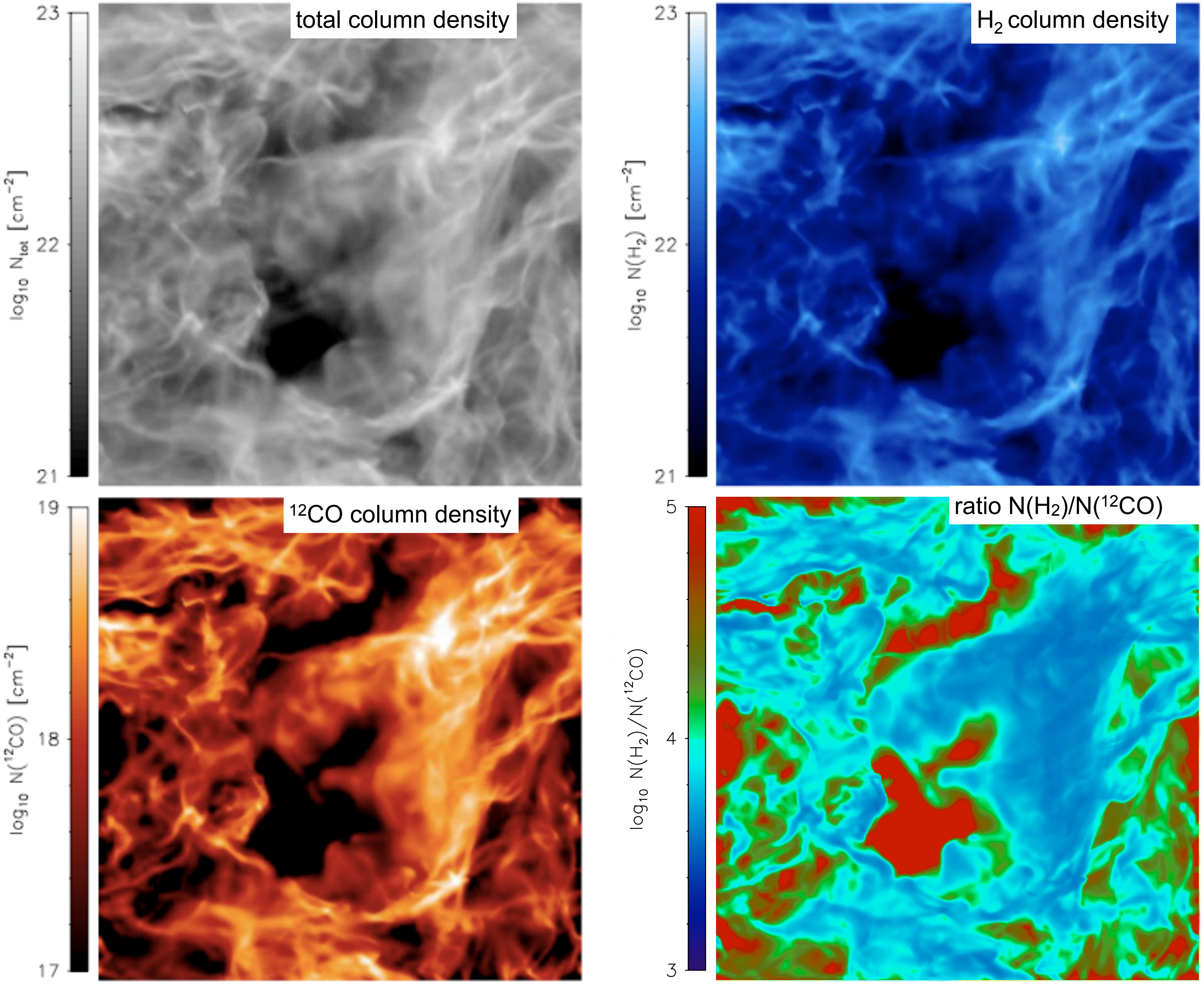

(Glover, Federrath, Mac Low, Klessen, 2010)

x-factor

- conversion rate between H_2 column density and CO emission (equivalent width W)

$$X = \frac{N_{\mathrm{H_2}}}{W} \ (\mathrm{cm^{-2}\,K^{-1}\,km^{-1}\,s})$$

- most mass H_2 determinations depend on X!
- in Milky Way X ~ few x 10^{22} $\mathrm{cm^{-2}}$ $\mathrm{K^{-1}}$ $\mathrm{km^{-1}}$ s ~ const.
- why is it constant?
- how does it vary with environmental condition?
  - metallicity
  - density, radiation field, etc.
    (“normal” gal. vs star burst)

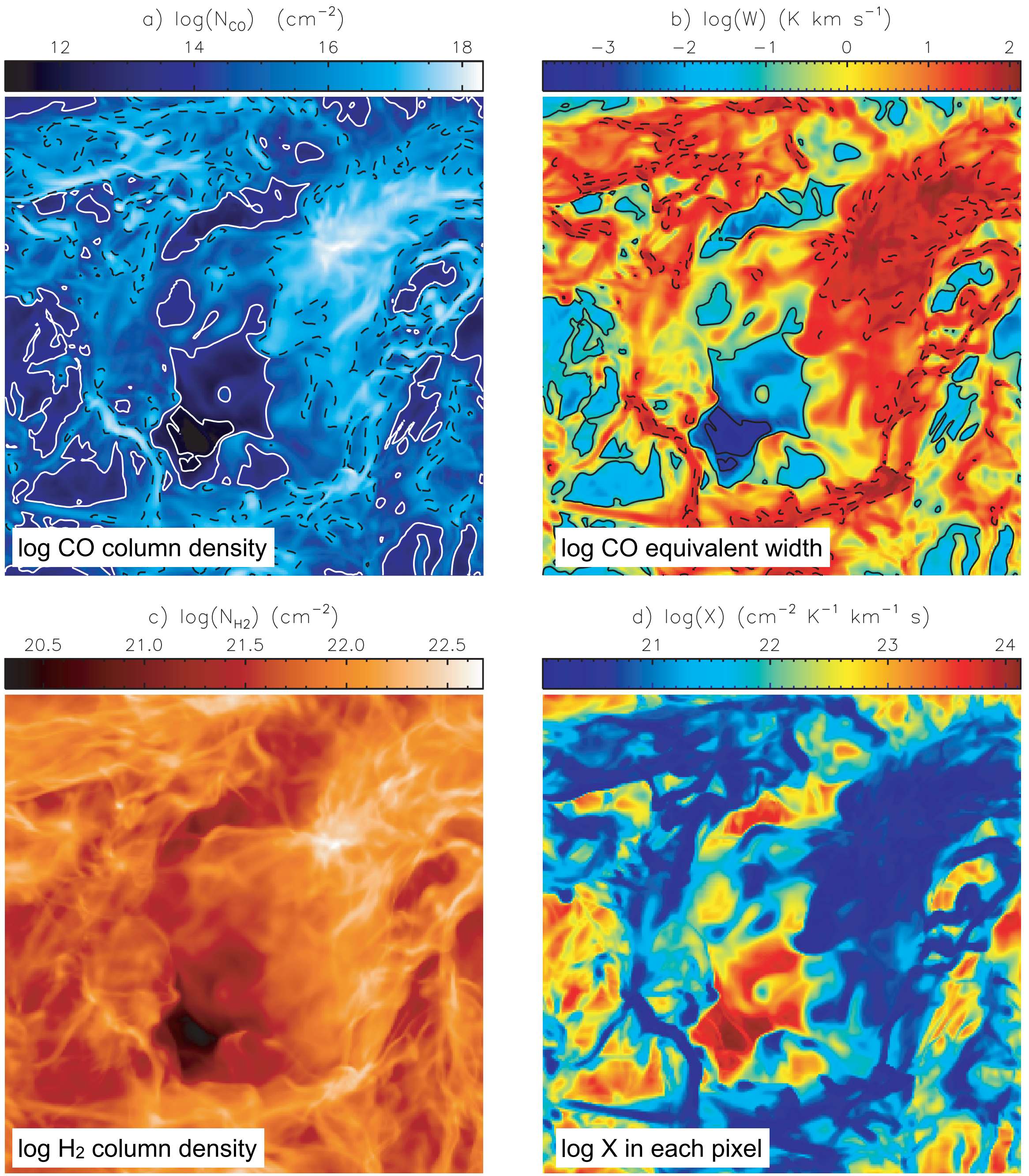

(Shetty, Glover, Dullemond, Klessen 2011)

Figure 4. Images of (a) N_{CO}, (b) W, (c) N_{H_2} and (d) the X factor of model n300-Z03. Each side has a length of 20 pc. In (a) and (b), solid contours indicate $\log(N_{CO}) = 12, 14$ and $\log(W) = -3, -1$; dashed contours are $\log(N_{CO}) = 16.5$ and $\log(W) = 1.5$ (see the text and Fig. 2d).

detailed analysis of typical
Galactic model cloud:
solar metallicity and
mean density 300 cm^{-3}

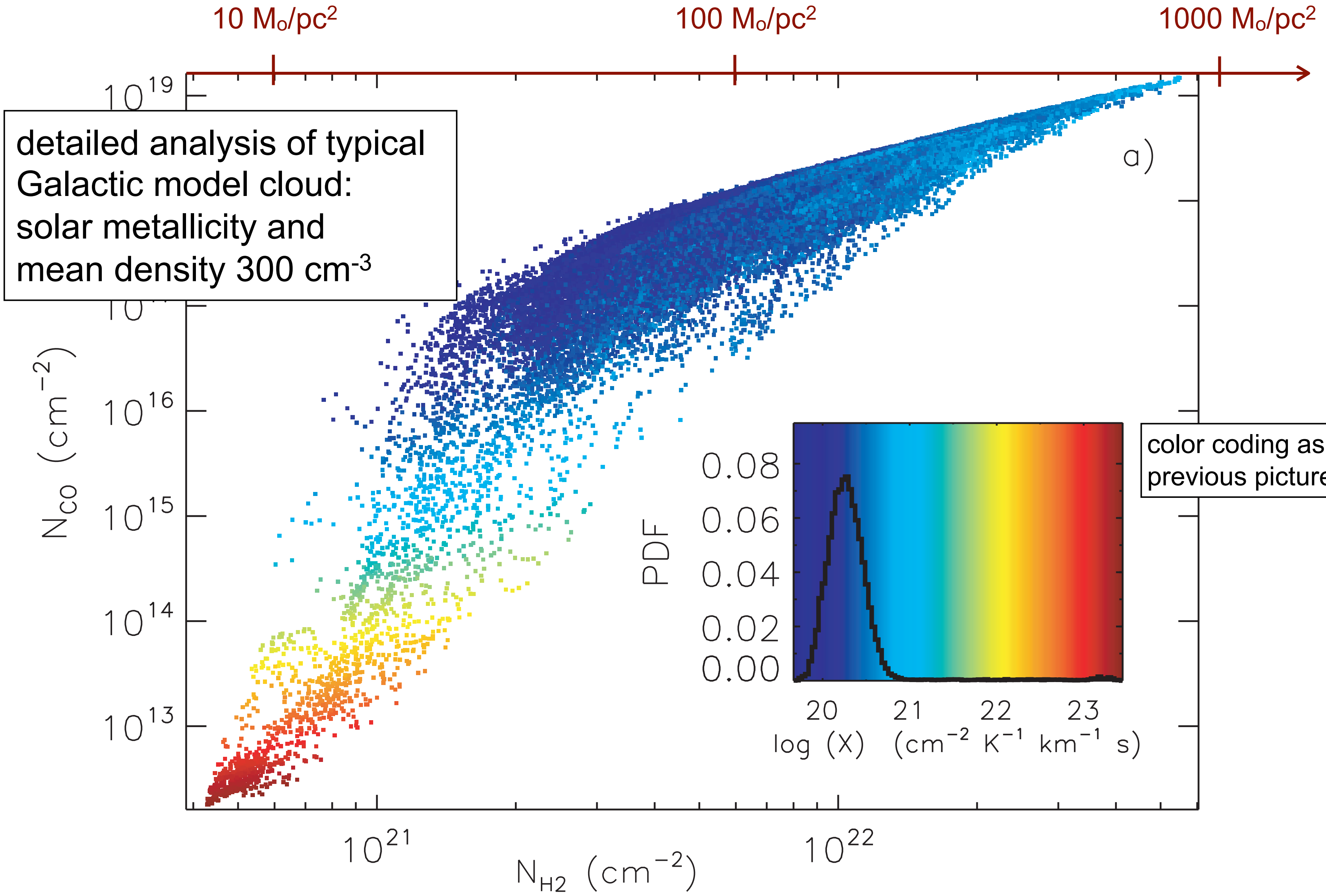

color coding as in
previous picture

(Shetty, Glover, Dullemond, Klessen 2011)

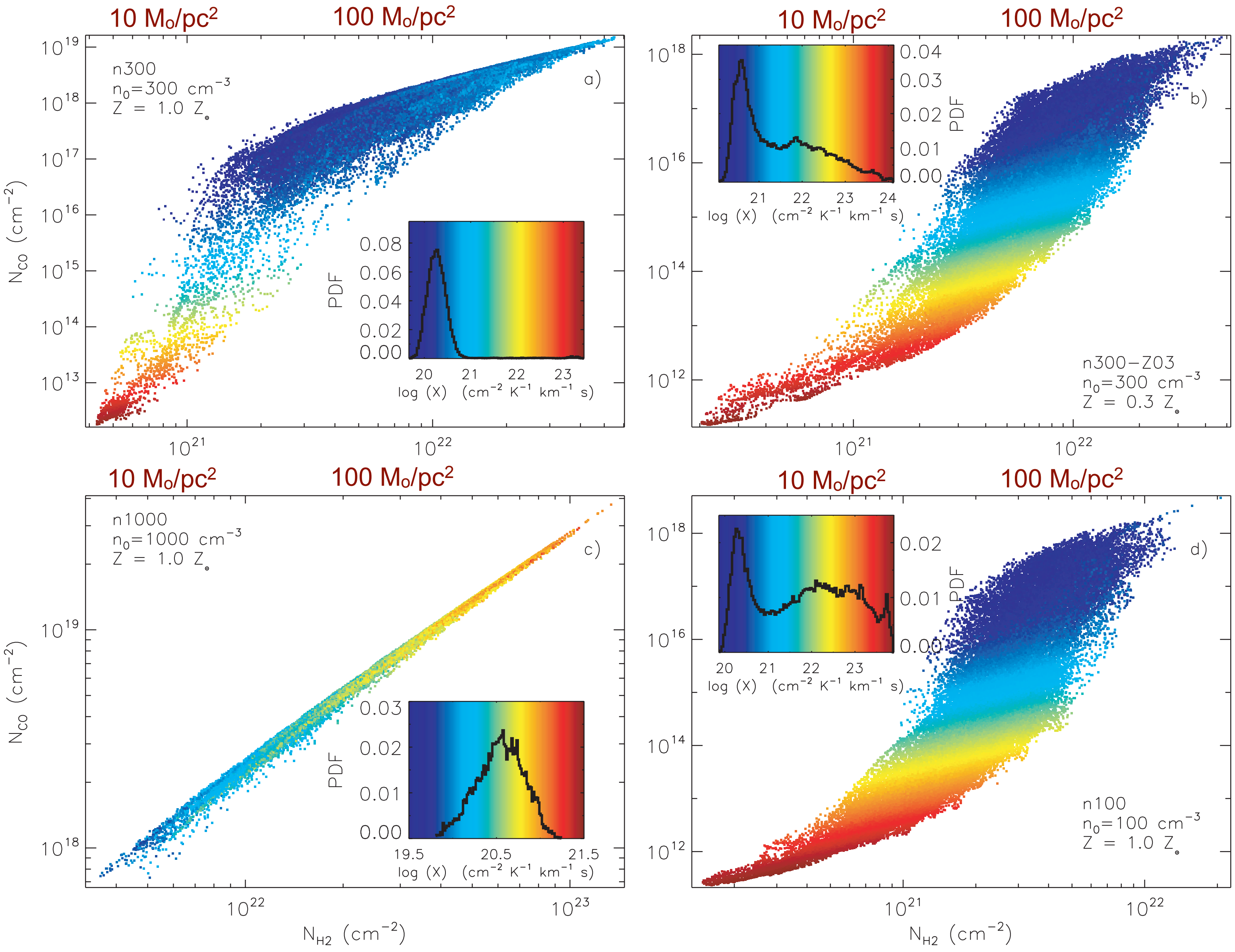

(Shetty, Glover, Dullemond, Klessen 2011)

Figure 5. *X* factor for four models. N_{CO} is plotted as a function of N_{H_2}. The colour of each point indicates the *X* factor. Inset figures show the colour scale and PDF of the *X* factor. The corresponding maps of N_{H_2}, N_{CO} and the *X* factor from model n300-Z03 are shown in Fig. 4.

observed x-factor

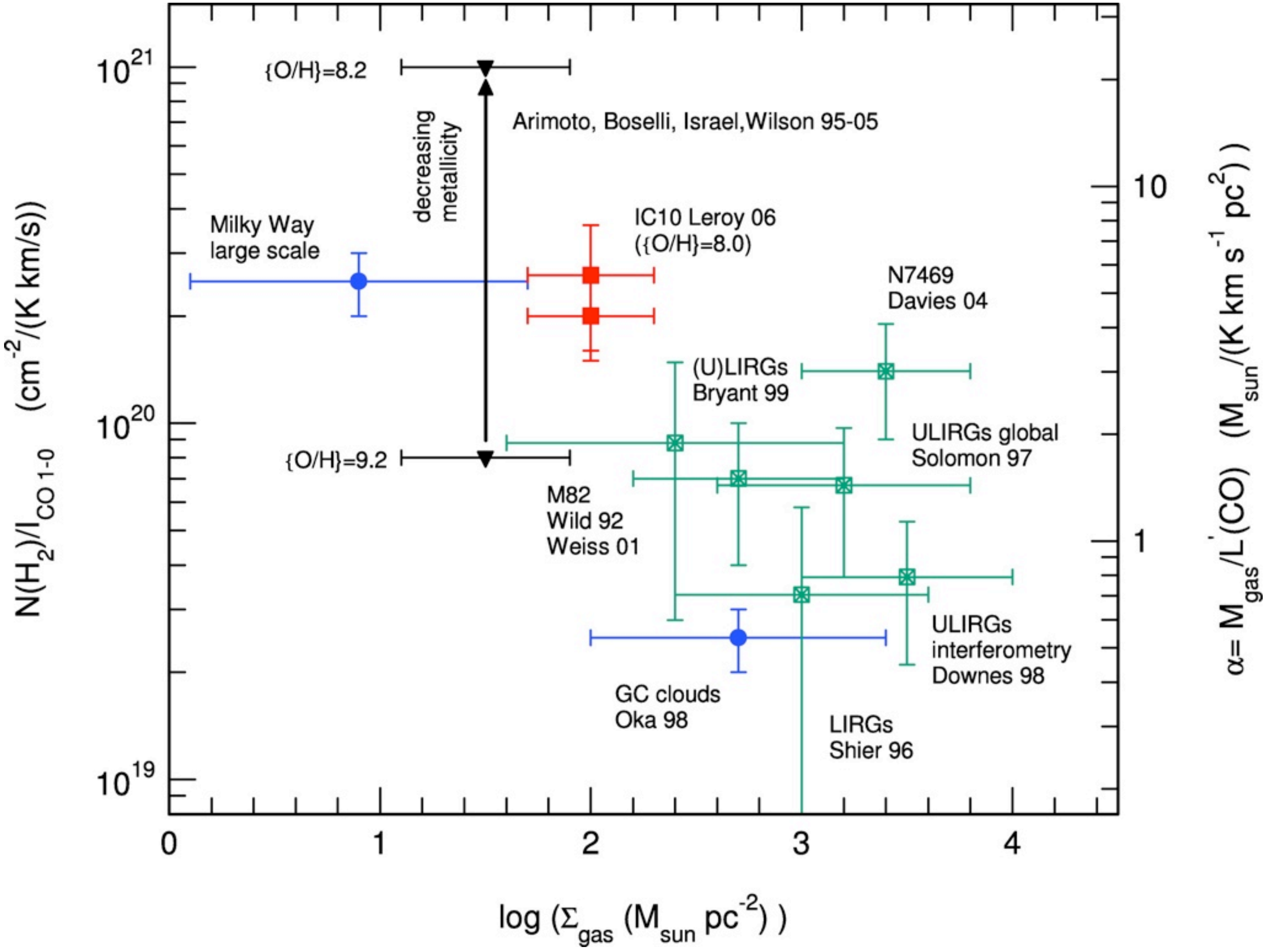

Tacconi et al. (2008)

derived x-factor

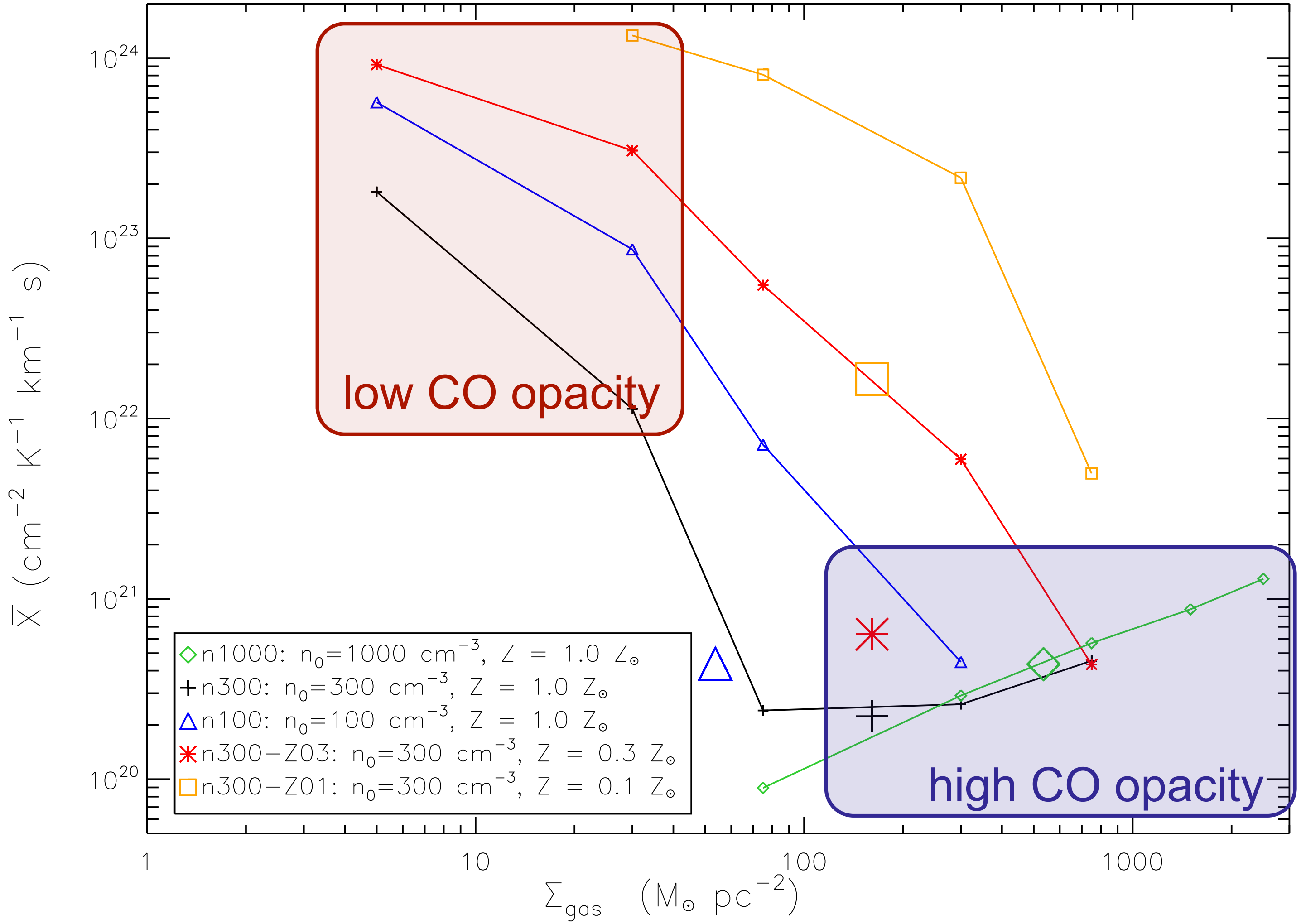

(Shetty, Glover, Dullemond, Klessen, MNRAS, 2011)

next steps

- extend range of model parameters
  - we are currently running *starburst galaxies* with higher density, and 1000x increased radiation field and/or 1000x increased cosmic ray intensity

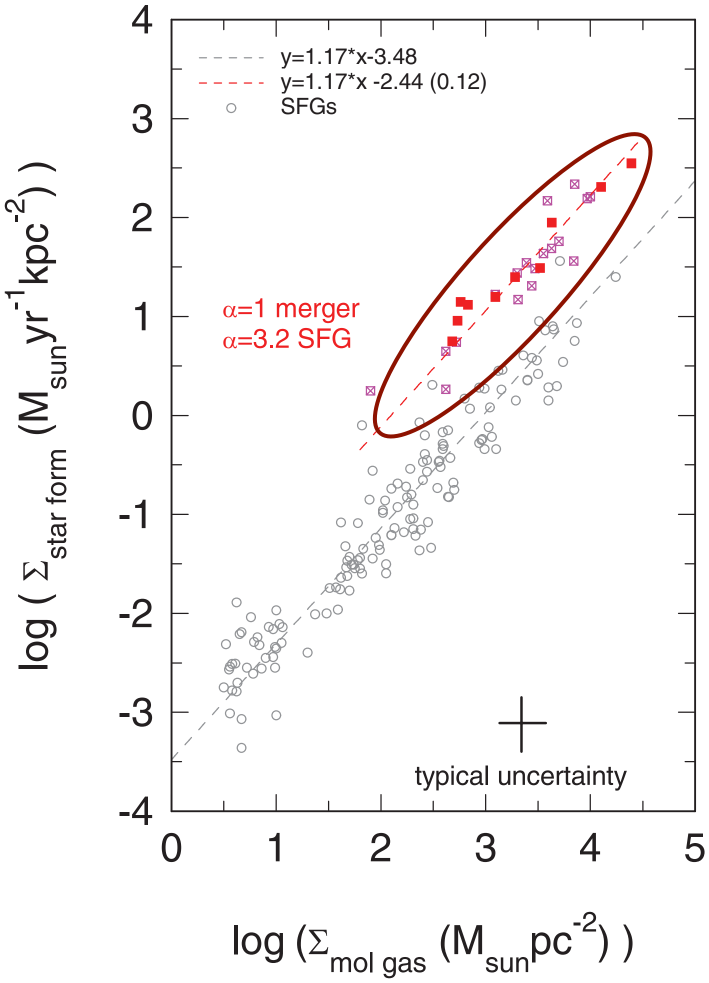

Genzel et al. (2010)

are molecules needed for star formation?

- it has been proposed that molecule formation (H_2, CO, etc.) is a prerequisite for star formation
  (e.g. Schaye 2004; Krumholz & McKee 2005; Elmegreen 2007; Krumholz et al. 2009)
- the idea is that CO is a necessary coolant for collapse
- however, also C+ is a very efficient coolant!
  (Glover & Clark 2011)

- to address this question, we performed dedicated simulations in Heidelberg

are molecules needed to form stars?

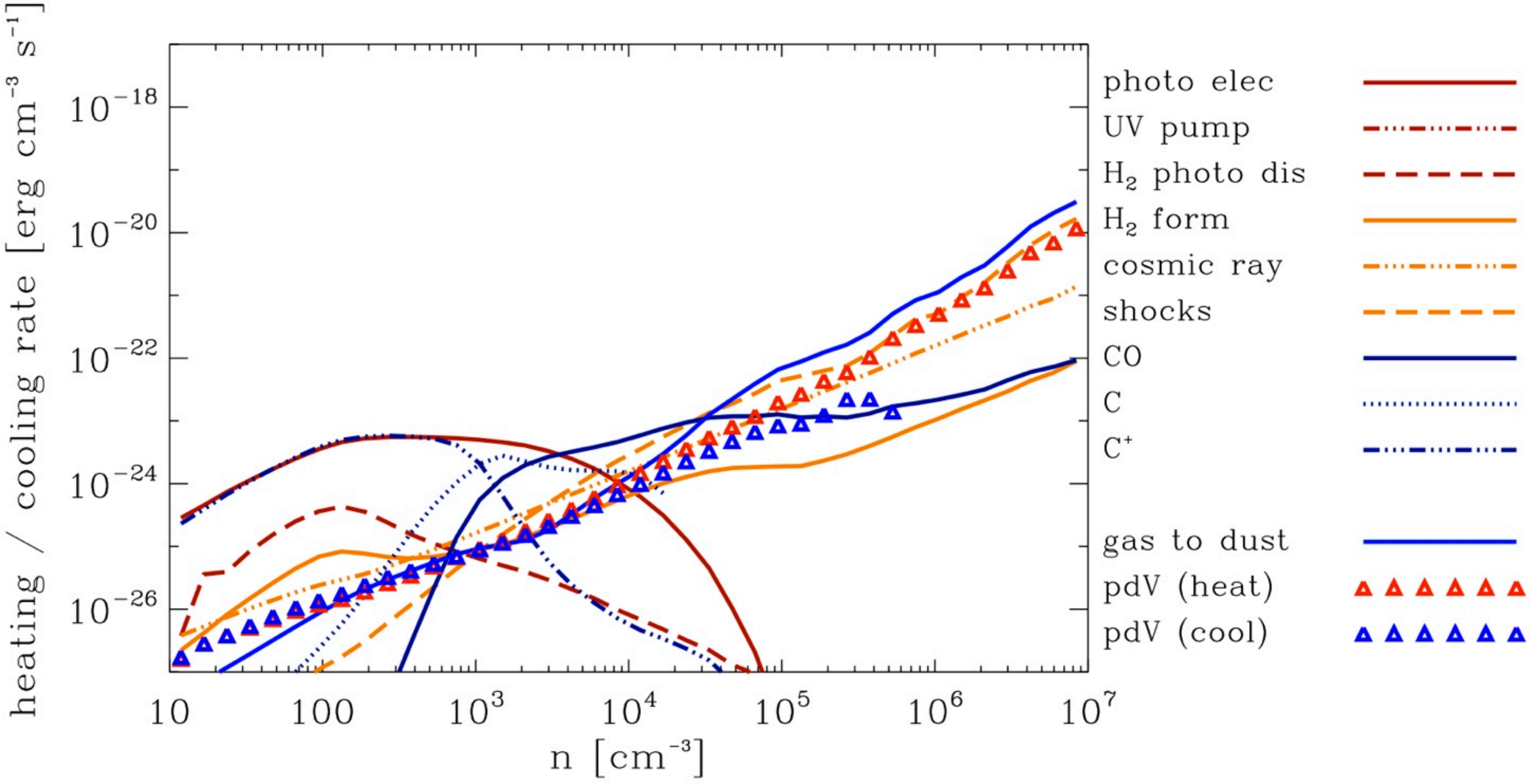

NO! CII, CI, provide equal amounts of cooling to CO . . .

image from Simon Glover

are molecules needed for star formation?

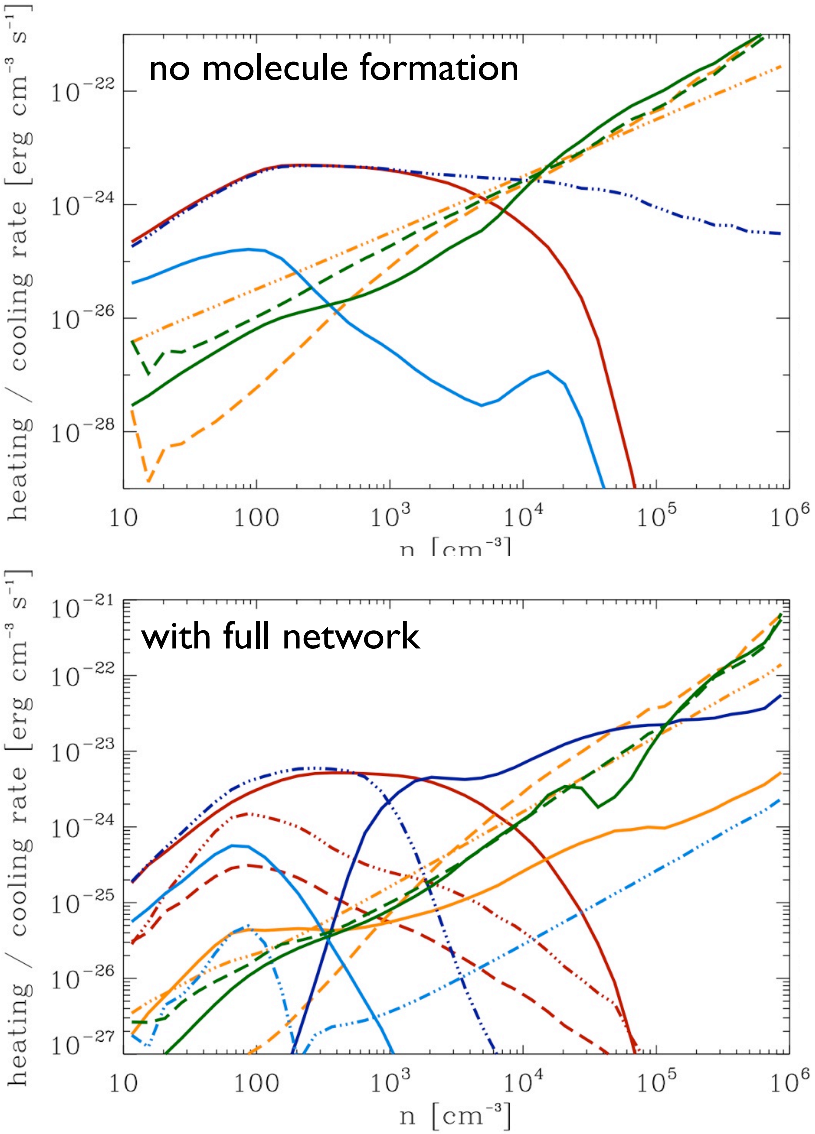

Glover & Clark (2011)

- presence of molecular gas has only very minor influence on ability of cloud to form stars
- C^+ is equally efficient coolant in atomic phase as CO in molecular
- what is crucial is the ability of cloud to shield itself from interstellar radiation field
- but clouds that are big/dense enough to shield themselves will be molecular!

this suggests that the correlation between H_2 and star formation is a coincidence

where is most energy lost?

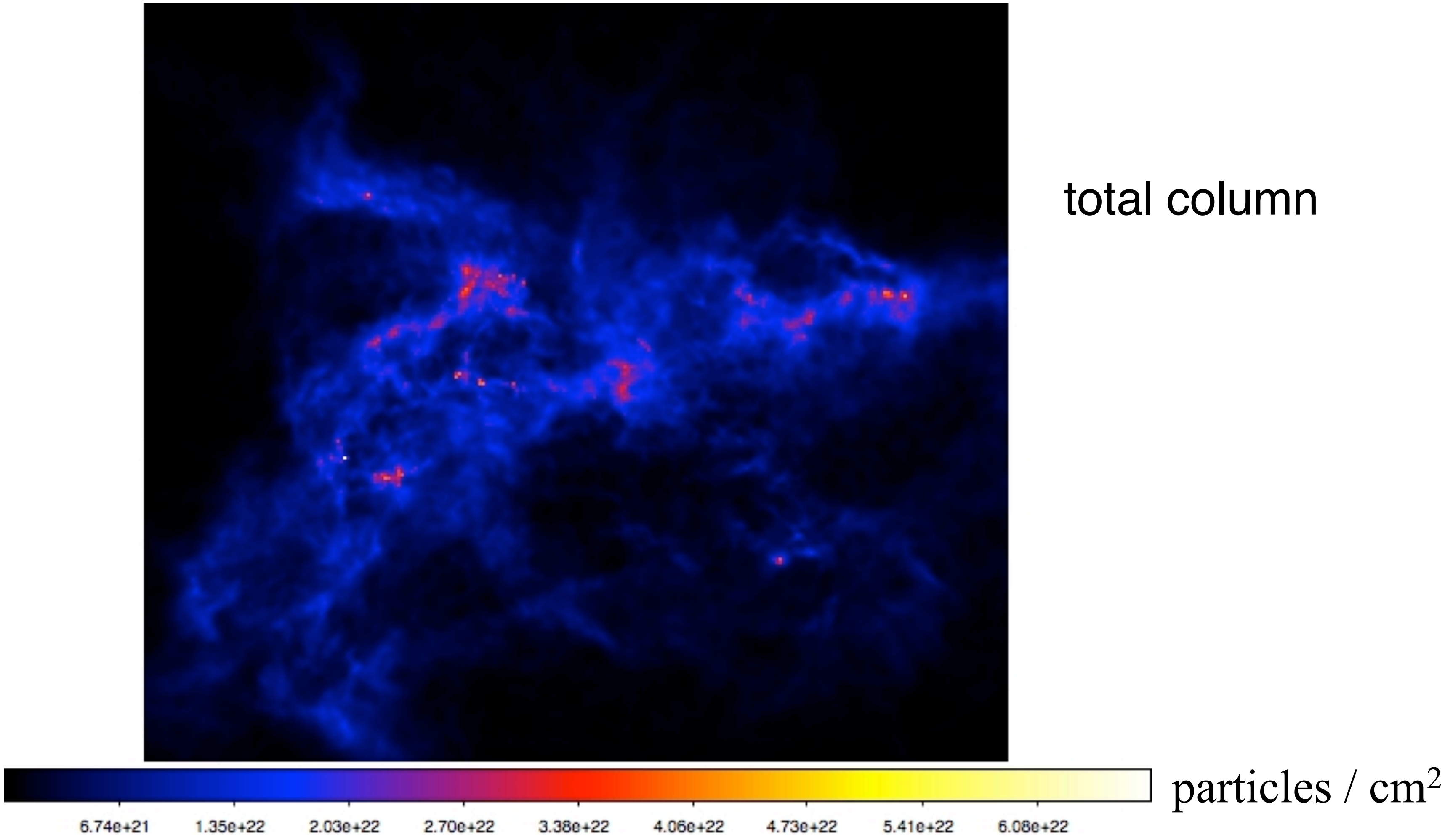

total column

images from Simon Glover

where is most energy lost?

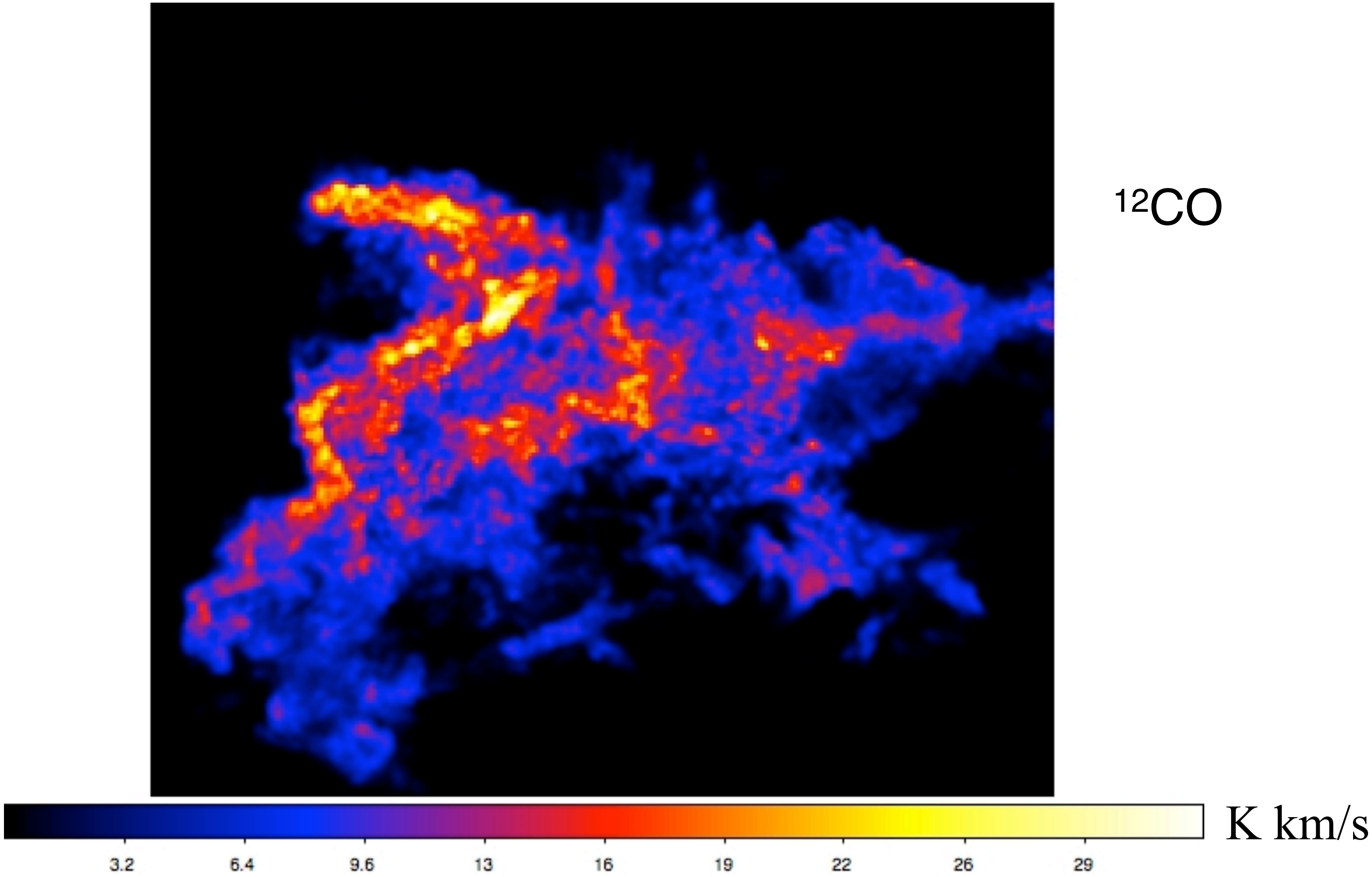

images from Simon Glover

where is most energy lost?

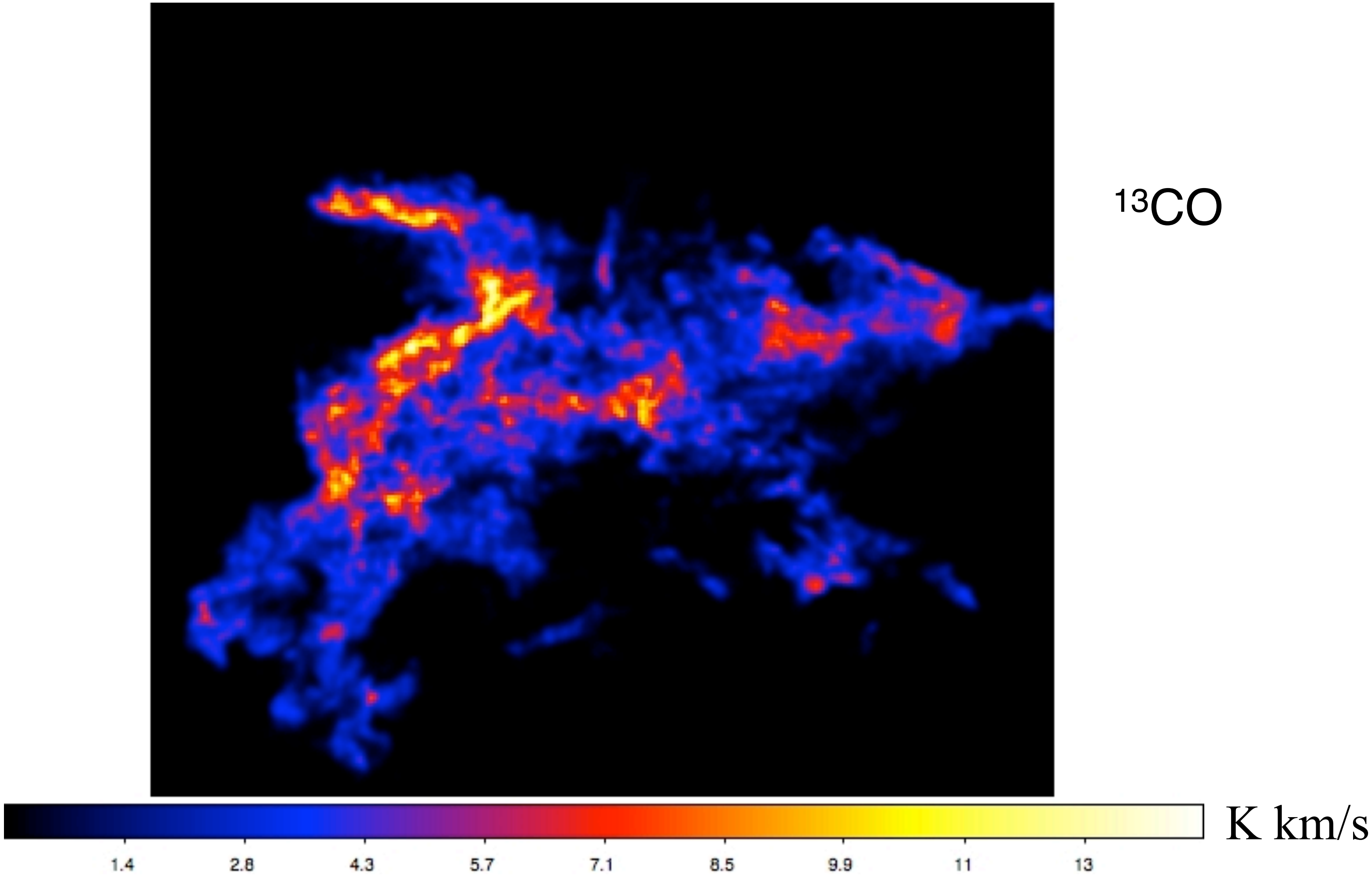

images from Simon Glover

where is most energy lost?

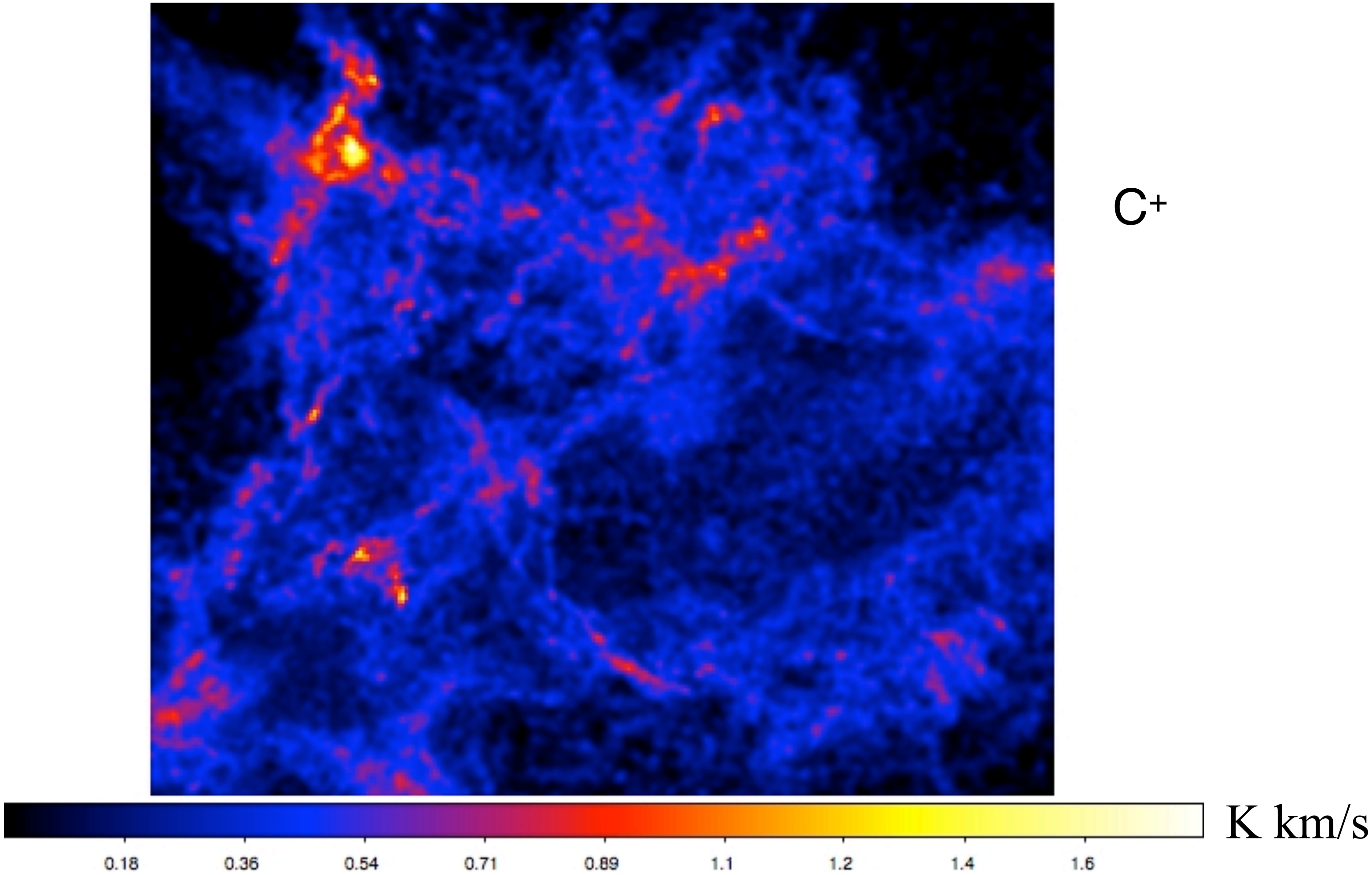

images from Simon Glover

theoretical approach

decrease in spatial scale / increase in density


Andromeda (R. Gendler)


NGC 602 in LMC (Hubble)


Proplyd in Orion (Hubble)

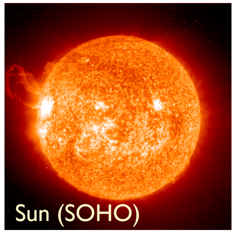
Sun (SOHO)


Earth

- density
  - density of ISM: few particles per cm^3
  - density of molecular cloud: few 100 particles per cm^3
  - density of Sun: 1.4 g/cm^3
- spatial scale
  - size of molecular cloud: few 10s of pc
  - size of young cluster: ~ 1 pc
  - size of Sun: 1.4×10^{10} cm

decrease in spatial scale / increase in density


Andromeda (R. Gendler)


NGC 602 in LMC (Hubble)


Proplyd in Orion (Hubble)

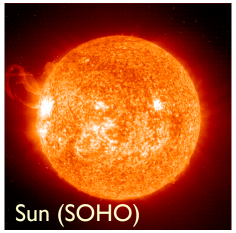
Sun (SOHO)


Earth

- contracting force
  - only force that can do this compression is ***GRAVITY***
- opposing forces
  - there are several processes that can oppose gravity
  - ***GAS PRESSURE***
  - ***TURBULENCE***
  - ***MAGNETIC FIELDS***
  - ***RADIATION PRESSURE***

decrease in spatial scale / increase in density


Andromeda (R. Gendler)


NGC 602 in LMC (Hubble)


Proplyd in Orion (Hubble)

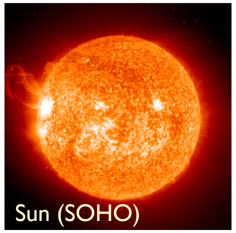
Sun (SOHO)


Earth

- contracting force
  - only force that can do this compression is ***GRAVITY***
- opposing forces
  - there are several processes that can oppose gravity
  - ***GAS PRESSURE***
  - ***TURBULENCE***
  - ***MAGNETIC FIELDS***
  - ***RADIATION PRESSURE***

Modern star formation theory is based on the complex interplay between *all* these processes.

early theoretical models

- *Jeans (1902):* Interplay between self-gravity and thermal pressure
  - stability of homogeneous spherical density enhancements against gravitational collapse
  - dispersion relation:

$$\boxed{\omega^2 = c_s^2 k^2 - 4\pi G \rho_0}$$

  - instability when $\omega^2 < 0$
  - minimal mass: $\boxed{M_J = \frac{1}{6}\pi^{-5/2} G^{-3/2} \rho_0^{-1/2} c_s^3 \propto \rho_0^{-1/2} T^{-3/2}}$

Sir James Jeans, 1877 - 1946

first approach to turbulence

- *von Weizsäcker (1943, 1951)* and *Chandrasekhar (1951):* concept of ***MICROTURBULENCE***
  - BASIC ASSUMPTION: separation of scales between dynamics and turbulence

    $\ell_{\text{turb}} \ll \ell_{\text{dyn}}$
  - then turbulent velocity dispersion contributes to effective soundspeed:

    $$\boxed{c_c^2 \mapsto c_c^2 + \sigma_{rms}^2}$$
  - → Larger effective Jeans masses → more stability
  - BUT: *(1) turbulence depends on k:* $\sigma_{rms}^2(k)$

    (2) supersonic turbulence → $\sigma_{rms}^2(k) >> c_s^2$ *usually*

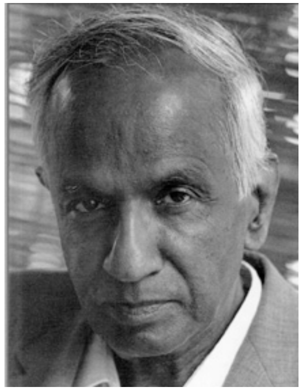

S. Chandrasekhar,
1910 - 1995

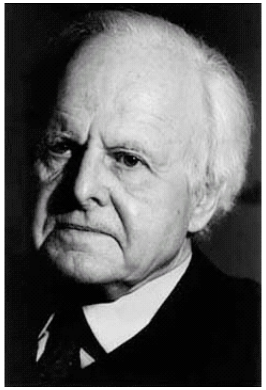

C.F. von Weiszäcker,
1912 - 2007

problems of early dynamical theory

- molecular clouds are *highly Jeans-unstable,*
  yet, they do *NOT* form stars at high rate
  and with high efficiency (Zuckerman & Evans 1974 conundrum)
  (the observed global SFE in molecular clouds is *~5%*)
  → *something prevents large-scale collapse.*
- all throughout the early 1990's, molecular clouds
  had been thought to be long-lived quasi-equilibrium
  entities.
- molecular clouds are *magnetized*

magnetic star formation

- *Mestel & Spitzer (1956):* Magnetic fields can prevent collapse*!!!*
  - Critical mass for gravitational collapse in presence of B-field

$$M_{cr} = \frac{5^{3/2}}{48\pi^2} \frac{B^3}{G^{3/2}\rho^2}$$

  - Critical mass-to-flux ratio (Mouschovias & Spitzer 1976)

$$\left[\frac{M}{\Phi}\right]_{cr} = \frac{\zeta}{3\pi}\left[\frac{5}{G}\right]^{1/2}$$

  - Ambipolar diffusion can initiate collapse

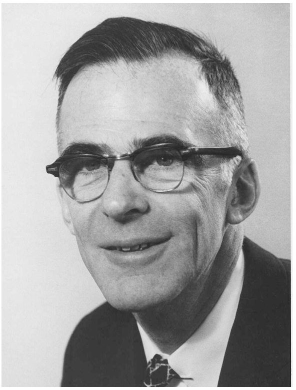

Lyman Spitzer, Jr., 1914 - 1997

“standard theory” of star formation

- BASIC ASSUMPTION: Stars form from magnetically highly subcritical cores
- Ambipolar diffusion slowly increases (M/Φ): $\tau_{AD} \approx 10\tau_{ff}$
- Once $(M/\Phi) > (M/\Phi)_{crit}$: dynamical collapse of SIS
  - Shu (1977) collapse solution
  - $dM/dt = 0.975\ c_s^3/G = \text{const.}$
- Was (in principle) only intended for isolated, low-mass stars

Frank Shu, 1943 -

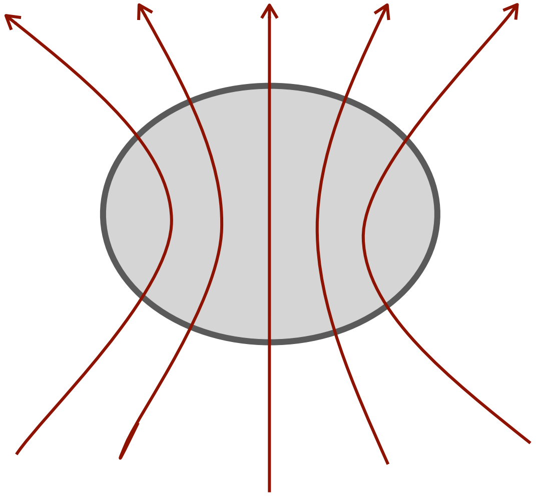

problems of “standard theory”

- Observed B-fields are weak, at most marginally critical (Crutcher 1999, Bourke et al. 2001)
- Magnetic fields cannot prevent decay of turbulence
  (Mac Low et al. 1998, Stone et al. 1998, Padoan & Nordlund 1999)
- Structure of prestellar cores
  (e.g. Bacman et al. 2000, Alves et al. 2001)
- Strongly time varying dM/dt
  (e.g. Hendriksen et al. 1997, André et al. 2000)
- More extended infall motions than predicted by the standard model
  (Williams & Myers 2000, Myers et al. 2000)
- Most stars form as binaries
  (e.g. Lada 2006)
- As many prestellar cores as protostellar cores in SF regions (e.g. André et al 2002)
- Molecular cloud clumps are chemically young
  (Bergin & Langer 1997, Pratap et al 1997, Aikawa et al 2001)
- Stellar age distribution small ($\tau_{ff} << \tau_{AD}$)
  (Ballesteros-Paredes et al. 1999, Elmegreen 2000, Hartmann 2001)
- Strong theoretical criticism of the SIS as starting condition for gravitational collapse
  (e.g. Whitworth et al 1996, Nakano 1998, as summarized in Klessen & Mac Low 2004)
- Standard AD-dominated theory is incompatible with observations
  (Crutcher et al. 2009, 2010ab, Bertram et al. 2011)

(see e.g. Mac Low & Klessen, 2004, Rev. Mod. Phys., 76, 125-194)

Observed B-fields are weak

B versus $N(H_2)$ from *Zeeman measurements*.
(from Bourke et al. 2001)

→ cloud cores are magnetically supercritical***!!!***

$(\Phi/M)_n > 1$ no collapse

$(\Phi/M)_n < 1$ collapse

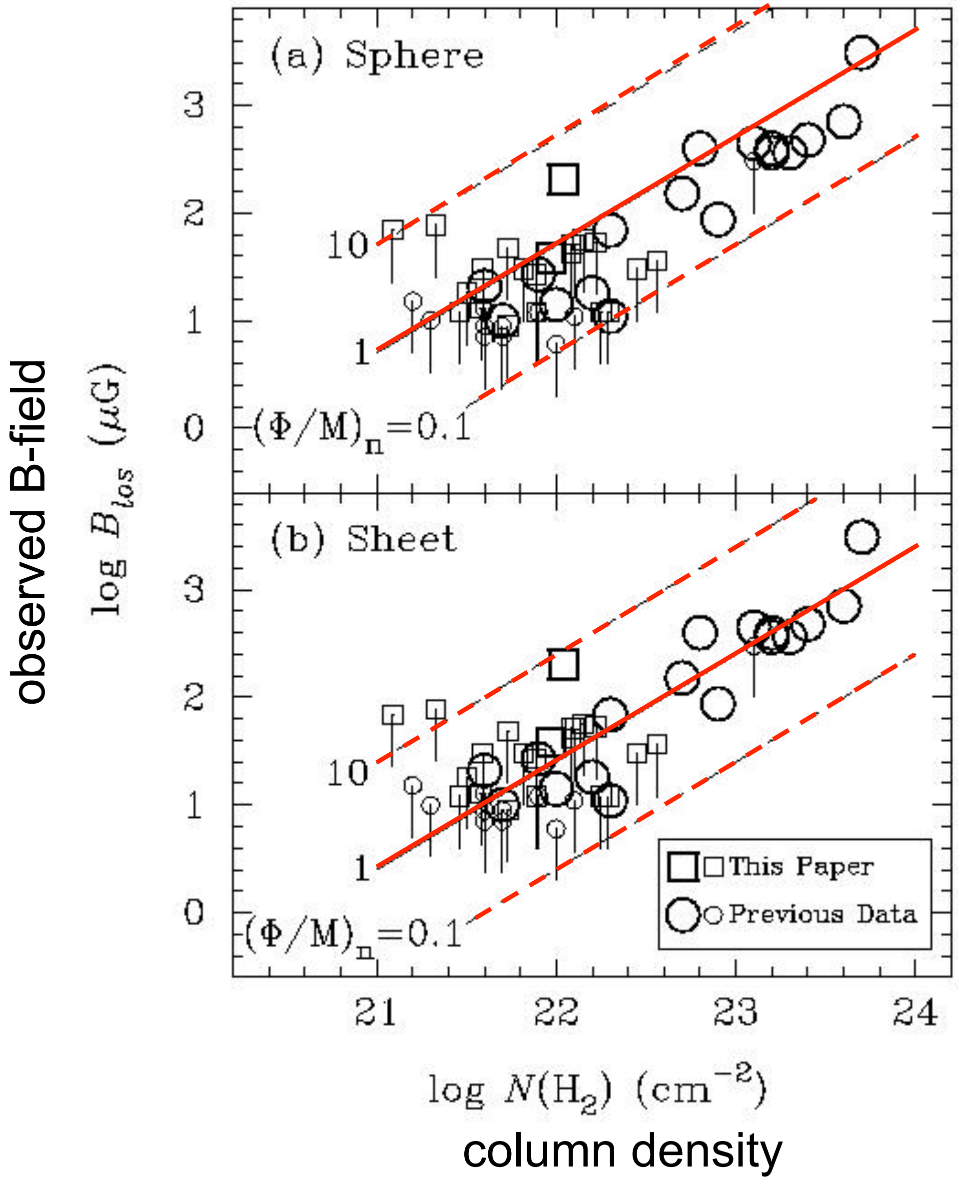

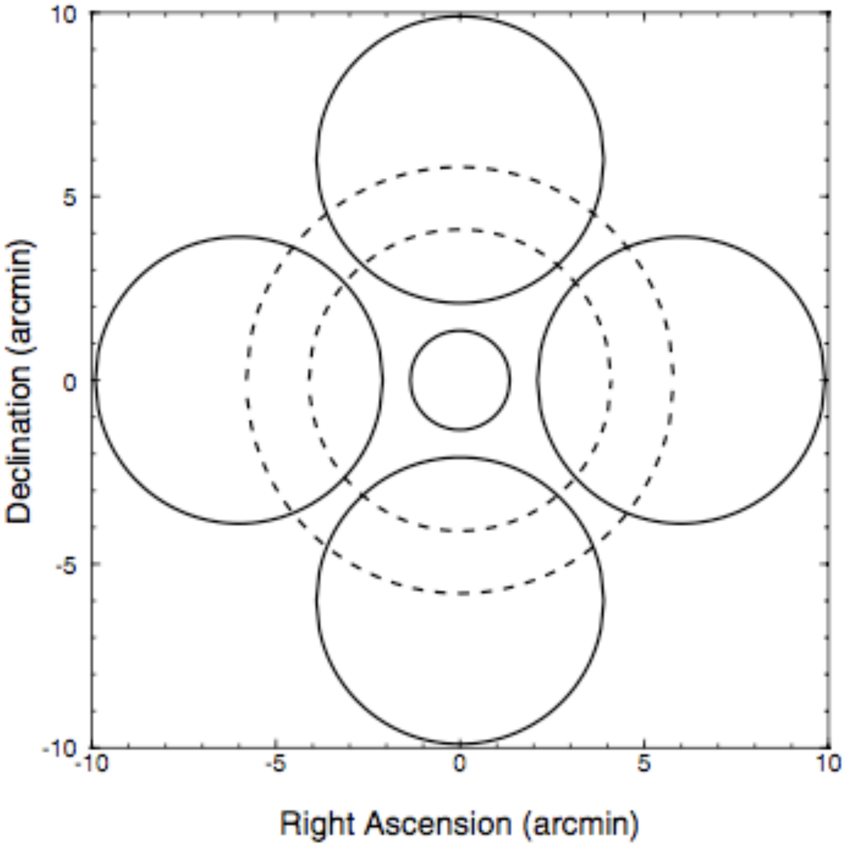

Fig. 1.— The Arecibo telescope primary beam (small circle centered at 0,0) and the four GBT telescope primary beams (large circles centered 6′ north, south, east, and west of 0,0. The dotted circles show the first sidelobe of the Arecibo telescope beam. All circles are at the half-power points.

Crutcher et al. (2009)

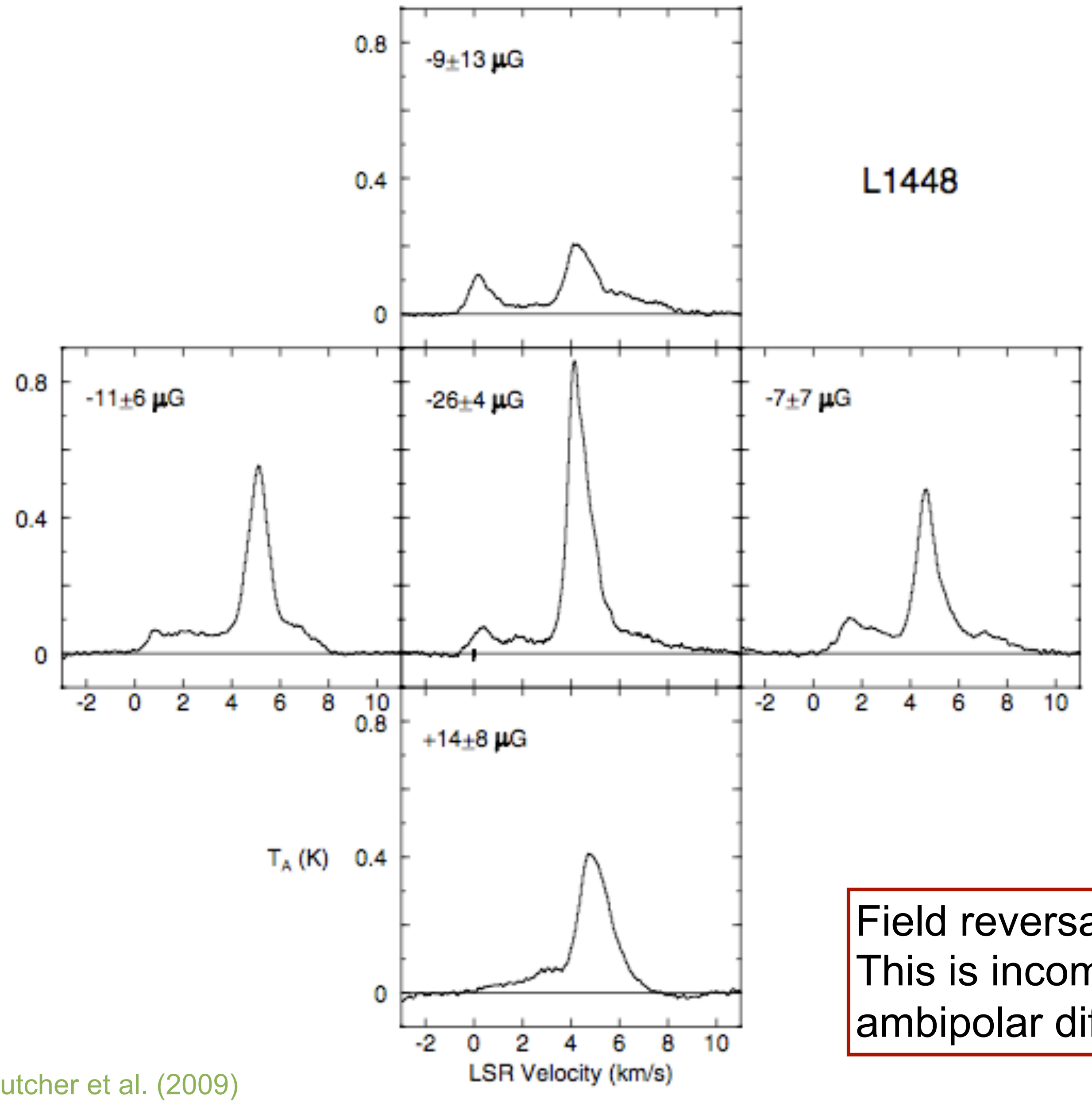

Crutcher et al. (2009)

Field reversal in the outer parts.
This is incompatible with “standard” ambipolar diffusion theory!

Fig. 2.— OH 1667 MHz spectra toward the core of L1448CO obtained with the Arecibo telescope (center panel) and toward each of the envelope positions 6′ north, south, east, and west of the core, obtained with the GBT. In the upper left of each panel is the inferred B_{LOS} and its 1σ uncertainty at that position. A negative B_{LOS} means the magnetic field points toward the observer, and vice versa for a positive B_{LOS}.

example: L1448

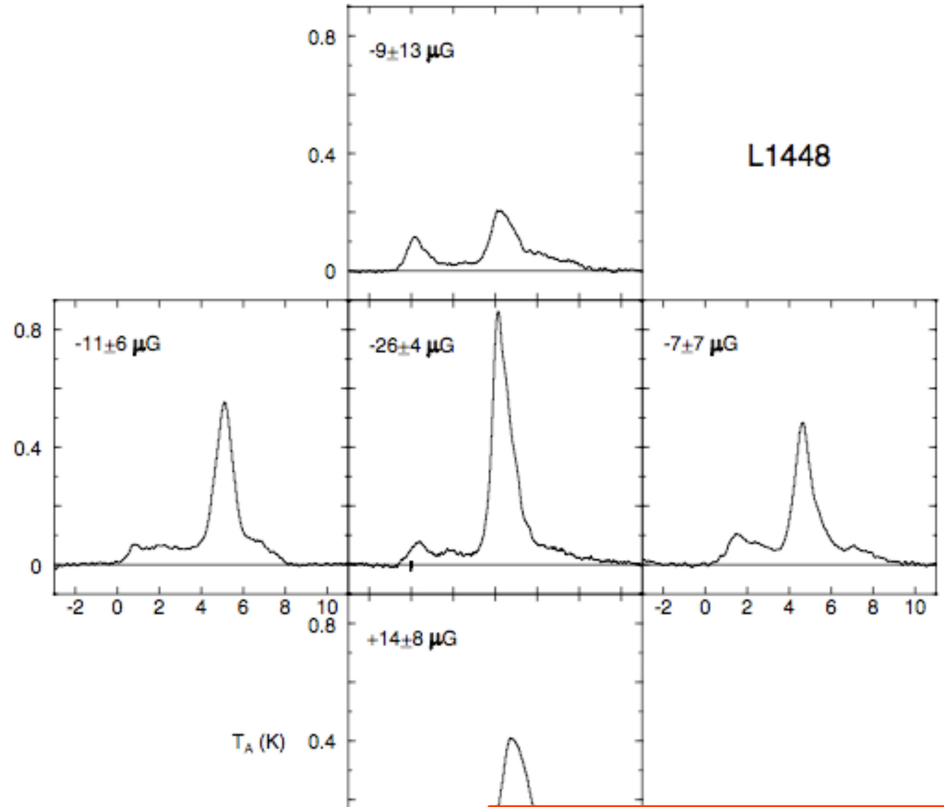

Fig. 2.— OH 1667 MHz spectra toward the
telescope (center panel) and toward each of the
west of the core, obtained with the GBT. In the
and its 1σ uncertainty at that position. A neg
toward the observer, and vice versa for a positi

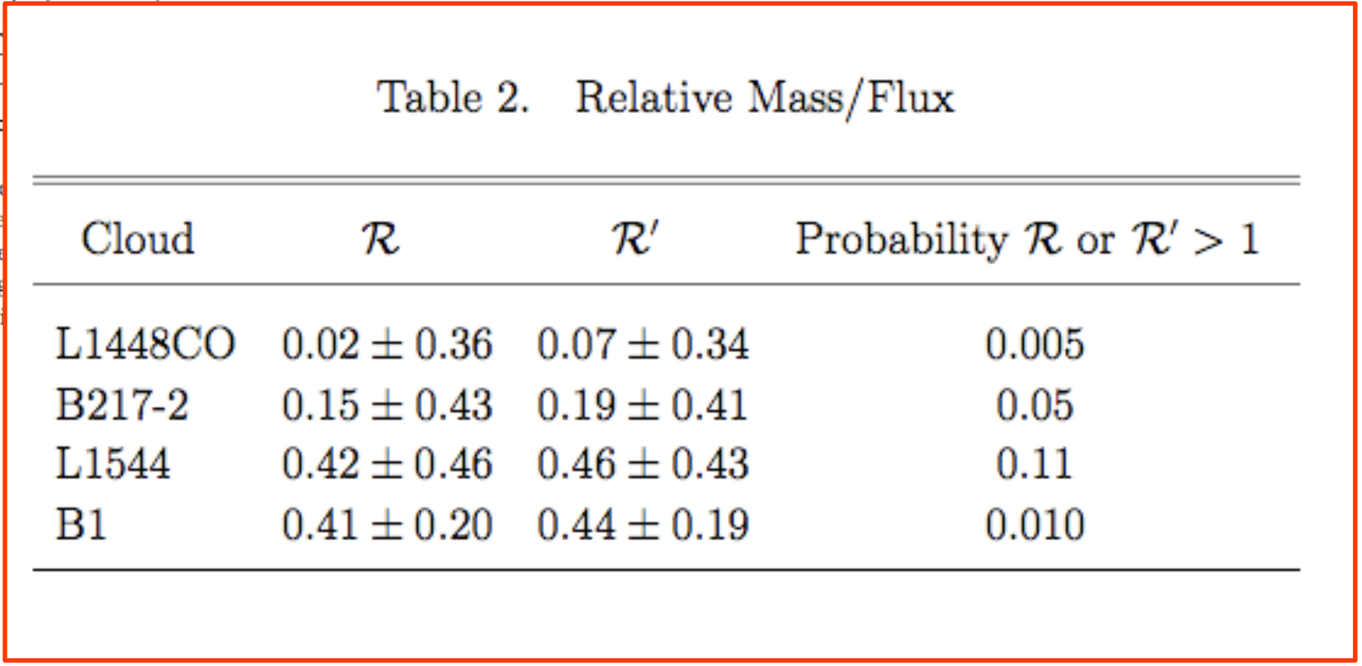

Table 2. Relative Mass/Flux

Cloud	$\mathcal{R}$	$\mathcal{R}'$	Probability $\mathcal{R}$ or $\mathcal{R}' > 1$
L1448CO	0.02 ± 0.36	0.07 ± 0.34	0.005
B217-2	0.15 ± 0.43	0.19 ± 0.41	0.05
L1544	0.42 ± 0.46	0.46 ± 0.43	0.11
B1	0.41 ± 0.20	0.44 ± 0.19	0.010

Crutcher et al. (2009)

Lunttila et al. (2008)

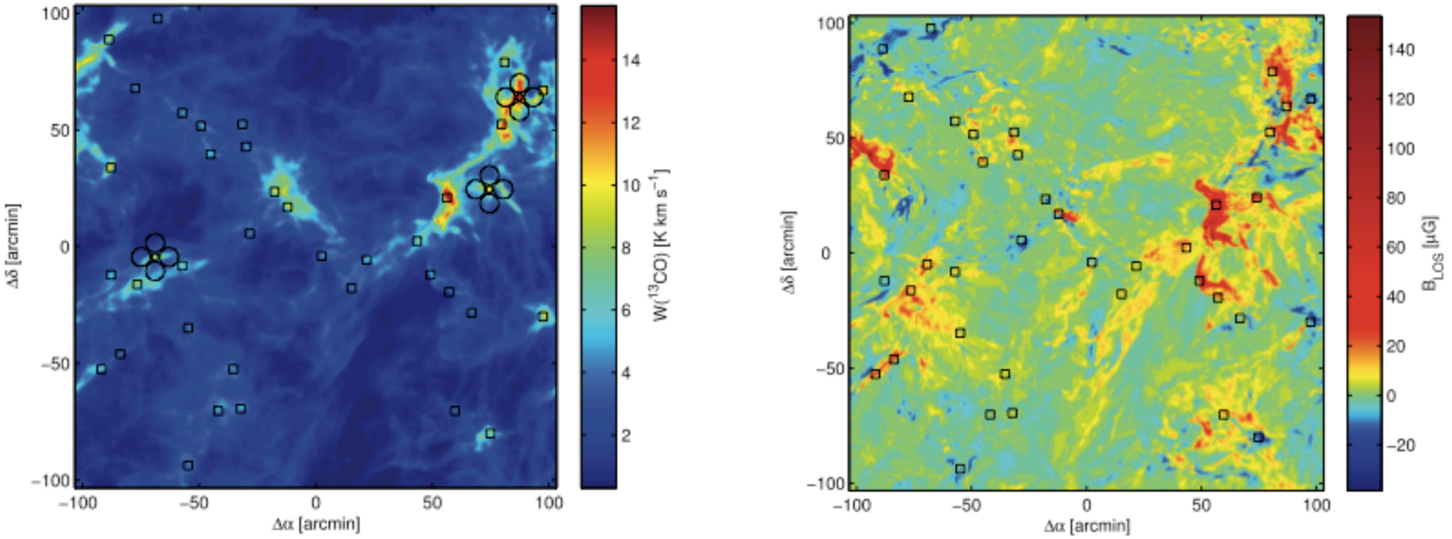

FIG. 1.—*Left*: Simulated ^{13}CO (1–0) map of the model in the *z*-axis direction. The locations of the cloud cores are shown with squares. The circles indicate the locations of telescope beams used in the synthetic observations of three cores. *Right*: Line-of-sight magnetic field strength as calculated from Zeeman splitting.

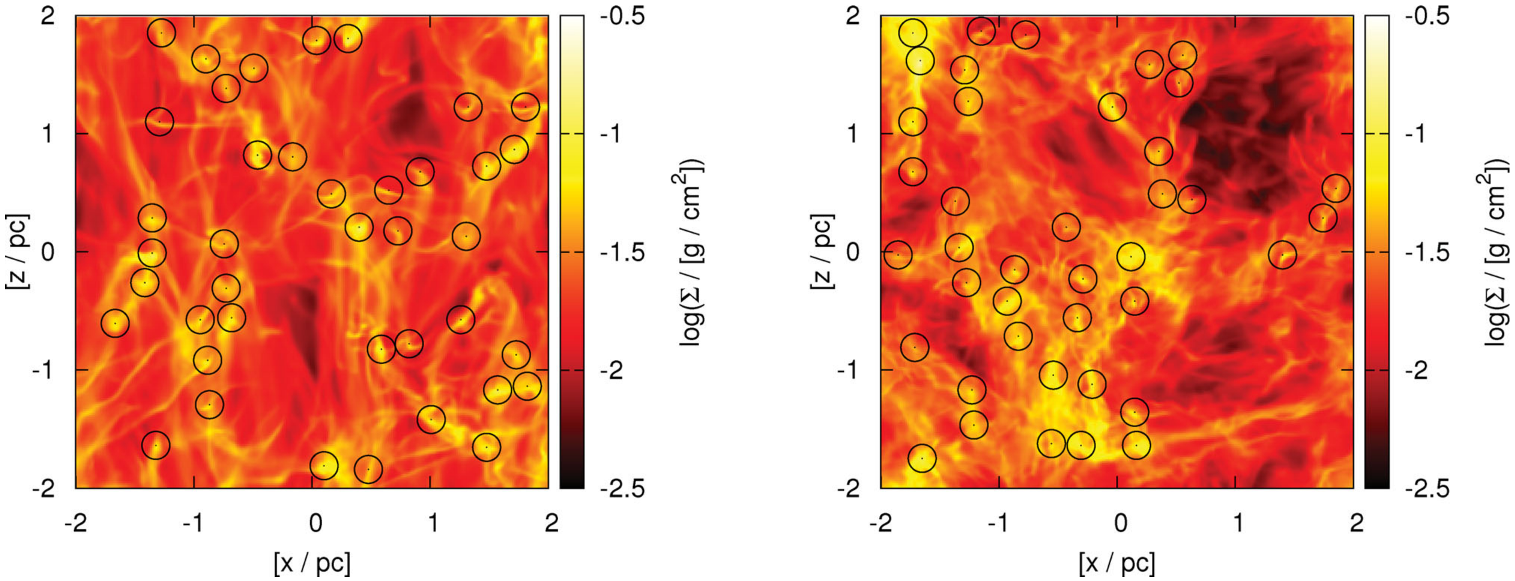

Bertram et al. (2012)

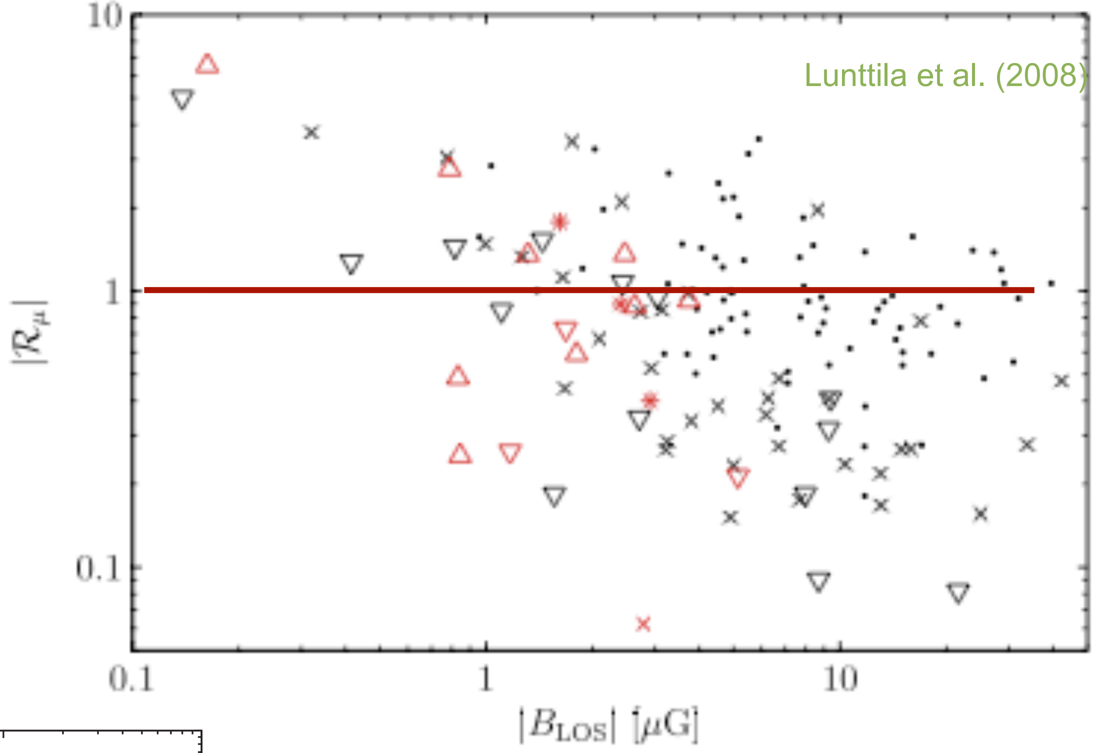
Lunttila et al. (2008)
10
1
0.1
$|\mathcal{R}_\mu|$
0.1
1
10
$|B_{\rm LOS}|$ [μG]

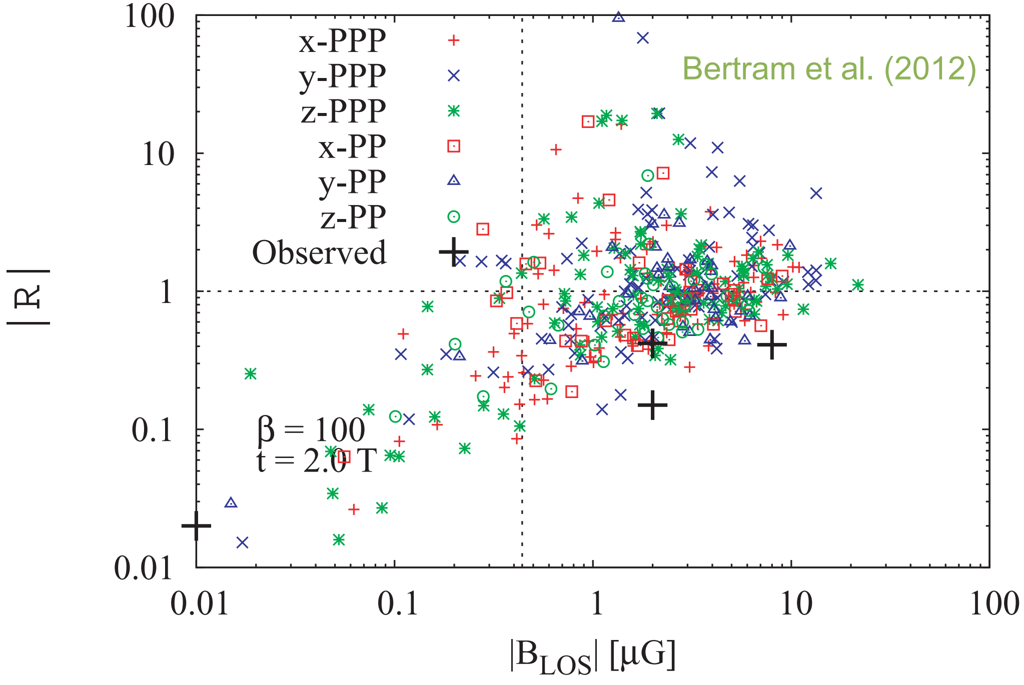
Bertram et al. (2012)
x-PPP
y-PPP
z-PPP
x-PP
y-PP
z-PP
Observed
β = 100
t = 2.0 T
100
10
1
0.1
0.01
|R|
0.01
0.1
1
10
100
$|B_{LOS}|$ [μG]

Molecular cloud dynamics

- **Timescale problem:** Turbulence *decays* on timescales *comparable to the free-fall time* τ_{ff} ($E \propto t^{-\eta}$ with $\eta \approx 1$).

(Mac Low et al. 1998,
Stone et al. 1998,
Padoan & Nordlund 1999)

- Magnetic fields (static or wave-like) *cannot* prevent loss of energy.

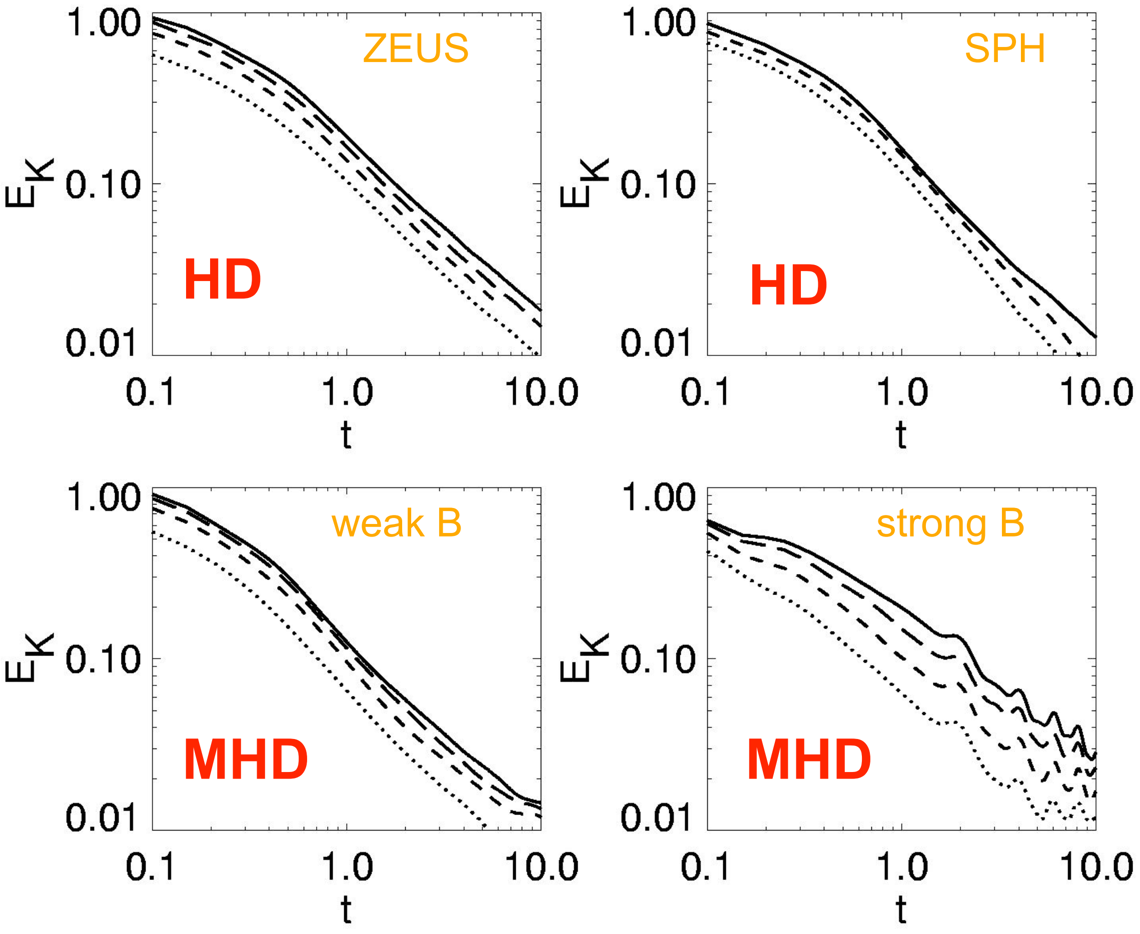

(Mac Low, Klessen, Burkert, & Smith, 1998, PRL)

gravoturbulent star formation

- BASIC ASSUMPTION:

star formation is controlled by interplay between supersonic turbulence and self-gravity

- turbulence plays a *dual role*:
  - on *large scales* it *provides support*
  - on *small scales* it can *trigger collapse*
- some predictions:
  - dynamical star formation timescale τ_{ff}
  - high binary fraction
  - complex spatial structure of embedded star clusters
  - and many more . . .

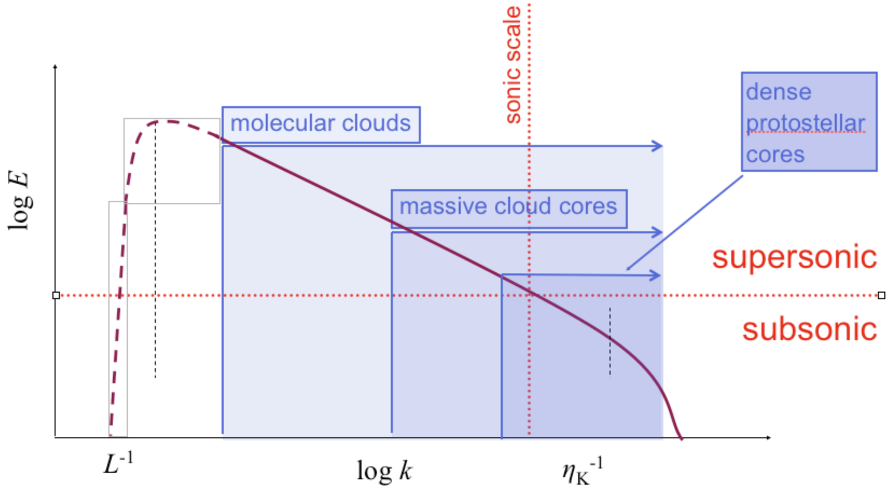

Mac Low & Klessen, 2004, Rev. Mod. Phys., 76, 125-194
McKee & Ostriker, 2007, ARAA, 45, 565

turbulent cascade in the ISM

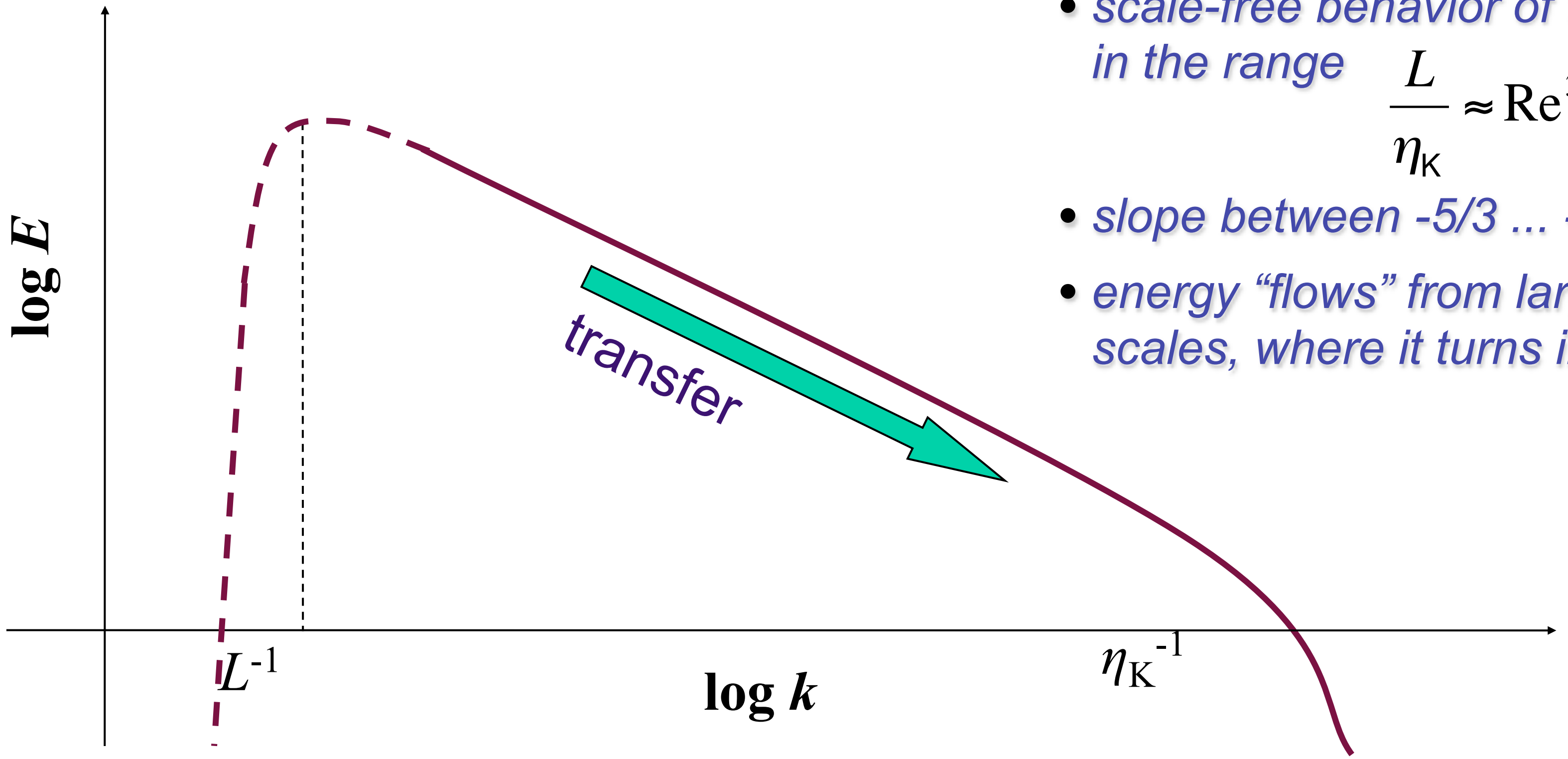

- *scale-free behavior of turbulence in the range* $\frac{L}{\eta_K} \approx \mathrm{Re}^{3/4}$
- *slope between -5/3 ... -2*
- *energy “flows” from large to small scales, where it turns into heat*

energy source & scale
NOT known
(supernovae, winds,
spiral density waves?)

dissipation scale not known
(ambipolar diffusion,
molecular diffusion?)

turbulent cascade in the ISM

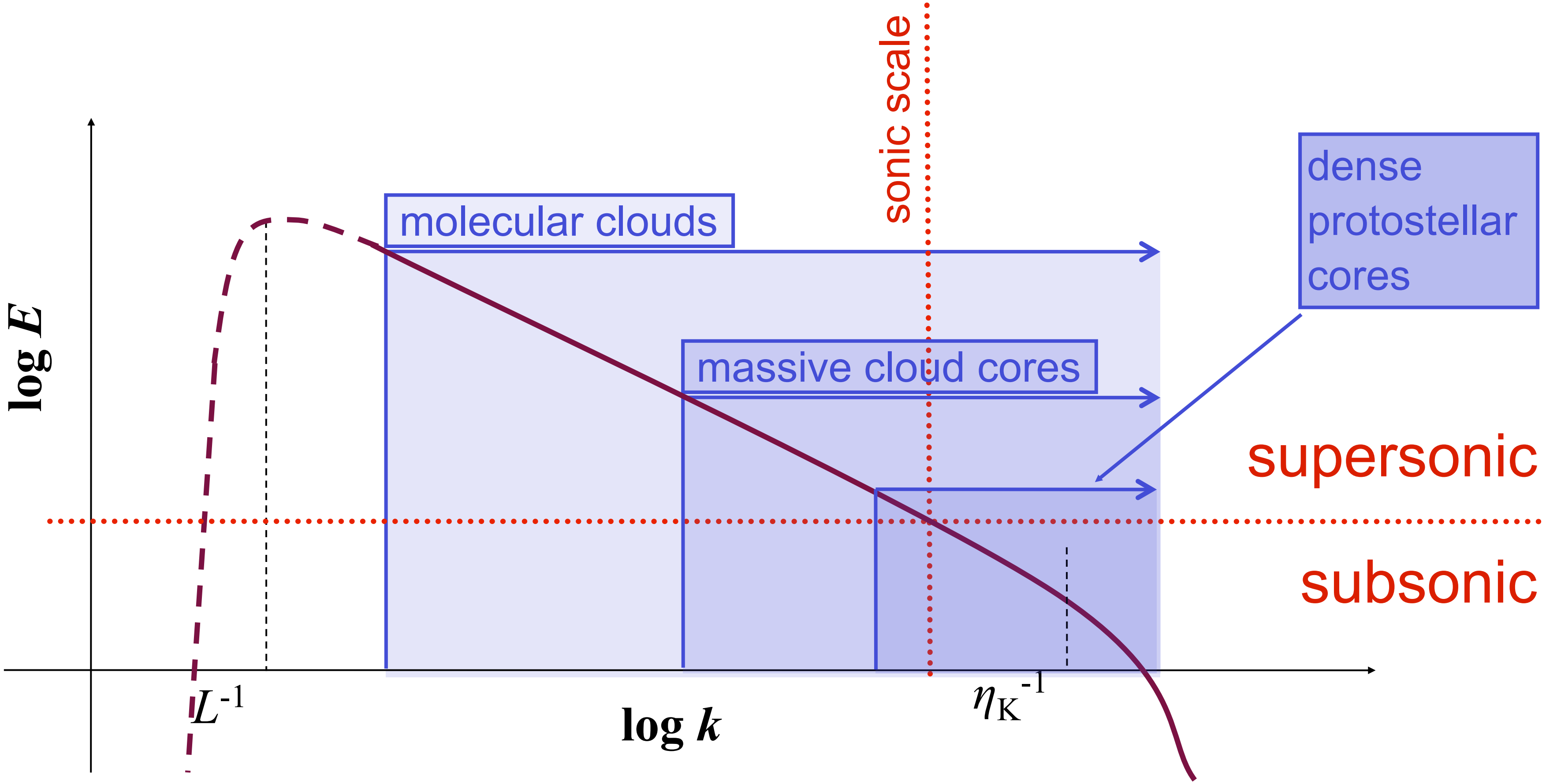

energy source & scale
NOT known
(supernovae, winds,
spiral density waves?)

$\sigma_{rms} << 1$ km/s
$M_{rms} \leq 1$
$L \approx 0.1$ pc

dissipation scale not known
(ambipolar diffusion,
molecular diffusion?)

dynamical SF in a nutshell

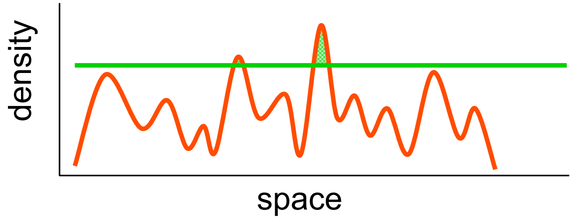

- interstellar gas is highly *inhomogeneous*
  - *gravitational instability*
  - *thermal instability*
  - *turbulent compression* (in shocks $\delta\rho/\rho \propto \mathcal{M}^2$; in atomic gas: $\mathcal{M} \approx 1...3$)
- cold *molecular clouds* can form rapidly in high-density regions at *stagnation points* of *convergent large-scale flows*
  - chemical *phase transition*: atomic → molecular
  - process is *modulated* by large-scale *dynamics* in the galaxy
- inside *cold clouds:* turbulence is highly supersonic ($\mathcal{M} \approx 1...20$)
  → *turbulence* creates large density contrast,
  gravity selects for collapse

→ ***GRAVOTUBULENT FRAGMENTATION***

- *turbulent cascade:* local compression *within* a cloud provokes collapse → formation of individual *stars* and *star clusters*

(e.g. Mac Low & Klessen, 2004, Rev. Mod. Phys., 76, 125-194)

Density structure of MC's

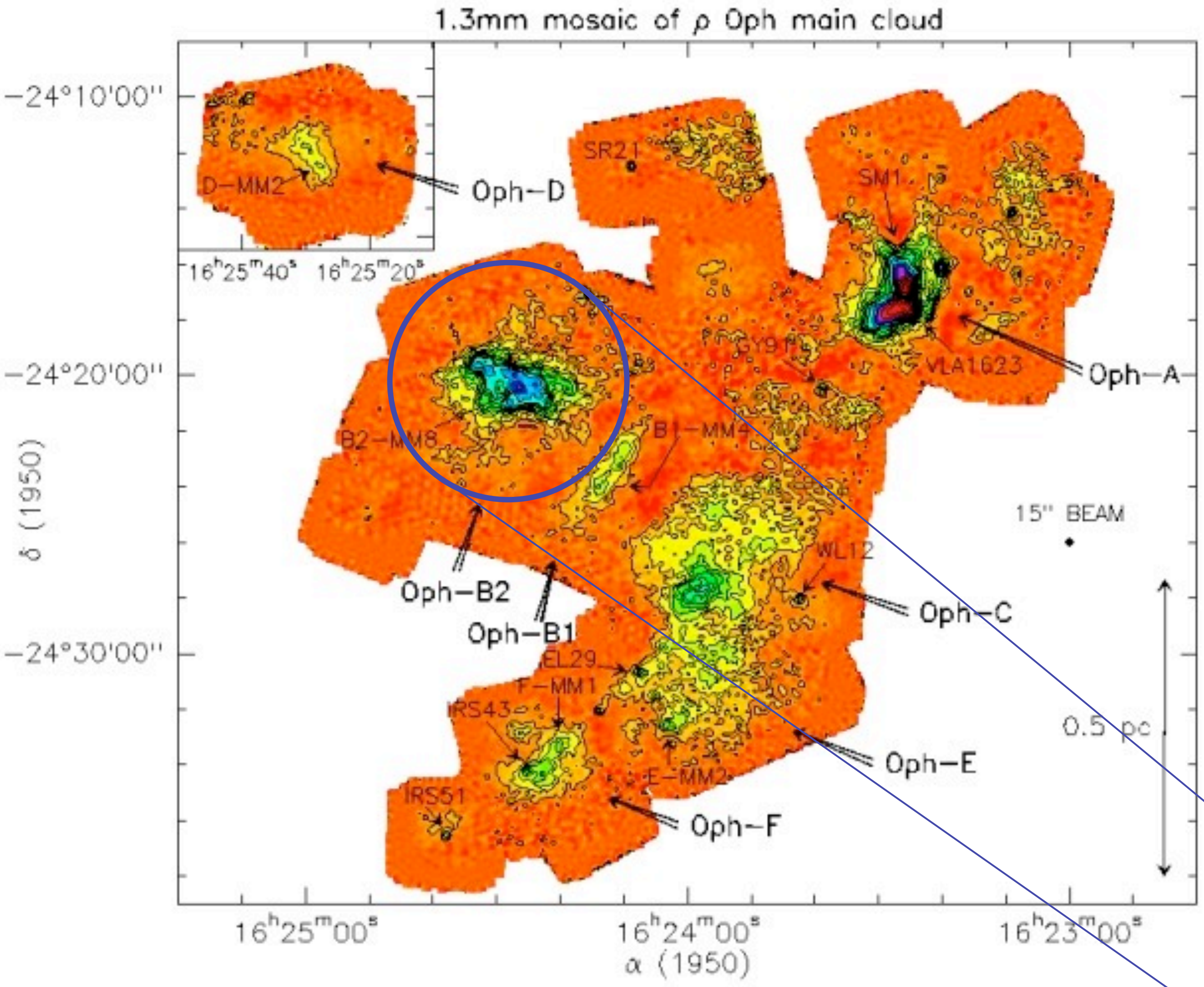

(Motte, André, & Neri 1998)

molecular clouds are highly inhomogeneous

stars form in the densest and coldest parts of the cloud

ρ-Ophiuchus cloud seen in dust emission

let's focus on a cloud core like this one

Evolution of cloud cores

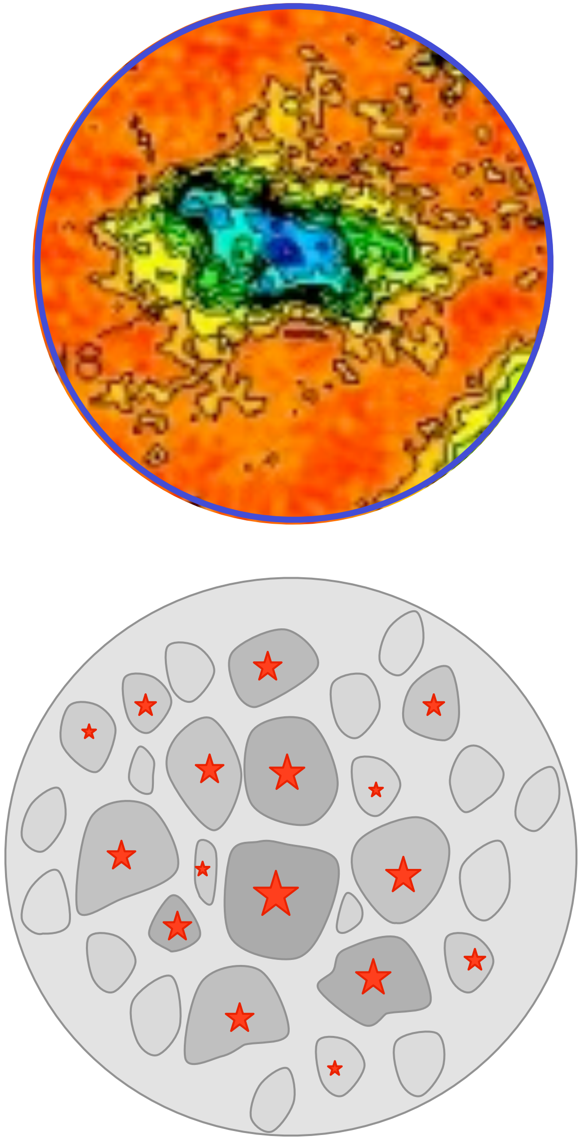

- How does this core evolve?
  Does it form one single massive star or cluster with mass distribution?

- Turbulent cascade „goes through“ cloud core
  --> NO *scale separation* possible
  --> NO *effective sound speed*
- Turbulence is supersonic!
  --> produces strong density contrasts:
  $\delta\rho/\rho \approx M^2$
  --> with typical $M \approx 10$ --> $\delta\rho/\rho \approx 100$!
- many of the shock-generated fluctuations are Jeans unstable and go into collapse
- --> expectation: *core breaks up and forms a cluster of stars*

Evolution of cloud cores

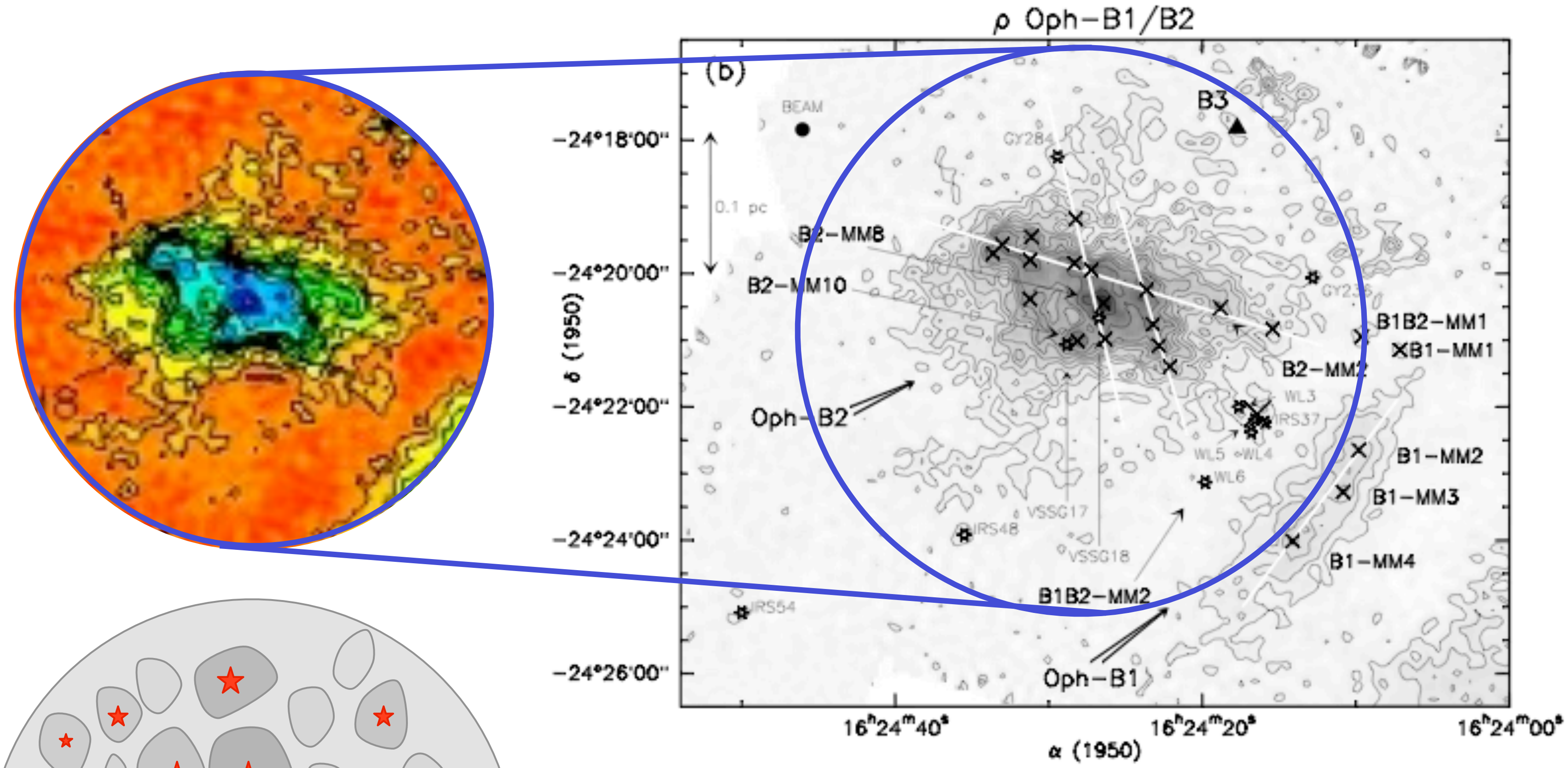

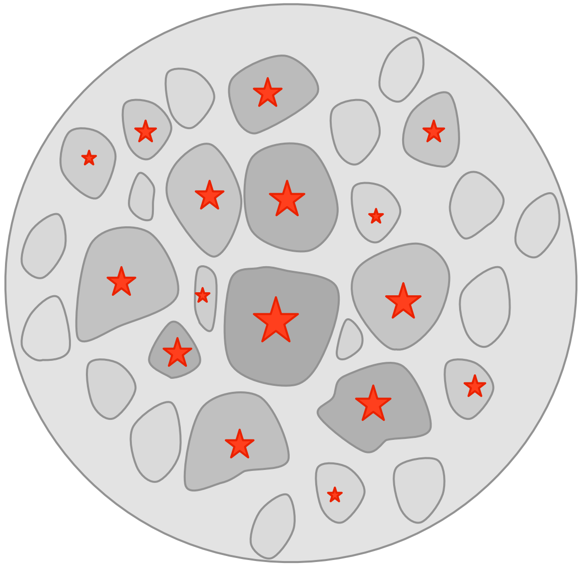

indeed ρ-Oph B1/2 contains several cores ("starless" cores are denoted by ×, cores with embedded protostars by ☆)

(Motte, André, & Neri 1998)

Formation and evolution of cores

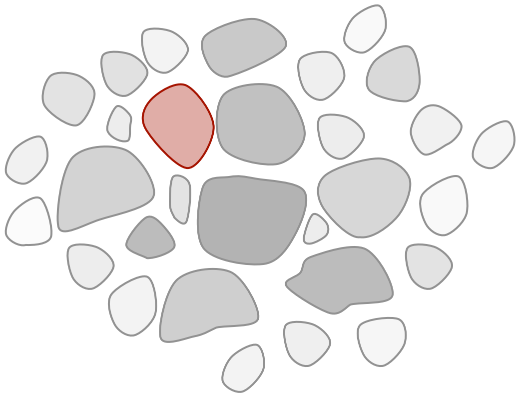

- protostellar cloud cores form at *stagnation point* in *convergent turbulent flows*

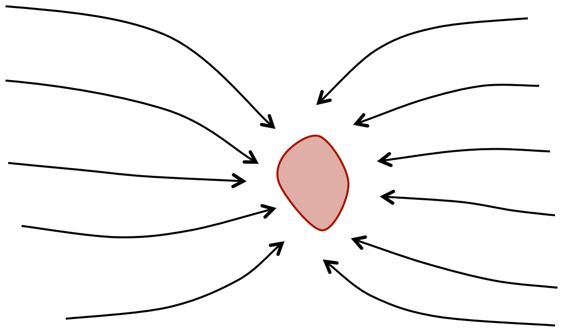

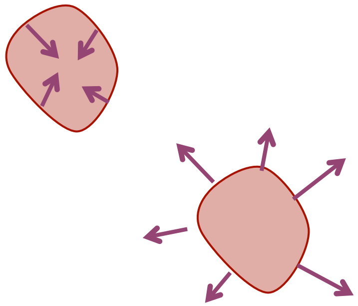

- if $M > M_{crit} \propto \rho^{-1/2} T^{3/2}$: collapse & star formation
- pf $M < M_{crit} \propto \rho^{-1/2} T^{3/2}$: reexpansion after end of external compression

(e.g. Vazquez-Semadeni et al 2005)

- typical timescale: $t \approx 10^4 \ldots 10^5$ yr

Formation and evolution of cores

What happens to distribution of cloud cores?

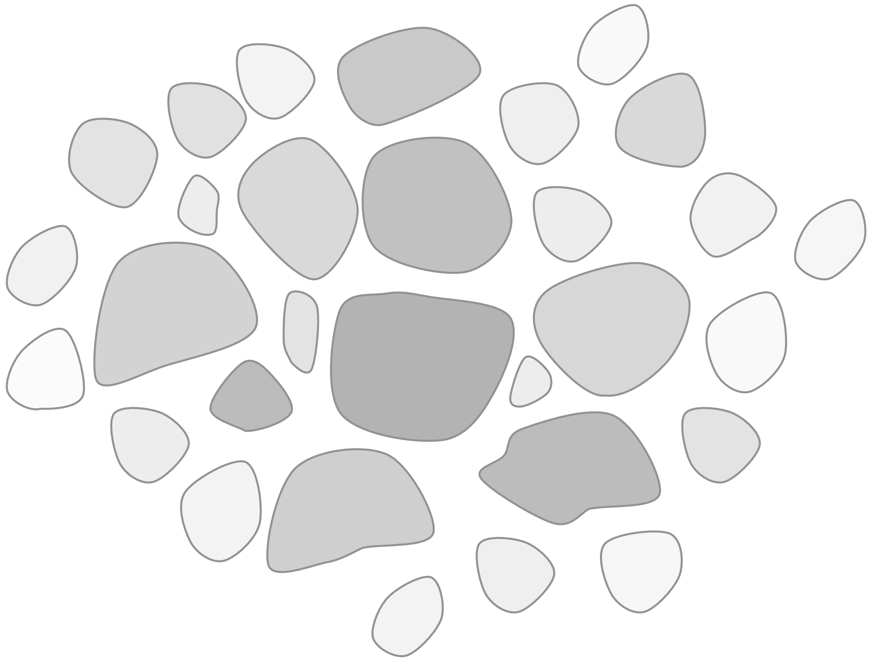

Two exteme cases:

(1) turbulence dominates energy budget:

$\alpha = E_{kin}/|E_{pot}| > 1$

--> individual cores do *not* interact

--> *collapse* of *individual* cores dominates *stellar mass growth*

--> *loose cluster of low-mass stars*

(2) turbulence decays, i.e. gravity dominates:

$\alpha = E_{kin}/|E_{pot}| < 1$

--> *global contraction*

--> core do *interact* while collapsing

--> *competition* influences *mass growth*

--> *dense cluster with high-mass stars*

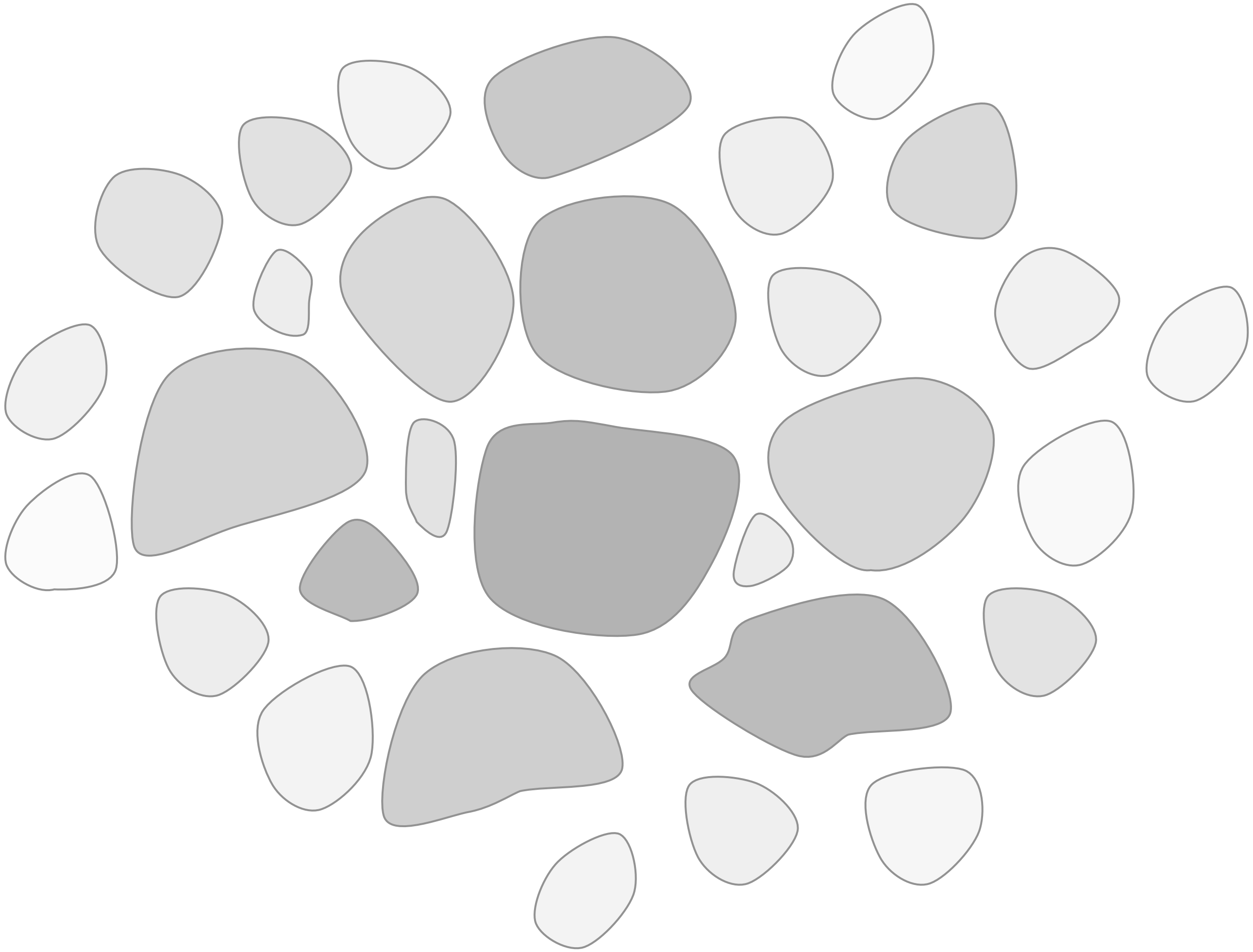

turbulence creates a hierarchy of clumps

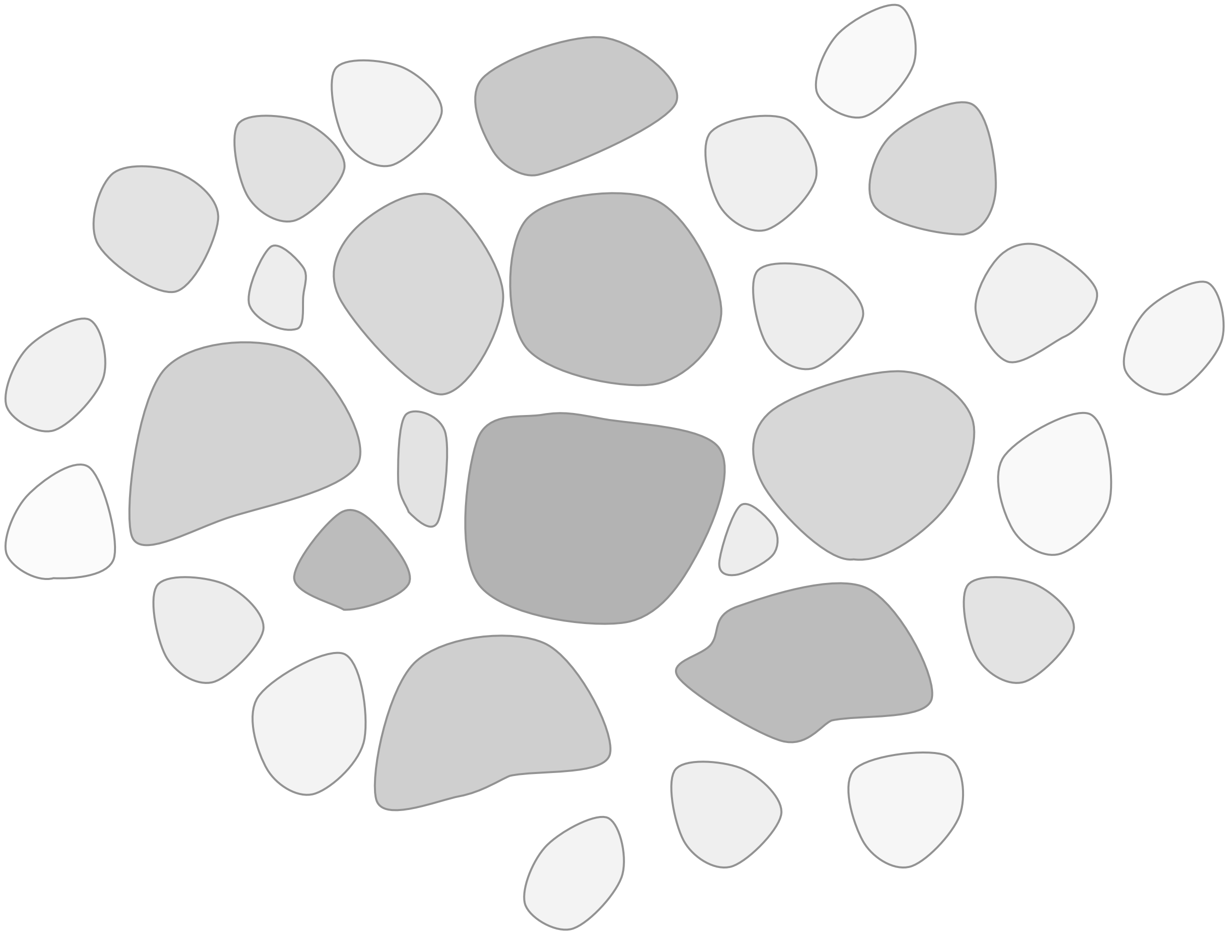

as turbulence decays locally, contraction sets in

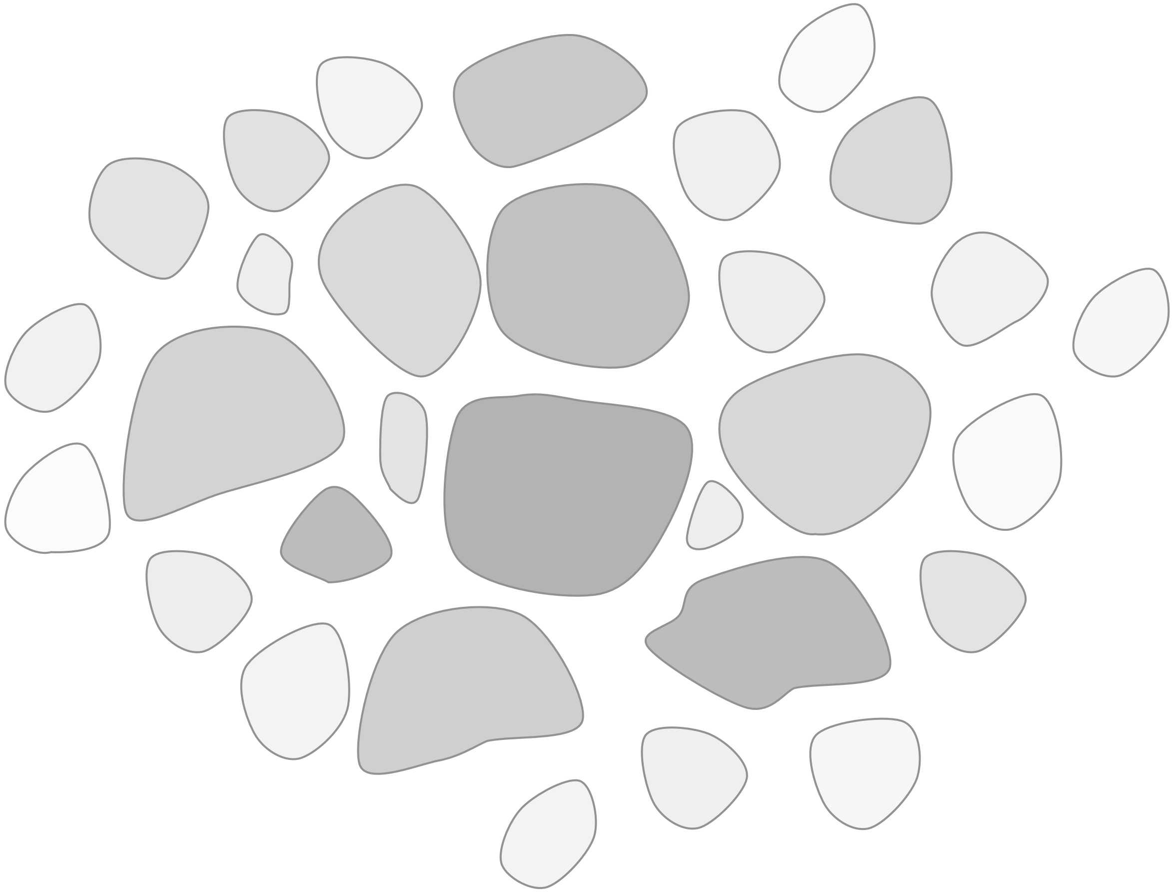

as turbulence decays locally, contraction sets in

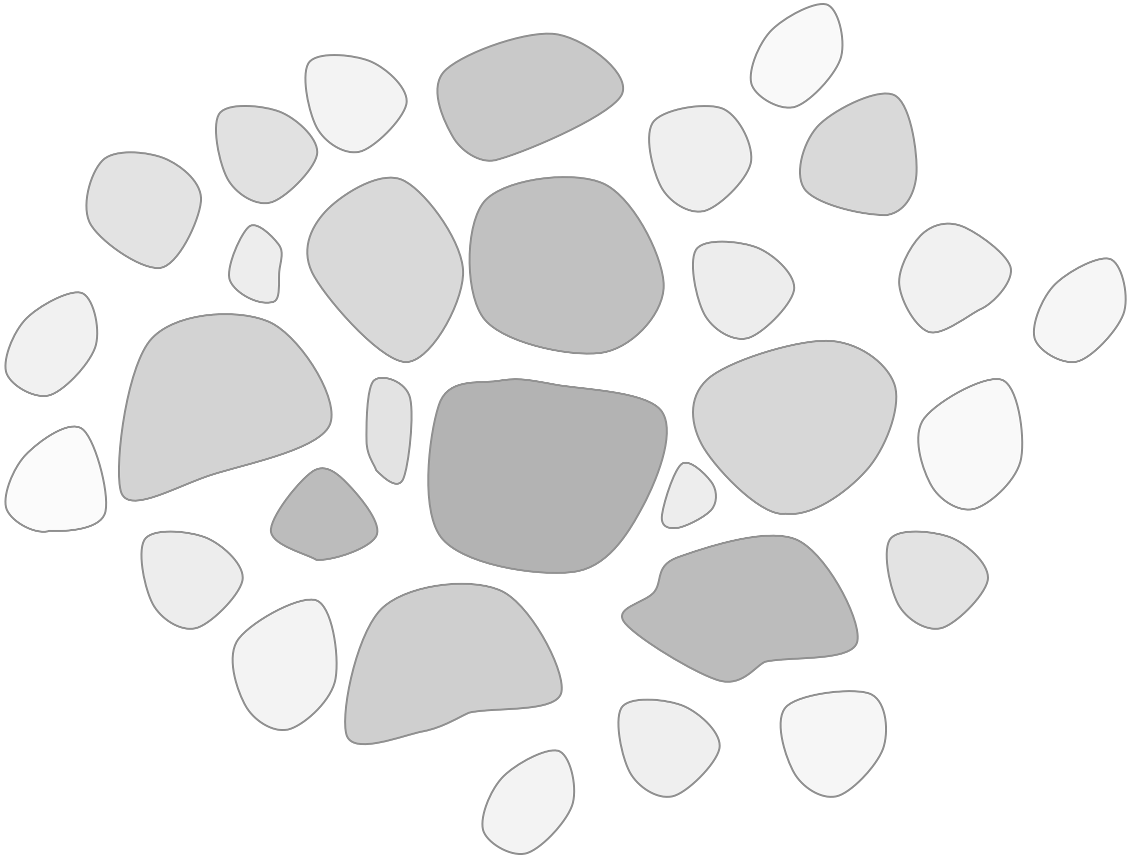

while region contracts, individual clumps collapse to form stars

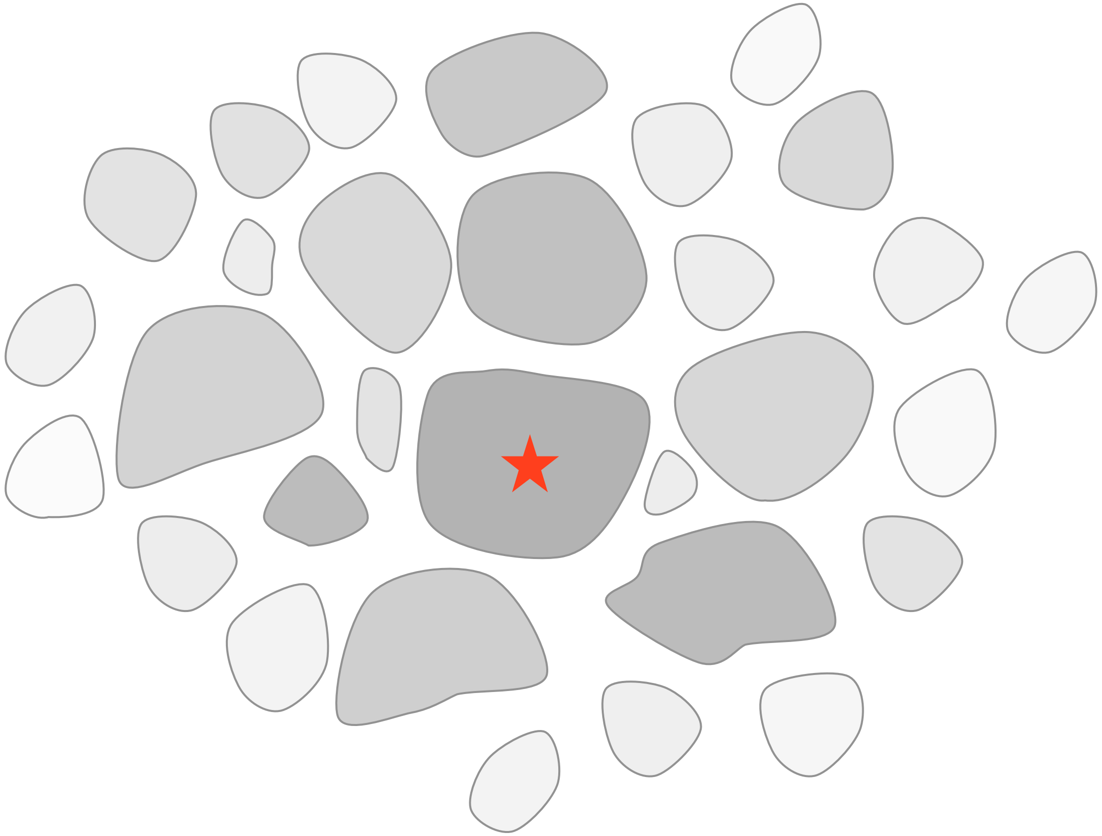

while region contracts, individual clumps collapse to form stars

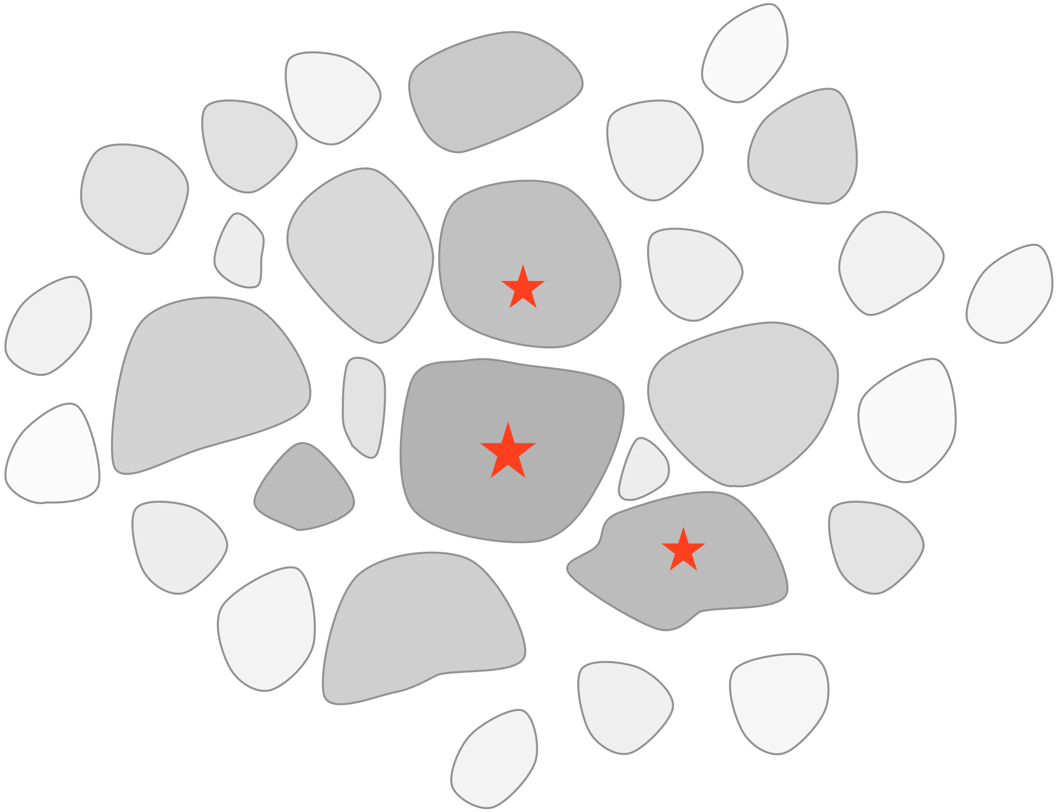

individual clumps collapse to form stars

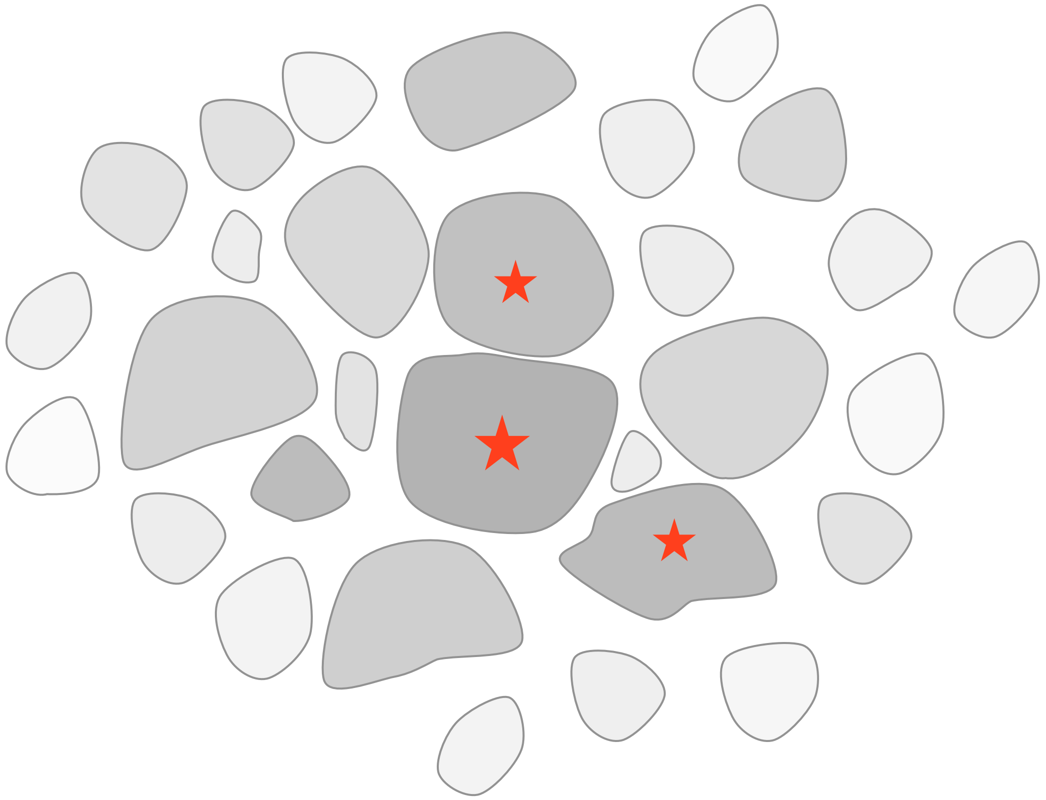

individual clumps collapse to form stars

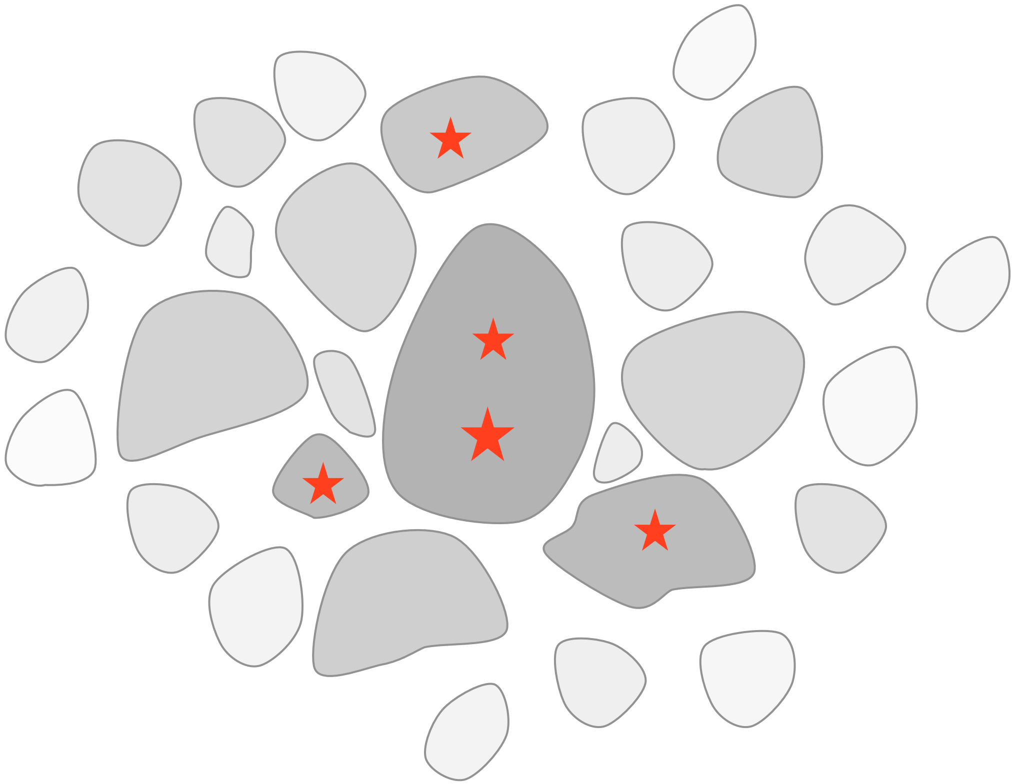

$\alpha = E_{kin}/|E_{pot}| < 1$

in *dense clusters*, clumps may merge while collapsing
--> then contain multiple protostars

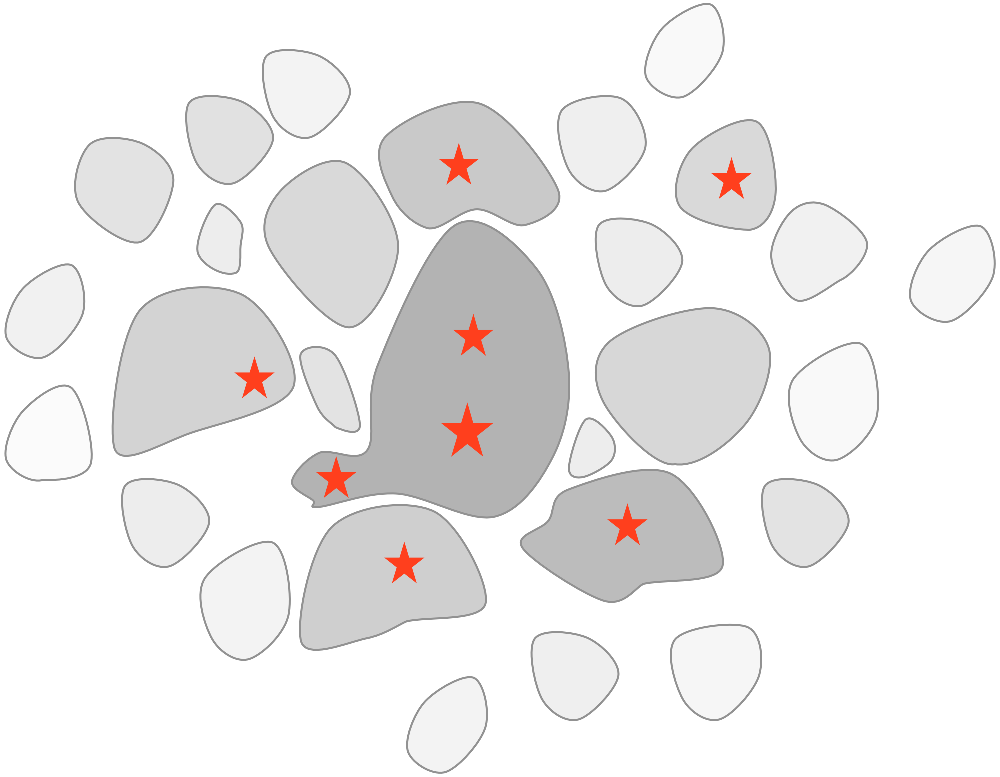

in *dense clusters*, clumps may merge while collapsing
--> then contain multiple protostars

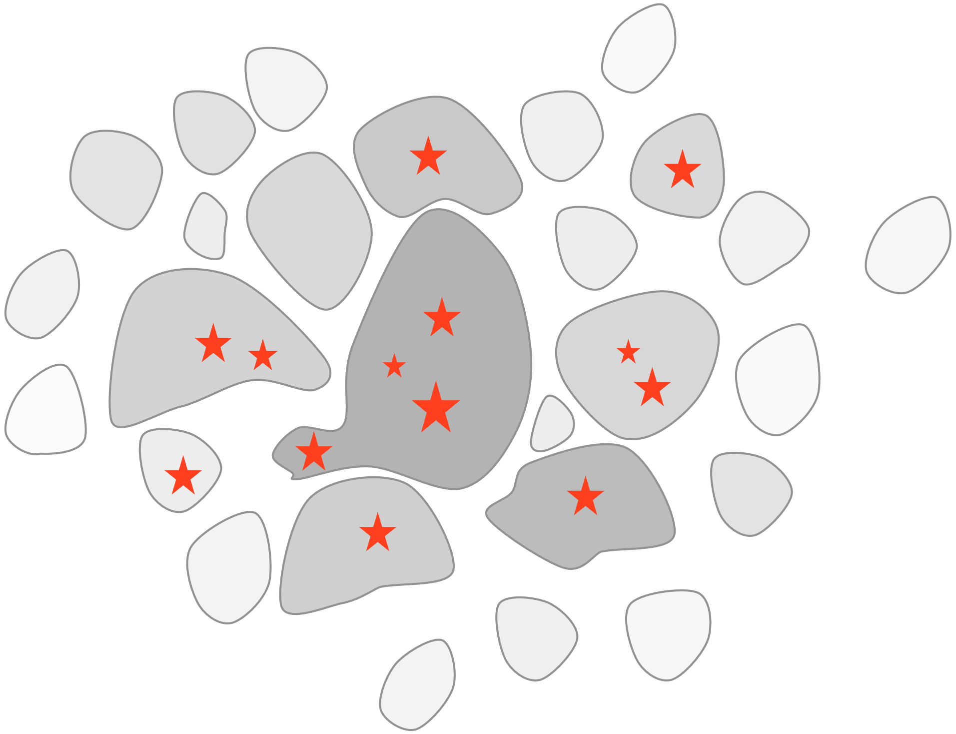

in *dense clusters*, clumps may merge while collapsing
--> then contain multiple protostars

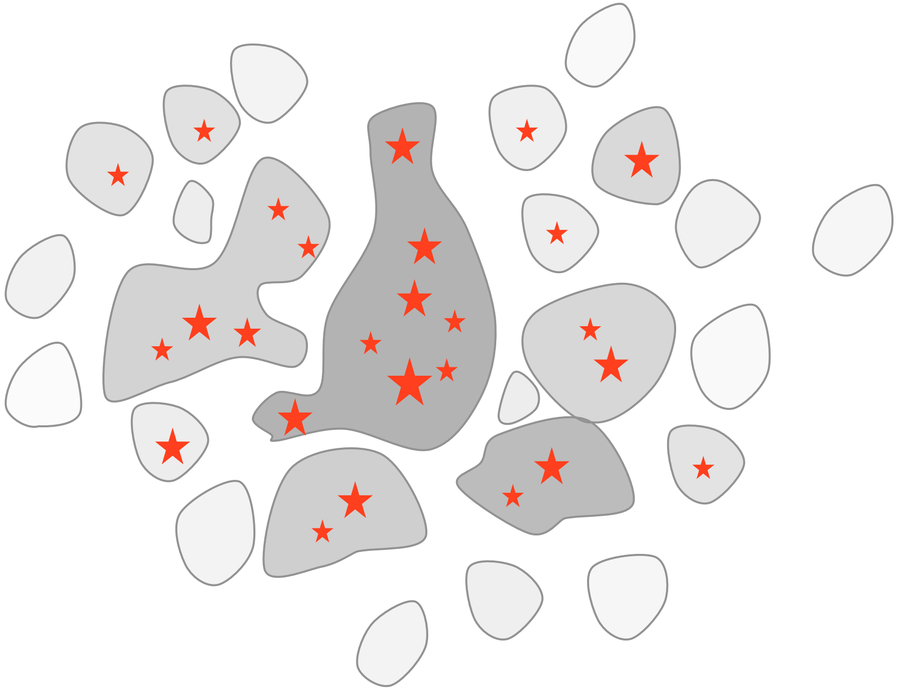

in *dense clusters*, competitive mass growth becomes important

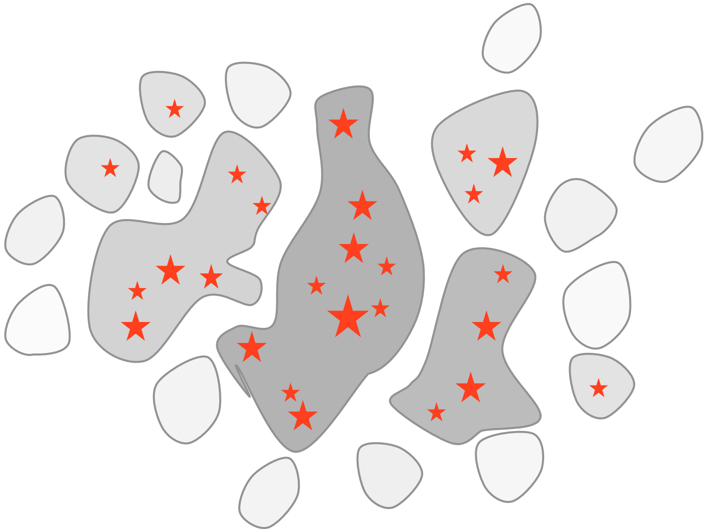

in *dense clusters*, competitive mass growth
becomes important

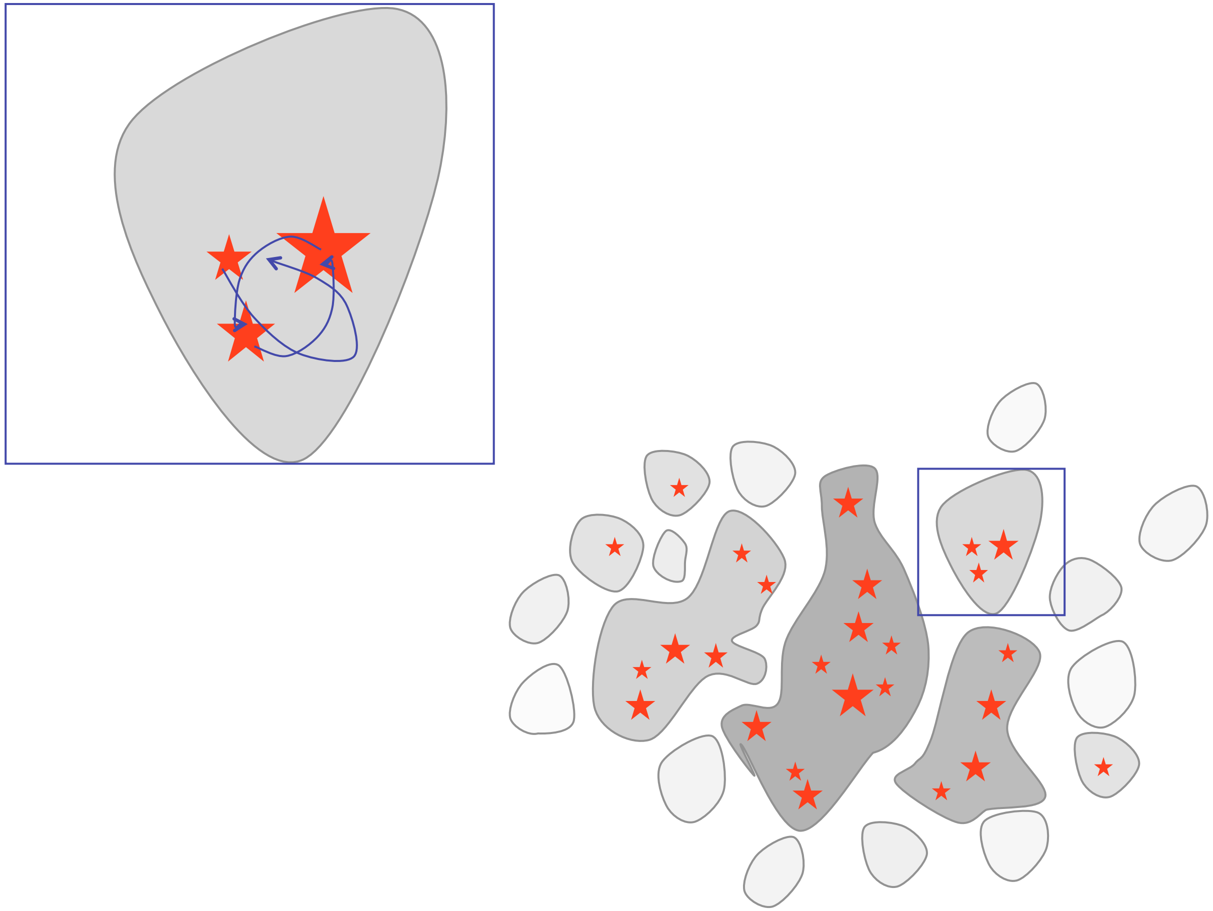

in *dense clusters*, *N*-body effects influence mass growth

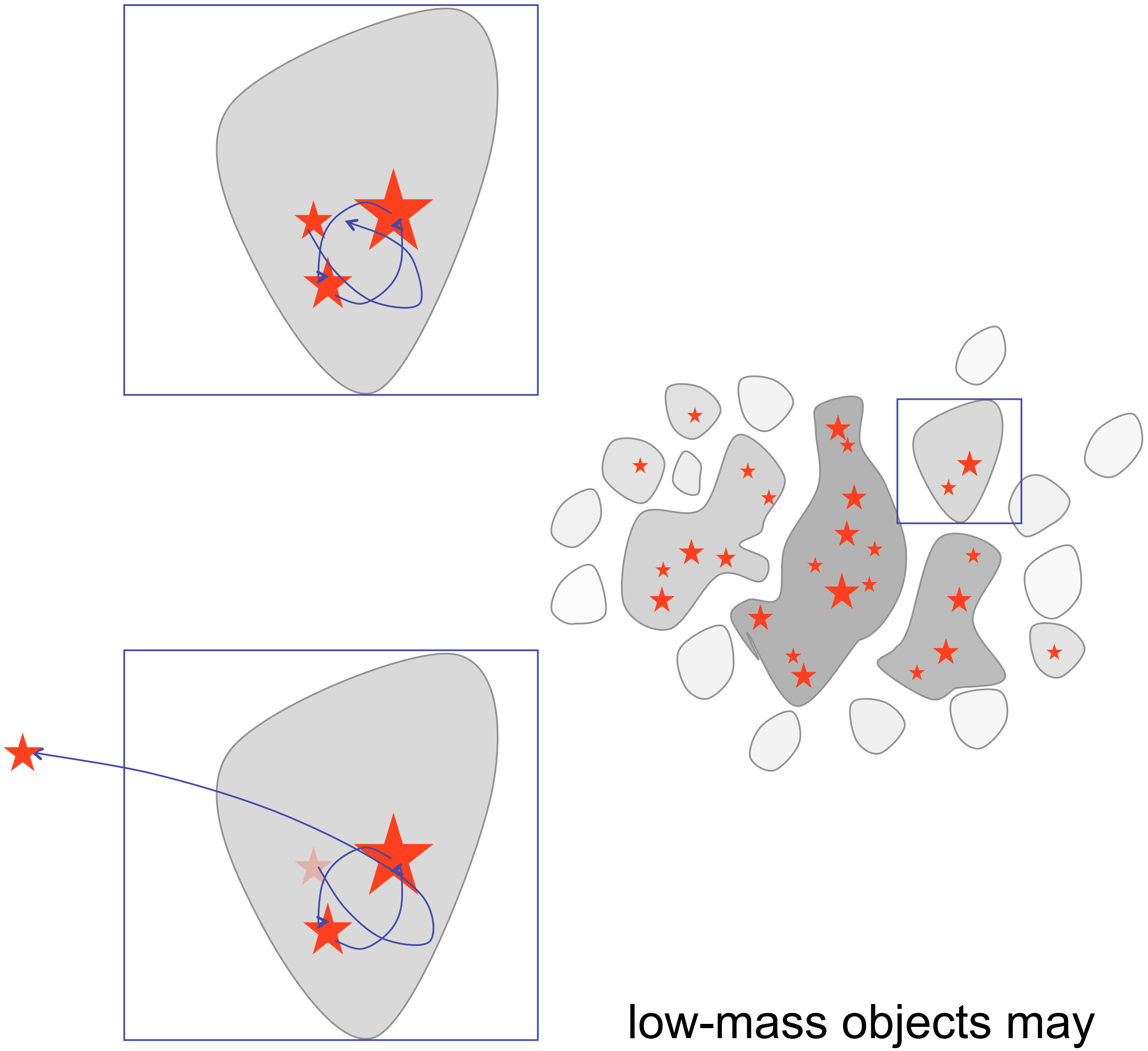

low-mass objects may
become ejected --> accretion stops

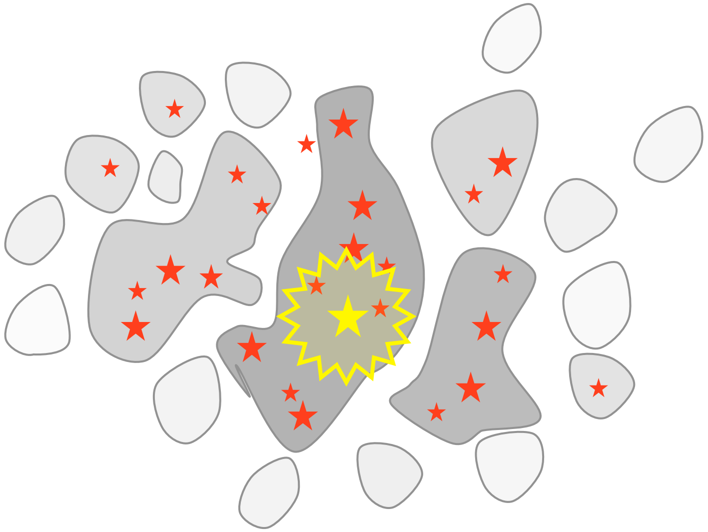

feedback terminates star formation

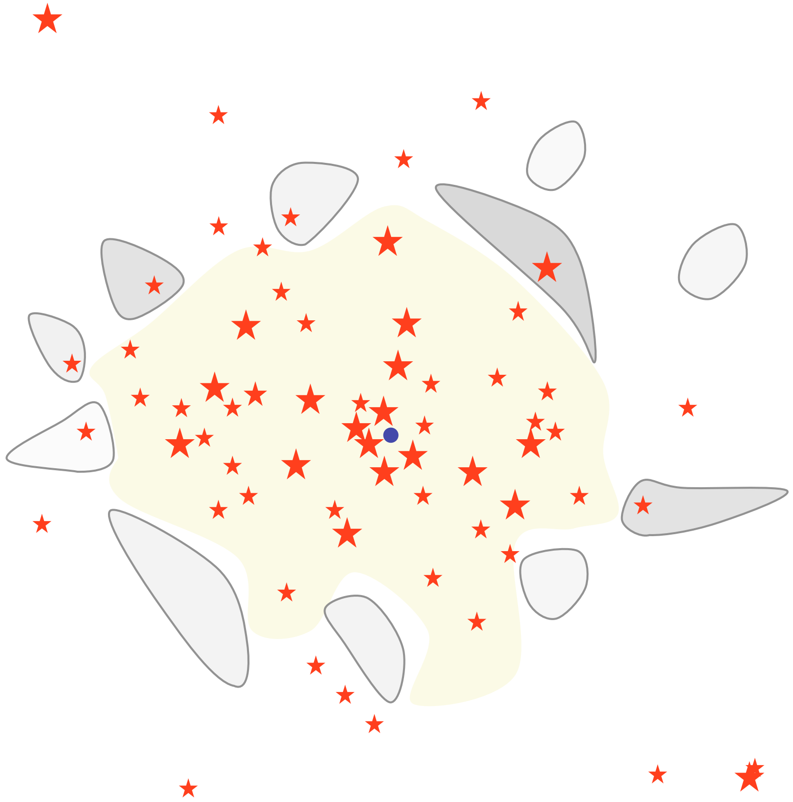

result: *star cluster*, possibly with H II region

NGC 602 in the LMC: Hubble Heritage Image

some concerns of simple model

- *energy balance*
  - in molecular clouds:

    kinetic energy ~ potential energy ~ magnetic energy > thermal energy
  - models based on HD turbulence misses important physics
  - in certain environments (Galactic Center, star bursts), energy density in *cosmic rays* and *radiation* is important as well
- *time scales*
  - star clusters form fast, but more slowly than predicted by HD only (feedback and magnetic fields do help)
  - initial conditions do matter
    (turbulence does not erase memory of past dynamics)
- *star formation efficiency (SFE)*
  - SFE in gravoturbulent models is too high (again more physics needed)

current status

- *stars form from the complex interplay of self-gravity and a large number of competing processes (such as turbulence, B-field, feedback, thermal pressure)*

- *the relative importance of these processes depends on the environment*
  - prestellar cores --> thermal pressure is important
    molecular clouds --> turbulence dominates $\}$ (Larson's relation: $\sigma \propto L^{1/2}$)
  - massive star forming regions (NGC602): radiative feedback is important
    small clusters (Taurus): evolution maybe dominated by external turbulence

- *star formation is regulated by various feedback processes*

- *star formation is closely linked to global galactic dynamics (KS relation)*

Star formation is intrinsically a multi-scale and multi-physics problem, where it is difficult to single out individual processes. Simple theoretical approaches usually fail.

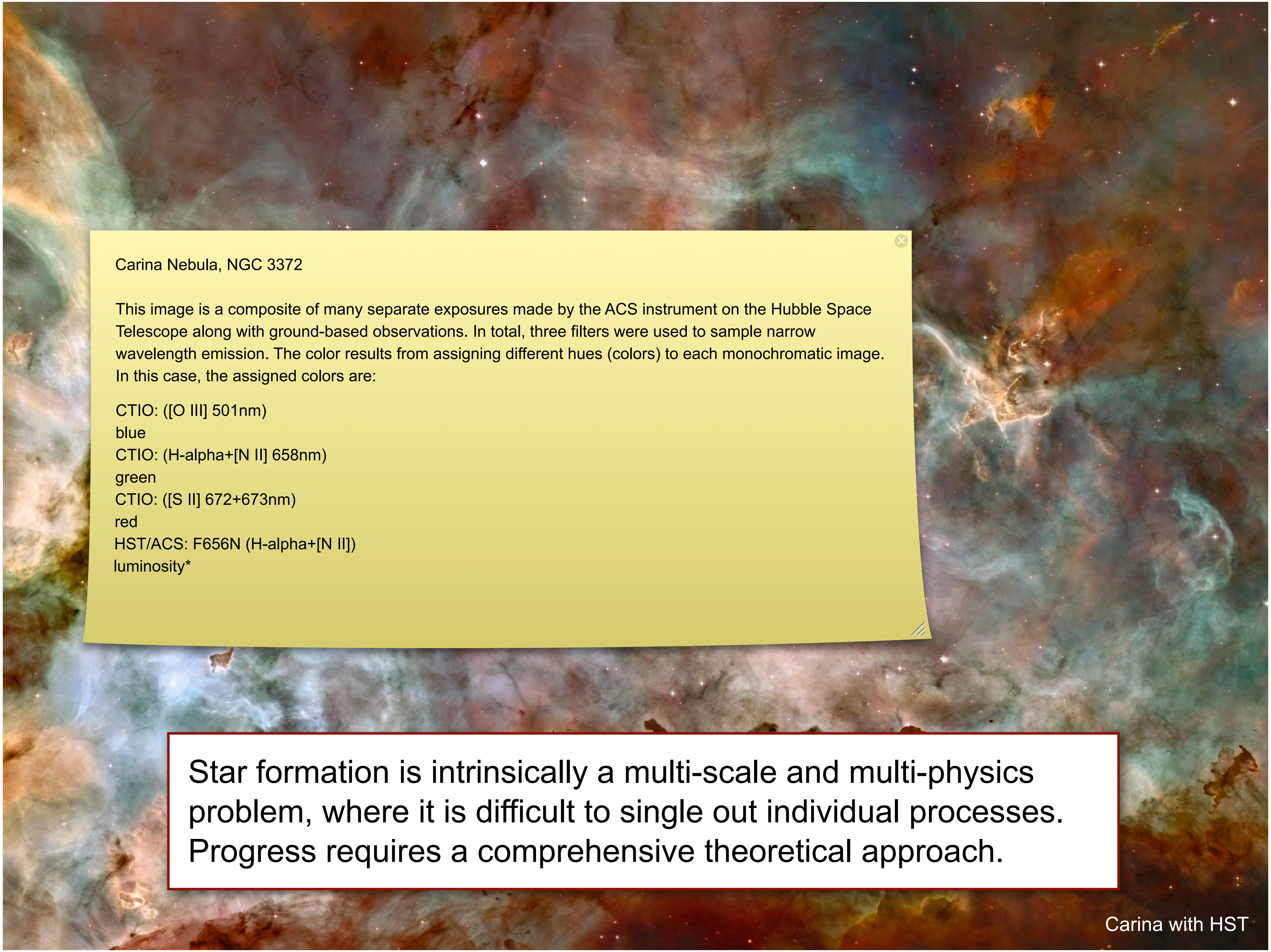

Carina Nebula, NGC 3372

This image is a composite of many separate exposures made by the ACS instrument on the Hubble Space Telescope along with ground-based observations. In total, three filters were used to sample narrow wavelength emission. The color results from assigning different hues (colors) to each monochromatic image. In this case, the assigned colors are:

CTIO: ([O III] 501nm)
blue
CTIO: (H-alpha+[N II] 658nm)
green
CTIO: ([S II] 672+673nm)
red
HST/ACS: F656N (H-alpha+[N II])
luminosity*

Star formation is intrinsically a multi-scale and multi-physics problem, where it is difficult to single out individual processes. Progress requires a comprehensive theoretical approach.

Carina with HST

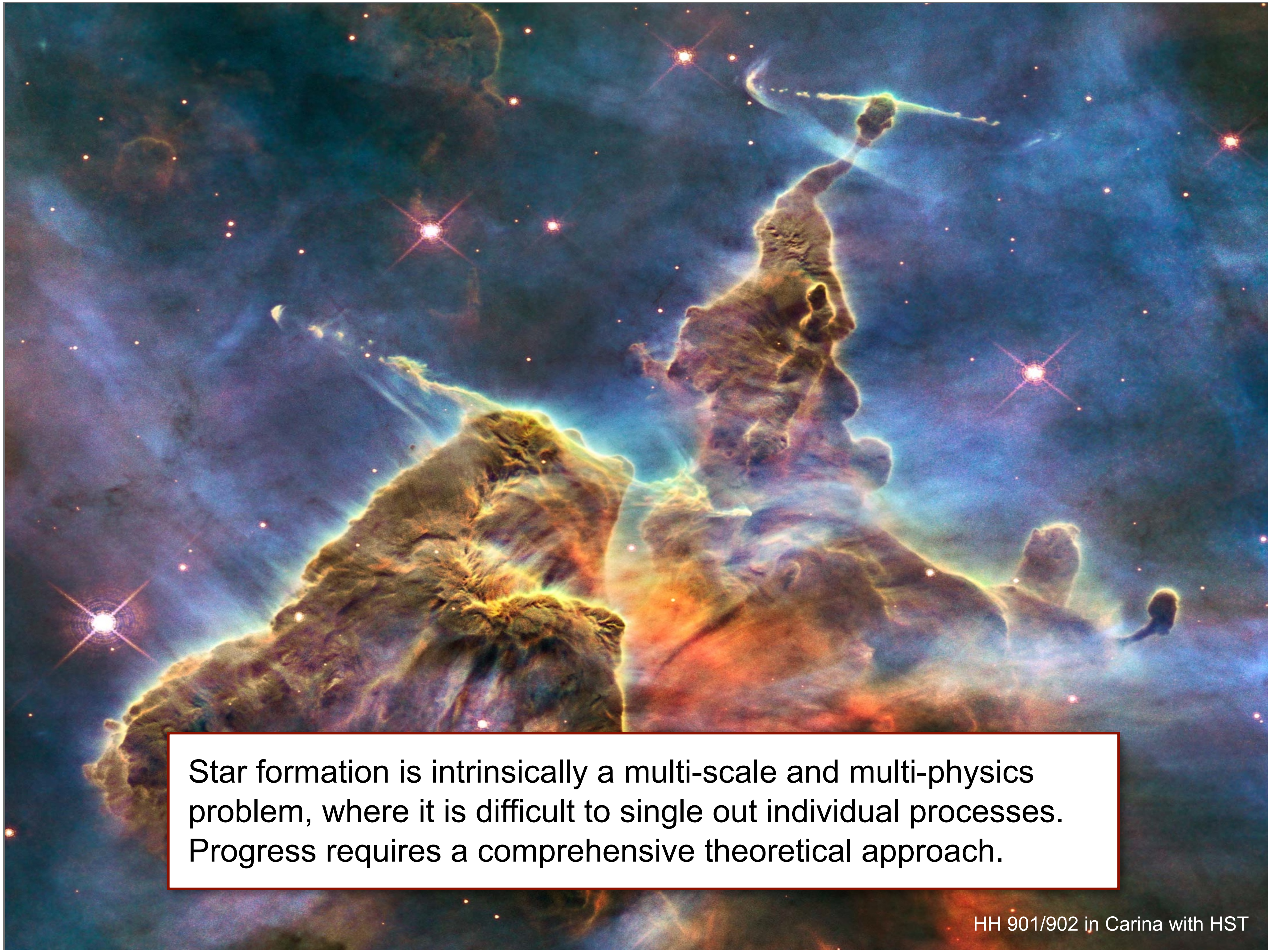

Star formation is intrinsically a multi-scale and multi-physics problem, where it is difficult to single out individual processes. Progress requires a comprehensive theoretical approach.

HH 901/902 in Carina with HST

selected open questions

- what processes determine the initial mass function (IMF) of stars?
- what are the initial conditions for star cluster formation?
  how does cloud structure translate into cluster structure?
- how do molecular clouds form and evolve?
- what drives turbulence?
- what triggers / regulates star formation on galactic scales?
- how does star formation depend on metallicity?
  how do the first stars form?
- star formation in extreme environments (galactic center, starburst, etc.),
  how does it differ from a more “normal” mode?

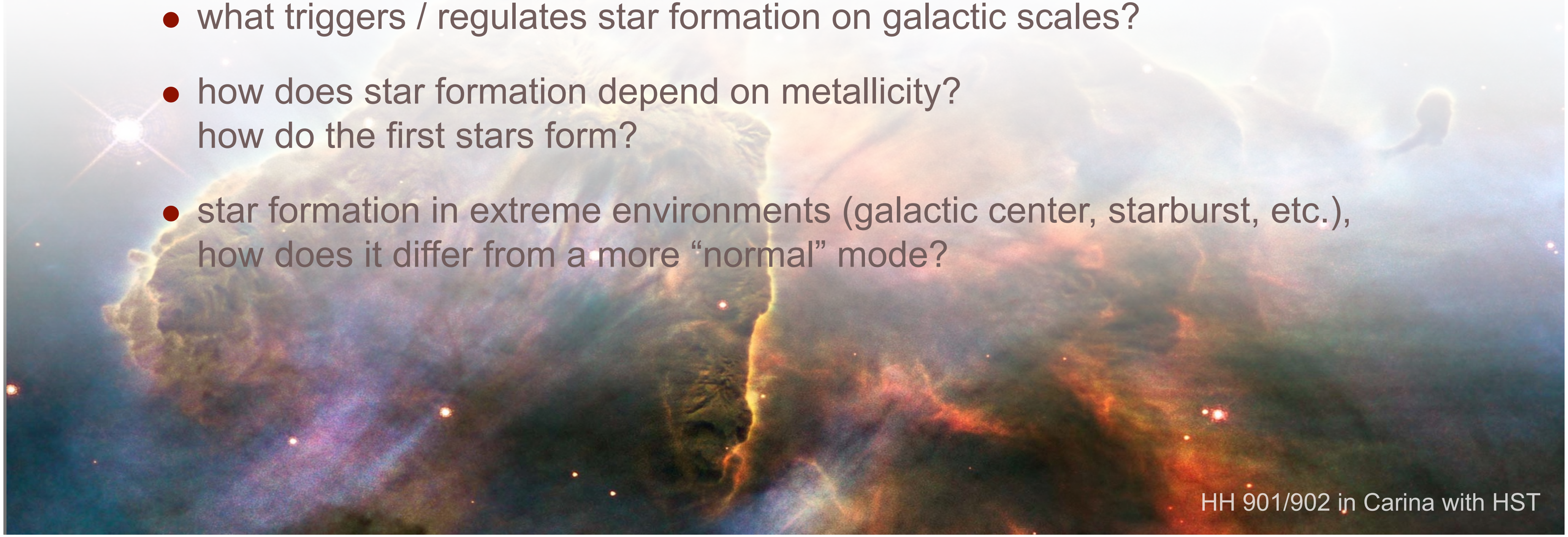

HH 901/902 in Carina with HST

initial mass function

stellar mass fuction

stars seem to follow a universal mass function at birth --> IMF

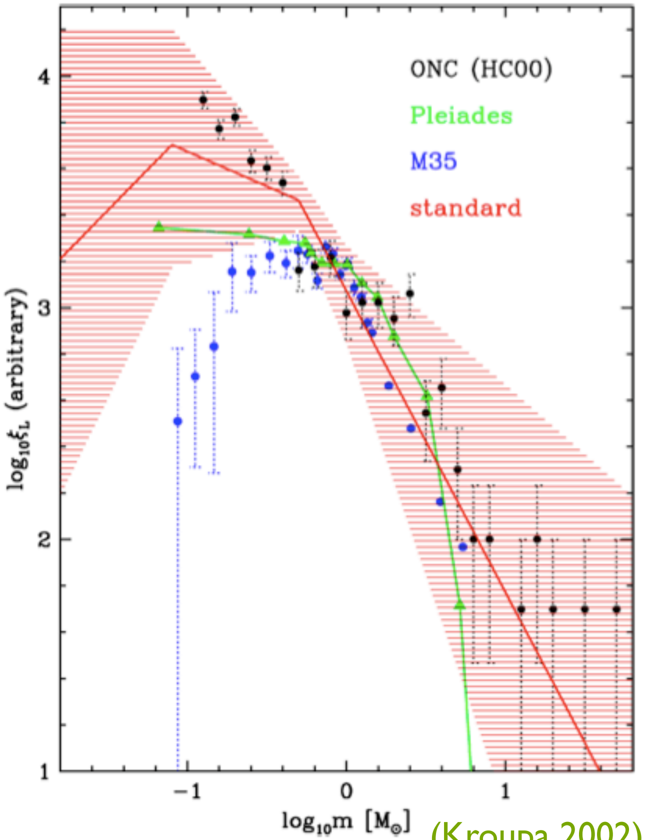

(Kroupa 2002)

Orion, NGC 3603, 30 Doradus
(Zinnecker & Yorke 2007)

stellar mass fuction

BUT: maybe variations with galaxy type (bottom heavy in the centers of large ellipticals)

from JAM (Jeans anisotropic multi Gaussian expansion) modeling

inferred excess of low-mass stars compared to Kroupa IMF

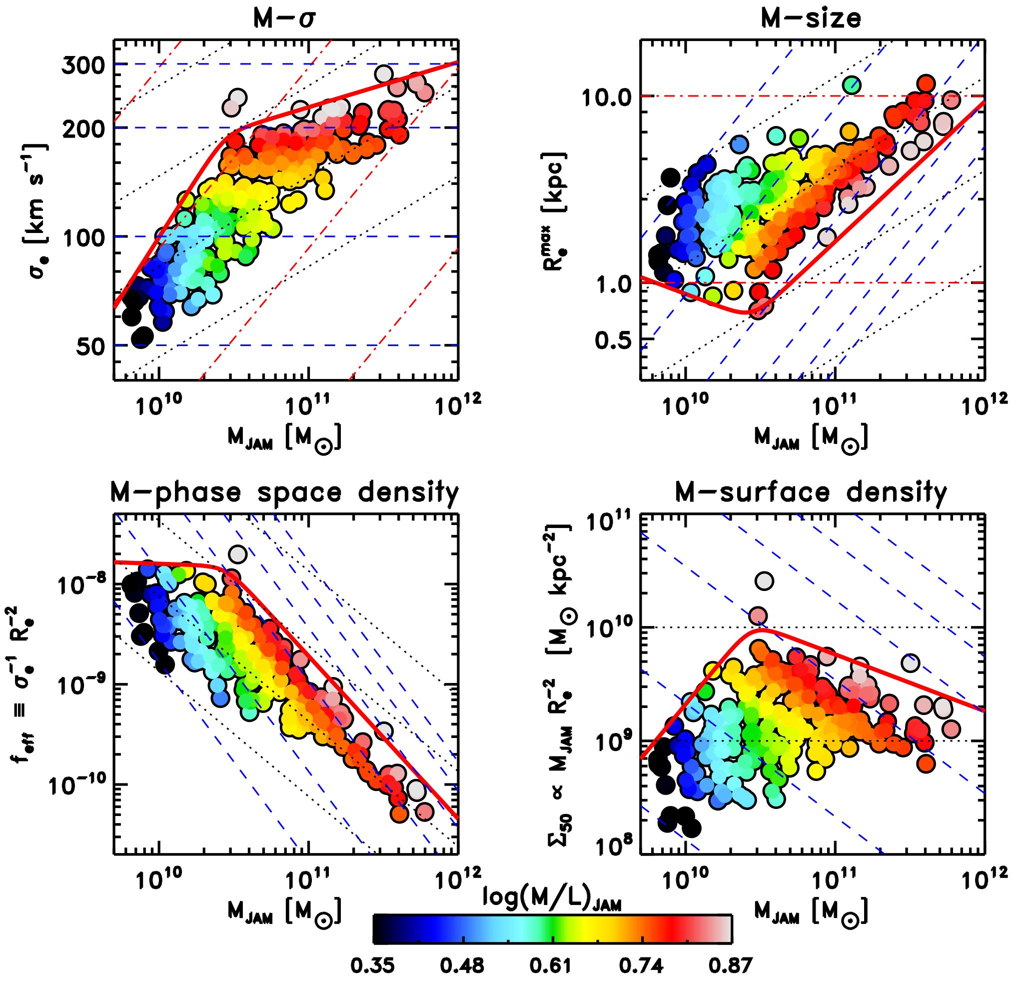

(Cappellari et al. 2012, Nature, 484, 485, Cappellari et al. 2012ab, MNRAS, submitted, also van Dokkum & Conroy 2010, Nature, 468, 940, Wegner et al. 2012, AJ, 144, 78, and others)

IMF

- distribution of stellar masses depends on
  - turbulent initial conditions
    --> mass spectrum of prestellar cloud cores
  - collapse and interaction of prestellar cores
    --> competitive accretion and *N*-body effects
  - thermodynamic properties of gas
    --> balance between heating and cooling
    --> EOS (determines which cores go into collapse)
  - (proto) stellar feedback terminates star formation
    ionizing radiation, bipolar outflows, winds, SN

(e.g. Larson 2003, Prog. Rep. Phys.; Mac Low & Klessen, 2004, Rev. Mod. Phys, 76, 125 - 194)

IMF

- distribution of stellar masses depends on
  - *turbulent initial conditions*
    --> mass spectrum of prestellar cloud cores ???
  - collapse and interaction of prestellar cores
    --> competitive accretion and *N*-body effects
  - thermodynamic properties of gas
    --> balance between heating and cooling
    --> EOS (determines which cores go into collapse)
  - (proto) stellar feedback terminates star formation
    ionizing radiation, bipolar outflows, winds, SN

(e.g. Larson 2003, Prog. Rep. Phys.; Mac Low & Klessen, 2004, Rev. Mod. Phys, 76, 125 - 194)

different statistical approaches

- there are different quantitative IMF based on turbulence
    - Padoan & Nordlund (2002, 2007)
    - Hennebelle & Chabrier (2008, 2009)
    - Hopkins (2012)
    - all relate the mass spectrum to statistical characteristics of the turbulent velocity fields

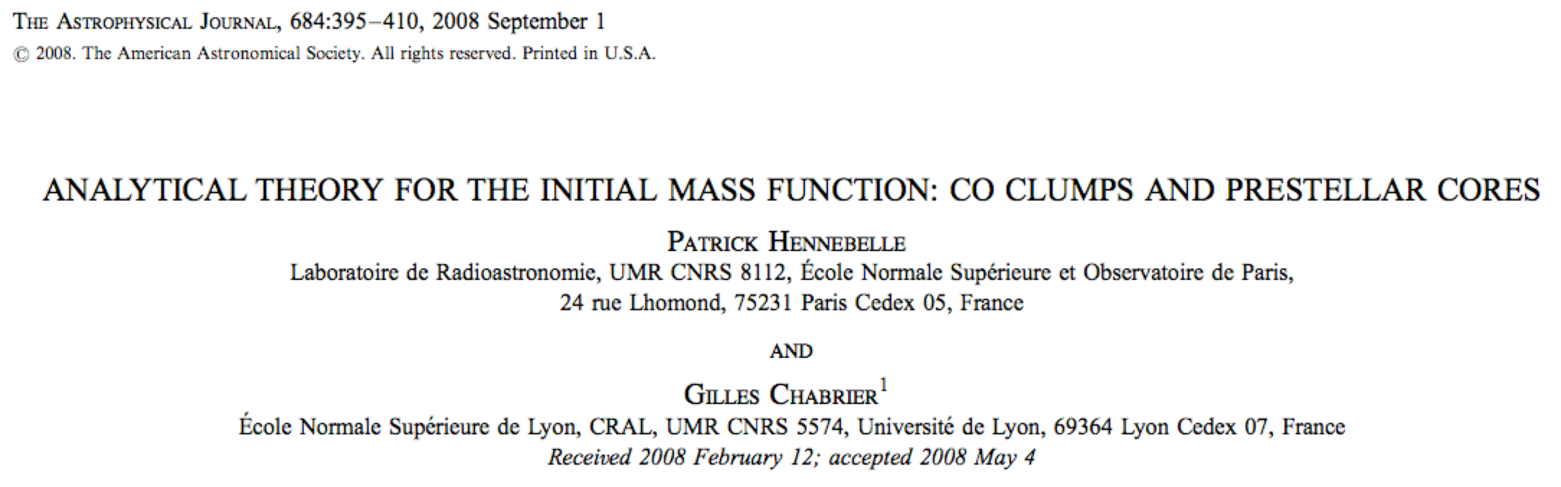

The Astrophysical Journal, 684:395–410, 2008 September 1

ANALYTICAL THEORY FOR THE INITIAL MASS FUNCTION: CO CLUMPS AND PRESTELLAR CORES

Patrick Hennebelle
Laboratoire de Radioastronomie, UMR CNRS 8112, École Normale Supérieure et Observatoire de Paris,
24 rue Lhomond, 75231 Paris Cedex 05, France

and

Gilles Chabrier[1]
École Normale Supérieure de Lyon, CRAL, UMR CNRS 5574, Université de Lyon, 69364 Lyon Cedex 07, France

Received 2008 February 12; accepted 2008 May 4

different statistical approaches

- there are different quantitative IMF based on turbulence
  - Padoan & Nordlund (2002, 2007)
  - Hennebelle & Chabrier (2008, 2009)
  - Hopkins (2012)
  - all relate the mass spectrum to statistical characteristics of the turbulent velocity fields

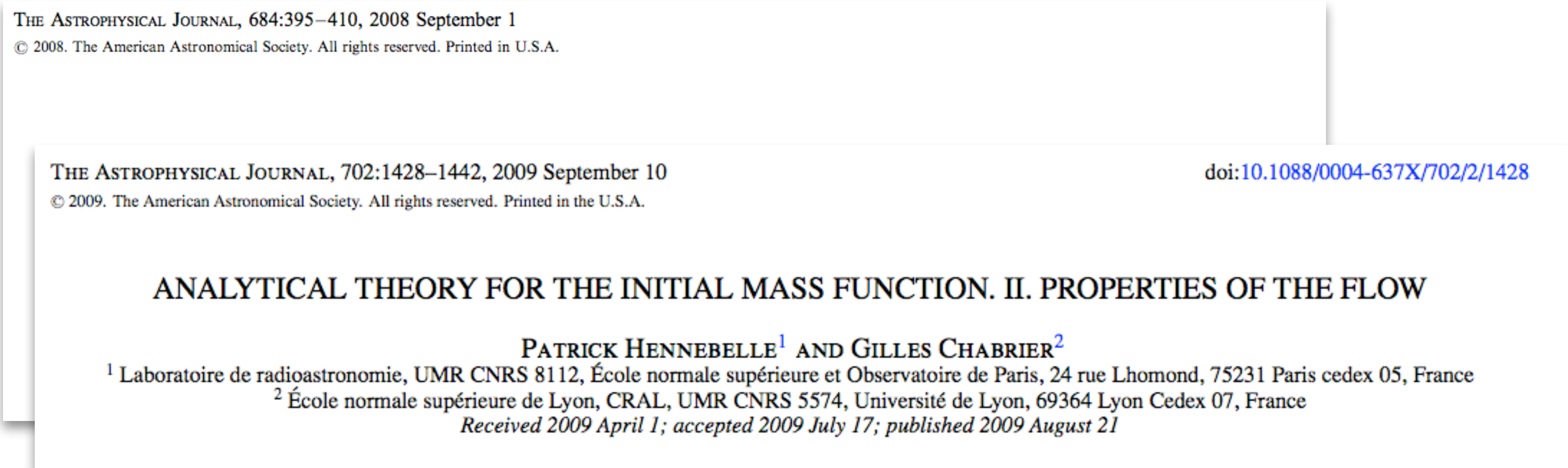

The Astrophysical Journal, 684:395–410, 2008 September 1

© 2008. The American Astronomical Society. All rights reserved. Printed in U.S.A.

The Astrophysical Journal, 702:1428–1442, 2009 September 10 doi:10.1088/0004-637X/702/2/1428

© 2009. The American Astronomical Society. All rights reserved. Printed in the U.S.A.

ANALYTICAL THEORY FOR THE INITIAL MASS FUNCTION. II. PROPERTIES OF THE FLOW

Patrick Hennebelle[1] and Gilles Chabrier[2]

[1] Laboratoire de radioastronomie, UMR CNRS 8112, École normale supérieure et Observatoire de Paris, 24 rue Lhomond, 75231 Paris cedex 05, France

[2] École normale supérieure de Lyon, CRAL, UMR CNRS 5574, Université de Lyon, 69364 Lyon Cedex 07, France

Received 2009 April 1; accepted 2009 July 17; published 2009 August 21

different statistical approaches

- there are different quantitative IMF based on turbulence
    - Padoan & Nordlund (2002, 2007)
    - Hennebelle & Chabrier (2008, 2009)
    - Hopkins (2012)
    - all relate the mass spectrum to statistical characteristics of the turbulent velocity fields

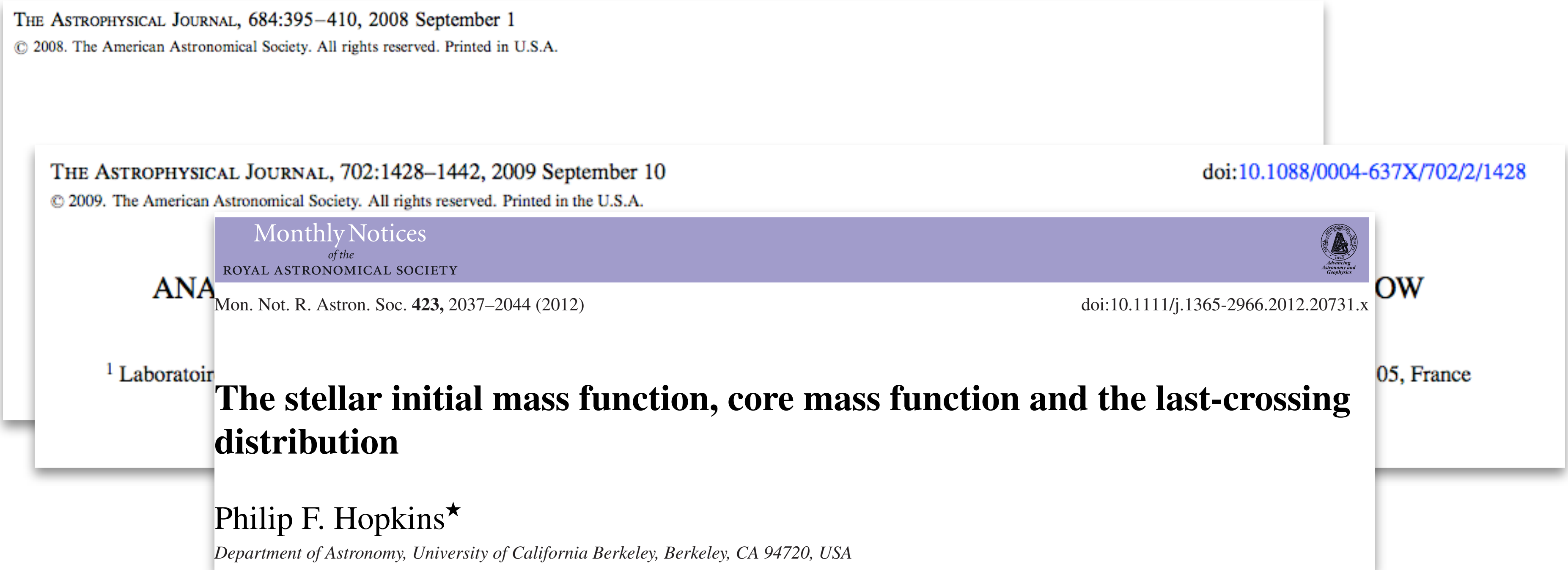

THE ASTROPHYSICAL JOURNAL, 684:395–410, 2008 September 1

THE ASTROPHYSICAL JOURNAL, 702:1428–1442, 2009 September 10 doi:10.1088/0004-637X/702/2/1428

ANA

OW

[1] Laboratoir

05, France

Monthly Notices
of the
ROYAL ASTRONOMICAL SOCIETY

Mon. Not. R. Astron. Soc. **423,** 2037–2044 (2012) doi:10.1111/j.1365-2966.2012.20731.x

The stellar initial mass function, core mass function and the last-crossing distribution

Philip F. Hopkins★

Department of Astronomy, University of California Berkeley, Berkeley, CA 94720, USA

different statistical approaches

- there are different quantitative IMF based on turbulence
  - Padoan & Nordlund (2002, 2007)
  - Hennebelle & Chabrier (2008, 2009)
  - Hopkins (2012)
  - all relate the mass spectrum to statistical characteristics of the turbulent velocity fields
- there are alternative approaches
  - IMF as closest packing problem / *sampling* problem in *fractal* clouds (Larson 1992, 1995, Elmegreen 1997ab, 2000ab, 2002)
  - IMF as purely *statistical* problem (Larson 1973, Zinnecker 1984, 1990, Adams & Fatuzzo 1996)
  - IMF from (proto)stellar *feedback* (Silk 1995, Adams & Fatuzzo 1996)
  - IMF from competitive *coagulation* (Murray & Lin 1995, Bonnell et al. 2001ab, etc.)

caveat: everybody gets the IMF!

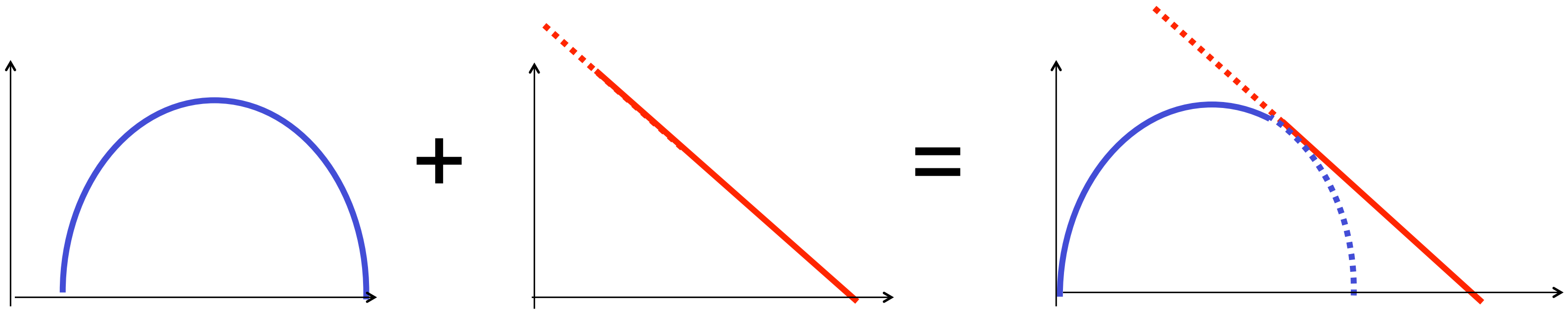

- combine scale free process → *POWER LAW BEHAVIOR*
  - turbulence (Padoan & Nordlund 2002, Hennebelle & Chabrier 2008)
  - gravity in dense clusters (Bonnell & Bate 2006, Klessen 2001)
  - universality: dust-induced EOS kink insensitive to radiation field (Elmegreen et al. 2008)

- with highly stochastic processes → central limit theorem → *GAUSSIAN DISTRIBUTION*
  - basically mean thermal Jeans length (or feedback)
  - universality: insensitive to metallicity (Clark et al. 2009, submitted)

caveat: everybody gets the IMF!

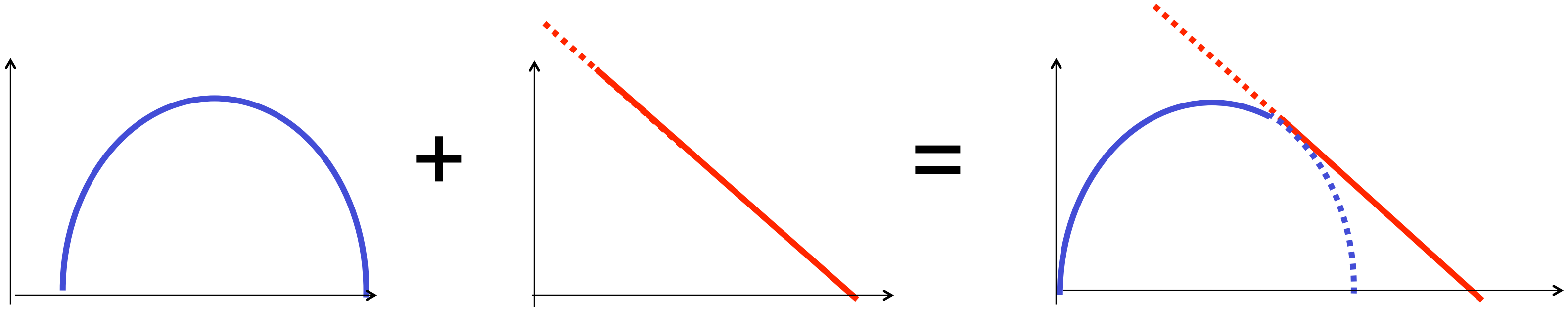

"everyone" gets the right IMF
→ better look for secondary indicators

- *stellar multiplicity*
- protostellar *spin* (including disk)
- *spatial distribution* + *kinematics* in young clusters
- *magnetic field strength* and *orientation*

caveat: dilatational vs. solenoidal

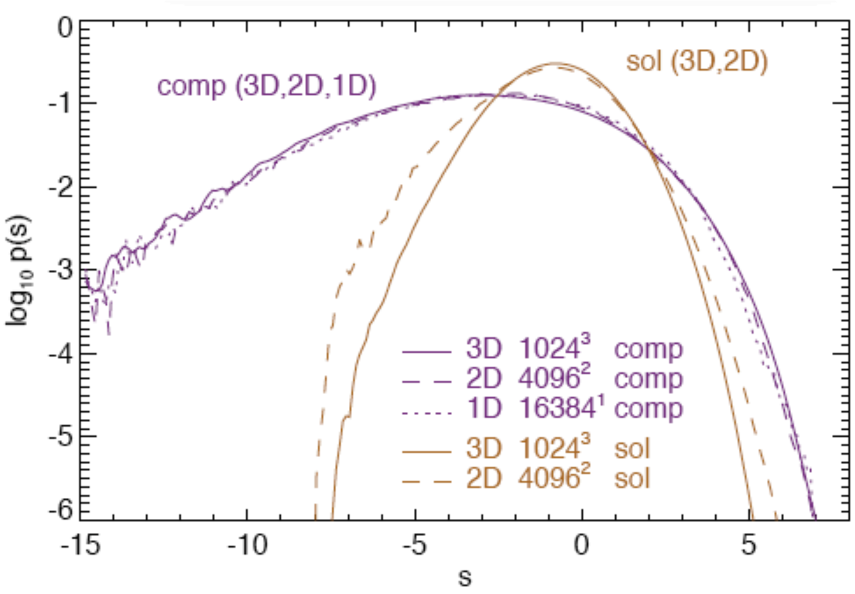

FIG. 3.— Volume-weighted density PDFs $p(s)$ obtained from 3D, 2D and 1D simulations with compressive forcing and from 3D and 2D simulations using solenoidal forcing. Note that in 1D, only compressive forcing is possible as in the study by Passot & Vázquez-Semadeni (1998). As suggested by eq. (5), compressive forcing yields almost identical density PDFs in 1D, 2D and 3D with $b{\sim}1$, whereas solenoidal forcing leads to a density PDF with $b{\sim}1/2$ in 2D and with $b{\sim}1/3$ in 3D.

Federrath, Klessen, Schmidt (2008a)

- density pdf depends on “dimensionality” of driving
  - relation between width of pdf and Mach number

$$\boxed{\sigma_\rho/\rho_0 = b\mathcal{M}}$$

  - with b depending on ζ via

$$\boxed{b = 1 + \left[\frac{1}{D} - 1\right]\zeta = \begin{cases} 1 - \frac{2}{3}\zeta & \text{, for } D = 3 \\ 1 - \frac{1}{2}\zeta & \text{, for } D = 2 \\ 1 & \text{, for } D = 1 \end{cases}}$$

  - with ζ being the ratio of dilatational vs. solenoidal modes:

$$\mathcal{P}^\zeta_{ij} = \zeta\mathcal{P}^\perp_{ij} + (1-\zeta)\mathcal{P}^{||}_{ij} = \zeta\delta_{ij} + (1-2\zeta)\frac{k_i k_j}{|k|^2}$$

caveat: dilatational vs. solenoidal

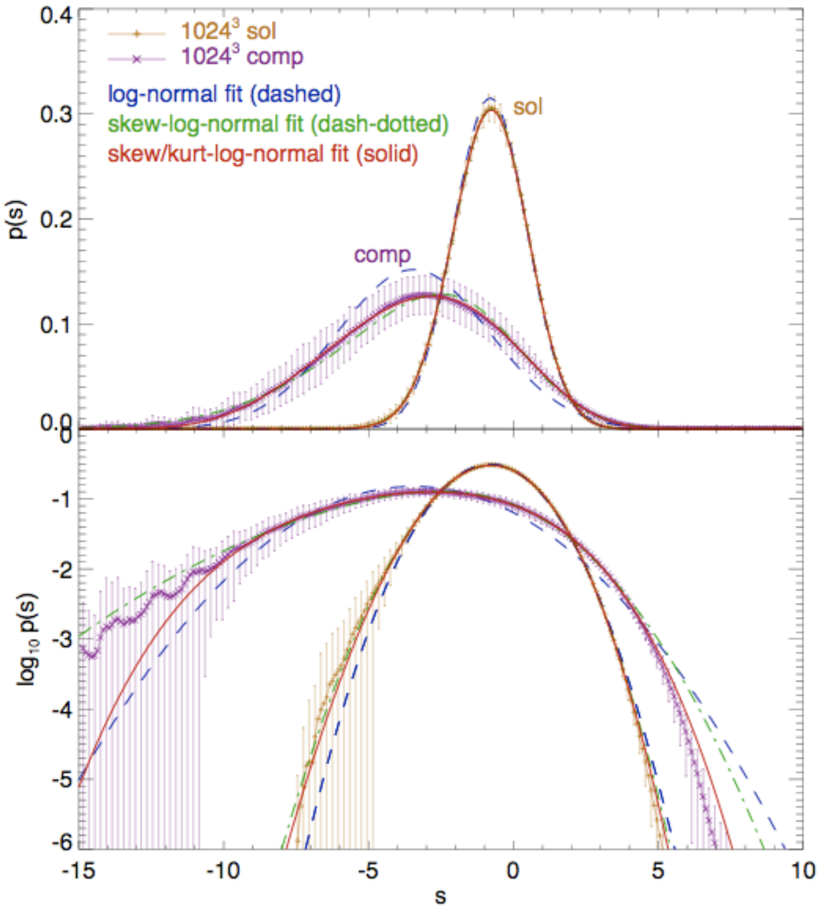

good fit needs 3rd and 4th moment of distribution!

Federrath, Klessen, Schmidt (2008b)

- density pdf depends on "dimensionality" of driving
  → is that a problem for the Krumholz & McKee model of the SF efficiency?
- density pdf of compressive driving is *NOT log-normal*
  → is that a problem for the Padoan & Nordlund, or Hennebelle & Chabrier IMF model?
- most "physical" sources should be *compressive* (convergent flows from spiral shocks or SN)

caveat: dilatational vs. solenoidal

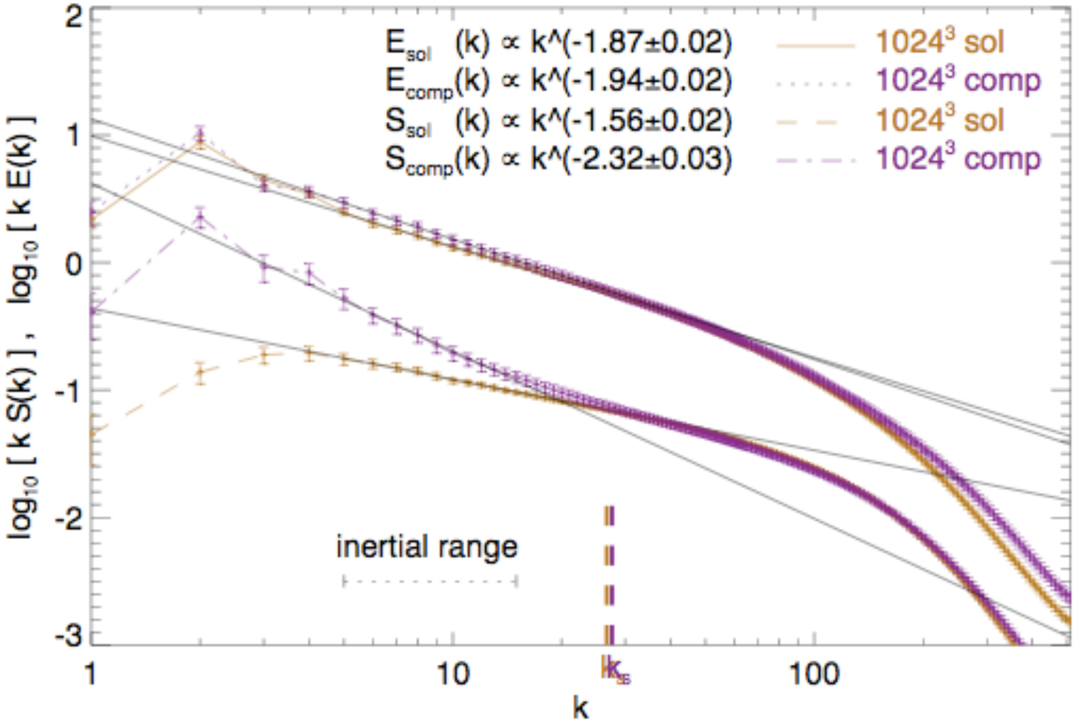

compensated density spectrum kS(k) shows clear break at sonic scale. below that shock compression no longer is important in shaping the power spectrum ...

- density power spectrum differs between dilatational and solenoidal driving!

→ dilatational driving leads to break at sonic scale!

- can we use that to determine driving sources from observations ?

Federrath, Klessen, Schmidt (2008b)

IMF

- distribution of stellar masses depends on
  - turbulent initial conditions
    --> mass spectrum of prestellar cloud cores
  - collapse and interaction of prestellar cores
    --> competitive mass growth and *N*-body effects
  - thermodynamic properties of gas
    --> balance between heating and cooling
    --> EOS (determines which cores go into collapse)
  - (proto) stellar feedback terminates star formation
    ionizing radiation, bipolar outflows, winds, SN

(e.g. Larson 2003, Prog. Rep. Phys.; Mac Low & Klessen, 2004, Rev. Mod. Phys, 76, 125 - 194)

example: model of Orion cloud

„model“ of Orion cloud:
15.000.000 SPH particles,
10^4 M_{sun} in 10 pc, mass resolution
0,02 M_{sun}, forms ~2.500
„stars“ (sink particles)

MASSIVE STARS
- form early in high-density gas clumps (cluster center)
- high accretion rates, maintained for a long time

LOW-MASS STARS
- form later as gas falls into potential well
- high relative velocities
- little subsequent accretion

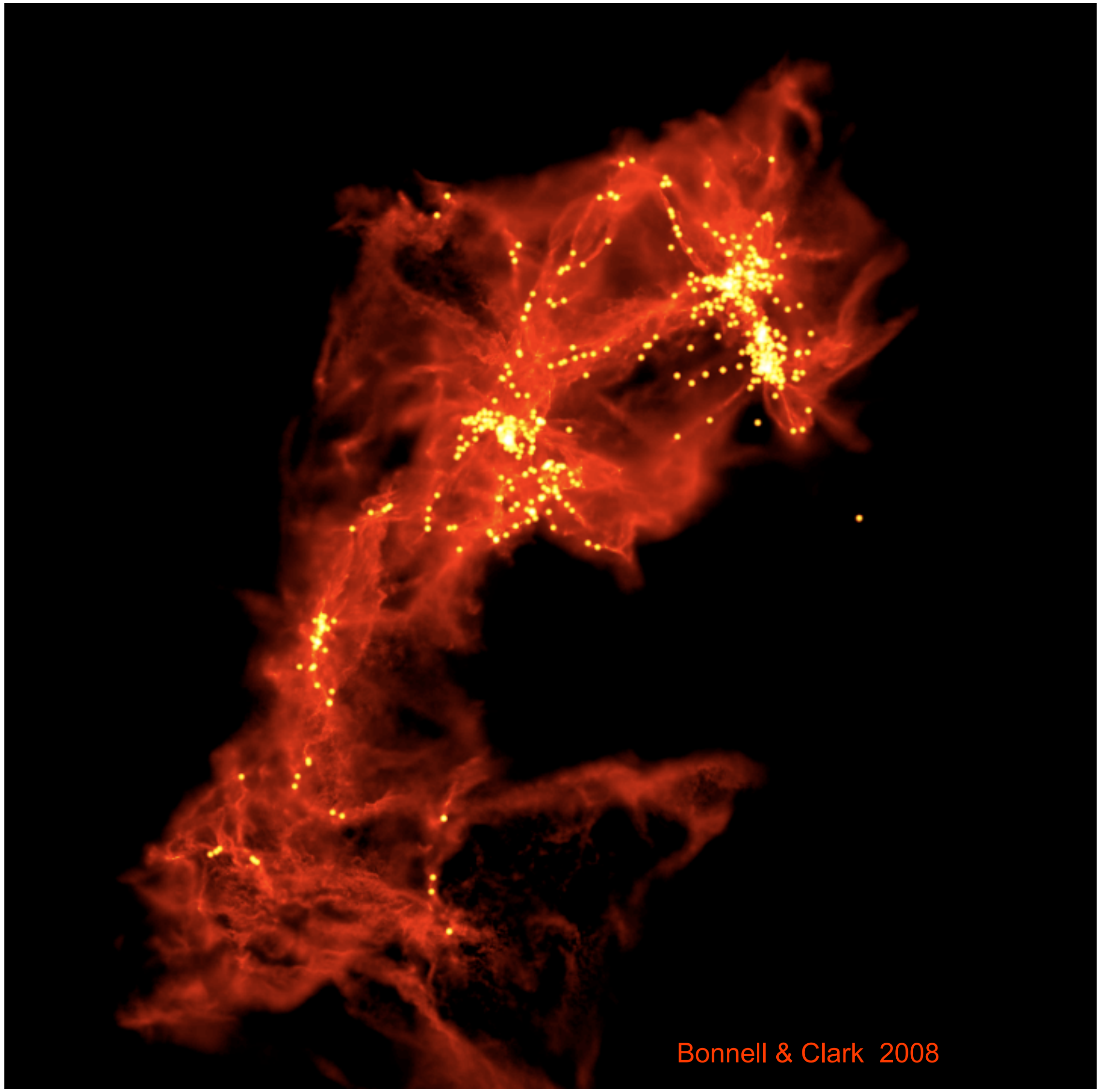

Bonnell & Clark 2008

Dynamics of nascent star cluster

in dense clusters protostellar interaction may be come important!

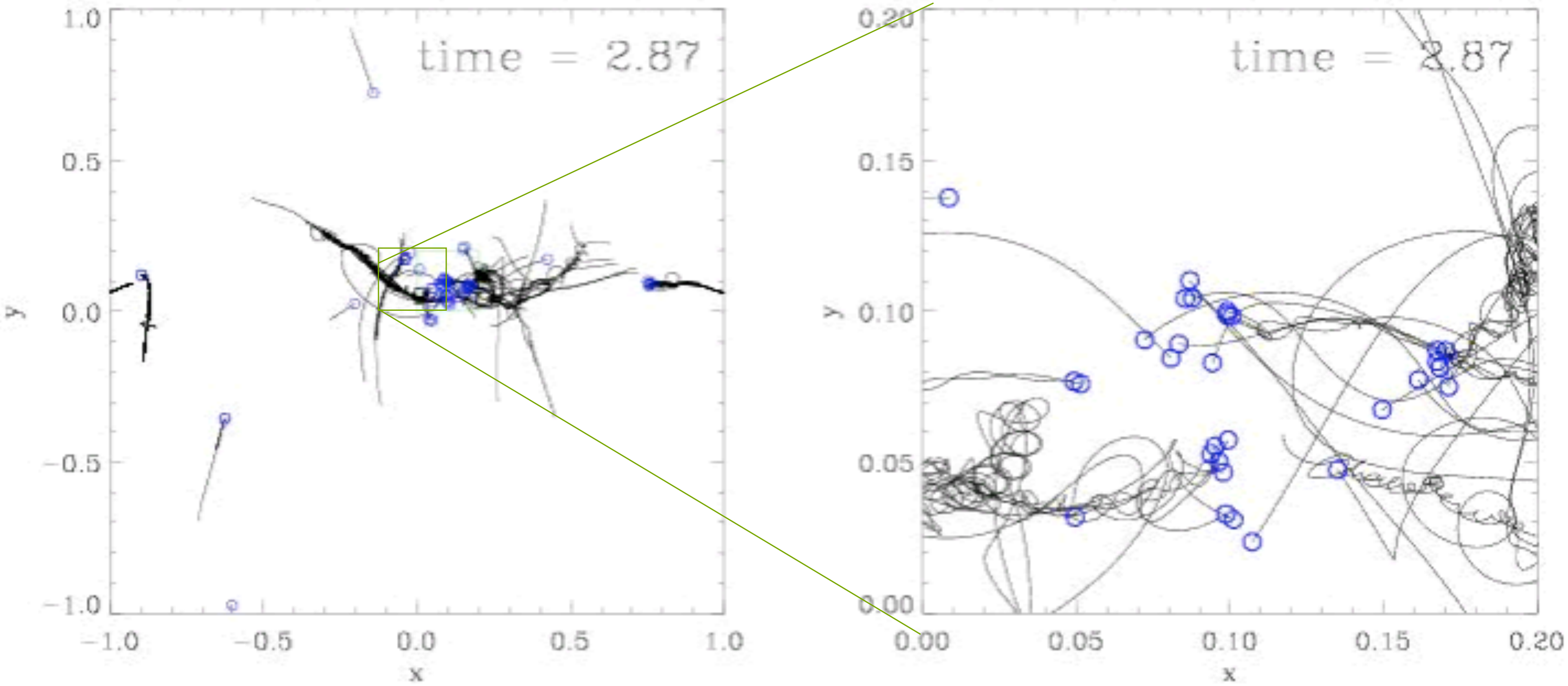

Trajectories of protostars in a nascent dense cluster created by gravoturbulent fragmentation
(from Klessen & Burkert 2000, ApJS, 128, 287)

accretion rates in clust

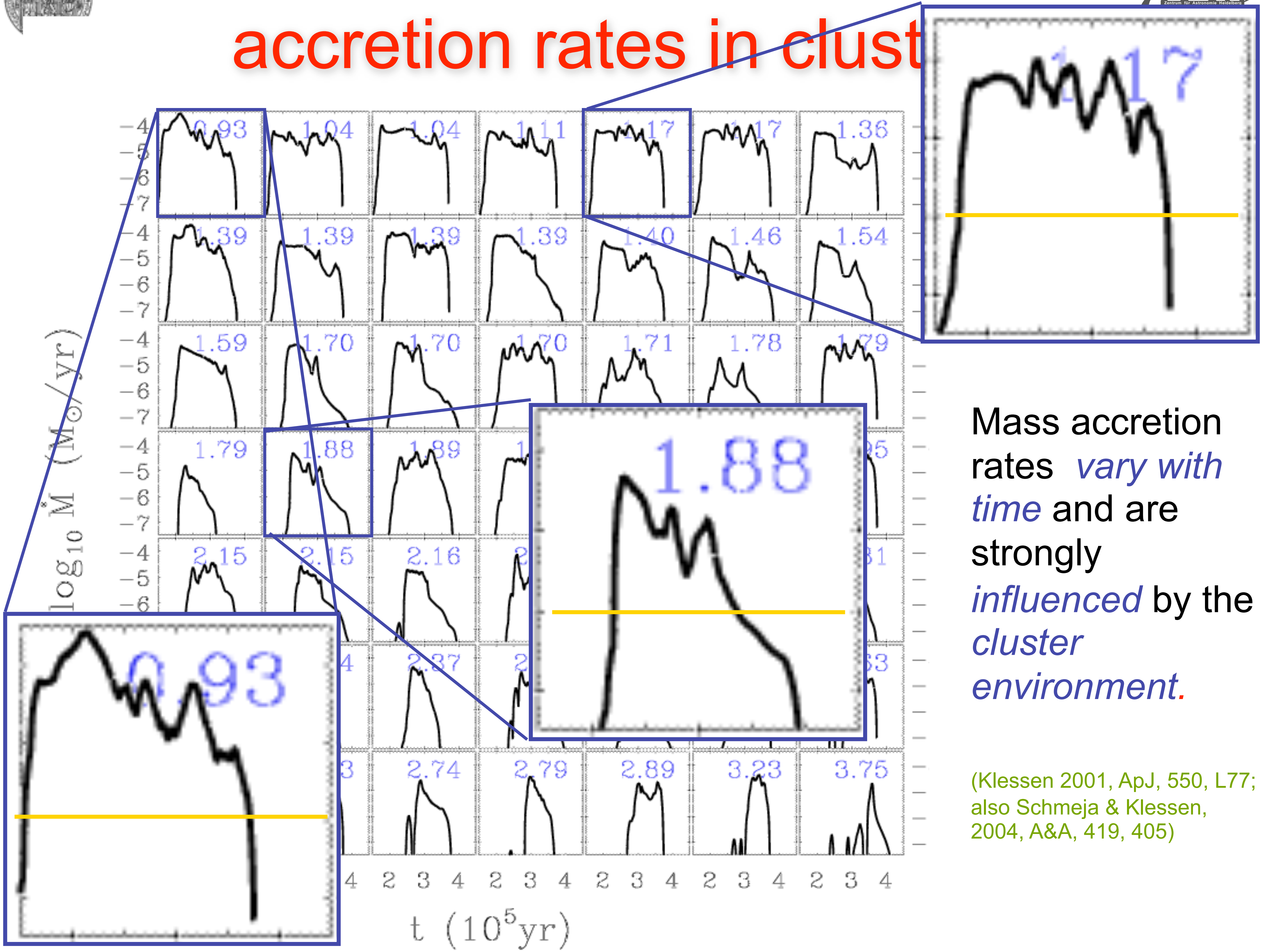

Mass accretion rates *vary with time* and are strongly *influenced* by the *cluster environment*.

(Klessen 2001, ApJ, 550, L77; also Schmeja & Klessen, 2004, A&A, 419, 405)

initial conditions for cluster formation

ICs of star cluster formation

- key question:
  - what is the initial density profile of cluster forming cores? how does it compare low-mass cores?
- observers answer:
  - very difficult to determine!
    - most high-mass cores have some SF inside
    - infra-red dark clouds (IRDCs) are difficult to study
  - but, new results with Herschel

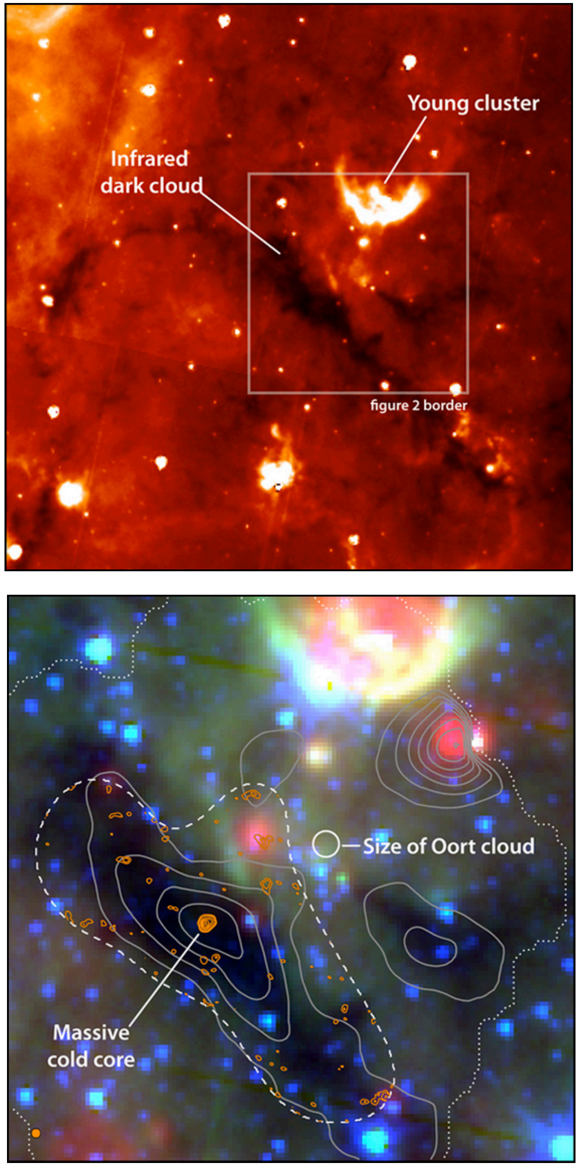

IRDC near Aquila rift, studied with the SMA: J. Swift & E. Churchwell

ICs of star cluster formation

- key question:
  - what is the initial density profile of cluster forming cores? how does it compare low-mass cores?
- observers answer:
  - very difficult to determine!
    - most high-mass cores have some SF inside
    - infra-red dark clouds (IRDCs) are difficult to study
  - but: new results with Herschel

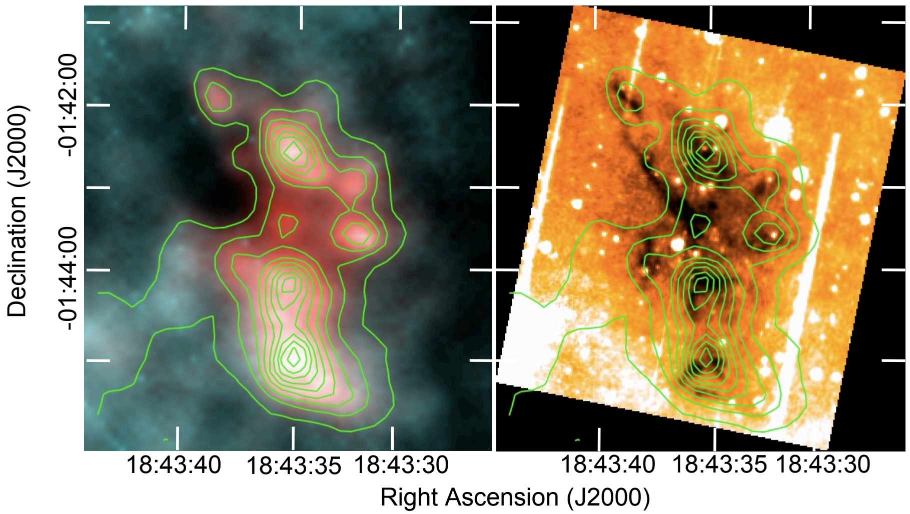

IRDC observed with Herschel, Peretto et al. (2010)

ICs of star cluster formation

- key question:
  - what is the initial density profile of cluster forming cores? how does it compare low-mass cores?
- theorists answer:
  - top hat (Larson Penston)
  - Bonnor Ebert (like low-mass cores)
  - power law $\rho \propto r^{-1}$ (logotrop)
  - power law $\rho \propto r^{-3/2}$ (Krumholz, McKee, et
  - power law $\rho \propto r^{-2}$ (Shu)
  - and many more

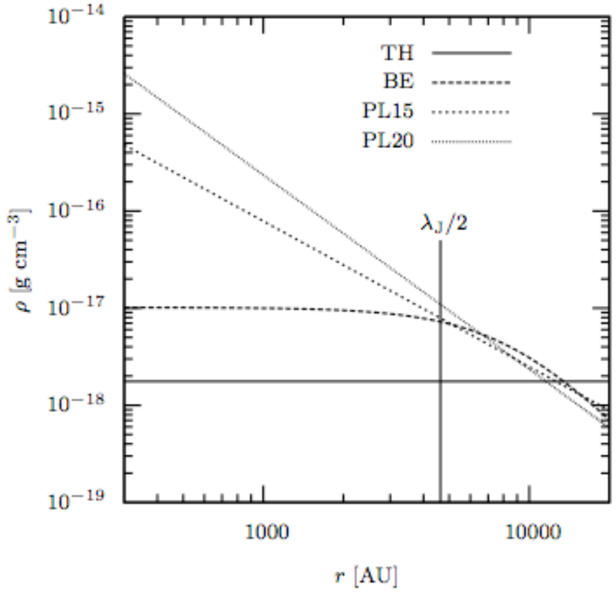

different density profiles

- does the density profile matter?

  .

  .

  .

- in comparison to
  - turbulence ...
  - radiative feedback ...
  - magnetic fields ...
  - thermodynamics ...

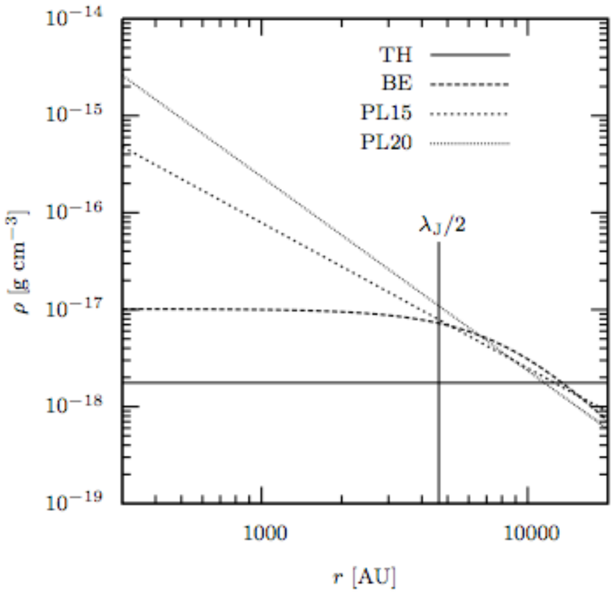

different density profiles

- address question in simple numerical experiment
- perform extensive parameter study
  - different profiles (top hat, BE, $r^{-3/2}$, r^{-3})
  - different turbulence fields
    - different realizations
    - different Mach numbers
    - solenoidal turbulence
      dilatational turbulence
      both modes
  - no net rotation, no B-fields
    (at the moment)

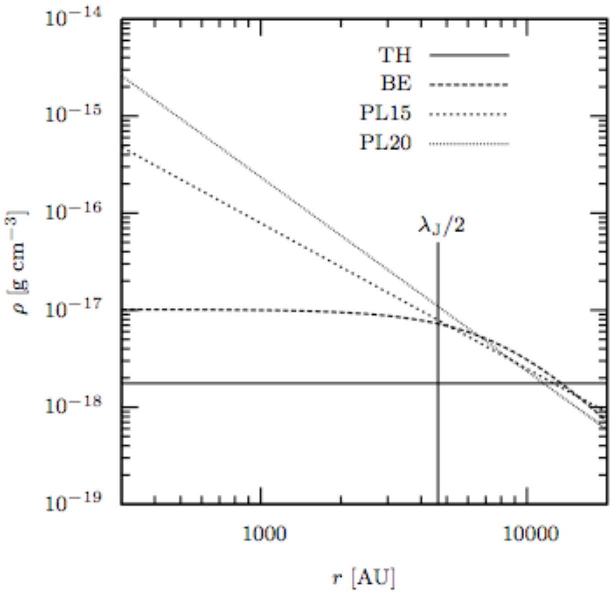

Girichids, Federrath, Banerjee, Klessen (2011abc)

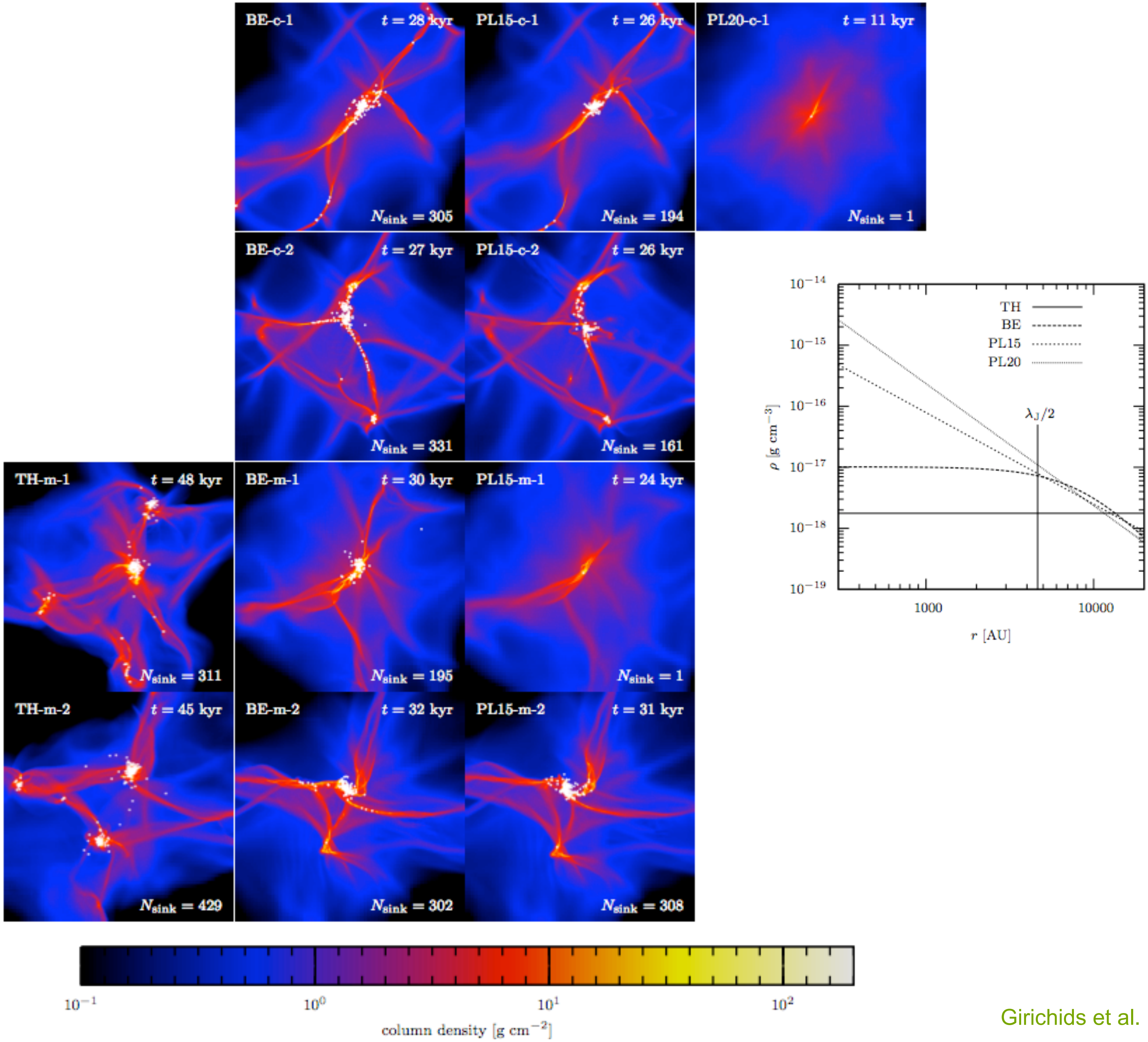

Girichids et al. (2011abc)

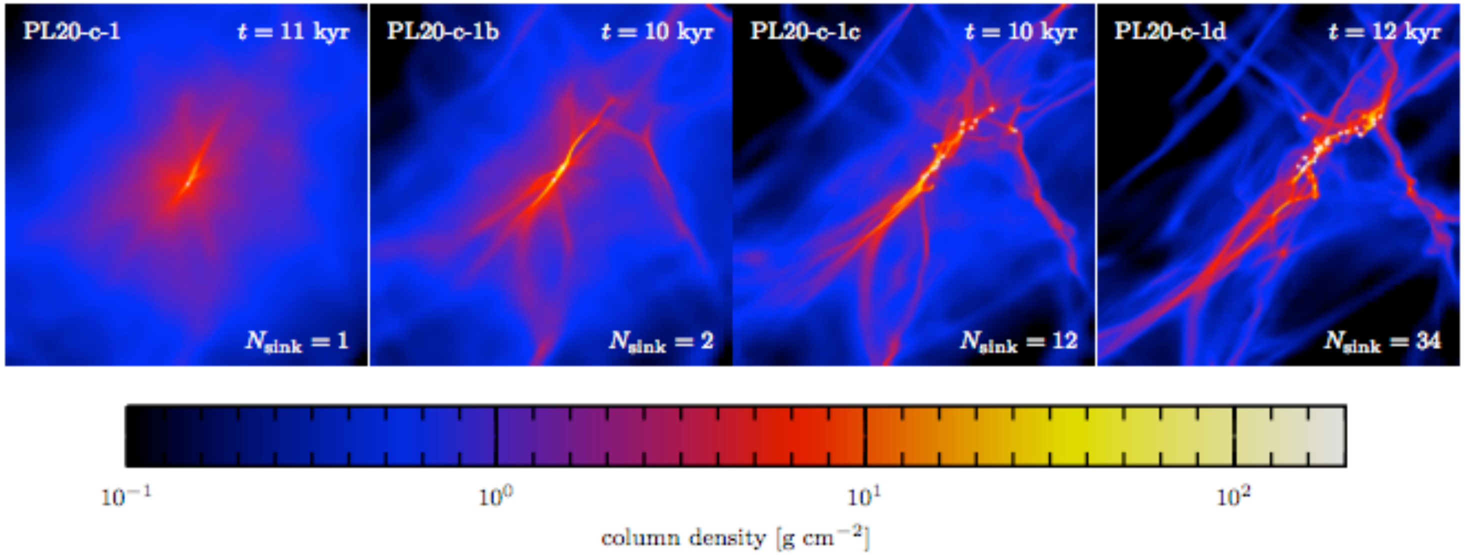

M=3 M=6 M=12 M=18

for the r^{-2} profile you need to crank up turbulence a lot to get some fragmentation!

Girichids et al. (2011abc)

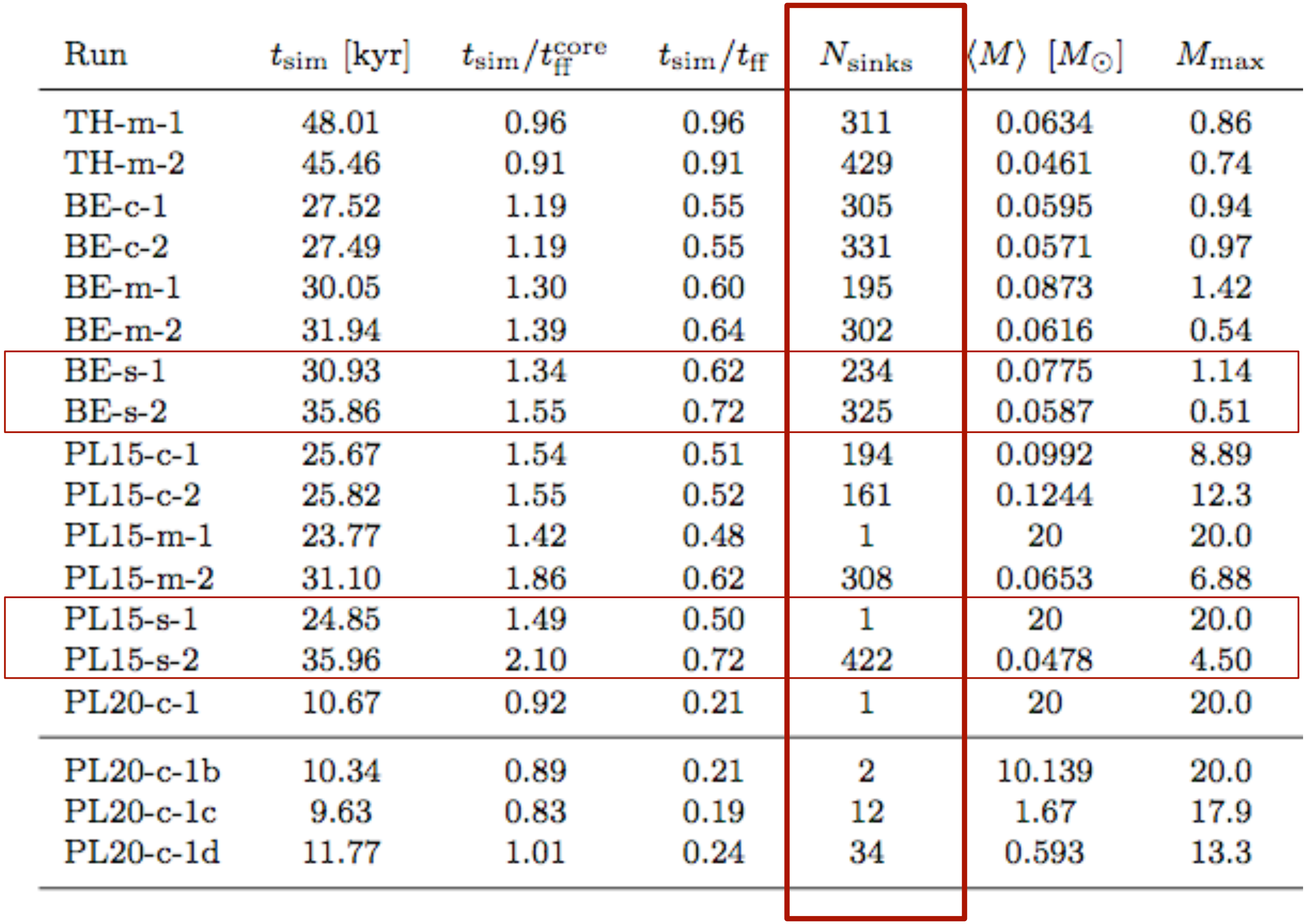

Run	$t_{\rm sim}$ [kyr]	$t_{\rm sim}/t_{\rm ff}^{\rm core}$	$t_{\rm sim}/t_{\rm ff}$	$N_{\rm sinks}$	$\langle M\rangle$ [$M_\odot$]	$M_{\rm max}$
TH-m-1	48.01	0.96	0.96	311	0.0634	0.86
TH-m-2	45.46	0.91	0.91	429	0.0461	0.74
BE-c-1	27.52	1.19	0.55	305	0.0595	0.94
BE-c-2	27.49	1.19	0.55	331	0.0571	0.97
BE-m-1	30.05	1.30	0.60	195	0.0873	1.42
BE-m-2	31.94	1.39	0.64	302	0.0616	0.54
BE-s-1	30.93	1.34	0.62	234	0.0775	1.14
BE-s-2	35.86	1.55	0.72	325	0.0587	0.51
PL15-c-1	25.67	1.54	0.51	194	0.0992	8.89
PL15-c-2	25.82	1.55	0.52	161	0.1244	12.3
PL15-m-1	23.77	1.42	0.48	1	20	20.0
PL15-m-2	31.10	1.86	0.62	308	0.0653	6.88
PL15-s-1	24.85	1.49	0.50	1	20	20.0
PL15-s-2	35.96	2.10	0.72	422	0.0478	4.50
PL20-c-1	10.67	0.92	0.21	1	20	20.0
PL20-c-1b	10.34	0.89	0.21	2	10.139	20.0
PL20-c-1c	9.63	0.83	0.19	12	1.67	17.9
PL20-c-1d	11.77	1.01	0.24	34	0.593	13.3

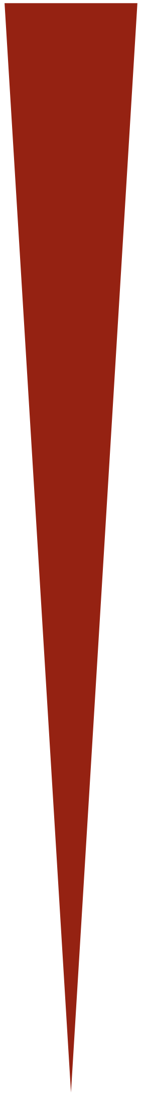

number of protostars

ICs with flat inner density profile form more fragments

Girichids et al. (2011abc)

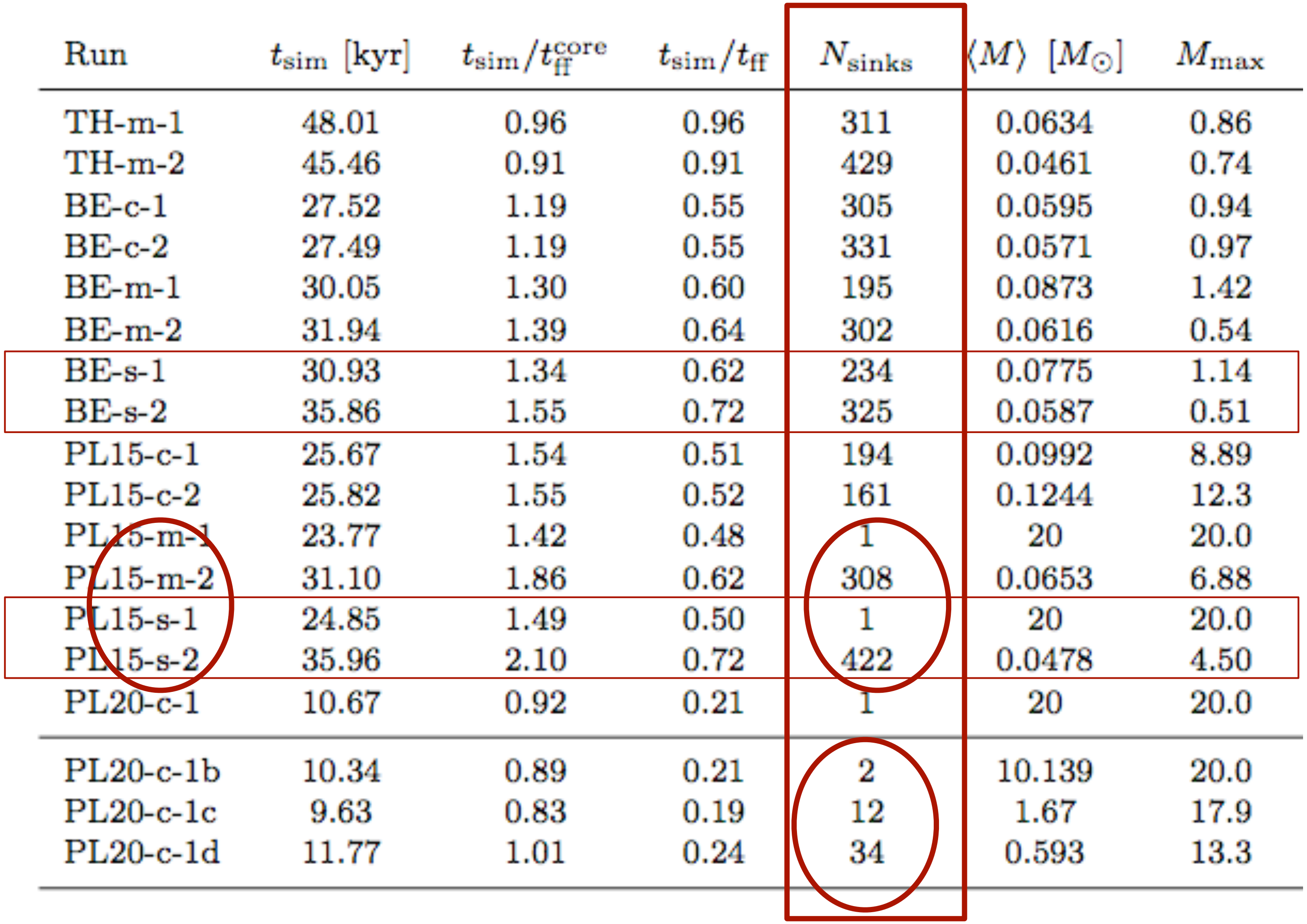

Run	$t_{\rm sim}$ [kyr]	$t_{\rm sim}/t_{\rm ff}^{\rm core}$	$t_{\rm sim}/t_{\rm ff}$	$N_{\rm sinks}$	$\langle M\rangle$ [$M_\odot$]	$M_{\rm max}$
TH-m-1	48.01	0.96	0.96	311	0.0634	0.86
TH-m-2	45.46	0.91	0.91	429	0.0461	0.74
BE-c-1	27.52	1.19	0.55	305	0.0595	0.94
BE-c-2	27.49	1.19	0.55	331	0.0571	0.97
BE-m-1	30.05	1.30	0.60	195	0.0873	1.42
BE-m-2	31.94	1.39	0.64	302	0.0616	0.54
BE-s-1	30.93	1.34	0.62	234	0.0775	1.14
BE-s-2	35.86	1.55	0.72	325	0.0587	0.51
PL15-c-1	25.67	1.54	0.51	194	0.0992	8.89
PL15-c-2	25.82	1.55	0.52	161	0.1244	12.3
PL15-m-1	23.77	1.42	0.48	1	20	20.0
PL15-m-2	31.10	1.86	0.62	308	0.0653	6.88
PL15-s-1	24.85	1.49	0.50	1	20	20.0
PL15-s-2	35.96	2.10	0.72	422	0.0478	4.50
PL20-c-1	10.67	0.92	0.21	1	20	20.0
PL20-c-1b	10.34	0.89	0.21	2	10.139	20.0
PL20-c-1c	9.63	0.83	0.19	12	1.67	17.9
PL20-c-1d	11.77	1.01	0.24	34	0.593	13.3

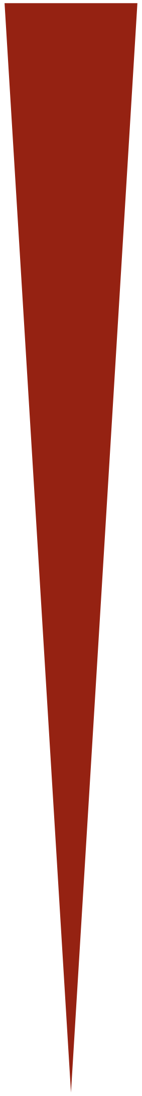

number of protostars

however, the real situation is very complex: details of the initial turbulent field matter

very high Mach numbers are needed to make SIS fragment

Girichids et al. (2011abc)

different density profiles

- different density profiles lead to very different fragmentation behavior
- fragmentation is strongly suppressed for very peaked, power-law profiles

- this is *good*, because it may explain some of the theoretical controversy, we have in the field
- this is *bad*, because all current calculations are “wrong” in the sense that the formation process of the star-forming core is neglected.

Girichids et al. (2011abc)

IMF

- distribution of stellar masses depends on
  - turbulent initial conditions
    --> mass spectrum of prestellar cloud cores
  - collapse and interaction of prestellar cores
    --> competitive accretion and *N*-body effects
  - *thermodynamic properties of gas*
    --> balance between heating and cooling
    --> EOS (determines which cores go into collapse)
  - (proto) stellar feedback terminates star formation
    ionizing radiation, bipolar outflows, winds, SN

(e.g. Larson 2003, Prog. Rep. Phys.; Mac Low & Klessen, 2004, Rev. Mod. Phys, 76, 125 - 194)

dependency on EOS

- degree of fragmentation depends on *EOS!*

- polytropic EOS: $\mathbf{p} \propto \rho^{\gamma}$
- $\gamma<1$: dense cluster of low-mass stars
- $\gamma>1$: isolated high-mass stars
- (see Li, Klessen, & Mac Low 2003, ApJ, 592, 975; also Kawachi & Hanawa 1998, Larson 2003)

dependency on EOS

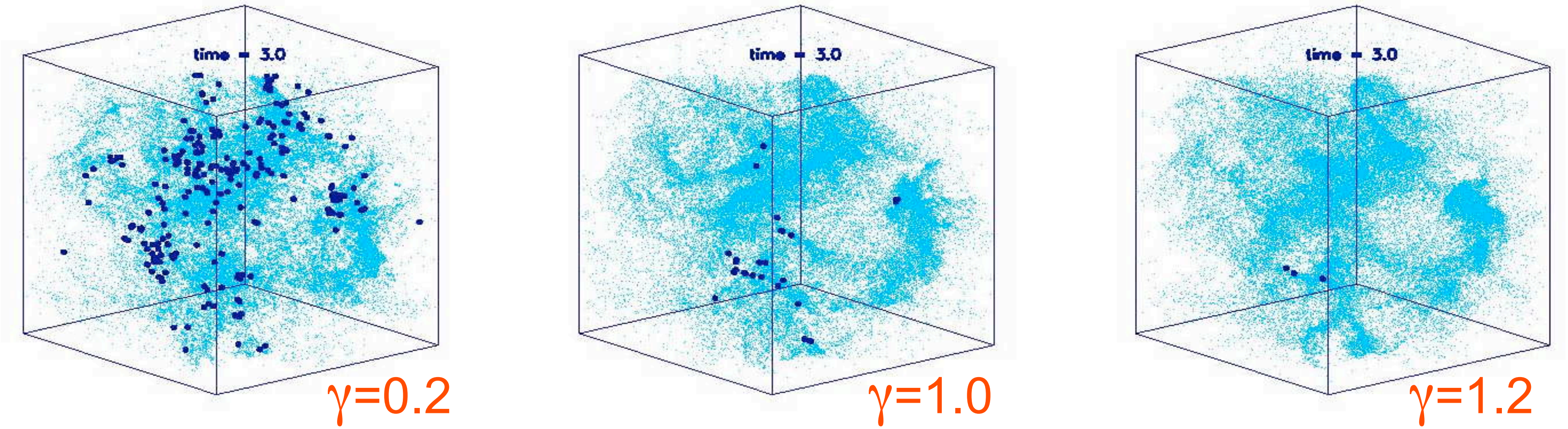

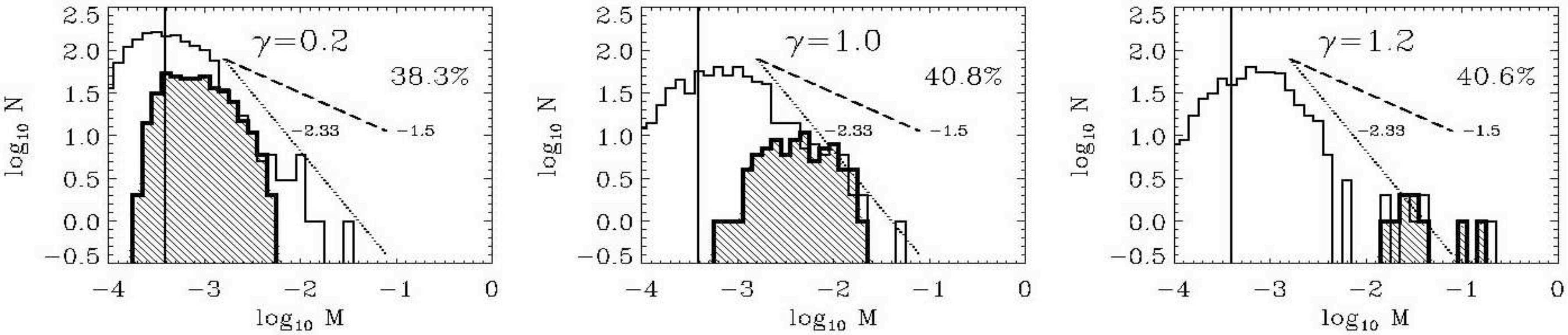

for γ<1 fragmentation is enhanced → *cluster of low-mass stars*

for γ>1 it is suppressed → formation of *isolated massive stars*

(from Li, Klessen, & Mac Low 2003, ApJ, 592, 975)

how does that work?

(1) $\mathbf{p} \propto \rho^{\gamma} \quad \rightarrow \quad \rho \propto \mathbf{p}^{1/\gamma}$

(2) $\mathbf{M}_{\mathbf{jeans}} \propto \gamma^{3/2}\, \rho^{(3\gamma-4)/2}$

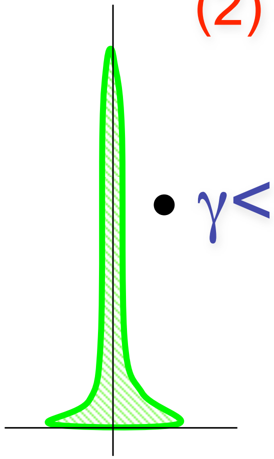

- $\gamma<1$: → *large* density excursion for given pressure
  → $\langle M_{jeans} \rangle$ becomes small
  → number of fluctuations with $M > M_{jeans}$ is large

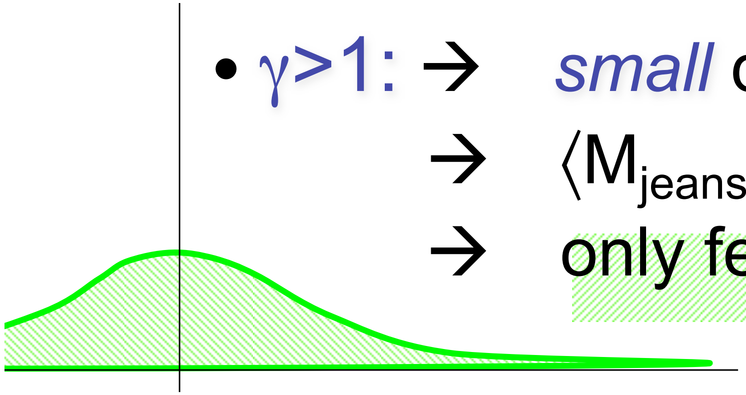

- $\gamma>1$: → *small* density excursion for given pressure
  → $\langle M_{jeans} \rangle$ is large
  → only few and massive clumps exceed M_{jeans}

EOS in different environments

EOS as function of metallicity

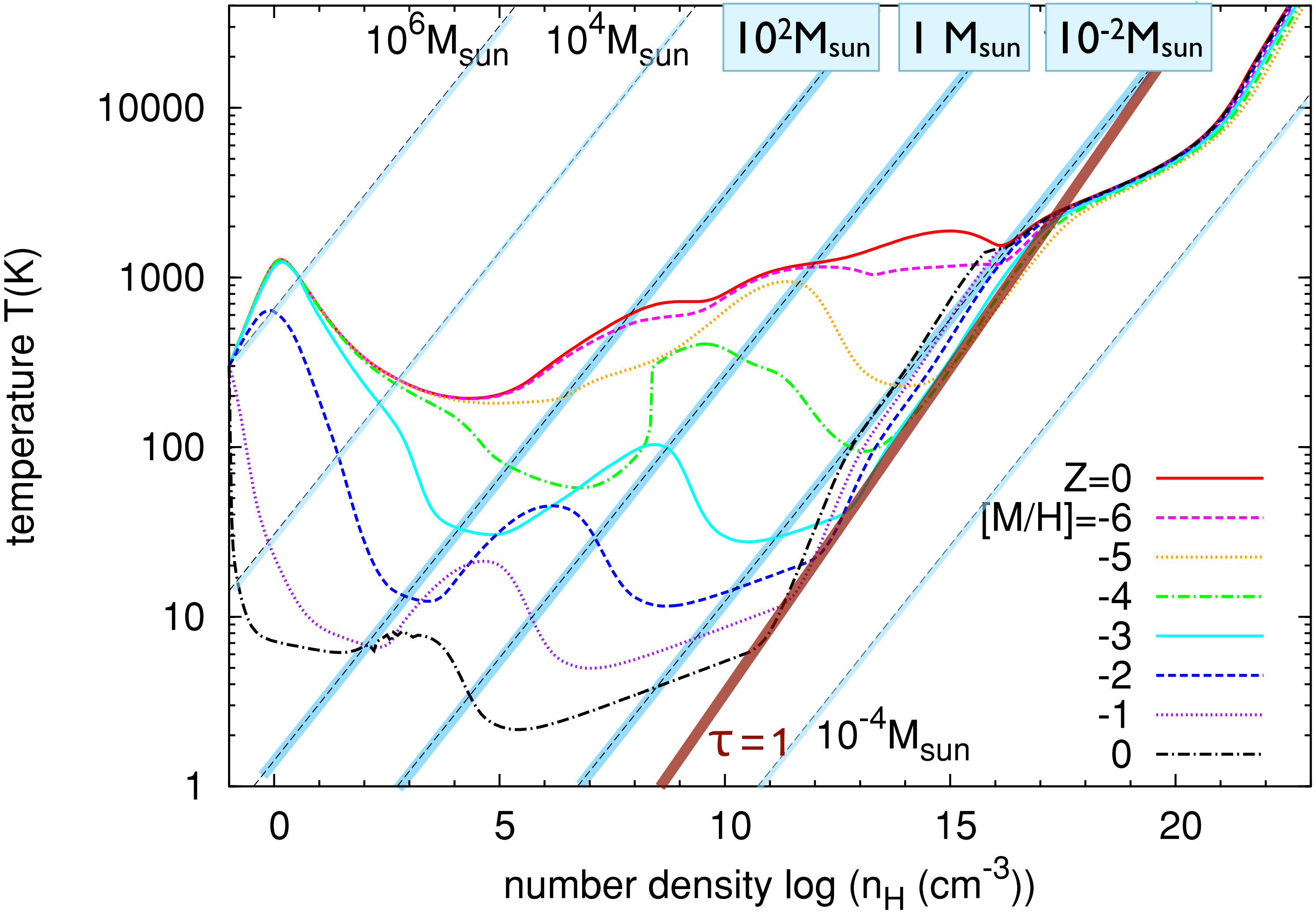

(Omukai et al. 2005, 2010)

EOS as function of metallicity

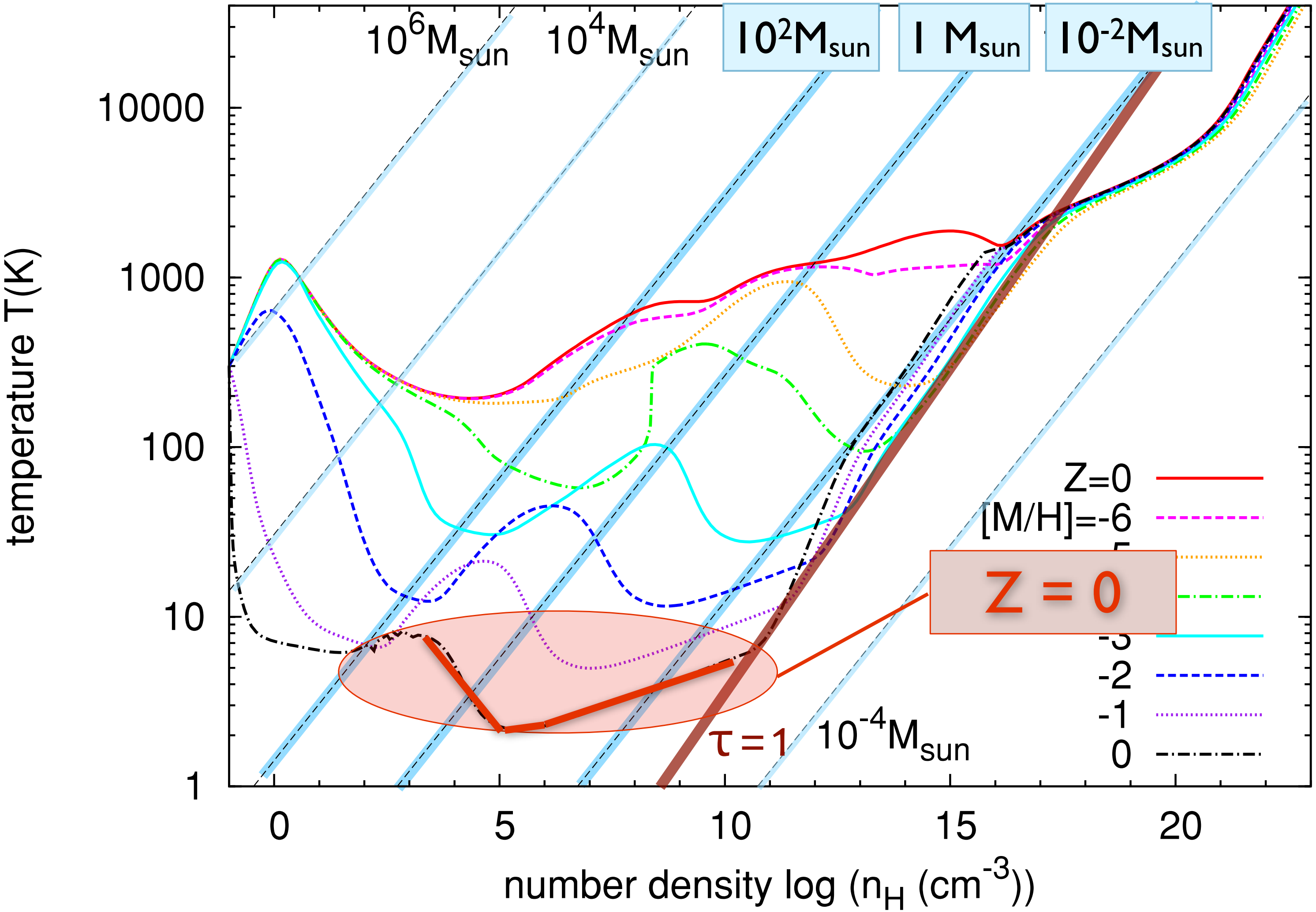

(Omukai et al. 2005, 2010)

present-day star formation

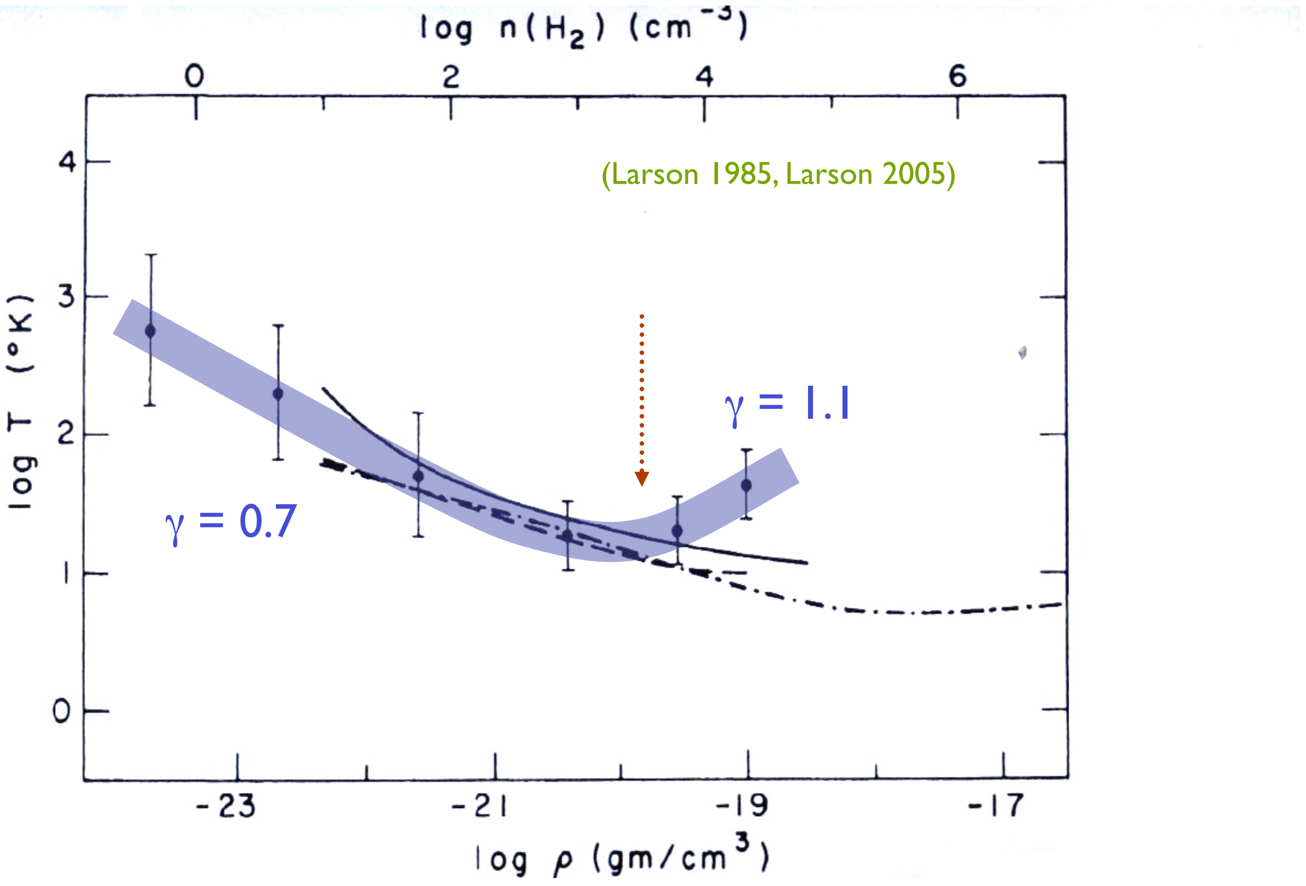

IMF in nearby molecular clouds

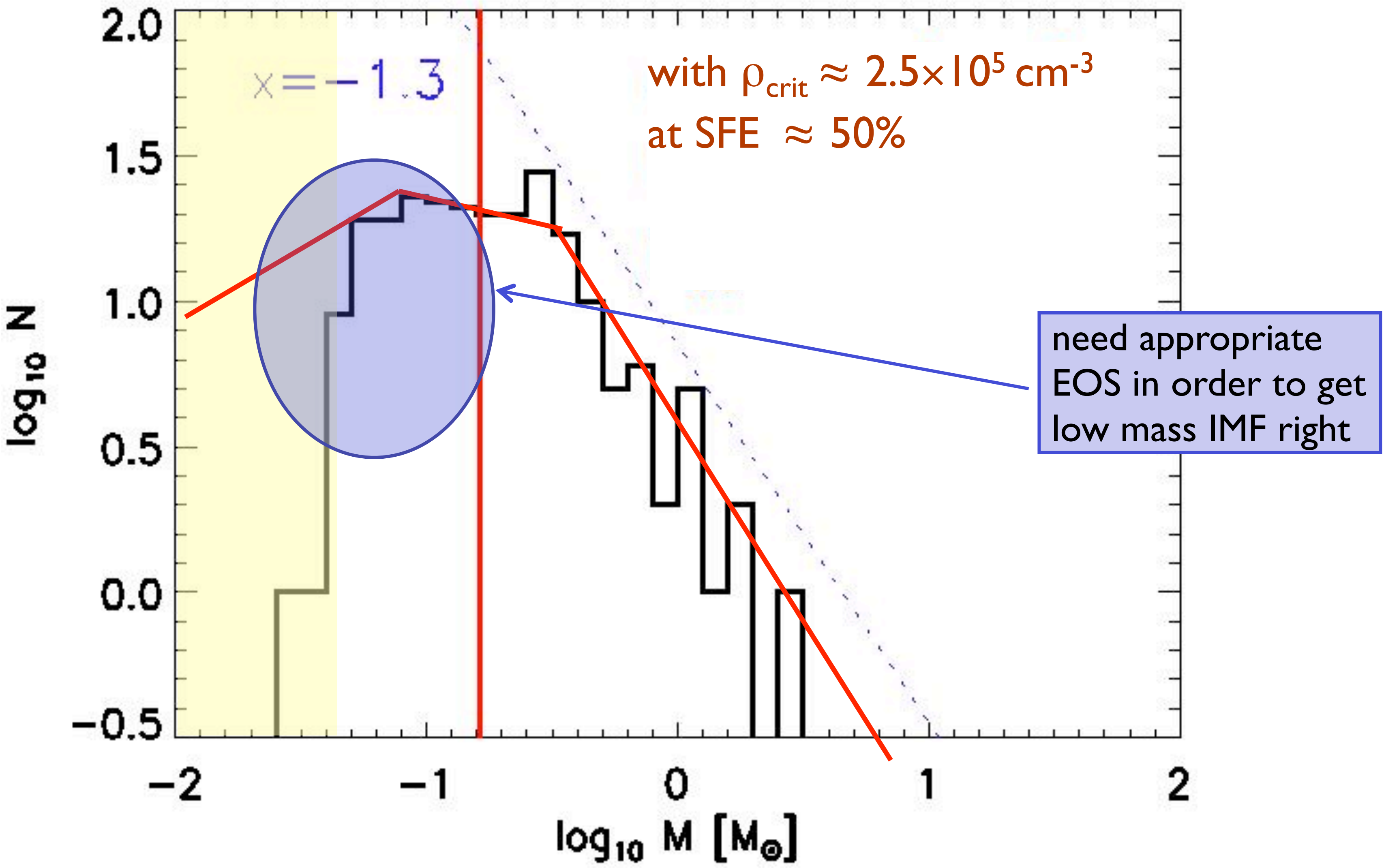

with $\rho_{crit} \approx 2.5 \times 10^5$ cm^{-3}
at SFE ≈ 50%

need appropriate EOS in order to get low mass IMF right

(Jappsen et al. 2005, A&A, 435, 611)

EOS as function of metallicity

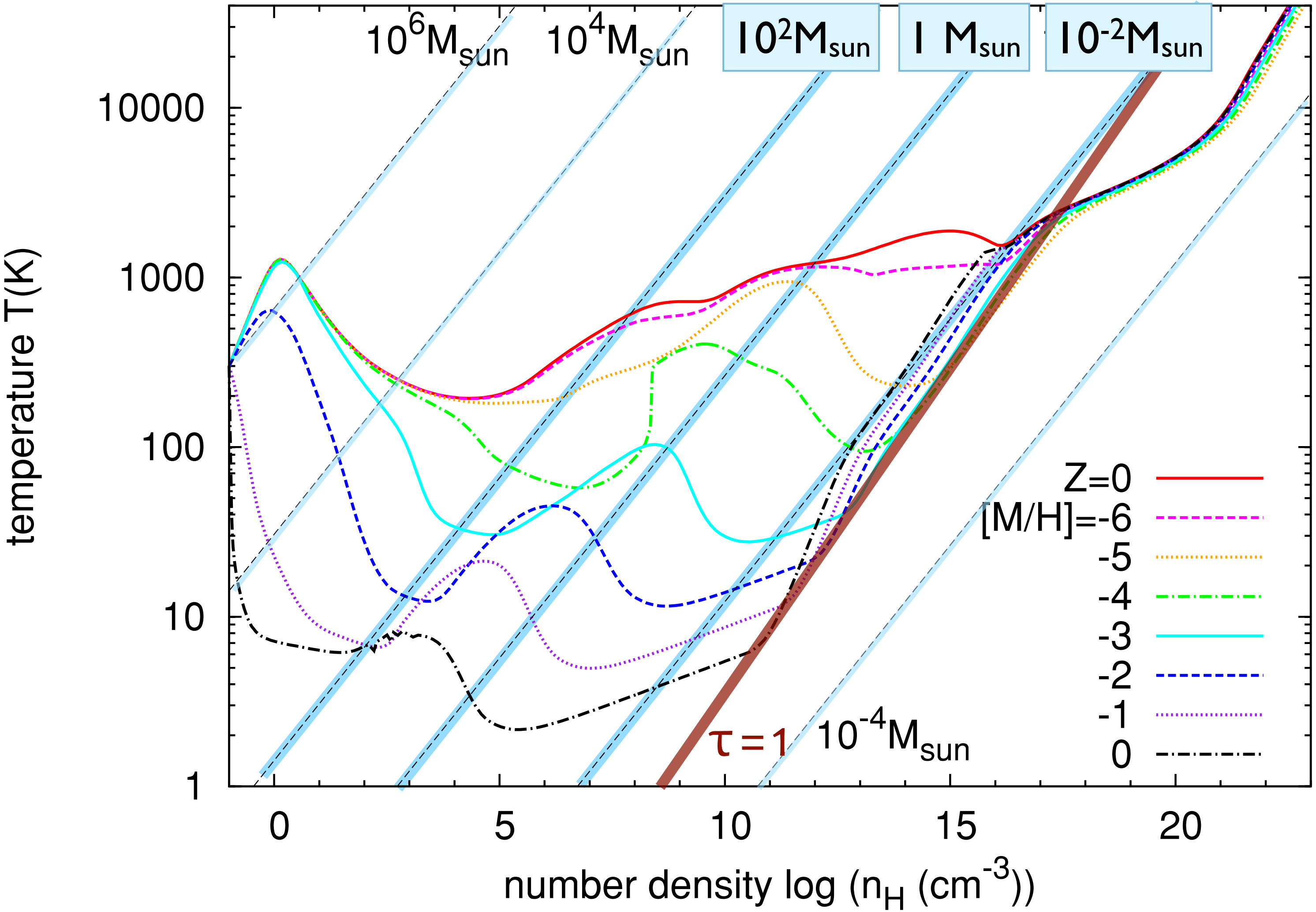

(Omukai et al. 2005, 2010)

EOS as function of metallicity

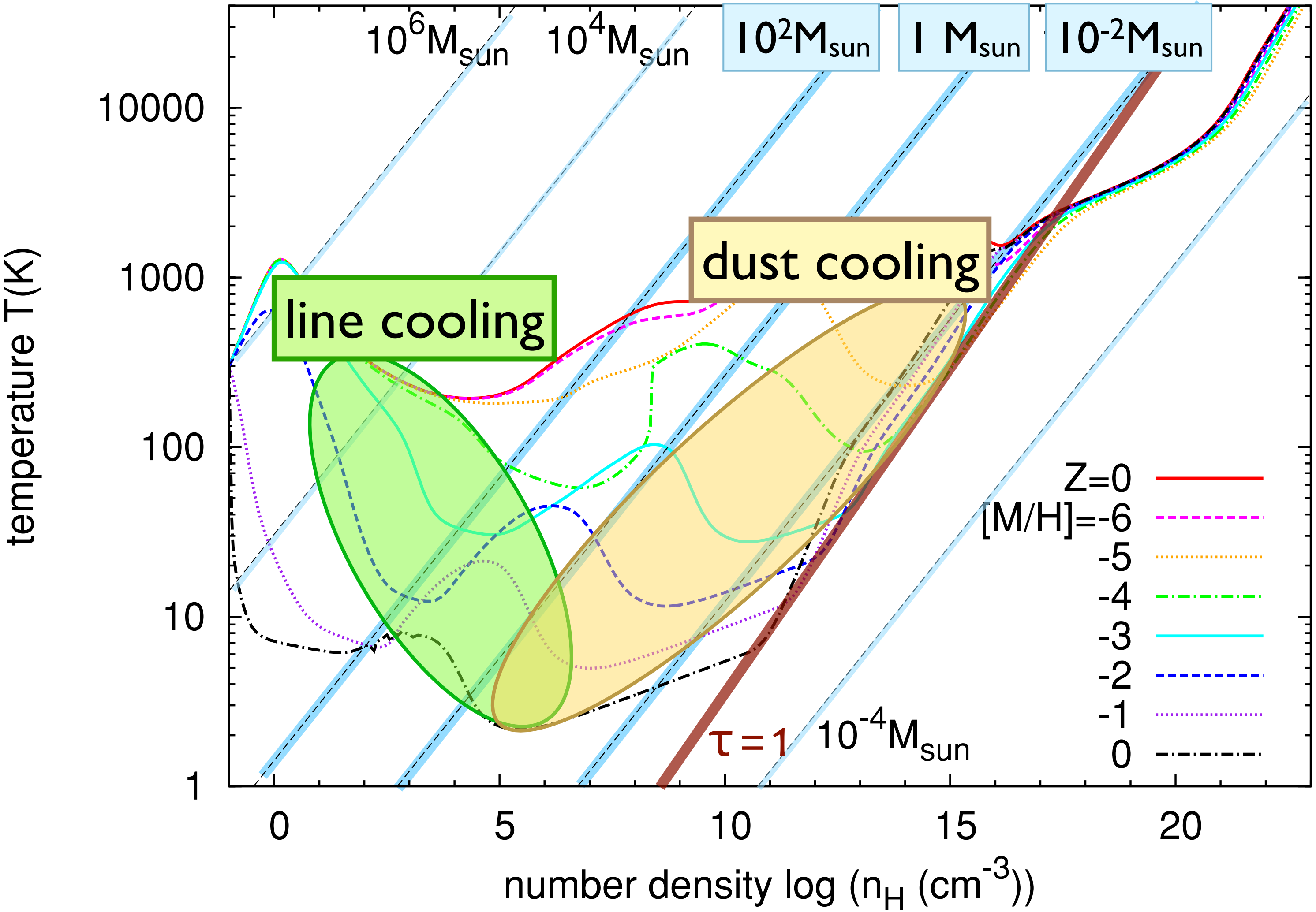

(Omukai et al. 2005, 2010)

transition: Pop III to Pop II.5

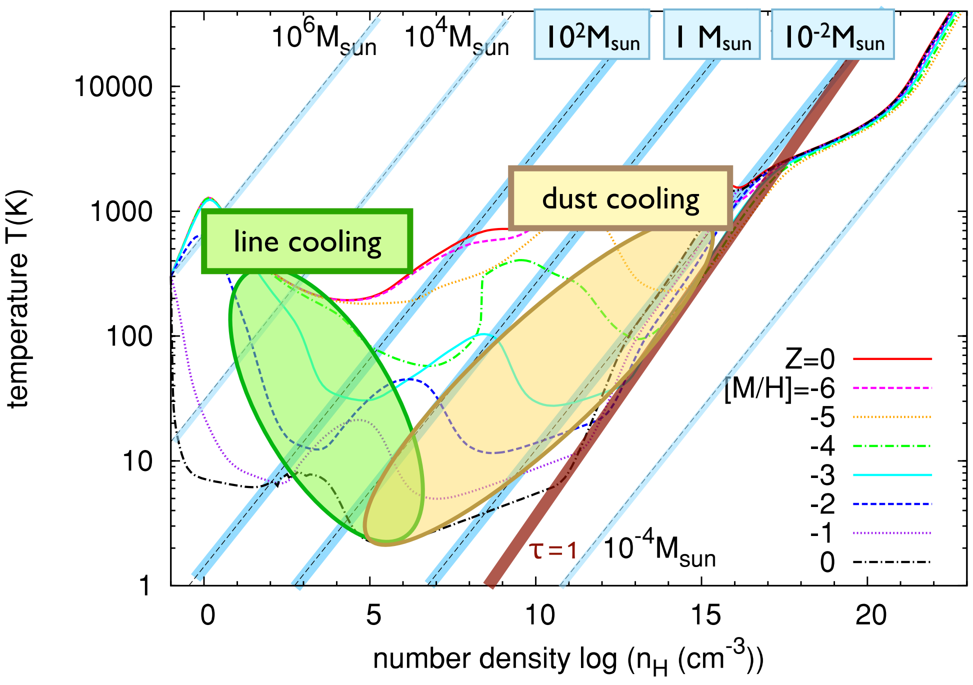

two competing models:

- cooling due to atomic fine-structure lines ($Z > 10^{-3.5}\ Z_{sun}$)
- cooling due to coupling between gas and dust ($Z > 10^{-5...-6}\ Z_{sun}$)

- which one is explains origin of extremely metal-poor stars *NB:* lines would only make very massive stars, with $M >$ few x10 M_{sun}.

(Omukai et al. 2005, 2010)

transition: Pop III to Pop II.5

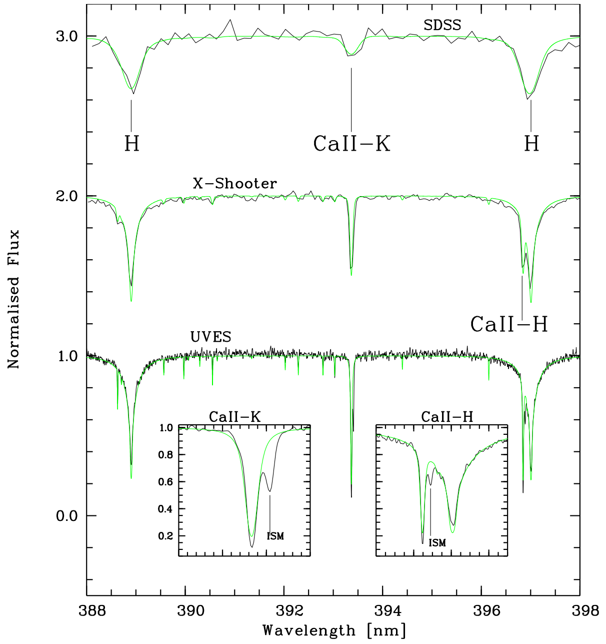

Element			[X/H]$_{1D}$		N lines	S_H	A(X)$_\odot$
		+3Dcor.	+NLTE cor.	+ 3D cor + NLTE cor			
C	≤ −3.8	≤ −4.5			G-band		8.50
N	≤ −4.1	≤ −5.0			NH-band		7.86
Mg I	−4.71 ± 0.11	−4.68 ± 0.11	−4.52 ± 0.11	−4.49 ± 0.12	5	0.1	7.54
Si I	−4.27	−4.30	−3.93	−3.96	1	0.1	7.52
Ca I	−4.72	−4.82	−4.44	−4.54	1	0.1	6.33
Ca II	−4.81 ± 0.11	−4.93 ± 0.03	−5.02 ± 0.02	−5.15 ± 0.09	3	0.1	6.33
Ti II	−4.75 ± 0.18	−4.83 ± 0.16	−4.76 ± 0.18	−4.84 ± 0.16	6	1.0	4.90
Fe I	−4.73 ± 0.13	−5.02 ± 0.10	−4.60 ± 0.13	−4.89 ± 0.10	43	1.0	7.52
Ni I	−4.55 ± 0.14	−4.90 ± 0.11			10		6.23
Sr II	≤ −5.10	≤ −5.25	≤ −4.94	≤ −5.09	1	0.01	2.92

(Caffau et al. 2011, 2012)

SDSS J1029151+172927

- is first ultra metal-poor star with Z ~ $10^{-4.5}$ Z_{sun} for all metals seen (Fe, C, N, etc.)
  [see Caffau et al. 2011]
- this is in regime, where metal-lines cannot provide cooling
  [e.g. Schneider et al. 2011, 2012, Klessen et al. 2012]

- new ESO large program to find more of these stars (120h x-shooter, 30h UVES)
  [PI E. Caffau]

(Schneider et al. 2011,2012, Klessen et al. 2012)

transition: Pop III to Pop II.5

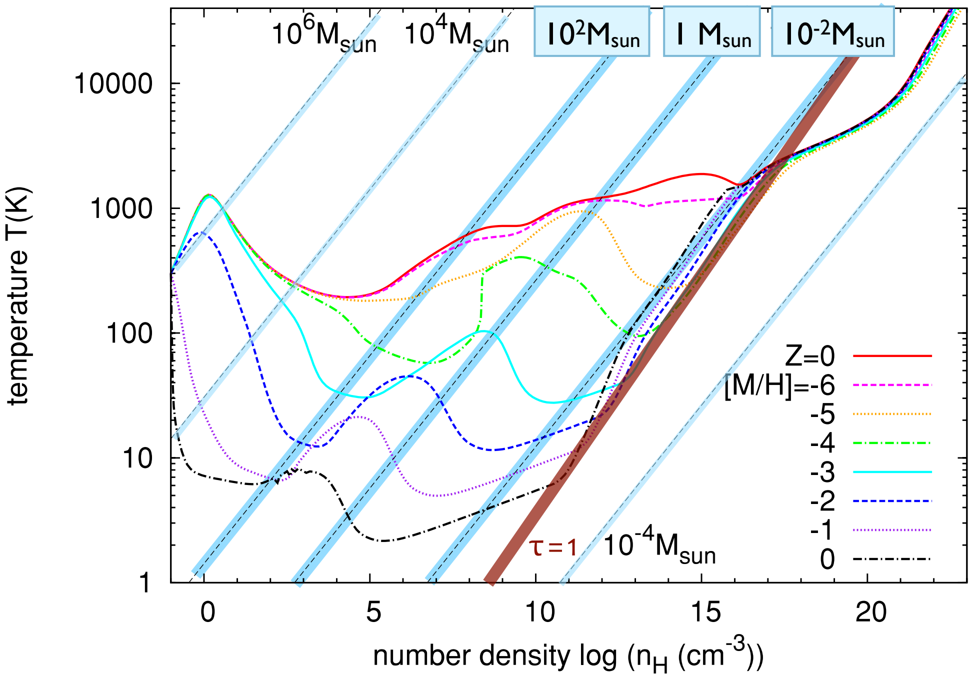

approach problem with high-resolution hydrodynamic calculations of central parts of high-redshift halos

- SPH (40 million particles)
- time-dependent chemistry (with dust)
- sink particles to model star formation
- external dark-matter potential

(Omukai et al. 2005, 2010)

transition: Pop III to Pop II.5

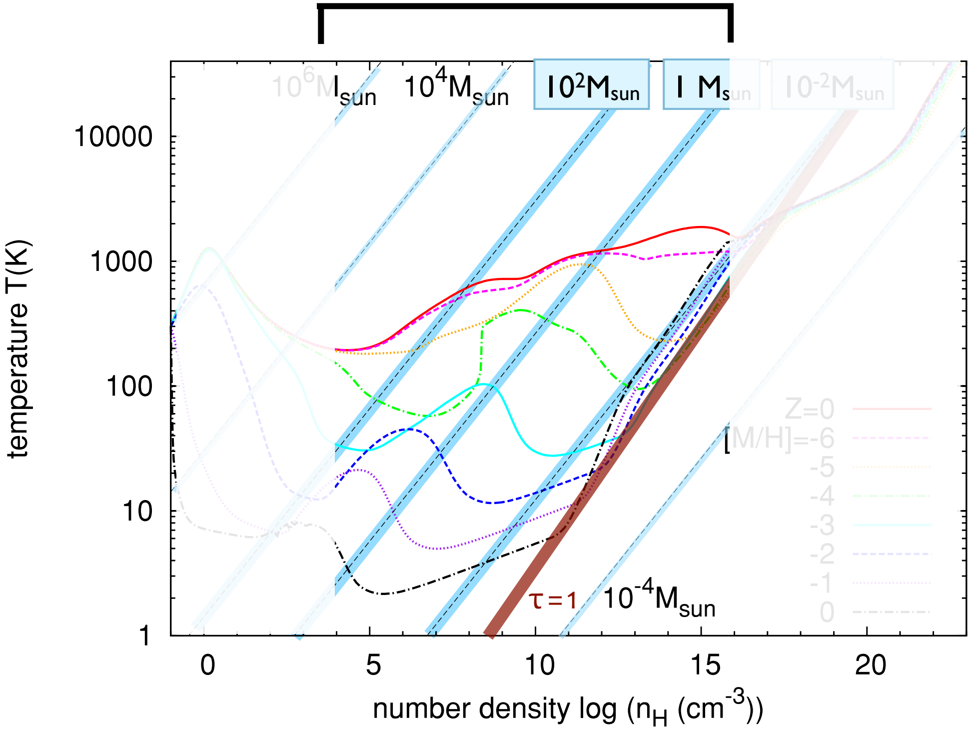

approach problem with high-resolution hydrodynamic calculations of central parts of high-redshift halos

- SPH (40 million particles)
- time-dependent chemistry (with dust)
- sink particles to model star formation
- external dark-matter potential
- focus on relevant density regime
  (i.e. include dust dip and optically thick regime)

(Omukai et al. 2005, 2010)

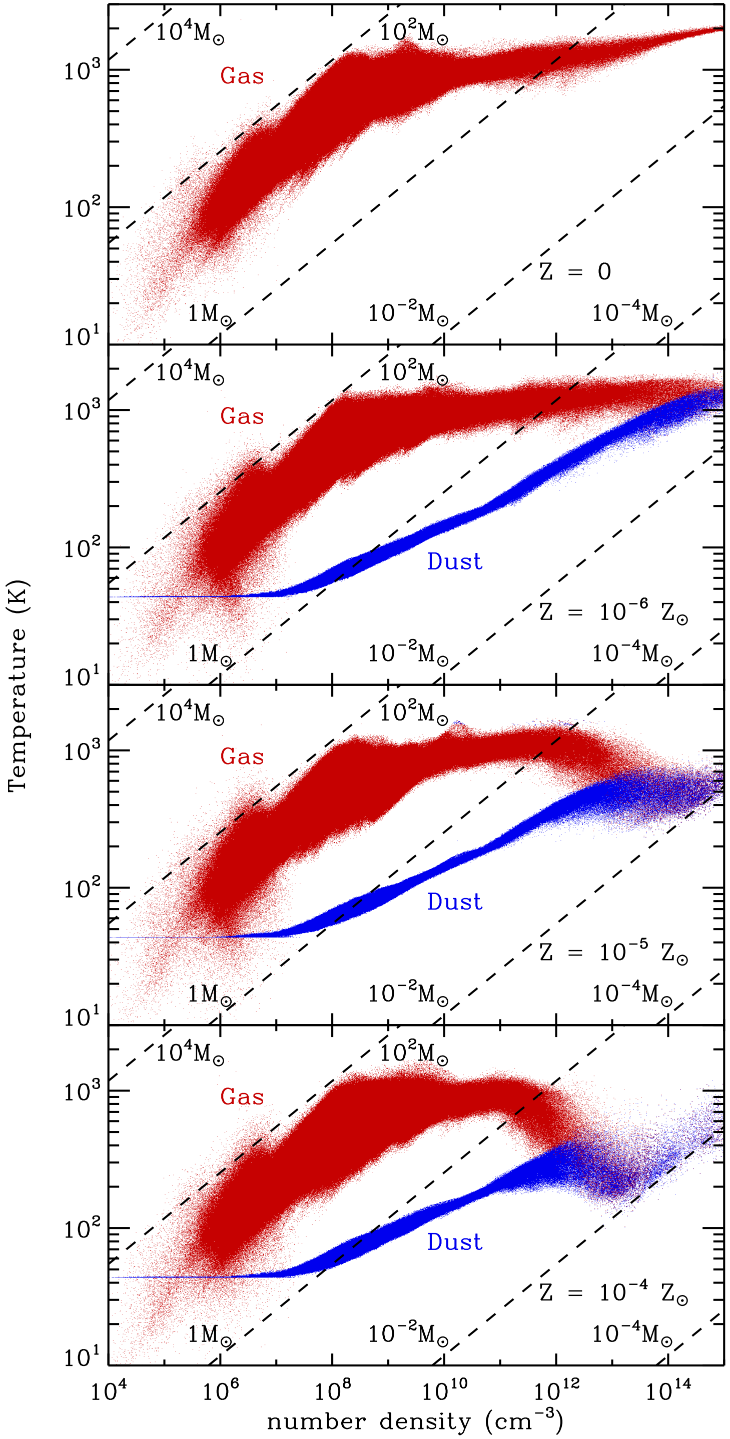

[M/H] = -ininity

[M/H] = -6

[M/H] = -5

[M/H] = -4

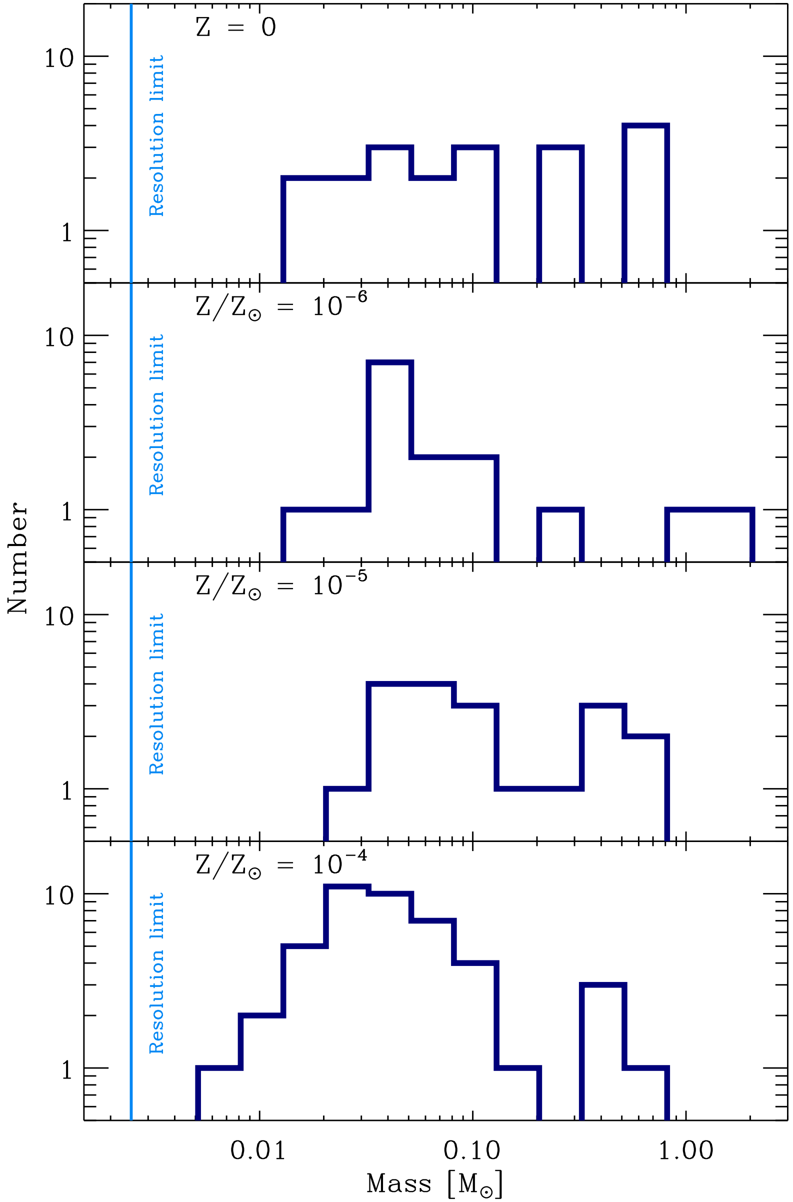

red : gas
blue: dust

Dopcke et al., 2012, submitted to ApJ, arXiv:1203.6842) hints for differences in mass spectrum

disk fragmentation mode

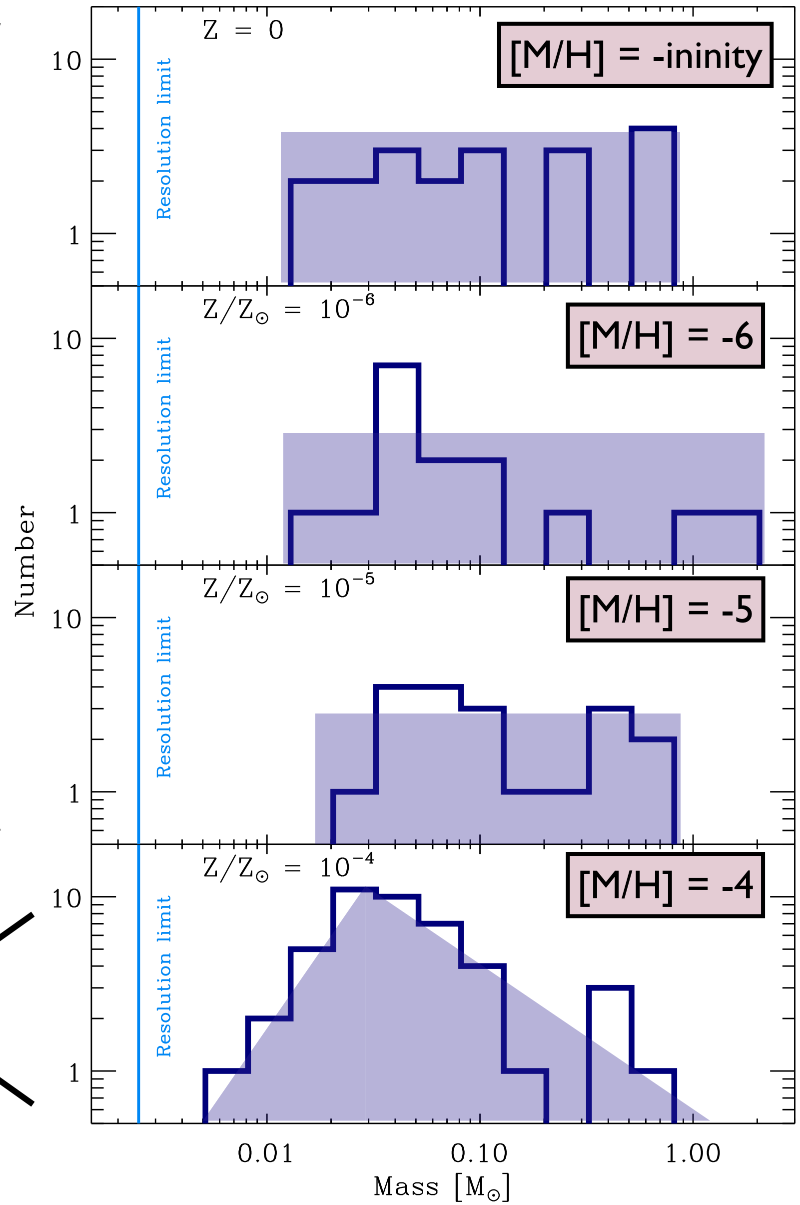

gravoturbulent fragmentation mode

Dopcke et al., 2012, submitted to ApJ, arXiv:1203.6842)

EOS as function of metallicity

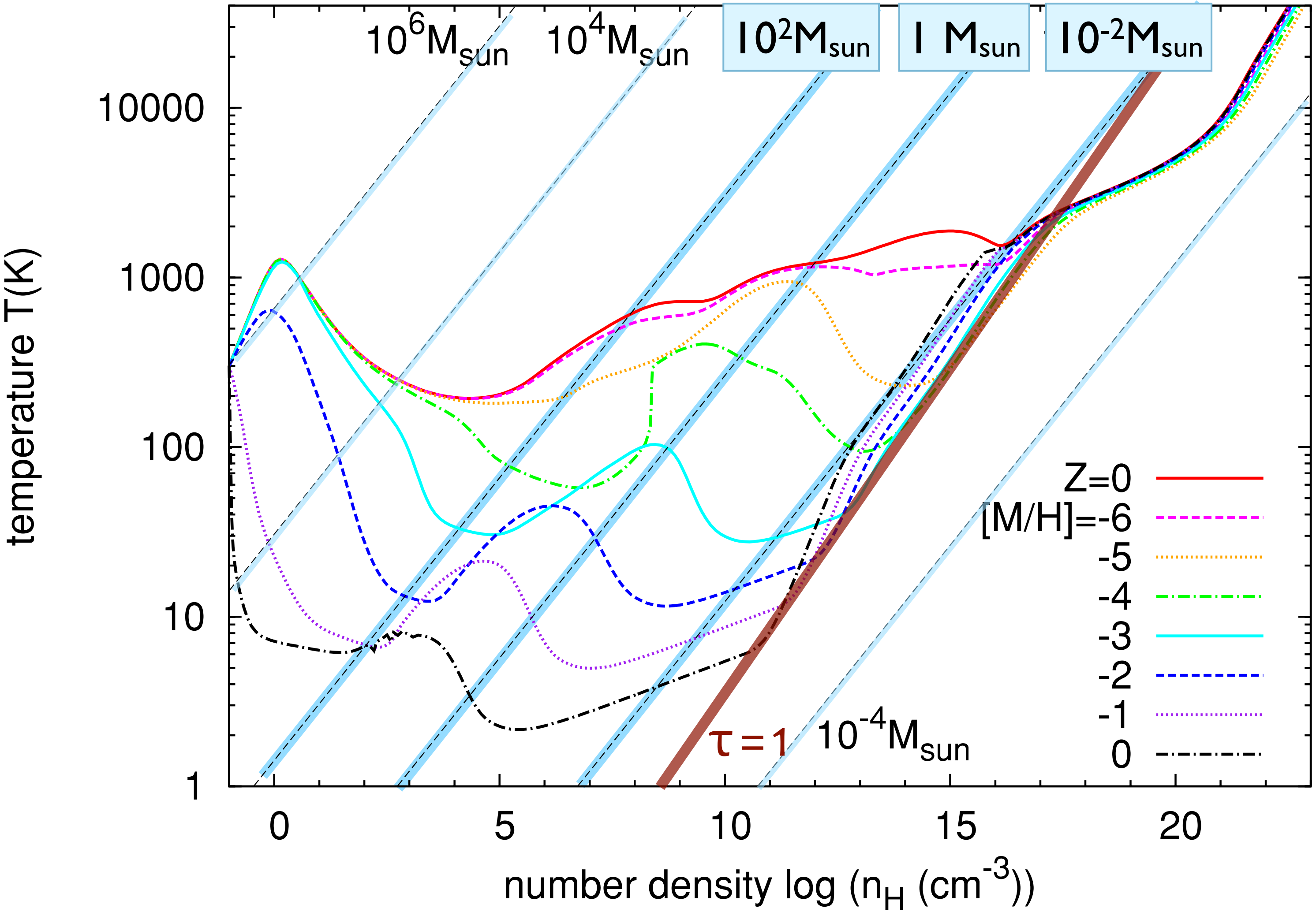

(Omukai et al. 2005, 2010)

EOS as function of metallicity

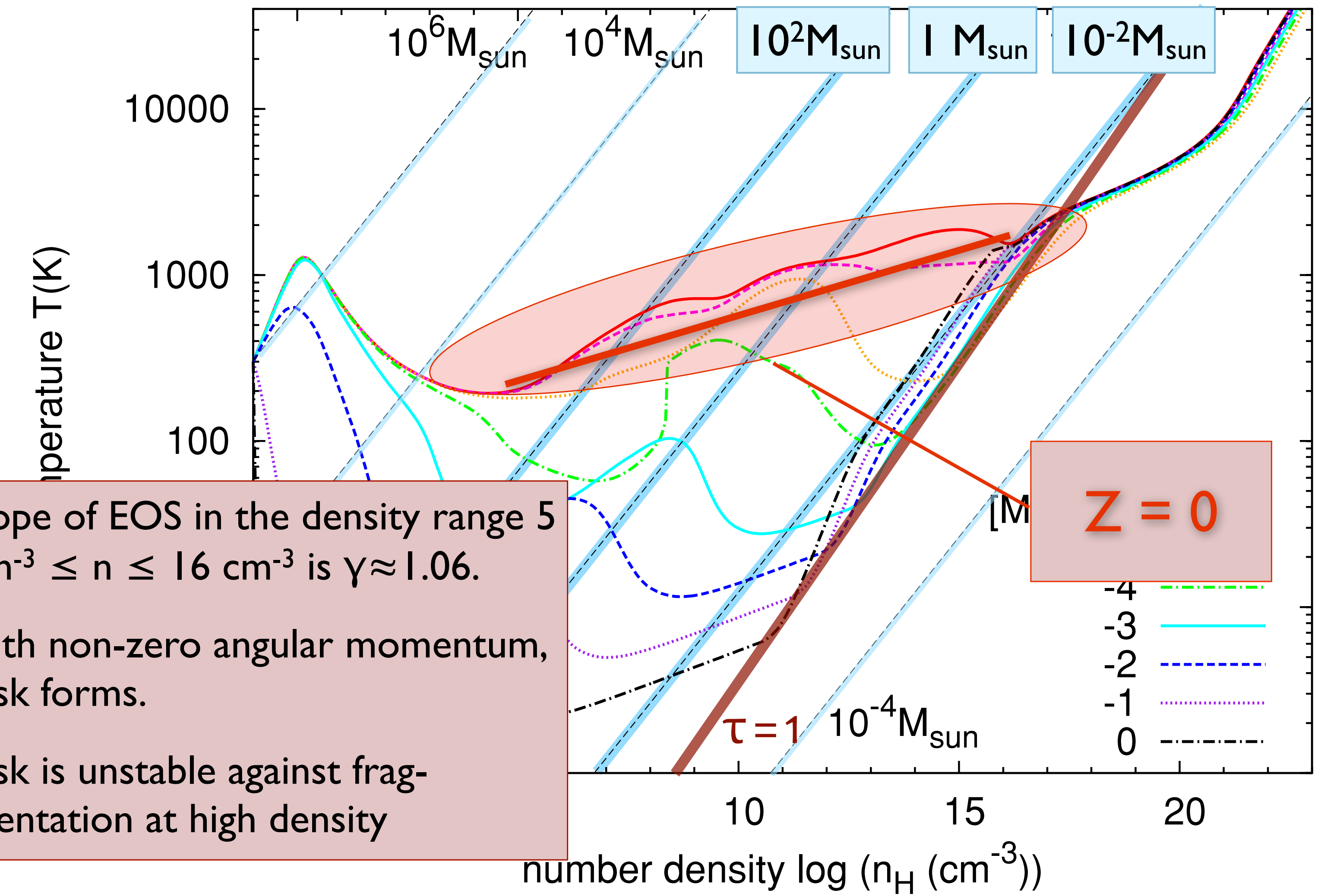

Z = 0

- slope of EOS in the density range 5 $cm^{-3} \leq n \leq 16\ cm^{-3}$ is $\gamma \approx 1.06$.
- with non-zero angular momentum, disk forms.
- disk is unstable against fragmentation at high density

(Omukai et al. 2005, 2010)

“classical” picture

- most current numerical simulations of Pop III star formation predict very massive objects

  (e.g. Abel et al. 2002, Yoshida et al. 2008, Bromm et al. 2009)

- similar for theoretical models (e.g. Tan & McKee 2004)

- there are some first hints of fragmentation, however

  (Turk et al. 2009, Stacy et al. 2010)

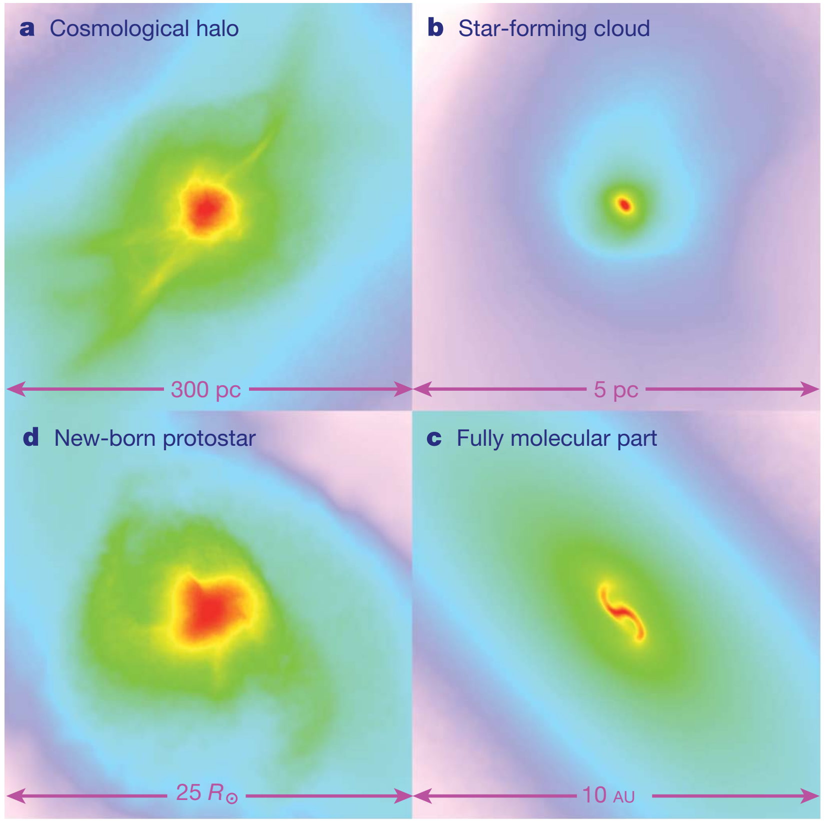

Figure 1 | Projected gas distribution around a primordial protostar. Shown is the gas density (colour-coded so that red denotes highest density) of a single object on different spatial scales. **a**, The large-scale gas distribution around the cosmological minihalo; **b**, a self-gravitating, star-forming cloud; **c**, the central part of the fully molecular core; and **d**, the final protostar. Reproduced by permission of the AAAS (from ref. 20).

(Yoshida et al. 2008, Science, 321, 669)

detailed look at accretion disk around first star

successive zoom-in calculation from cosmological initial conditions (using SPH and new grid-code AREPO)

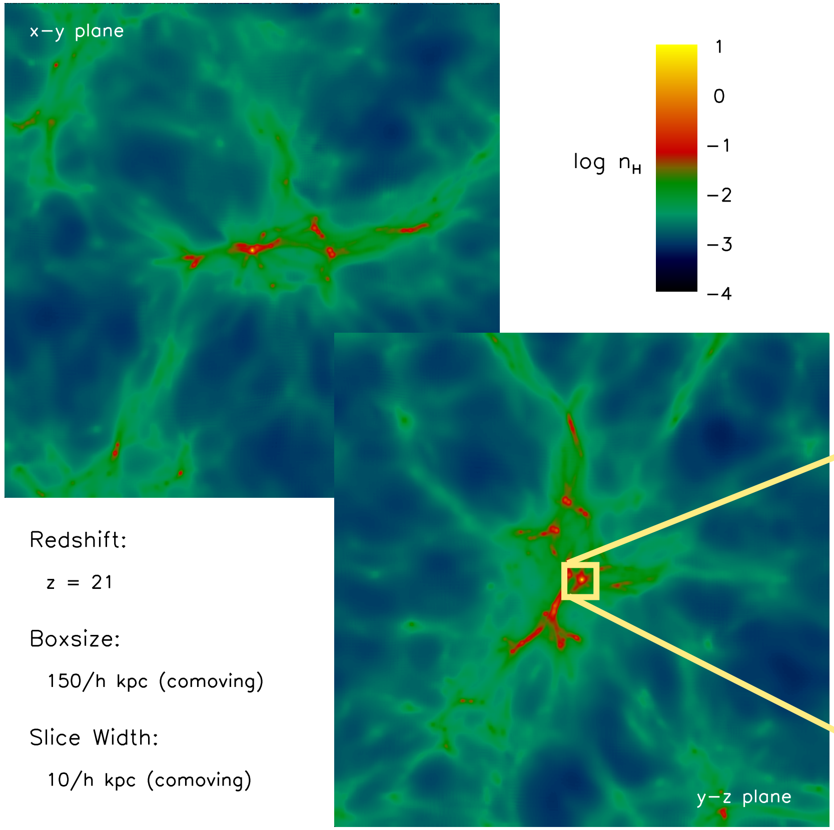

(Greif et al., 2007, ApJ, 670, 1)

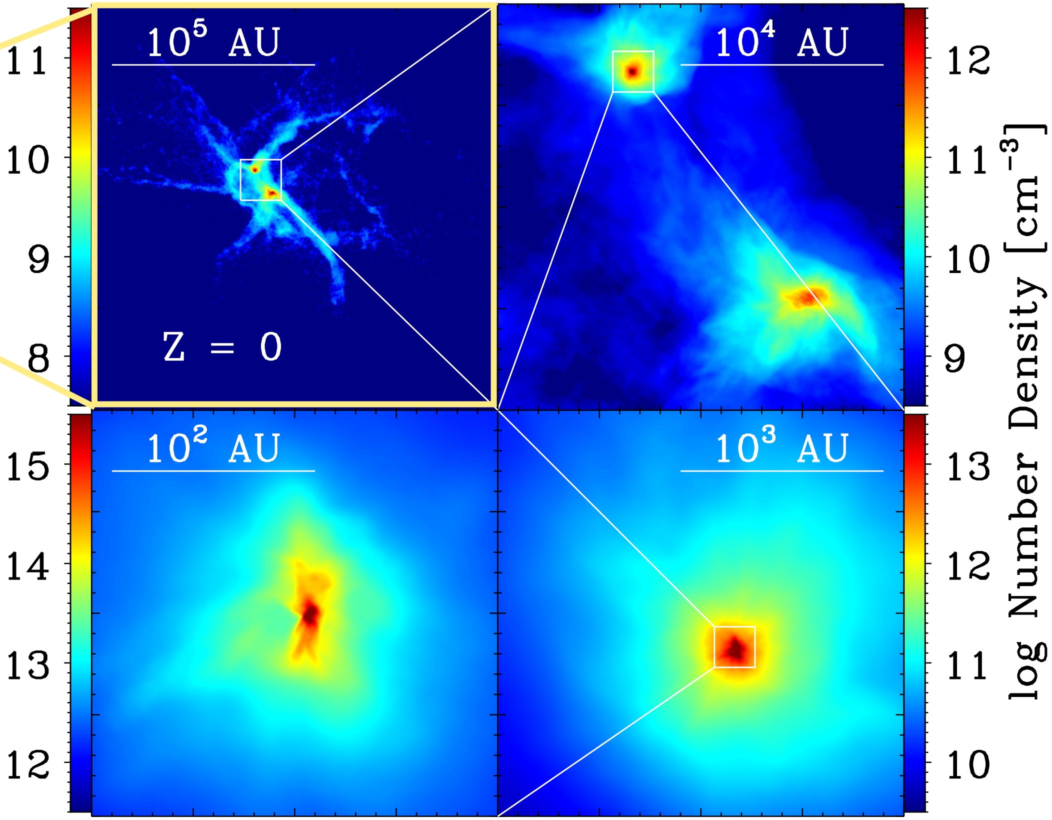

(Greif et al. 2011, ApJ, 737, 75, Greif et al. 2012, MNRAS, 424, 399, Dopcke et al. 2012, ApJ submitted, arXiv1203.6842)

detailed look at accretion disk around first star

successive zoom-in calculation from cosmological initial conditions (using SPH and new grid-code AREPO)

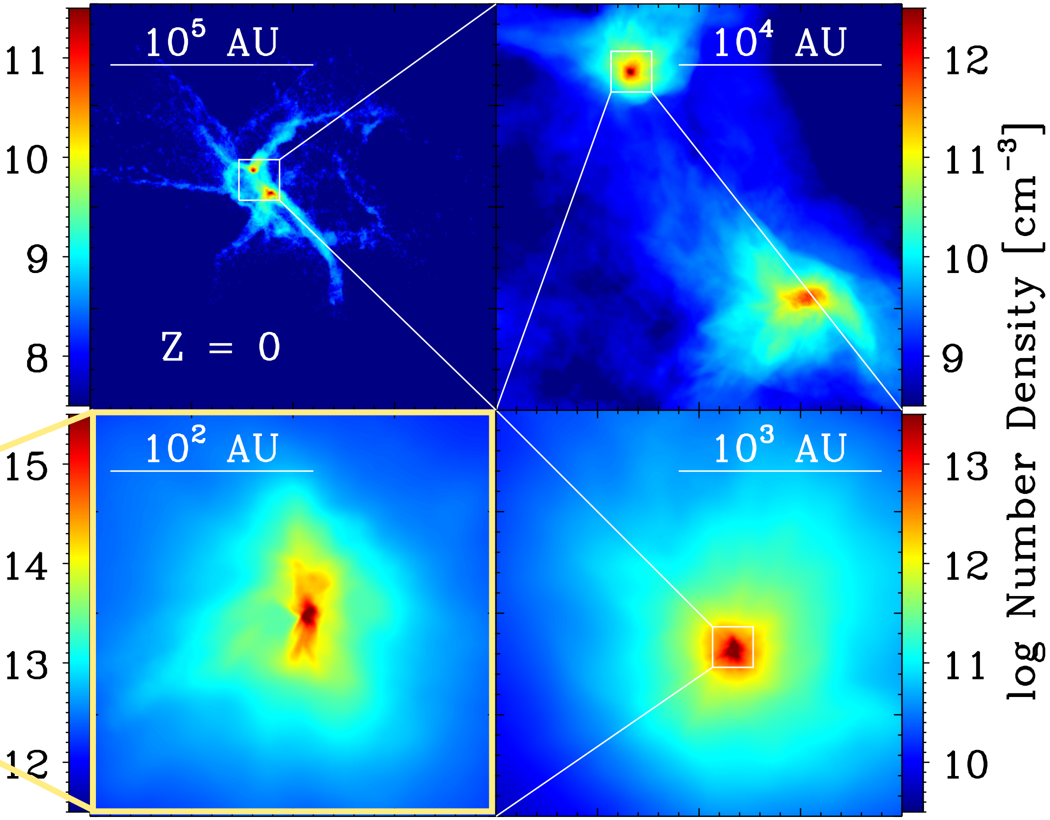

what is the time evolution of accretion disk around first star to form?

(Greif et al. 2011, ApJ, 737, 75, Greif et al. 2012, MNRAS, 424, 399, Dopcke et al. 2012, ApJ submitted, arXiv1203.6842) detailed look at accretion disk

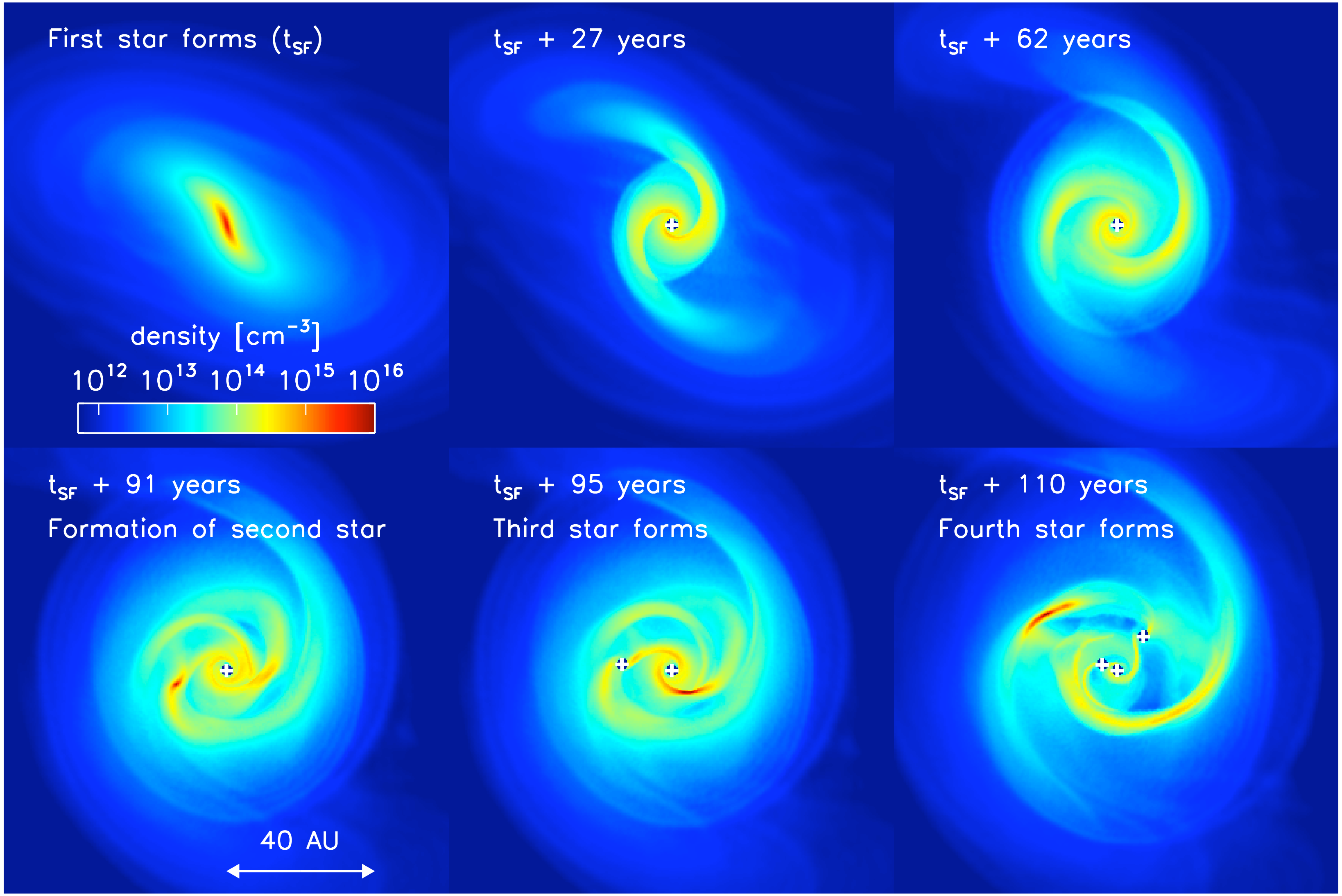

Figure 1: Density evolution in a 120 AU region around the first protostar, showing the build-up of the protostellar disk and its eventual fragmentation. We also see ‘wakes’ in the low-density regions, produced by the previous passage of the spiral arms.

(Clark et al. 2011b, Science, 331, 1040)

important disk parameters

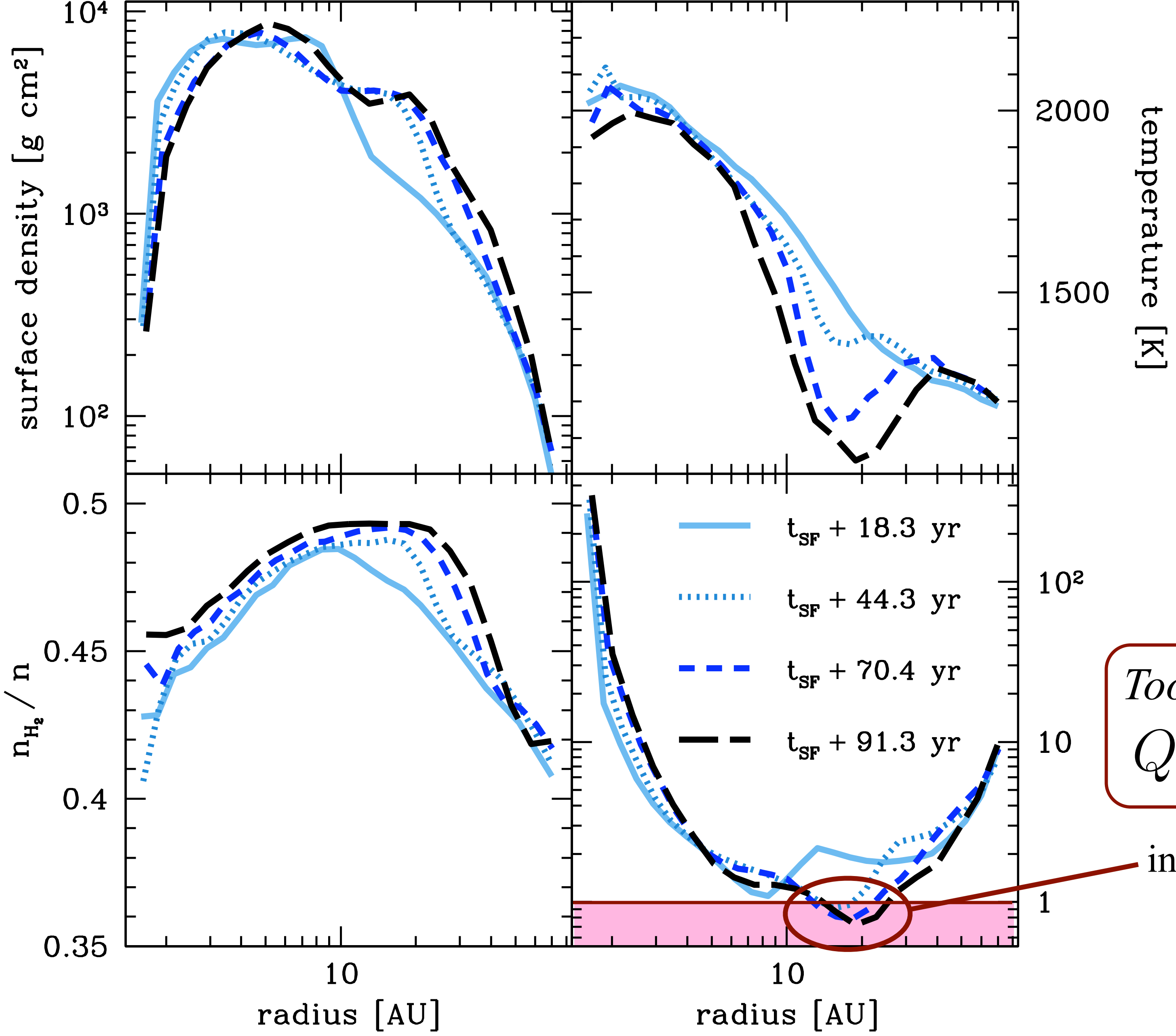

Toomre Q:

$$Q = c_{\rm s}\kappa/\pi G\Sigma$$

instability for *Q<1*

(Clark et al. 2011b, Science, 331, 1040)

similar study with very different numerical method (AREPO)

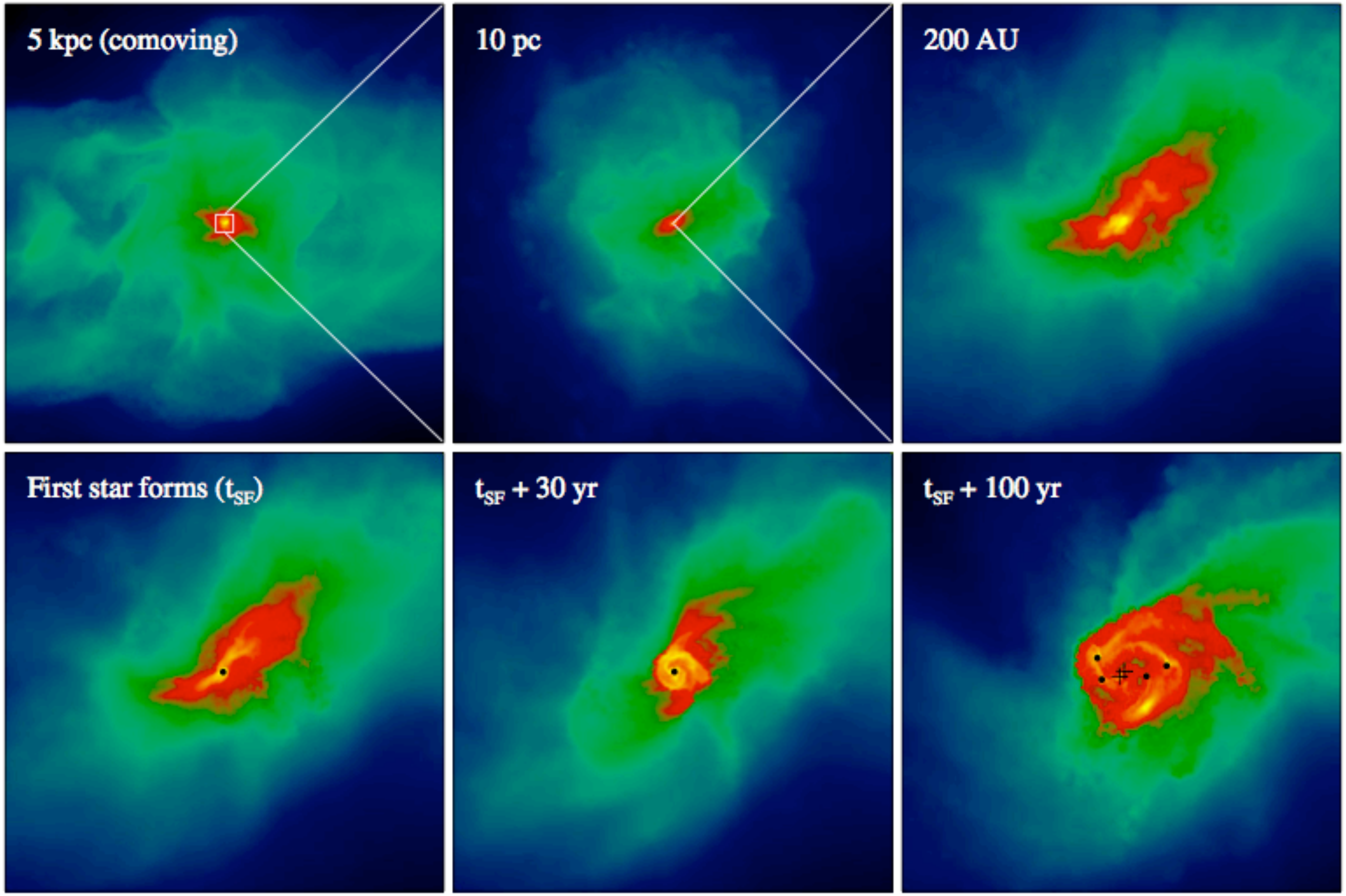

one out of five halos

(Greif et al. 2011a, ApJ)

expected mass spectrum

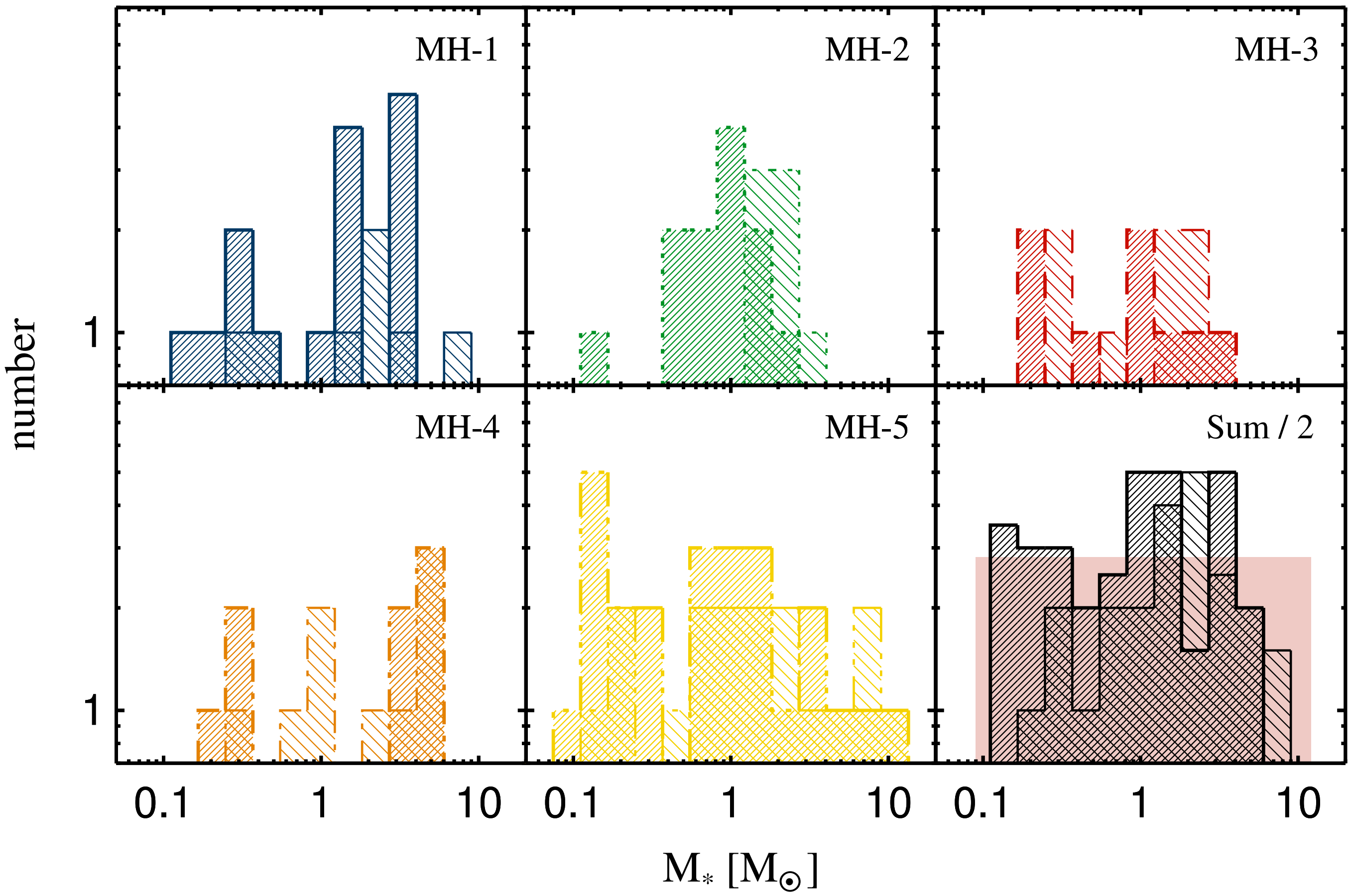

we see "flat"
mass spectrum

(Greif et al. 2011, ApJ, 737, 75, also Dopcke et al. 2012 ApJ submitted, arXiv1203.6842)

expected mass spectrum

- *expected IMF is flat* and covers a wide range of masses
- implications
  - because slope > -2, most *mass is in massive objects* as predicted by most previous calculations
  - most high-mass Pop III stars should be in *binary systems* --> source of *high-redshift gamma-ray bursts*
  - because of ejection, some *low-mass objects* (< 0.8 $M_\odot$) might have *survived* until today and could potentially be found in the Milky Way
- consistent with abundance patterns found in second generation stars

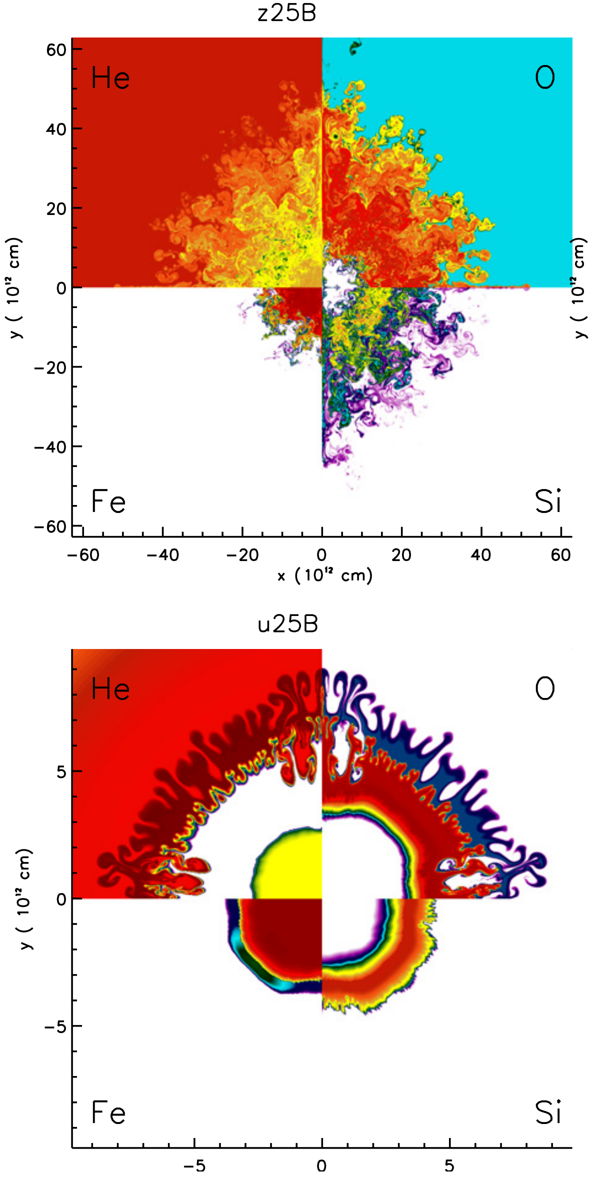

(Joggerst et al. 2009, 2010)

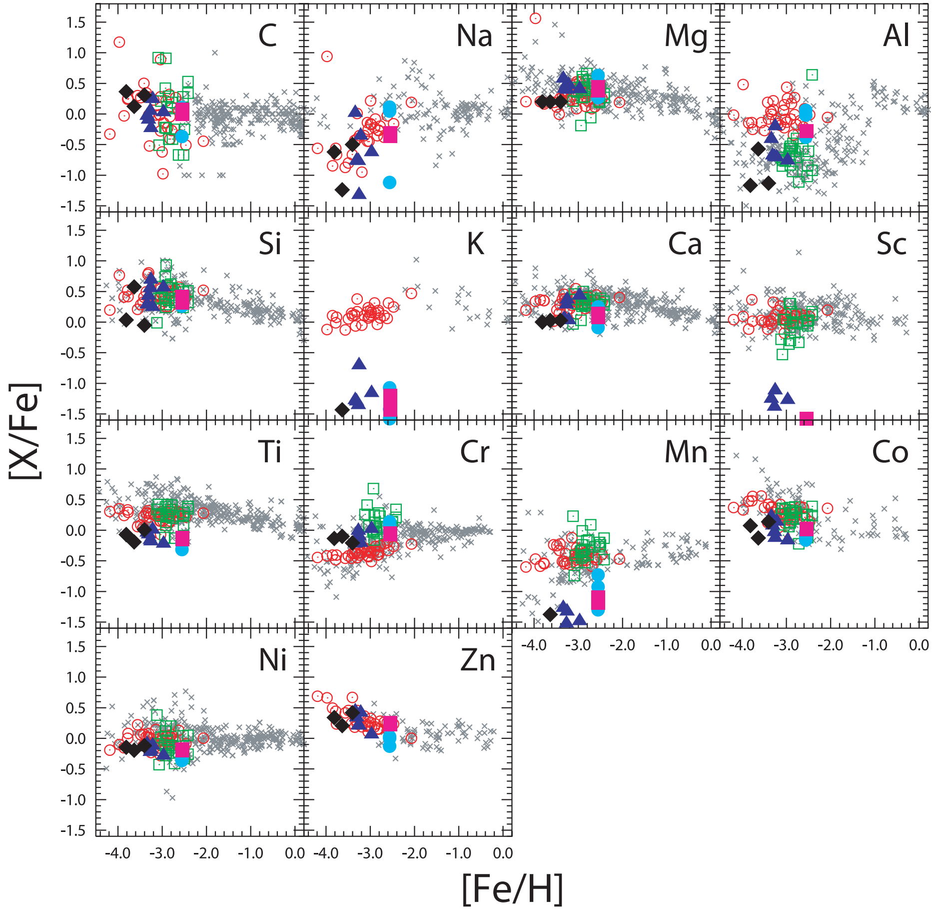

(Tominaga et al. 2007)

The metallicities of extremely metal-poor stars in the halo are consistent with the yields of core-collapse supernovae, i.e. progenitor stars with 20 - 40 M$_\odot$

(e.g. Tominaga et al. 2007, Izutani et al. 2009, Joggerst et al. 2009, 2010)

primordial star formation

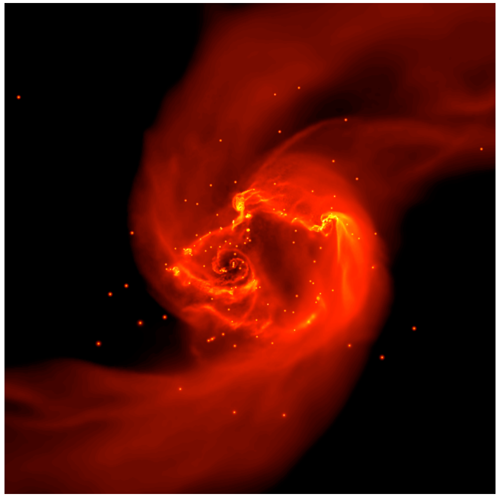

- just like in present-day SF, we expect
  - *turbulence*
  - *thermodynamics*
  - *feedback*
  - *magnetic fields*

  to influence first star formation.
- masses of first stars still *uncertain* (surprises from new generation of high-resolution calculations that go beyond first collapse)
- disks unstable: first stars should be *binaries* or *part of small clusters*
- effects of feedback less important than in present-day SF

IMF

- distribution of stellar masses depends on
  - turbulent initial conditions
    --> mass spectrum of prestellar cloud cores
  - collapse and interaction of prestellar cores
    --> competitive accretion and *N*-body effects
  - *thermodynamic properties of gas*
    --> balance between heating and cooling
    --> EOS (determines which cores go into collapse)
  - (proto) stellar feedback terminates star formation
    ionizing radiation, bipolar outflows, winds, SN

high-mass star formation

We want to address the following questions:

- how do massive stars (and their associated clusters) form?
- what determines the upper stellar mass limit?
- what is the physics behind observed HII regions?

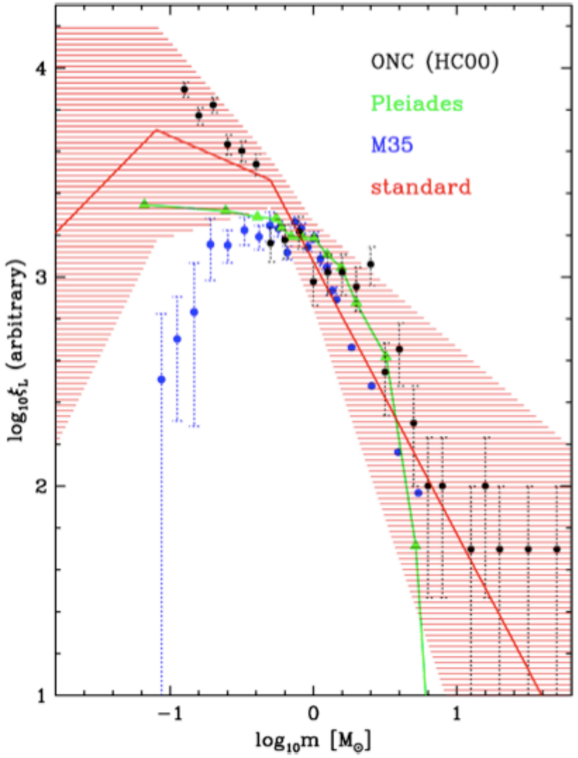

IMF (Kroupa 2002)

Rosetta nebula (NGC 2237)

(proto)stellar feedback processes

- radiation pressure on dust particles
- ionizing radiation
- stellar winds
- jets and outflows

ionization

- few numerical studies so far (e.g. Dale 2007, Gritschneder et al. 2009), detailed collapse calculations with ionizing and non-ionizing feedback still missing
- HII regions around massive stars are directly observable --> direct comparison between theory and observations

our (numerical) approach

- focus on collapse of individual high-mass cores...
  - massive core with 1,000 $M_\odot$
  - Bonnor-Ebert type density profile
    (flat inner core with 0.5 pc and rho ~ $r^{-3/2}$ further out)
  - initial m=2 perturbation, rotation with $\beta = 0.05$
  - sink particle with radius 600 AU and threshold density of 7×10^{-16} g cm^{-3}
  - cell size 100 AU

Peters et al. (2010a, ApJ, 711, 1017), Peters et al. (2010b, ApJ, 719, 831), Peters et al. (2010c, ApJ, 725, 134)

our (numerical) approach

- method:
  - FLASH with ionizing and non-ionizing radiation using raytracing based on hybrid-characteristics
  - protostellar model from Hosokawa & Omukai
  - rate equation for ionization fraction
  - relevant heating and cooling processes
  - some models include magnetic fields
  - *first 3D MHD calculations that consistently treat both ionizing and non-ionizing radiation in the context of high-mass star formation*

Peters et al. (2010a,b,c)

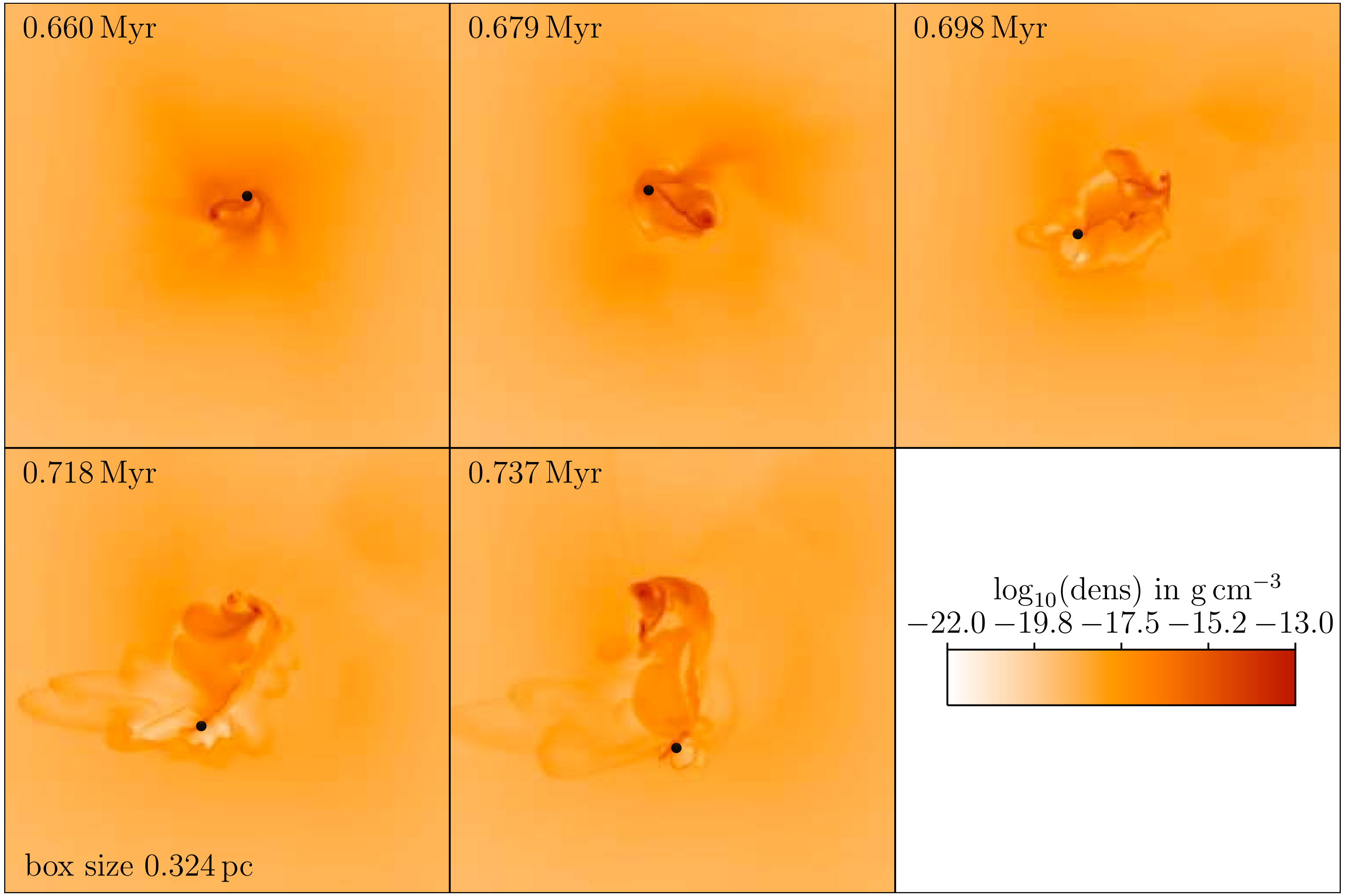

- disk is gravitationally unstable and fragments
- we suppress secondary sink formation by “Jeans heating”
- H II region is shielded effectively by dense filaments
- ionization feedback does not cut off accretion!

Peters et al. (2010a,b,c)

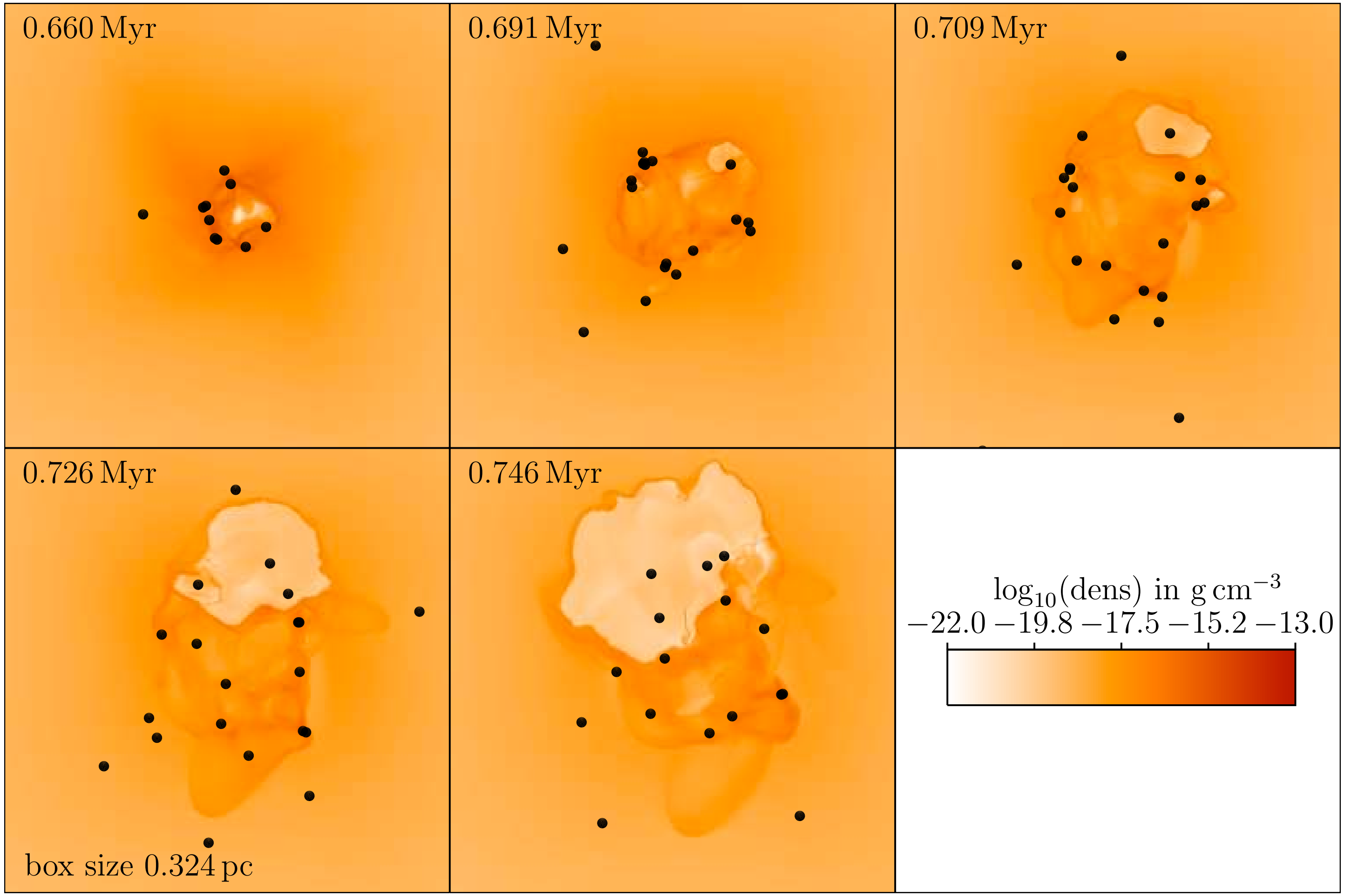

- all protostars accrete from common gas reservoir
- accretion flow suppresses expansion of ionized bubble
- cluster shows “fragmentation-induced starvation”
- halting of accretion flow allows bubble to expand

Peters et al. (2010a,b,c)

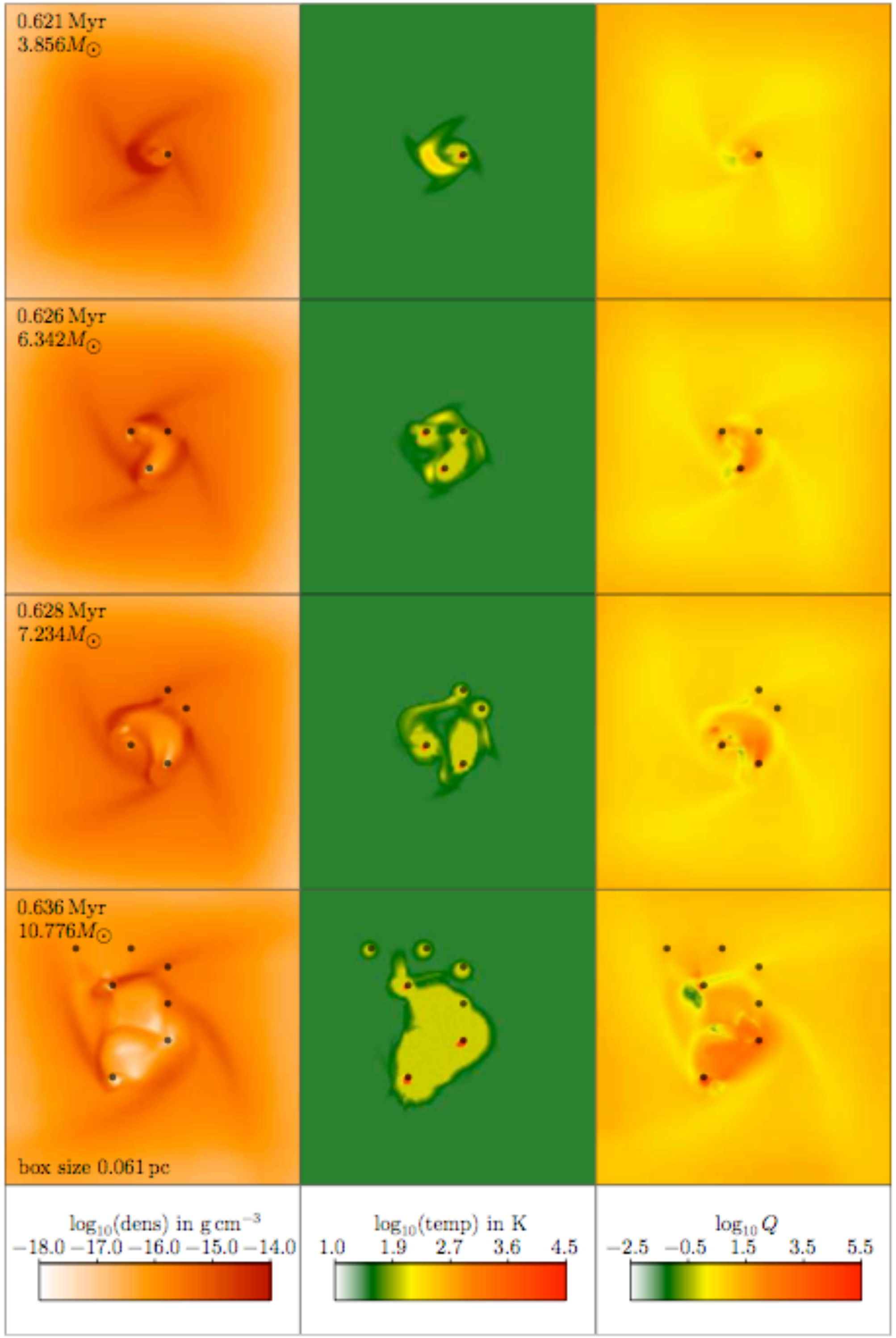

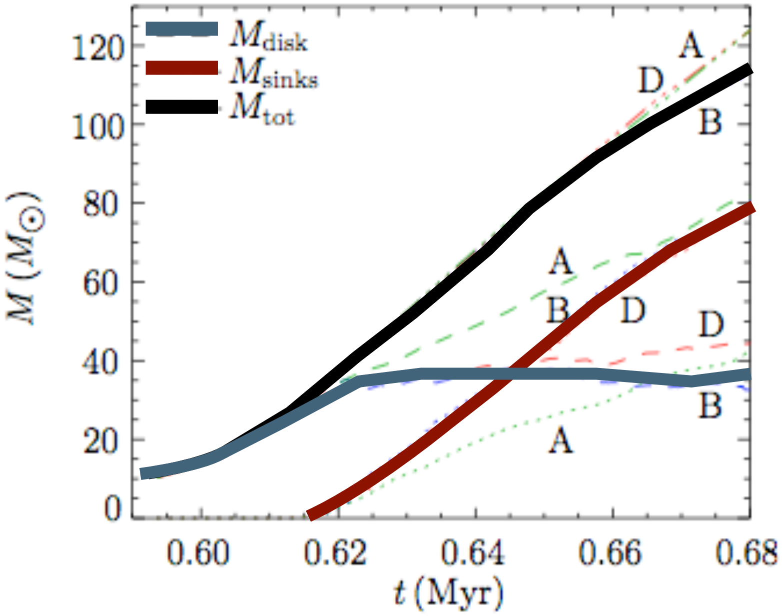

mass load onto the disk exceeds inward transport
--> becomes gravitationally unstable (see also Kratter & Matzner 2006, Kratter et al. 2010)

fragments to form multiple stars --> explains why high-mass stars are seen in clusters

Peters et al. (2010a, ApJ, 711, 1017),
Peters et al. (2010b, ApJ, 719, 831),
Peters et al. (2010c, ApJ, 725, 134)

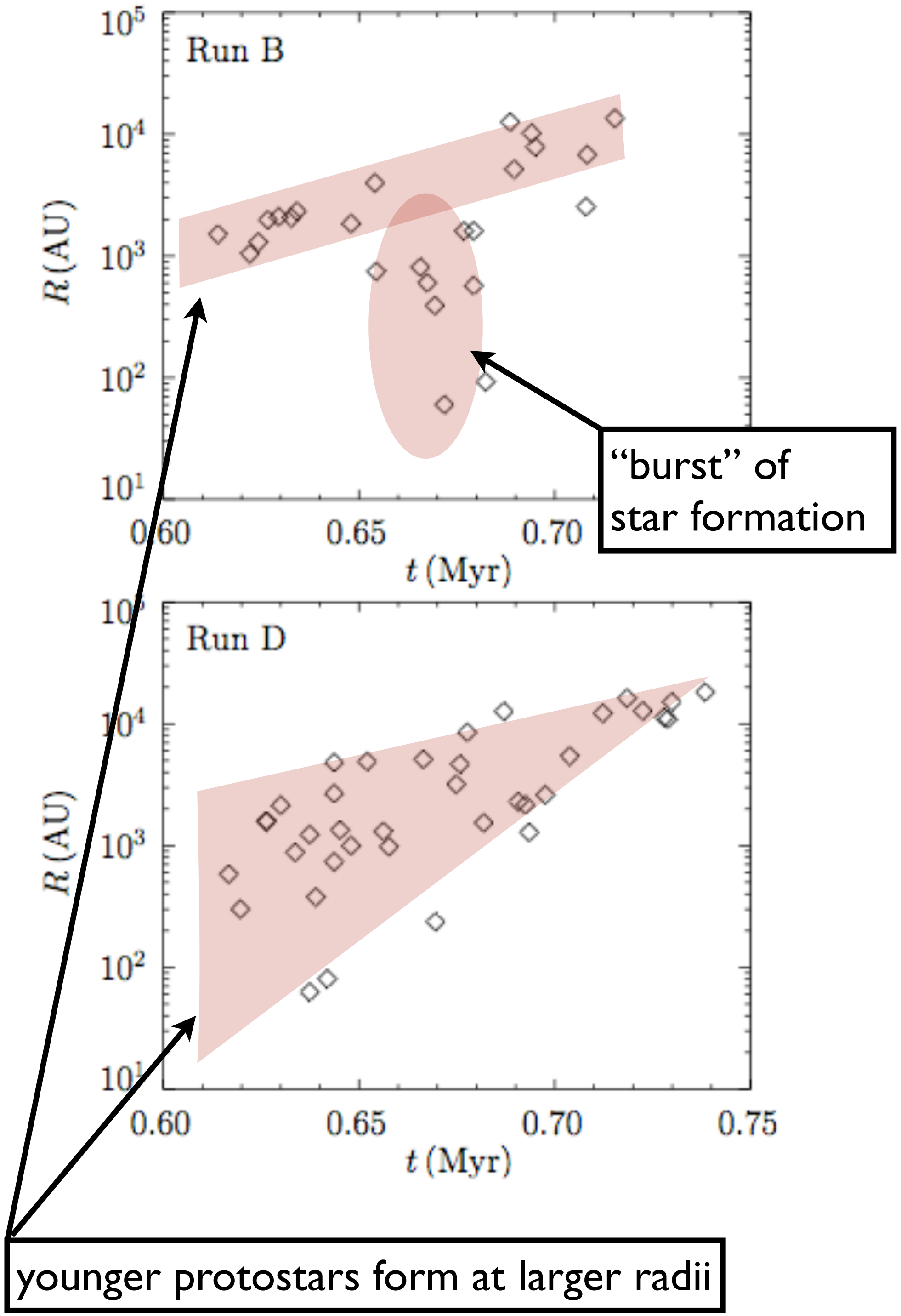

“burst” of star formation

younger protostars form at larger radii

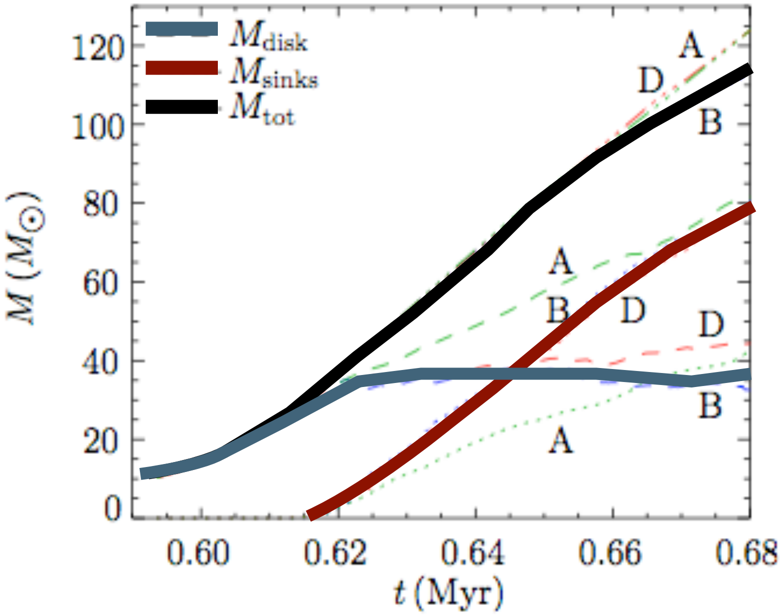

mass load onto the disk exceeds inward transport
--> becomes gravitationally unstable (see also Kratter & Matzner 2006, Kratter et al. 2010)

fragments to form multiple stars --> explains why high-mass stars are seen in clusters

Peters et al. (2010a, ApJ, 711, 1017),
Peters et al. (2010b, ApJ, 719, 831),
Peters et al. (2010c, ApJ, 725, 134)

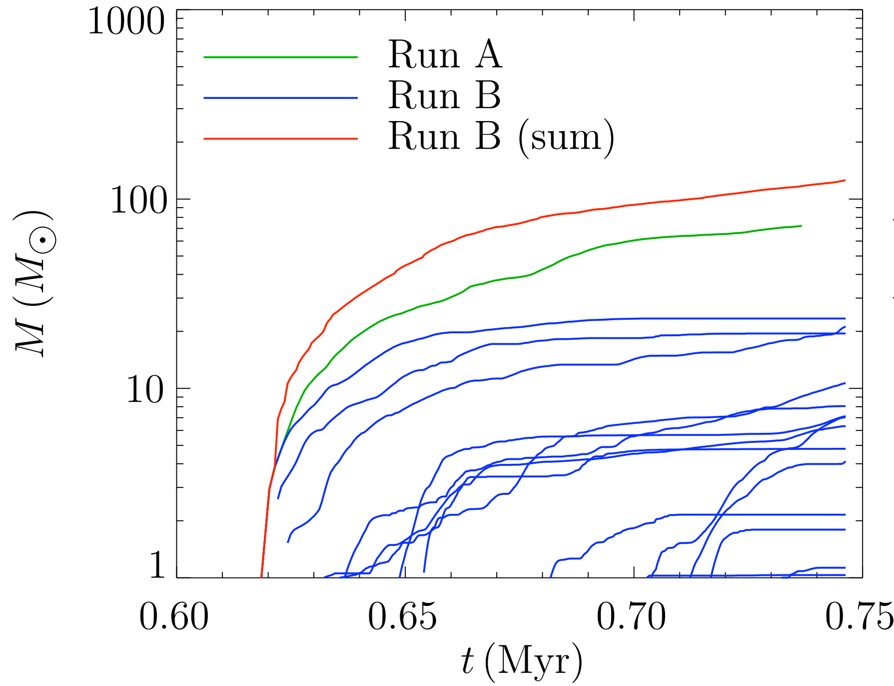

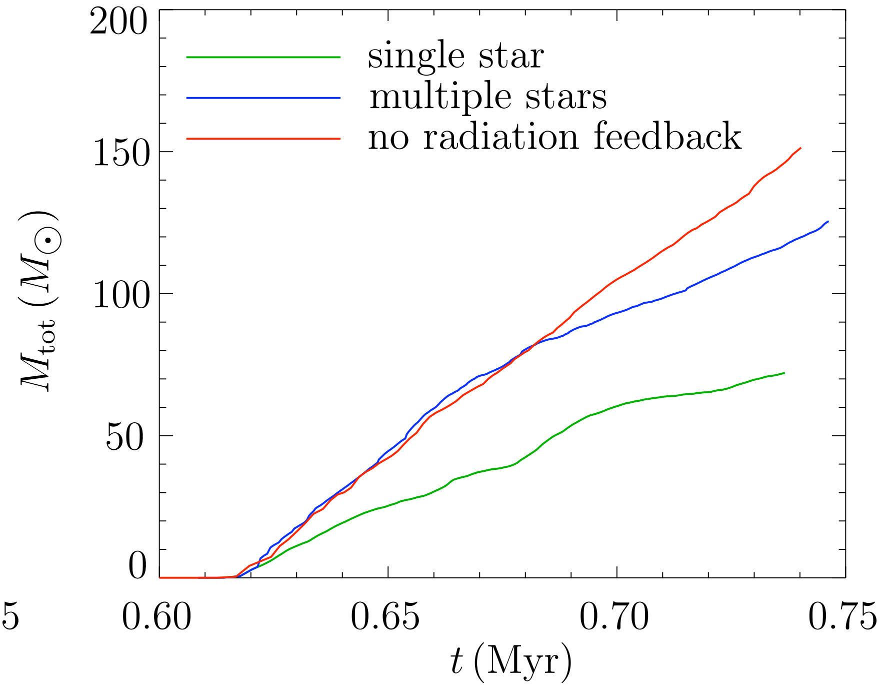

- compare with control run without radiation feedback
- total accretion rate does not change with accretion heating
- expansion of ionized bubble causes turn-off
- no triggered star formation by expanding bubble

Peters et al. (2010a, ApJ, 711, 1017), Peters et al. (2010b, ApJ, 719, 831), Peters et al. (2010c, ApJ, 725, 134)

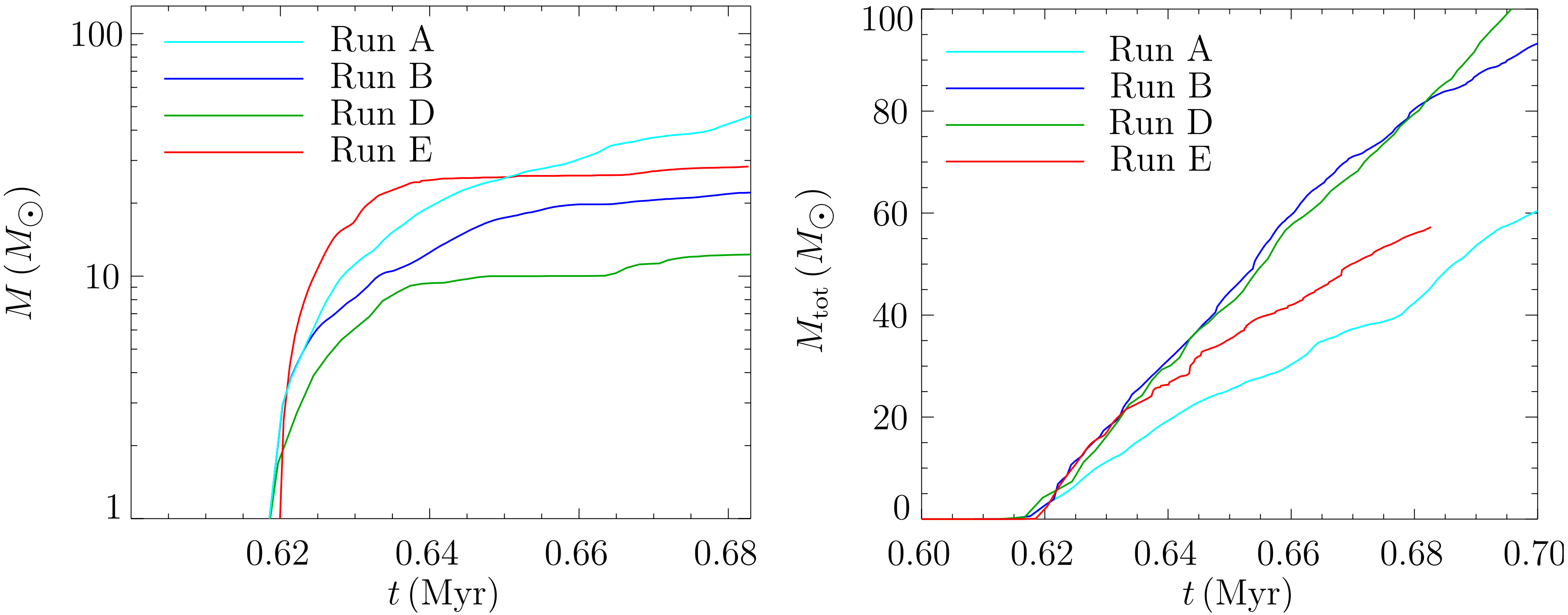

- magnetic fields lead to weaker fragmentation
- central star becomes more massive (magnetic breaking

Peters et al. (2010a, ApJ, 711, 1017), Peters et al. (2010b, ApJ, 719, 831), Peters et al. (2010c, ApJ, 725, 134), Peters et al. (2011, ApJ, 729, 72

Fragmentation-induced starvation in a complex cluster

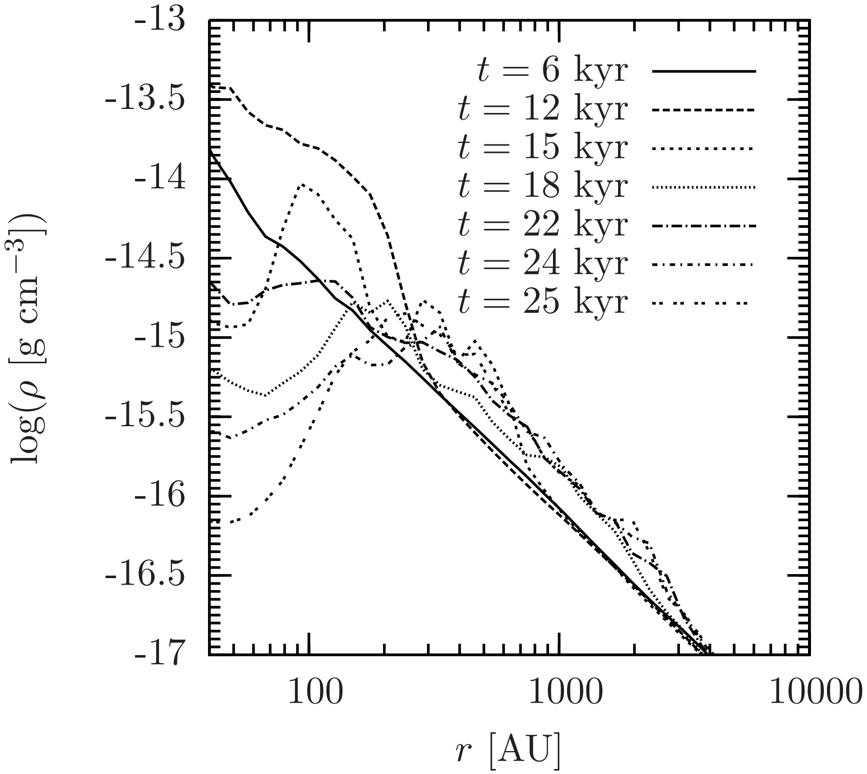

gas density as function of radius at different times

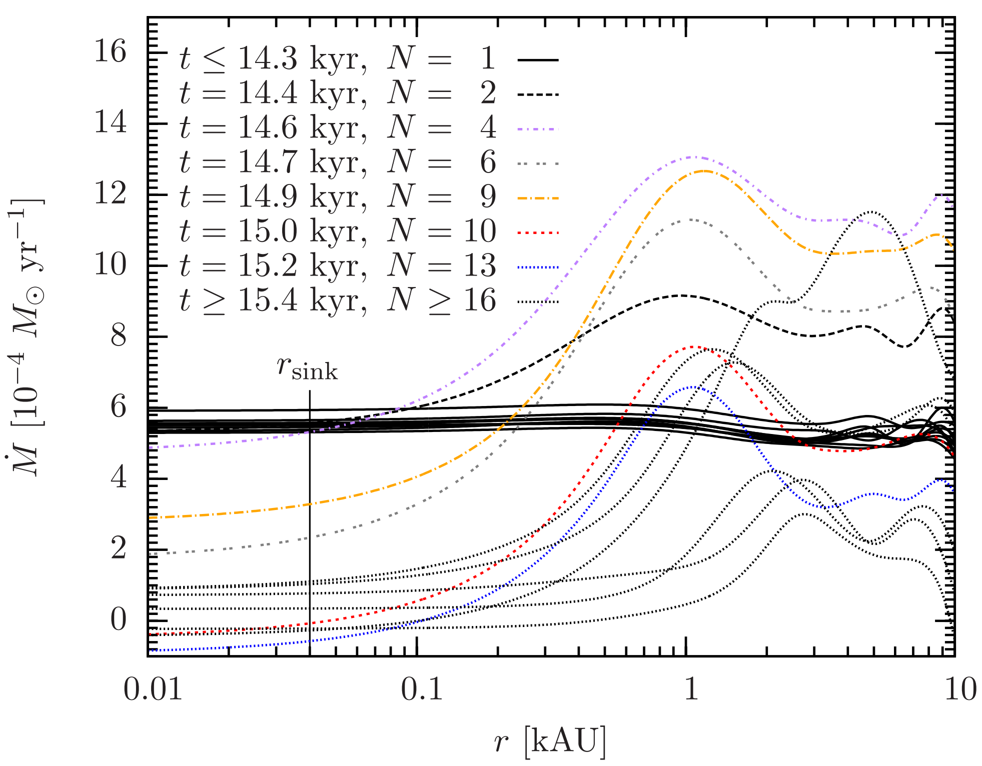

mass flow towards the center as function of radius at different times

Girichidis et al. (2011a,b)

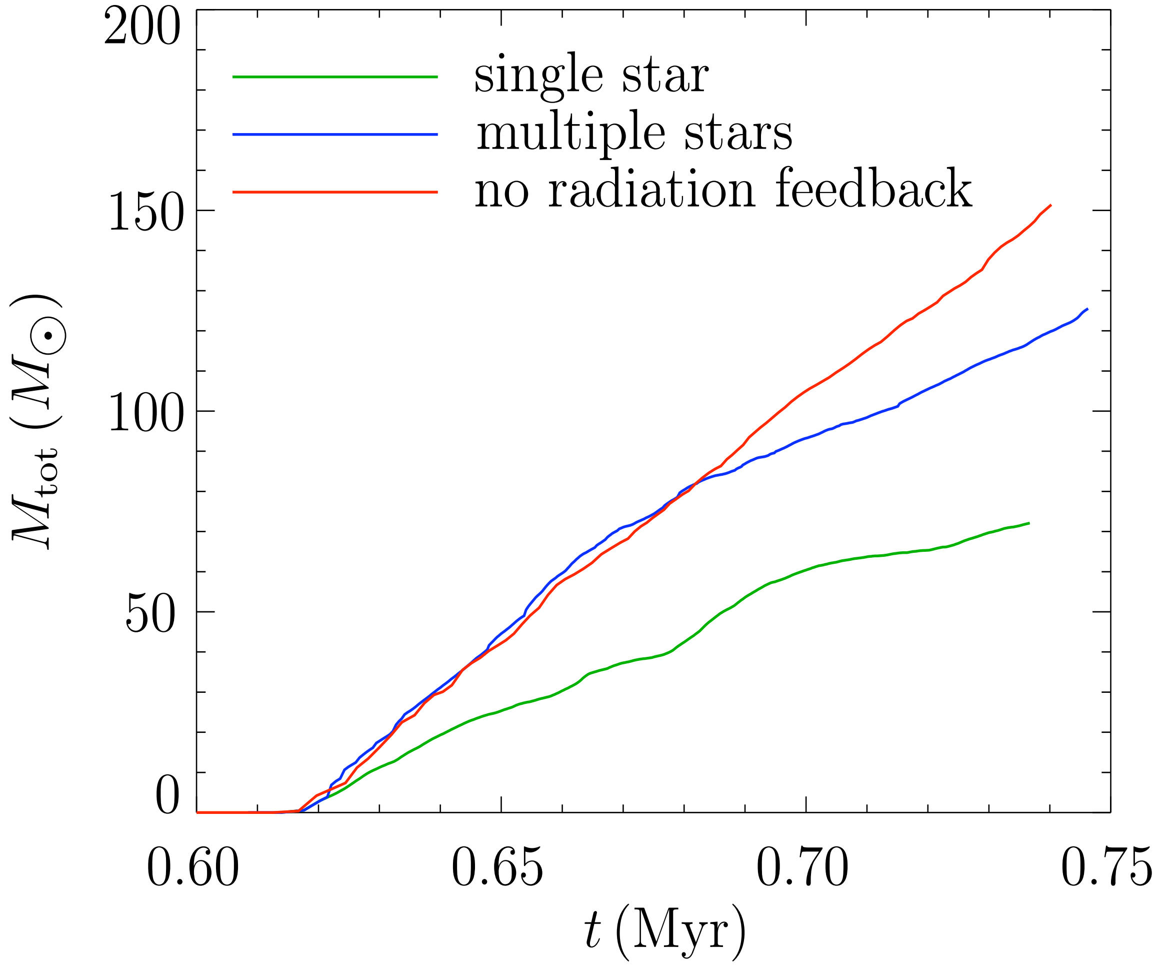

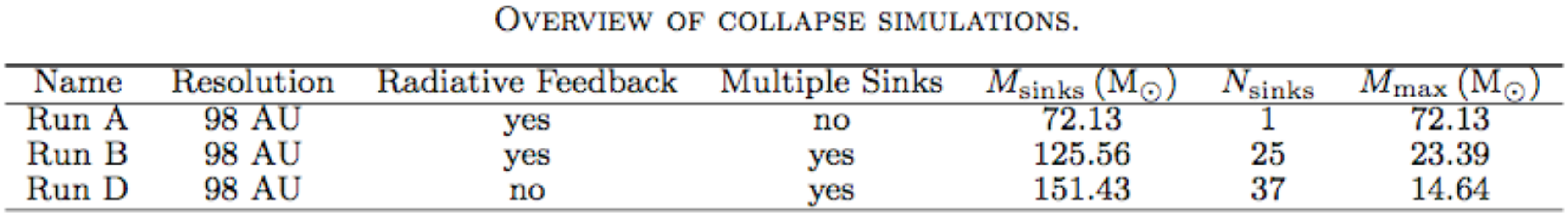

OVERVIEW OF COLLAPSE SIMULATIONS.

Name	Resolution	Radiative Feedback	Multiple Sinks	$M_{\rm sinks}$ ($M_\odot$)	$N_{\rm sinks}$	$M_{\rm max}$ ($M_\odot$)
Run A	98 AU	yes	no	72.13	1	72.13
Run B	98 AU	yes	yes	125.56	25	23.39
Run D	98 AU	no	yes	151.43	37	14.64

Peters et al. (2010a,b,c)

relation between maximum stellar mass and total stellar mass

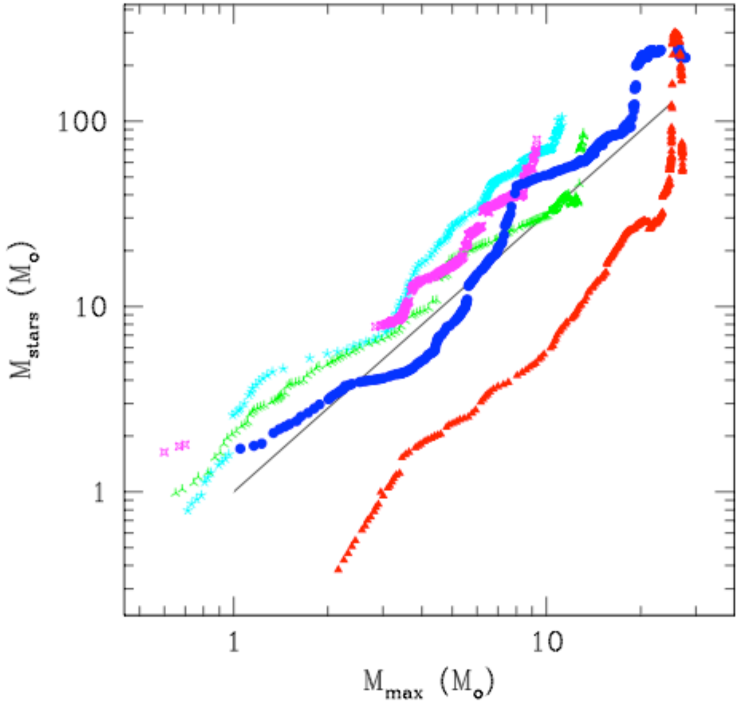

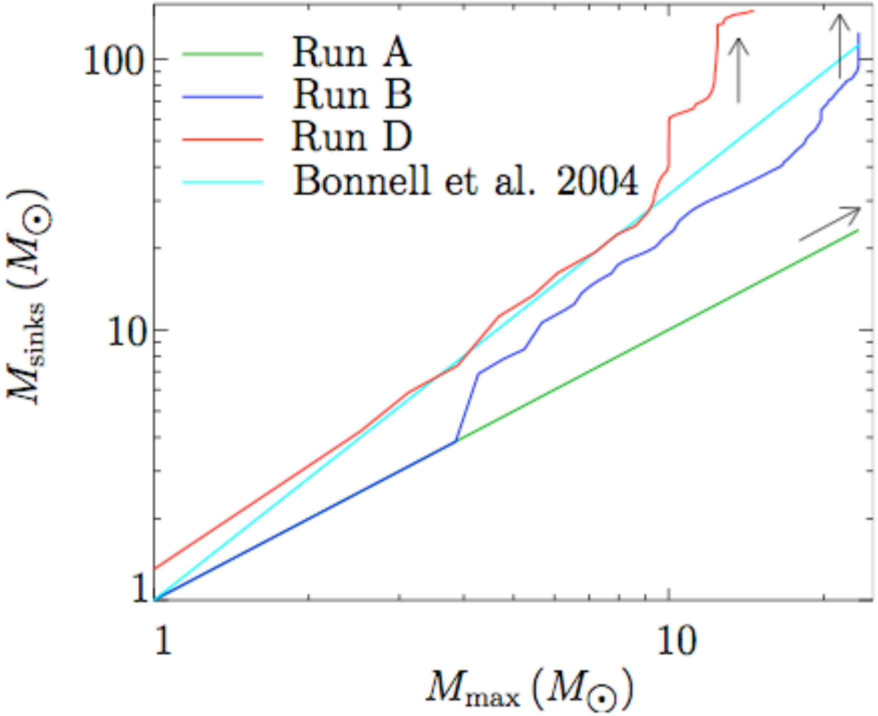

Bonnell et al. (2004):
competitive accretion

Peters et al. (2010):
fragmentation-induced starvation

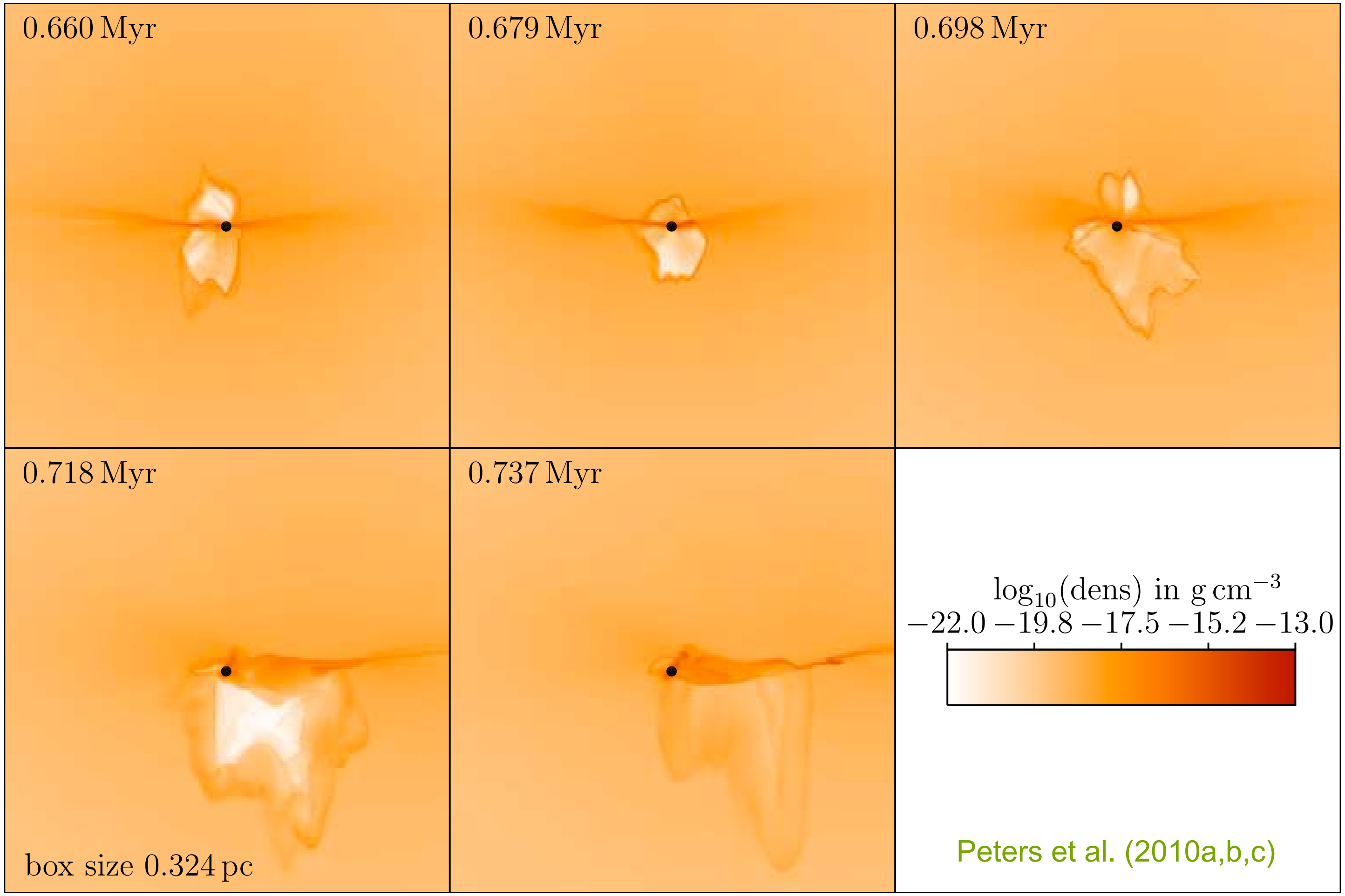

Peters et al. (2010a,b,c)

- thermal pressure drives bipolar outflow
- filaments can effectively shield ionizing radiation
- when thermal support gets lost, outflow gets quenched again
- no direct relation between mass of star and size of outflow

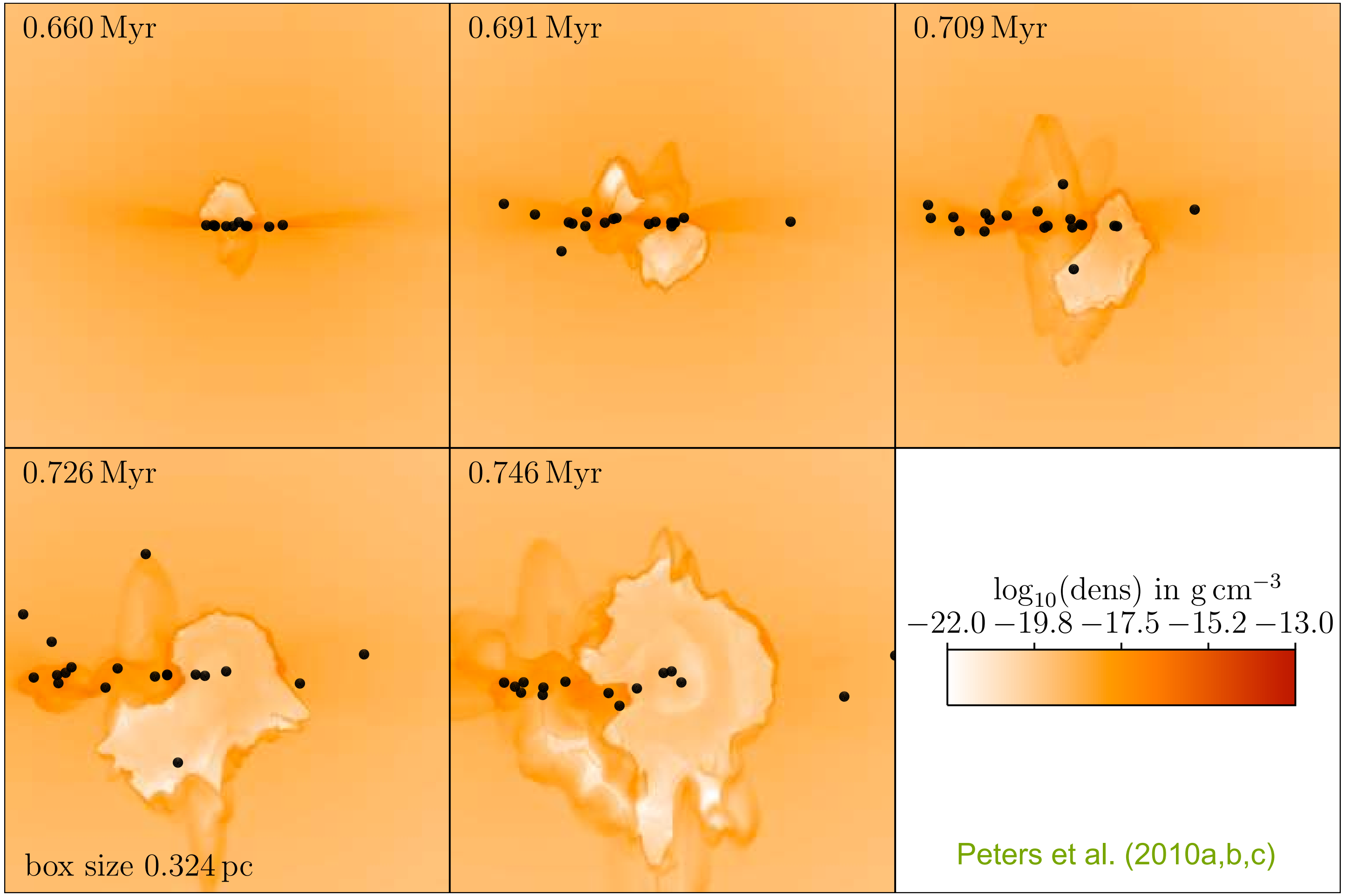

Peters et al. (2010a,b,c)

- bipolar outflow during accretion phase
- when accretion flow stops, ionized bubble can expand
- expansion is highly anisotropic
- bubbles around most massive stars merge

- numerical data can be used to generate continuum maps
- calculate free-free absorption coefficient for every cell
- integrate radiative transfer equation (neglecting scattering)
- convolve resulting image with beam width
- VLA parameters:
    - distance $2.65\,\mathrm{kpc}$
    - wavelength $2\,\mathrm{cm}$
    - FWHM $0\farcs14$
    - noise $10^{-3}\,\mathrm{Jy}$

Peters et al. (2010a, ApJ, 711, 1017), Peters et al. (2010b, ApJ, 719, 831), Peters et al. (2010c, ApJ, 725, 134)

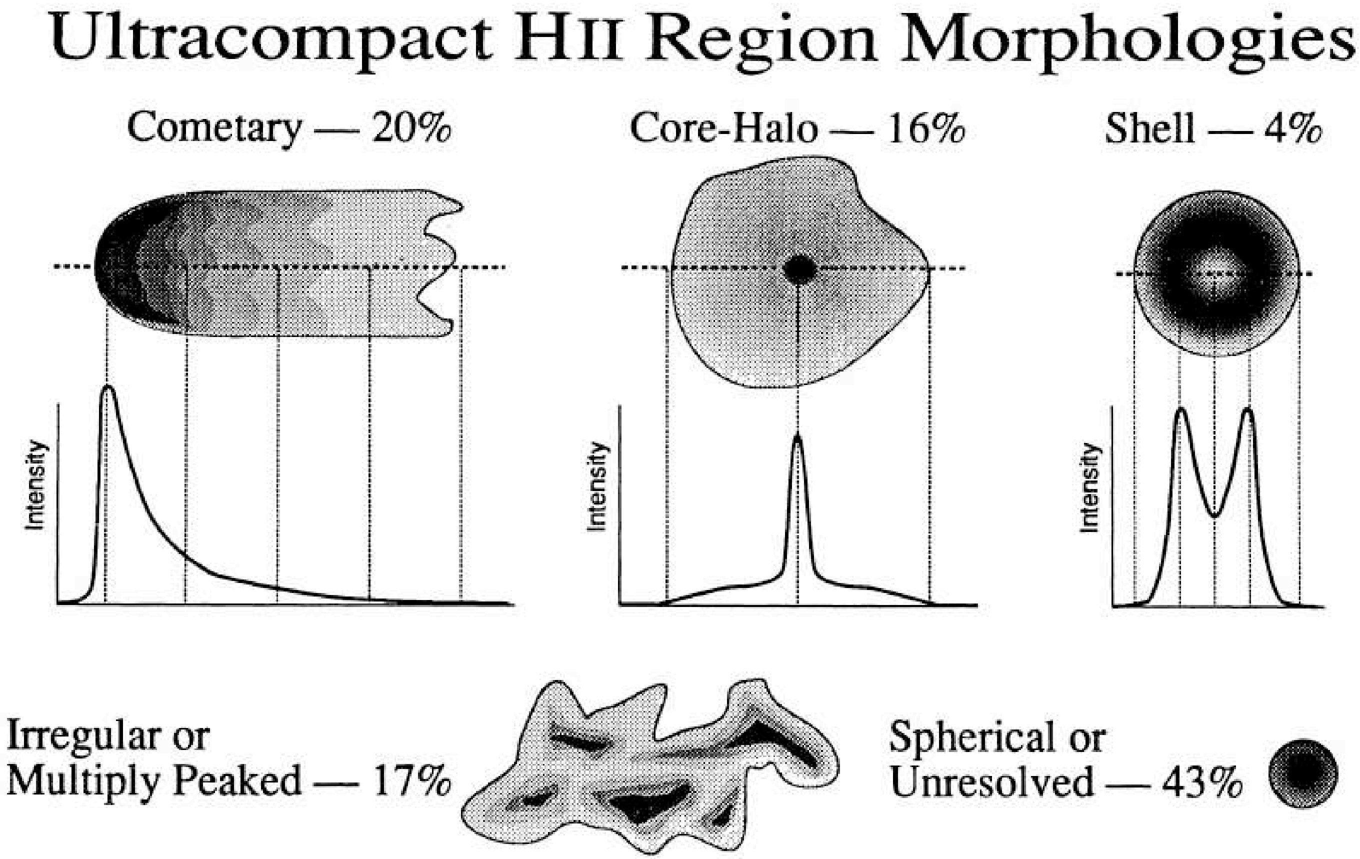

- Wood & Churchwell 1989 classification of UC H II regions
- Question: What is the origin of these morphologies?
- UC H II lifetime problem: Too many UC H II regions observed!

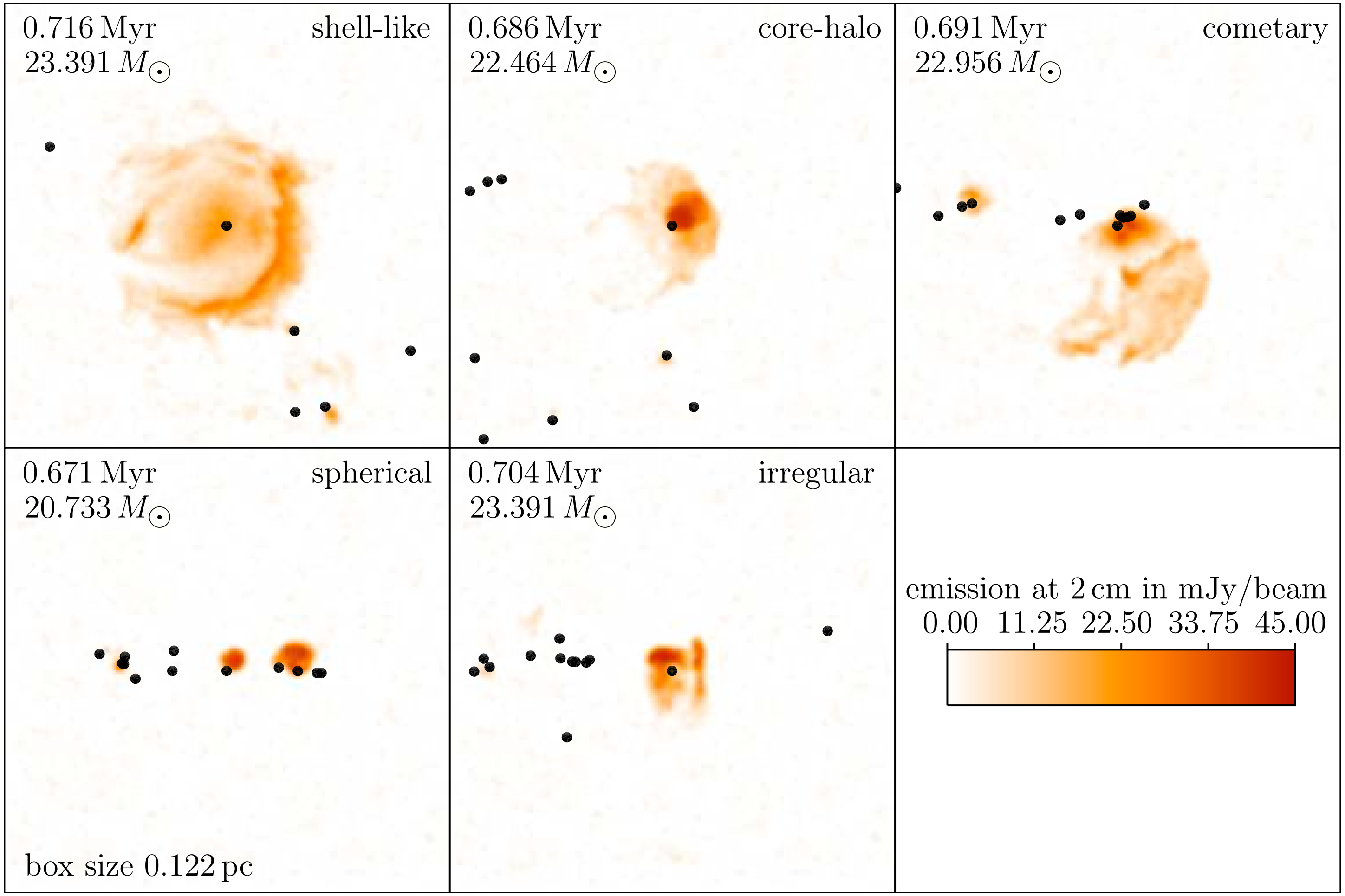

- synthetic VLA observations at $2\,\mathrm{cm}$ of simulation data
- interaction of ionizing radiation with accretion flow creates high variability in time and shape
- flickering resolves the lifetime paradox!

Peters et al. (2010a,b,c)

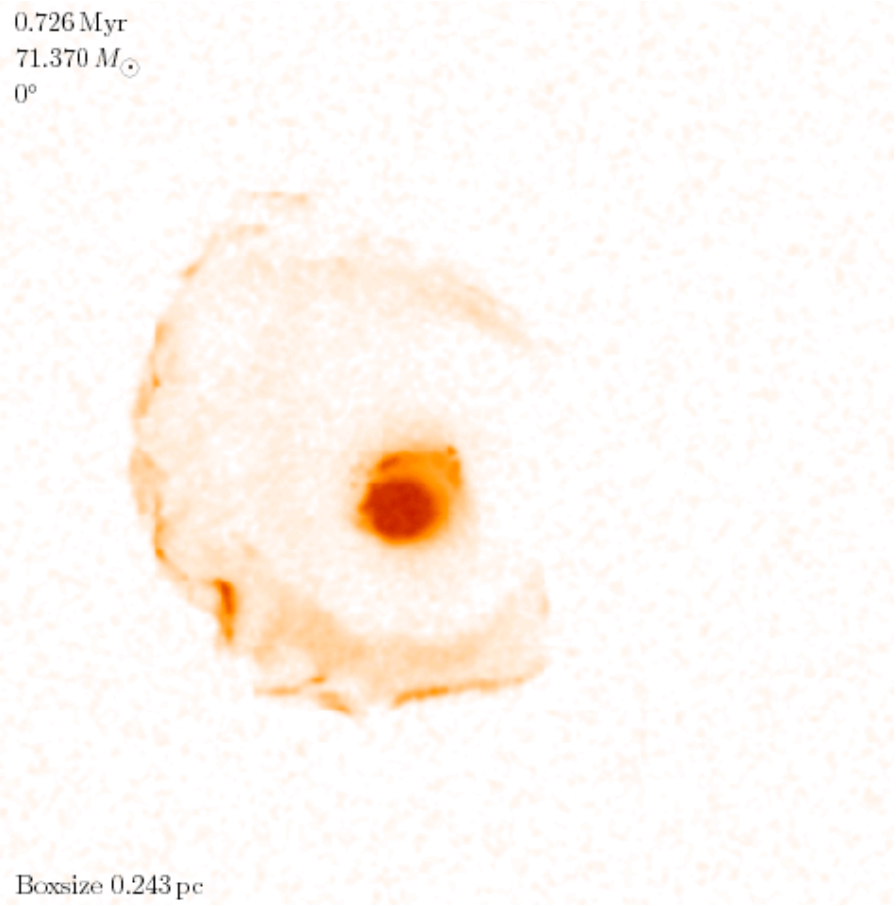

Morphology of HII region depends on viewing angle

Peters et al. (2010a,b,c)

Type	WC89	K94	single	multiple
Spherical/Unresolved	43	55	19	60 ± 5
Cometary	20	16	7	10 ± 5
Core-halo	16	9	15	4 ± 2
Shell-like	4	1	3	5 ± 1
Irregular	17	19	57	21 ± 5

WC89: Wood & Churchwell 1989, K94: Kurtz et al. 1994

- statistics over 25 simulation snapshots and 20 viewing angles
- statistics can be used to distinguish between different models
- single sink simulation does not reproduce lifetime problem

Peters et al. (2010a,b,c)

time variability

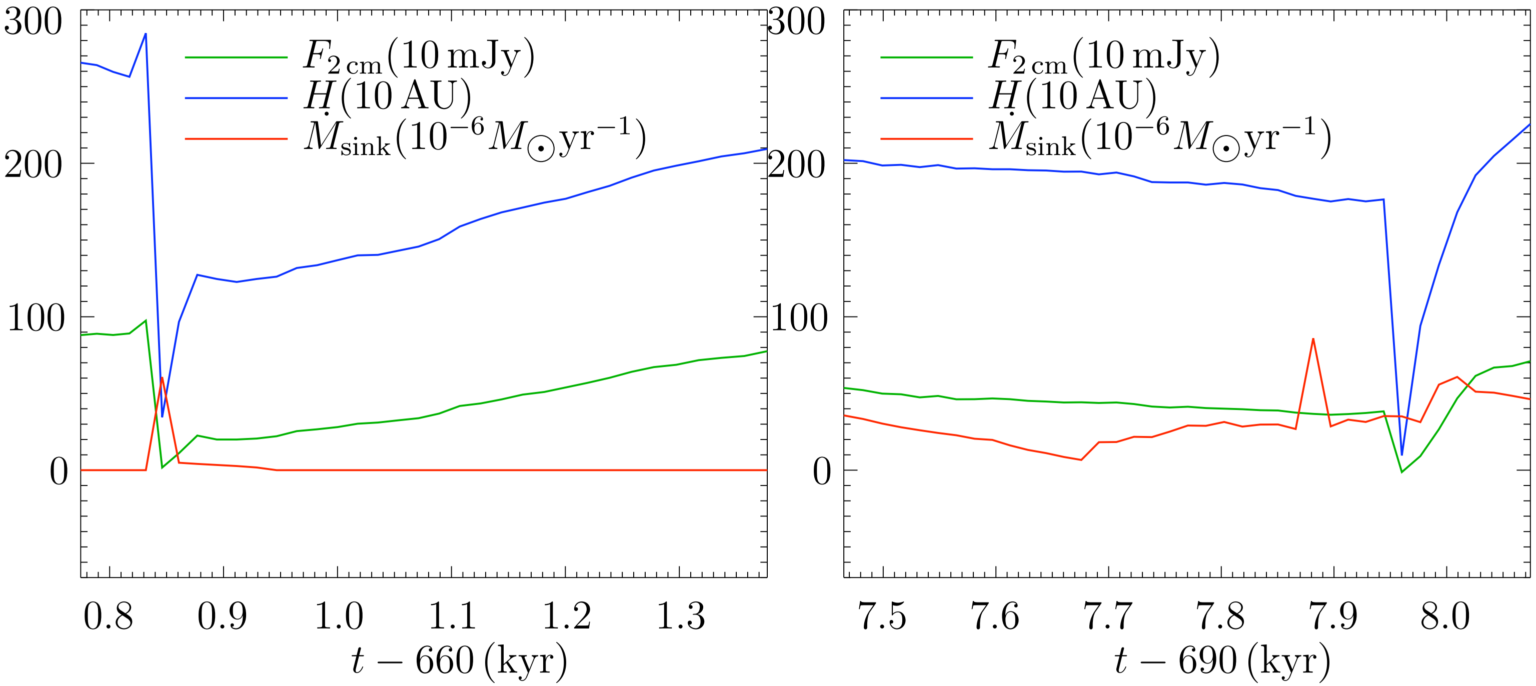

- correlation between accretion events and H II region changes
- time variations in size and flux have been observed
- changes of size and flux of $5\text{–}7\%\mathrm{yr}^{-1}$ match observations

Franco-Hernández et al. 2004, Rodríguez et al. 2007, Galván-Madrid et al. 2008

(Galvan-Madrid et al. 2011)

Some results

- ionization feedback cannot stop accretion
- ionization drives bipolar outflows
- HII regions show high variability in time and shape
- all classified morphologies can be observed in one run
- lifetime of HII regions determined by accretion timescale (and not by expansion time)
- rapid accretion through dense and unstable flows
- fragmentation limits further accretion of massive stars

Peters et al. (2010a, ApJ, 711, 1017), Peters et al. (2010b, ApJ, 719, 831), Peters et al. (2010c, ApJ, 725, 134), Peters et al. (2011, ApJ, 729, 72

summary

Star formation is intrinsically a multi-scale and multi-physics problem. Many different processes need to be considered simultaneously.

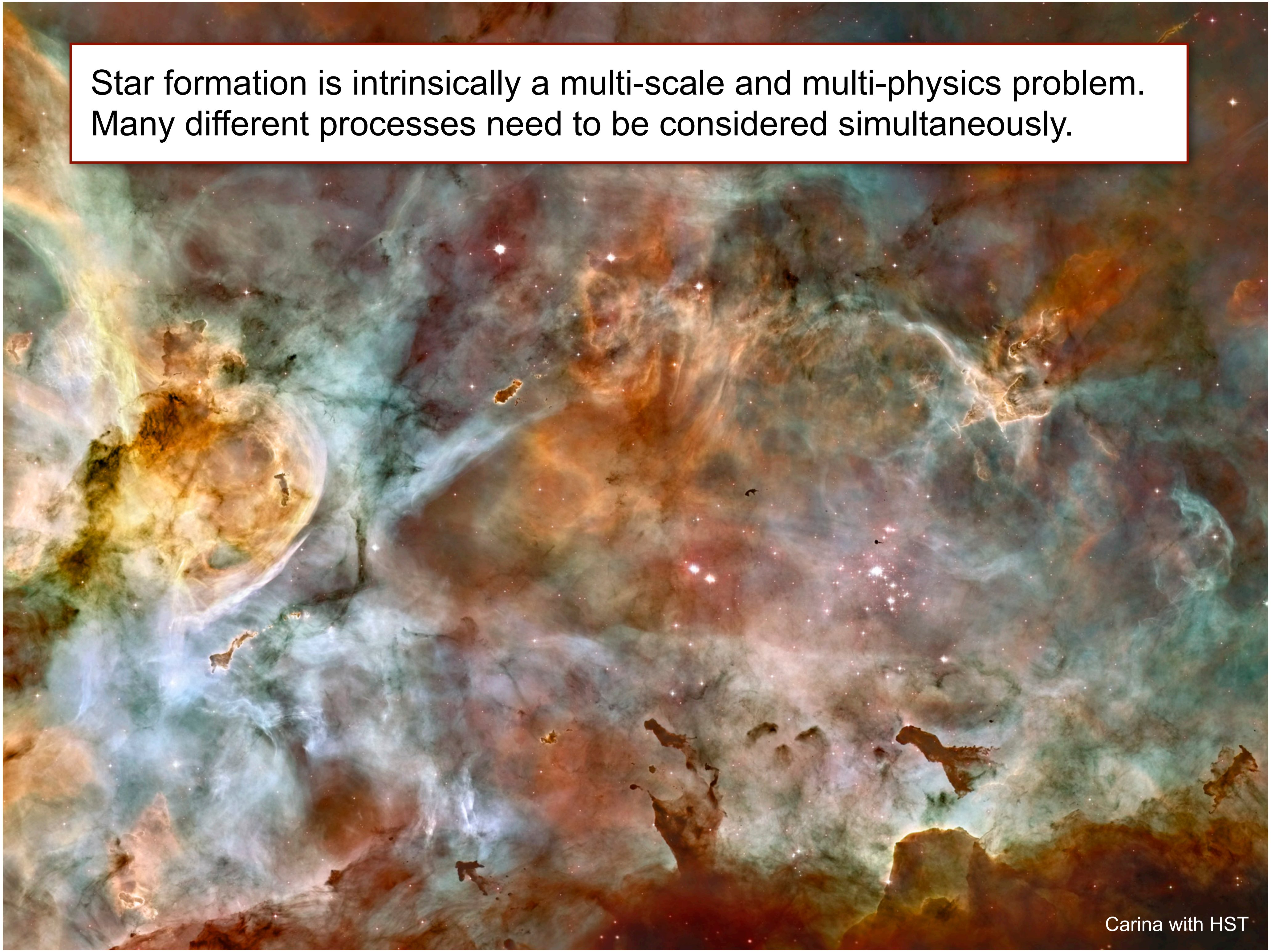

Carina with HST

Star formation is intrinsically a multi-scale and multi-physics problem. Many different processes need to be considered simultaneously.

- stars form from the **complex interplay** of **self-gravity** and a large number of competing processes (such as **turbulence**, **B-field**, **feedback**, **thermal pressure**)
- **thermodynamic properties** of the gas (heating vs cooling) play a key role in the star formation process
- detailed studies require the **consistent treatment** of many **different physical and chemical processes** (theoretical and computational challenge)
- star formation is **regulated** by several **feedback loops**, which are still poorly understood

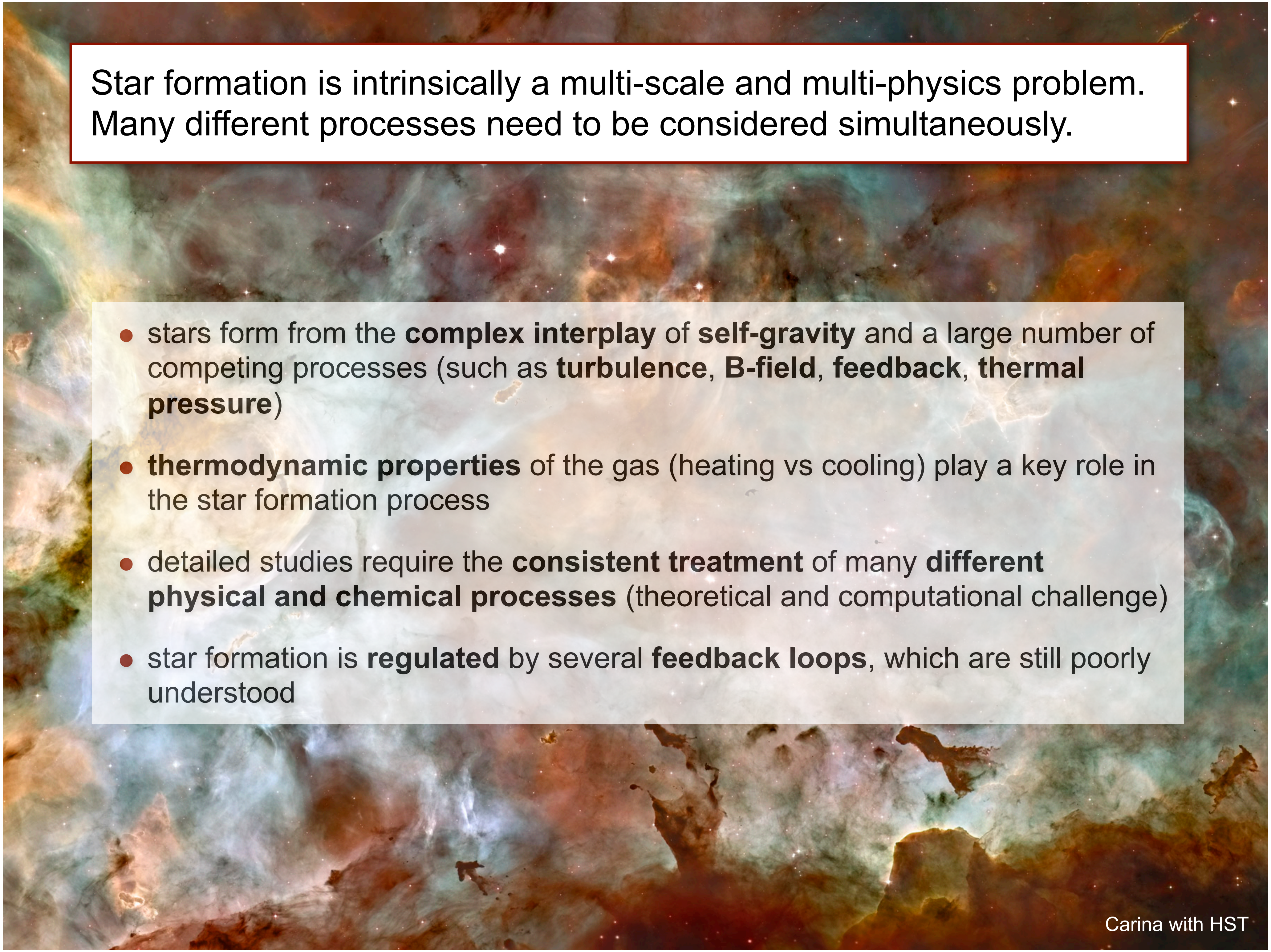

Carina with HST

Protostars and Planets VI in Summer 2013

Protostars and Planets VI in Summer 2013

www.ppvi.org

Thanks!